Indian J. Chem. Vol. 27A No. 12 pp. 1013-1116
December 1988
CODEN:IJOCAP ISSN: 0019-5103
27A(12) 1013-1116 (1988)

74
27/4/89

Indian Journal of
CHEMISTRY

SECTION A
(Inorganic, Physical, Theoretical & Analytical)

Published by
PUBLICATIONS & INFORMATION DIRECTORATE, CSIR, NEW DELHI
in association with
THE INDIAN NATIONAL SCIENCE ACADEMY, NEW DELHI

A RANGE OF HIGH PRECISION, HIGH QUALITY RECORDING INSTRUMENTS FOR THE DISCRIMINATING RESEARCH SCIENTIST

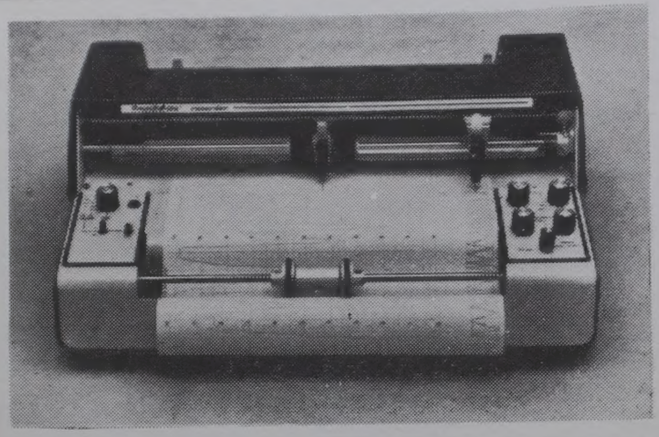

Series 5000 Strip Chart Recorder

The series 5000 Strip Chart Recorder and the series 2000 XY Recorder are well proven instruments incorporating State of the Art Circuitry. A wide range of models offer tremendous flexibility to the user. With over 5000 installations, these instruments are the preferred choice of discriminating users all over India.

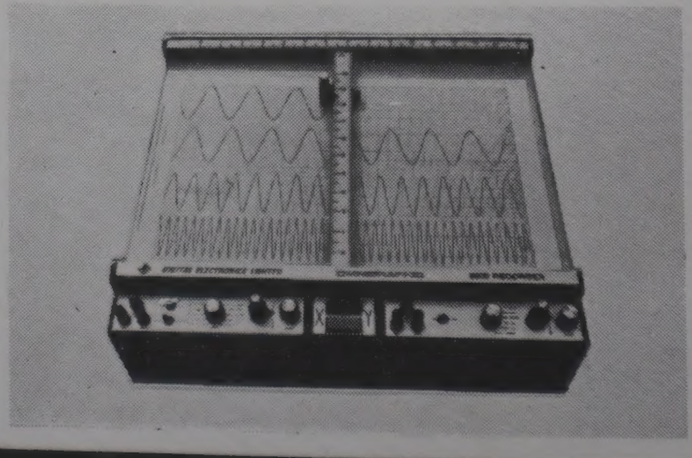

Series 2000 XY Recorder

Another quality product from

DIGITAL ELECTRONICS LIMITED

Reliability in Recording Instruments.

Digilog House 74/II, Marol Industrial Area MIDC, Andheri (East), Bombay- 400 093 Tel: 634 09 01, 632 86 76 Grams: 'DIGILOG'

A Company in collaboration with houston instrument

Special Effects/DE/25/86

RENEWAL NOTICE

Your subscription which expires with the despatch of December 1988 issue of the journal, stands for renewal. We request you to be so good as to return the enclosed order form duly filled early, so as to ensure continuity in despatch.

Sales & Distribution Officer

DATED:

The Sales & Distribution Officer
PUBLICATIONS & INFORMATION DIRECTORATE
HILLSIDE ROAD, NEW DELHI-110012 (INDIA)

Dear Sir,

Please renew my subscription/enrol me as subscriber to:

			Rs.	$	£
1	Journal of Scientific & Industrial Research	(Monthly)	200.00	70.00	45.00
2	Indian Journal of Chemistry, Section A	(Monthly)	300.00	100.00	70.00
3	Indian Journal of Chemistry, Section B	(Monthly)	300.00	100.00	70.00
4	Indian Journal of Experimental Biology	(Monthly)	250.00	85.00	55.00
5	Indian Journal of Technology	(Monthly)	250.00	85.00	55.00
6	Indian Journal of Pure & Applied Physics	(Monthly)	250.00	85.00	55.00
7	Indian Journal of Biochemistry & Biophysics	(Bimonthly)	125.00	42.00	28.00
8	Indian Journal of Radio & Space Physics	(Bimonthly)	125.00	42.00	28.00
9	Indian Journal of Marine Sciences	(Quarterly)	125.00	42.00	28.00
10	Indian Journal of Textile Research	(Quarterly)	125.00	42.00	28.00
11	Research & Industry	(Quarterly)	125.00	42.00	28.00
12	Current Literature on Science of Science	(Monthly)	100.00	30.00	12.00
13	Medicinal & Aromatic Plants Abstracts	(Bimonthly)	225.00	75.00	50.00

(Please tick off the periodicals you would like to subscribe).

for one year from January 1989 for which I/we have remitted to you a sum of Rs .....£ ..... $ ..... by Cheque/Demand Draft No. ..... dated ..... in favour of PUBLICATIONS & INFORMATION DIRECTORATE, NEW DELHI.

COMPLETE MAILING ADDRESS

Name .....

Address .....

Country/State .....

(Signature)

Note:
1. Subscribers at annual rates for all the periodicals are enlisted for the full volumes, i.e. for the period from January to December only.
2. The Cheque Demand Draft may plese be drawn in favour of "PUBLICATIONS & INFORMATION DIRECTORATE, NEW DELHI". Banking charges shall be borne by the subscriber. For inland outstation cheques please add Rs. 3.50. For foreign cheques please add $ 1.00 or £ 0.45.
3. The supply will commence on receipt of subscription in advance.

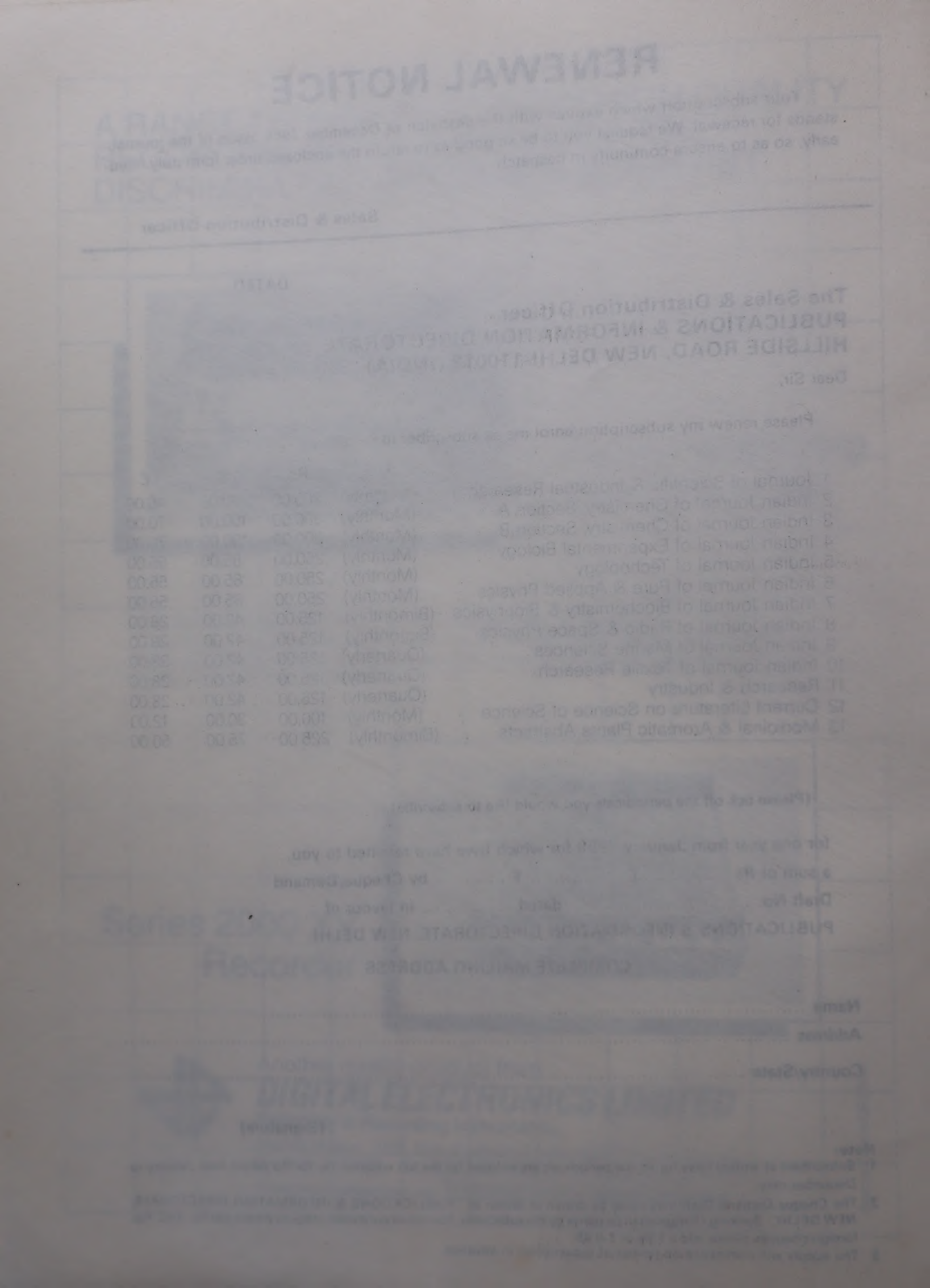

INDIAN JOURNAL OF CHEMISTRY

Section A: Inorganic, Physical, Theoretical & Analytical Chemistry

Editorial Board

Prof. C.N.R. Rao
Director
Indian Institute of Science
Bangalore 560 012

Prof. R.P. Rastogi
Vice-Chancellor
Banaras Hindu University
Varanasi 221 005

Prof. A.R. Vasudeva Murthy
Department of Inorganic &
Physical Chemistry
Indian Institute of Science
Bangalore 560 012

Prof. J.C. Kuriacose
Department of Chemistry
Indian Institute of Technology
Madras 600 036

Prof. D.V.S. Jain
Department of Chemistry
Panjab University
Chandigarh 160 014

Prof. P. Natarajan
Department of Inorganic Chemistry
University of Madras
Madras 600 025

Prof. N.K. Ray
Department of Chemistry
University of Delhi
Delhi 110 007

Prof. A. Chakravorty
Department of Inorganic Chemistry
Indian Association for the
Cultivation of Science
Calcutta 700 032

Prof. S. Mitra
Tata Institute of Fundamental Research
Bombay 400 005

Dr K.N. Rao
Chemistry Division
Bhabha Atomic Research Centre
Trombay, Bombay 400 085

Prof. S.M. Khopkar
Department of Chemistry
Indian Institute of Technology
Powai, Bombay 400 076

Prof. P.T. Manoharan
Department of Chemistry
Indian Institute of Technology
Madras 600 036

Dr A.C. Dash
Department of Chemistry
Utkal University
Bhubaneswar 751 004

Shri S.P. Ambasta, Editor-in-Chief
(*Ex-officio*)

Editors

S.S. Saksena — B.C. Sharma — S. Sivakamasundari

Assistant Editor

S.K. Bhasin

Published by the Publications & Information Directorate (CSIR), Hillside Road, New Delhi 110 012

Editor-in-Chief: S.P. Ambasta

Copyright, 1988, by the Council of Scientific & Industrial Research, New Delhi 110 012

The Indian Journal of Chemistry is issued monthly in two sections: A and B. Communications regarding contributions for publication in the journal should be addressed to the Editor, Indian Journal of Chemistry, Publications & Information Directorate, Hillside Road, New Delhi 110 012.

Correspondence regarding subscriptions and advertisements should be addressed to the Sales & Distribution Officer, Publications & Information Directorate, hillside Road, New Delhi 110 012.

The Publications & Information Directorate (CSIR) assumes no responsibility for the statements and opinions advanced by contributors. The Editorial Board in its work of examining papers received for publication is assisted, in an honorary capacity by a large number of distinguished scientists, working in various parts of India.

Annual Subscription: Rs. 300.00 £ 70.00 $ 100.00; 50% discount admissible to research workers and students and 25% discount to non-research individuals on annual subscription.

Single Copy: Rs. 30.00 £ 7.00 $ 10.00

Payments in respect of subscriptions and advertisements may be sent by cheque, bank draft, money order or postal order marked payable to Publications & Information Directorate, Hillside Road, New Delhi 110 012.

Claims for missing numbers will be allowed only if received within 3 months of the date of issue of the journal plus the time normally required for postal delivery of the journal and the claim.

Indian Journal of Chemistry

Sect. A: Inorganic, Physical, Theoretical & Analytical

VOLUME 27A NUMBER 12 DECEMBER 1988

CONTENTS

Communication

A non-local pseudopotential in FSGO model study: Some typical organic molecules . 1013
S Kaur, V Saxena, R C Rastogi & N K Ray*

Papers

Intramicellar Quenching of Singlet Emission of 5,10,15,20-Tetraphenylporphyrin by Nitroaromatics 1016
V Hanumantha Rao & V Krishnan*

Mechanism of Solidification of Binary Naphthalene-Benzoic Acid Eutectic System . . . 1021
P S Bassi*, B L Sharma, N K Sharma & Shiv Kumar

Effect of *p*H, Urea, EDTA & Deoxycholate on Metachromasia Induced by Heteropoly-anions 1025
Shyam Narain Ram, K D S Yadav*, B Sharma & Chanan Singh

Kinetics of Halogenation of Sulphacetamide & Sulphanilamide by Trichloroisocyanuric Acid 1028
P S Radhakrishnamurti*, N K Rath & M Yedukondalu

Kinetics & Mechanism of Oxidation of Substituted Benzyl Alcohols by Sodium Bis-[2-ethyl-2-hydroxybutanoato(2-)]oxochromate(V) 1031
G Sreelatha, M Prasada Rao, B Sethuram* & T Navaneeth Rao

Oxidation by Fe(VI): Kinetics of Fe(VI) Oxidation of Alcohols 1035
K Laxmi Venkat Rao, M Prasada Rao, B Sethuram* & T Navaneeth Rao

Characterization & Polymerization Studies on Silica-supported Titanium(IV) Complexes 1040
G C Ofunne*, B L Booth & P J T Tait

Synthesis of Carbene Complexes of Iron from gem-Dichlorocyclopropylcycloalkanes . 1047
S S Alam, M A Hashem* & S S Ullah

Synthesis & Reactions of Isotetralenetricarbonyliron 1050
M N Abser, M A Hashem, S E Kabir & S S Ullah*

Alkoxy Boron-bridged Macrocyclic Compounds of Nickel(II) with 1,1′,8,8′-Tetraalkoxy-1,8-dibora-4,5,11,12-tetraphenyl-3,6,10,13-tetraaza-2,7,9,14-tetraoxatetradecacyclo-3,5,10,12-tetraene & 1,1′,9,9′-Tetraalkoxy-1,9-dibora-4,6,12,14-tetramethyl-3,7,11,15-tetraaza-2,8,10,16-tetraoxacyclohexadeca-3,6,11,14-tetraene 1053
H C Rai*, Jaya Tiwary & Rekha Kumari

Intercalated Compounds of Cu(II) Montmorillonite Clay with 1,2-Diaminoethane & 1,2-Diaminopropane 1056
Nitin Labhasetwar & O P Shrivastava*

(*Continued overleaf*)

Synthesis & Characterisation of Imidodi(thiocarbonic acid O-alkyl ester) Derivatives of Triphenylphosphine Complexes of Rhodium(I) & Ruthenium(II) 1060
S Sumathy, S Ayyavoo, V Chinnusamy & K Natarajan*

Synthesis, Characterization & Antifungal Properties of Some Four-coordinate Nickel(II) & Four- & Five-coordinate Copper(II) Complexes Containing Tridentate Thiosemicarbazones & Heterocyclic Bases 1064
M Akbar Ali*, M H Kabir, M Nazimuddin, S M M H Majumder, M T H Tarafder & M A Khair

Tetrad Effect in the Solution Stabilities of Mixed Ligand Complexes of Lanthanides . 1068
Sangeeta Verma & M C Saxena*

ctance Studies of Tetraalkylammonium Iodides in Dimethyl Sulphoxide-Water Mixtures 1073
S Das & D K Hazra*

Spectrophotometric Study of Acid-Base Equilibria of Sudan Green in Mixed Water-Organic Solvent Media 1080
M M Seleim, K A Idriss*, Magda S Saleh & H Sedaira

Notes

On the Counting of Conjugated Circuits in Benzenoid Hydrocarbons 1084
I Gutman

Dimerization & Subsequent Complexation of 1,5,9-Cyclododecatriene with Hexacarbonyltungsten 1087
K A Azam, M B H Howlader, S E Kabir & S S Ullah*

Linear Free Energy Correlation in Substitution Reactions of Octahedral Cobalt(III) Complexes 1089
Anadi C Dash* & Ajaya K Patnaik

Enthalpies of Mixing of Polyoxypropyleneglycols with Benzene, Ethanol & Water at 321.35 K 1092
R Parashar* & S C Sharma

Electroreduction of Samarium(III) in Calcium Nitrate Tetrahydrate Melt 1095
C K Bhaskare* & K N Ganage

Compounds of Vanadium(IV) with Imidazoles & Piperidines 1097
Tankeswar Bora* & (Mrs) Meena Devi

Ternary Complexes of Copper(II) Involving Barbituric Acid and Some of Its Derivatives 1100
Rohitashva M Tripathi, (Mrs) Ranjana Ghose & Animesh K Ghose*

Synthesis, Characterisation & Antimicrobial Studies of Co(II) & Ni(II) Complexes with Some Pyrazoles 1102
Zahid Hussain Chohan*, Misbahul Ain Khan & Mohammad Moazzam

Synthesis & Characterization of Thorium(IV) & Dioxouranium(VI) Complexes of 4-{(N-Benzoyl)amino}antipyrine 1105
R K Agarwal*, H K Rawat & A K Srivastava

Thorium Nitrate Complexes of Some Schiff Bases Derived from Substituted Benzaldehydes & Amino Compounds 1109
Babu Kuncheria & P Indrasenan*

Evaluation of Formation Constants of Pyridine Adducts of (Resacetophenoneoximato)-nickel(II) 1111
Arvind T Rane* & Deepawati R Nepali

Spectrophotometric Determination of Co(II), Ni(II) & Cu(II) Using Sodium 1-Amidino-azo-2-hydroxynaphthalene-4-sulphonate 1114
V Pradhan & R P Singh*

Book Reviews

Chemical Crystallography with Pulsed Neutrons and Synchrotron X-rays (Editors: M A Carrando & G A Jeffrey) 1116
L M Pant

Authors for correspondence are indicated by (*)

AUTHOR INDEX

Abser M N 1050
Agarwal R K 1105
Akbar Ali M 1064
Alam S S 1047
Ayyavoo S 1060
Azam K A 1087

Bassi P S 1021
Bhaskare C K 1095
Booth B L 1040
Bora Tankeswar 1097

Chinnusamy V 1060
Chohan Zahid Hussain 1102

Das S 1073
Dash Anadi C 1089

Ganage K N 1095
Ghose Animesh 1100
Ghose Ranjana 1100
Gutman I 1084

Hanumantha Rao V 1016
Hashem M A 1047,1050
Hazra D K 1073
Howlader M B H 1087

Idriss K A 1080
Indrasenan P 1109

Kabir M H 1064
Kabir S E 1050,1087
Kaur S 1013
Khair M A 1064
Khan Misbahul Ain 1102
Krishnan V 1016
Kuncheria Babu 1109

Labhasetwar Nitin 1056
Laxmi Venkat Rao K 1035

Majumder S M M H 1064
Meena Devi 1097
Moazzam Mohammad 1102

Natarajan K 1060
Navaneeth Rao T 1031,1035
Nazimuddin M 1064
Nepali Deepawati R 1111

Ofunne G C 1040

Pant L M 1116
Parashar R 1092
Patnaik Ajaya K 1089
Pradhan V 1114
Prasada Rao M 1031,1035

Radhakrishnamurti P S 1028
Rai H C 1053
Rane Arvind T 1111
Rastogi R C 1013
Rath N K 1028
Rawat H K 1105
Ray N K 1013
Rekha Kumari 1053

Saleh Magada S 1080
Saxena M C 1068
Saxena V 1013
Sedaira H 1080
Seleim M M 1080
Sethuram B 1031,1035
Sharma B 1025
Sharma B L 1021
Sharma N K 1021
Sharma S C 1092
Shiv Kumar 1021
Shrivastava O P 1056
Shyam Narain Ram 1025
Singh Chanan 1025
Singh R P 1114
Sreelatha G 1031
Srivastava A K 1105
Sumathy S 1060

Tait P J T 1040
Tarafder M T H 1064
Tiwary Jaya 1053
Tripathi Rohitashva M 1100

Ullah S S 1047,1050,1087

Verma Sangeeta 1068

Yadav K D S 1025
Yedukondalu M 1028

Indian Journal of Chemistry
Vol. 27A, December 1988, pp. 1013-1015

Communication

A non-local pseudopotential in FSGO model study: Some typical organic molecules†

S KAUR, V SAXENA, R C RASTOGI & N K RAY*
Department of Chemistry, University of Delhi, Delhi 110 007

Received 27 October 1988; accepted 15 November 1988

A non-local pseudopotential has been used in the FSGO (Floating Spherical Gaussian Orbital) model to study valence electronic structures and equilibrium geometries of ethane, ethylene, acetylene, cyclopropane, methanol, formaldehyde, methylamine and methyl cyanide. Predicted average electric polarizabilities (α) and magnetic susceptibilities (χ) are also reported. The results of present 'valence-electron only' studies are in excellent agreement with those obtained from all-electron calculations. Calculations for α and χ values for a number of hydrocarbons, alcohols, aldehydes, ethers, amines and nitriles have also been made assuming approximate transferability of bond and lone pair gaussians. The predicted values are in good agreement with other estimates.

The FSGO model of Frost[1] is quite interesting since the wavefunctions obtained in this simple ab-initio model are always susceptible to simple interpretation in terms of chemical ideas and intuition. This model describes the electronic structures of molecules in terms of core, bond and lone pair gaussians. Several[2-16] attempts have been made to simulate the core electrons using different model potentials. Recently Grundler and Walther[17] have used a non-local pseudopotential in FSGO model to successfully study the electronic structures of first row hydrides and some diatoms. We have presently used this pseudopotential to study the electronic structures and equilibrium geometries of some hydrocarbons, methyl alcohol, methyl amine and methyl cyanide.

In this model the localised orbitals are constructed using single normalized spherical gaussian functions as depicted by Eq. (1)

$$\phi_i = (2/\pi\rho_i^2)^{3/4} \exp[-(r-R_i)^2/\rho_i^2] \quad \ldots (1)$$

with orbital radius ρ_i, and position R_i. A single determinant wavefunction is used for the singlet ground state of the molecule and energy is minimized by a direct search procedure with respect to all parameters: orbital radii (ρ_i), orbital positions (R_i) and nuclear positions.

The pseudopotential suggested by Grundler and Walther[17] is of the form (2)

$$V_c(i) = -Zc/r_{ci} + (k_c/\rho_c^2)|c><c| \quad \ldots (2)$$

where Zc is the core charge and $|c><c|$ is the non-local projection operator. This contains the gaussian function

$$\phi_c = (2/\pi\rho_c^2) \exp[-(r-R_c)^2/\rho_c^2]$$

All valence electron calculations reported here have been performed with complete geometry optimization and retaining only the restrictions of full FSGO calculations with respect to the position of lone-pair gaussians[18] and representation of double and triple bonds[19]. The predicted equilibrium geometries are given in Table 1 and excellent agreement can be seen between the results of present valence-electron studies and those obtained from all-electron FSGO studies. Some of the bond angles predicted in methanol and methyl amine are in poor agreement with experiment both for the all-electron FSGO model and present pseudopotential FSGO calculations. Same observation can also be made for the results of calculation[17] for water and ammonia molecules. This is a known shortcoming of the FSGO model itself[25] due to the poor approximation of the lone-pair orbital by single gaussian.

We have used the symmetry adapted double perturbation theory of Amos and Yoffe[20] to calculate the average electric polarizabilities and magnetic susceptibilities of the systems studied here. Present "valence-electron only" results are in excellent agreement with all-electron FSGO results and other estimates (see Table 2).

Bhargava and Ray[21,22] earlier have successfully studied the average electric polarizabilities (α) and magnetic susceptibilities (χ) of a number of hydrocarbons, alcohols, ethers and amines assuming the approximate transferability (see Blustin and Linnet)[23] of core, bond and lone-pair gaussians. They have also shown that the core contributions are negligibly small so that the average electric polarizabilities and magnetic susceptibilities can be well estimated from the contributions of bond and lone pair gaussians. The same concept has been used here to estimate α and χ values for a series of hydrocarbons, alcohols, aldehydes, ethers, amines and nitriles. The bond and lone pair gaussions needed for these calculations have been obtained from pseudopotential FSGO calculations using experimental geometry for ethane, methyl alcohol, formaldehyde, methylamine and methyl cyanide.

† Dedicated to Prof. P.T. Narsimhan on his 60th birthday

Table 1—Calculated Equilibrium Geometries (Å, degree)

Molecule	Bond distances & bond angles	Present calculation	FSGO[a]	Obsd.[b]
Ethane	C–H	1.14	1.12	1.093
	C–C	1.53	1.50	1.534
	∠H–C–H	108.1	108.2	109.1
Ethylene	C–H	1.12	1.10	1.086
	C=C	1.38	1.35	1.337
	∠H–C–H	118.7	118.7	117.3
Acetylene	C–H	1.09	1.08	1.059
	C≡C	1.23	1.21	1.205
Cyclopropane	C–H	1.13	1.12	1.123
	C–C	1.56	1.53	1.510
	∠H–C–H	113.8	114.5	114.4
Formaldehyde	C–H	1.12	1.11	1.116
	C=O	1.17	1.16	1.208
	∠H–C–H	108.4	109.4	116.5
Methanol	C–H	1.14	1.13	1.094
	C–O	1.29	1.27	1.425
	O–H	0.90	0.89	0.945
	∠H–C–H	105.1	104.9	108.6
	∠C–O–H	89.8	89.9	108.5
Methylamine	C–H	1.14	1.13	1.093
	N–H	1.02	1.01	1.011
	C–N	1.44	1.43	1.474
	∠H–C–H	105.98	105.96	109.47
	∠C–N–H	90.85	90.92	109.8
	∠H–N–H	89.06	89.08	105.9
Methyl cyanide	C–H	1.13	1.11	1.104
	C–C	1.53	1.54	1.458
	C≡N	1.18	1.16	1.157
	∠–H–C–H	112.8	110.4	109.47

(a) Results for hydrocarbons are taken from reference 19 along with the listed experimental bond lengths and bond angles.
(b) Observed results for systems other than hydrocarbons are taken from the tables of reference 26.

Table 2—Calculated Average Electric Polarizabilities (α)[a] and Magnetic Susceptibilities (χ)[b]

System	α			χ		
	Present	FSGO[c]	Obsd.[d]	Present	FSGO[c]	Obsd.[d]
Ethane	43.7	42.1	44.7	24.1	24.0	27.4
Ethylene	38.9	36.9	42.2	20.9	20.7	15.3
Acetylene	33.5	31.6	34.9	17.7	17.5	12.5
Cyclopropane	60.0	57.5	56.4	32.0	31.7	39.9
Methanol	27.3	26.0	32.5	18.6	18.3	21.9
Formaldehyde	22.2	19.0	—	15.1	14.7	—
Methylamine	37.2	35.7	—	22.8	22.1	—
Methyl cyanide	43.5	41.4	44.3	25.7	25.4	27.6

(a) All quantities are in units of 10^{-25} cm^3.
(b) All quantities are in units of -1×10^{-6} c.g.s. units.
(c) Results for hydrocarbons are taken from reference 20.
(d) Obtained from references 24 and 25.

Results of these studies are given in Table 3 and good agreement can be seen with other estimates.

It appears from the results of present study that the non-local pseudopotential used here is quite adequate in mimicking the results of all-electron FSGO calculations. The valence-electron wave-function obtained in the present model can be successfully used to estimate the average electron polarizabilities and magnetic susceptibilities of the systems studied here. Work is in progress to study

Table 3—Calculated Average Electric Polarizabilities (α)[a] and Magnetic Susceptibilities (χ)[b] of Some Typical Organic Molecules

System	α		χ	
	Present	Obs.[c]	Present	Obs.[c]
n-Butane	80.66	81.8	44.70	50.3
n-Hexane	117.56	118.9	65.24	74.3
n-Octane	154.46	155.4	85.78	96.9
Ethanol	48.22	51.1	29.74	33.7
Butanol	85.14	87.6	50.28	56.3
Propionaldehyde	58.63	63.4	36.02	34.3
Diethyl ether	85.76	89.2	49.46	55.1
Dibutyle ether	159.38	162.5	91.48	—
1-Cyanoethane	62.54	62.9	36.12	38.8
1-Cyanohexane	136.36	137.2	77.23	—
1-Aminobutane	92.57	95.5	53.00	58.9
1-Aminoheptane	147.95	150.6	83.81	—

(a) All quantities are in units of 10^{-25} cm^3.
(b) All quantities are in units of -1×10^{-6} c.g.s. units.
(c) Obtained from references 24 and 25.

other molecular systems (organometallics and hydrogen bonded) and other expection values (both in co-ordinate and momentum space). These results will be reported elsewhere.

Acknowledgement

One of the authors (VS) is thankful to the CSIR, New Delhi for a research fellowship. All calculations reported here were carried out on a Hewlett Packard (HP-9050) computer bought under the COSIST programme of the UGC, New Delhi.

References

1 Frost A A, *J chem Phys*, **47** (1967) 3707.
2 Barthelat J C & Durand P H, *Chem Phys Lett*, **16** (1972) 63.
3 Barthelat J C & Durand P H, *Chem Phys Lett*, **40** (1976) 407.
4 Barthelat J C & Durand P H, *Theor Chim Acta*, **27** (1972) 109.
5 Ray N K & Switalski J D, *J chem Phys*, **63** (1975) 5053.
6 Ray N K & Switalski J D, *Theor Chim Acta*, **41** (1976) 329.
7 Ray N K & Mahendru S P, *Chem Phys Lett*, **54** (1978) 42.
8 Ray N K, Mahendru S P & Switalski J D, *Chem Phys Lett*, **47** (1977) 563.
9 Mahendru S P & Ray N K, *Chem Phys Lett*, **50** (1977) 497.
10 Semkow A M, Suthers R A & Linnet J W, *Chem Phys Lett*, **32** (1975) 116.
11 Topiol S, Frost A A, Ratner M A & Moskowitz J W, *J chem Phys*, **65** (1976) 4467.
12 Topiol S, Frost A A, Moskowitz J W & Ratner M A, *J chem Phys*, **66** (1977) 5130.
13 Topiol S, Frost A A, Ratner M A, Moskowitz J W & Melius C F, *Theor Chim Acta*, **45** (1977) 177.
14 Topiol S, Moskowitz J W, Frost A A & Ratner M A, *J chem Soc Faraday Trans II*, **74** (1978) 1521.
15 Ratner M A, Frost A A, Topiol S & Sabin J R, *J chem Soc Faraday Trans II*, **74** (1978) 324.
16 Toman J J, Frost A A, Topiol S, Jacobson S & Ratner M A, *Theor Chim Acta*, **58** (1981) 285.
17 Grundler W & Walther P, *Chem Phys Lett*, **150** (1988) 275.
18 Frost A A, *J phys Chem*, **72** (1968) 1289.
19 Frost A A & Rouse R A, *J Am chem Soc*, **90** (1968) 1965.
20 Amos A T & Yoffe J A, *J chem Phys*, **63** (1975) 4723.
21 Bhargava S & Ray N K, *Proc Indian Acad Sci*, **88A** (1979) 367.
22 Bhargava S, Bakshi A K & Ray N K, *Indian J Chem*, **19A** (1980) 1203.
23 Blustin P H & Linnet J W, *J chem Soc Faraday Trans II*, **70** (1974) 274.
24 Kier L B & Hall L H, *Molecular connectivity in chemistry & drug research*, (Academic Press, New York) 1976.
25 Heberditzl W, *Theory and application of molecular diamagnetism*, edited by L.N. Mulay & E.A. Boudreaux, (John Wiley, New York) 1976.
26 Dewar M J S & Thiel W, *J Am chem Soc*, **99** (1977) 4907.

Indian Journal of Chemistry
Vol. 27A, December 1988, pp. 1016-1020

Intramicellar Quenching of Singlet Emission of 5,10,15,20-Tetraphenylporphyrin by Nitroaromatics

V HANUMANTHA RAO & V KRISHNAN*
Department of Inorganic and Physical Chemistry, Indian Institute of Science, Bangalore 560 012, India

Received 29 *June* 1988; *accepted* 18 *July* 1988

The singlet emission quenching of 5,10,15,20-tetraphenylporphyrin (H_2TPP) by diverse nitroaromatic compounds nas been studied in neutral, anionic and cationic surfactant solutions. The apparent Stern-Volmer (S-V) constants calculated from the analytical quencher concentration have large magnitudes. This has been explained in terms of compartmentalisation of quencher molecules in small volume element of the micellar psuedophase. The mean occupancy number of quencher molecules per micelle, $\bar{n}$, and the partition constants of the quencher molecules between the aqueous and micellar pseudophase have been evaluated from the fluorescence quenching at various micellar concentrations. The partition constants are found to be dependent on the nature of the micelles and follow the order: CTAB > SDS > Triton X-100. This is interpreted in terms of ion-dipole interactions of the micelles with quencher molecules. The real S-V constants (K_{SV}^{real} calculated from $\bar{n}$ values vary with the micellar system in the order Triton X-100 > SDS > CTAB. This is attributed to the different diffusional characteristics of quenchers in various micelles.

Studies on several photoprocesses in organized assemblies are of considerable importance because of their potential applications in the area of solar energy conversion. This has been the subject of many reviews and monographs[1-5]. The possibility of obtaining a net chemical conversion through a process in which both the light absorbing substrate and the quencher are recycled has been illustrated by Schmell and Whitten[6].

Amongst the various photoprocesses, the most widely investigated one is the quenching of the luminescence intensity. These studies permit the evaluation of a range of properties of the system such as, size of the micelles, aggregation numbers, partition and association constants, rate of entry and exit of molecules, and effects induced by the presence of the solubilizates on the structure of the pseudophase. The excited state properties of porphyrins are ably suited for mimicking many photosynthetic processes. In view of this, tetraphenylporphyrin (H_2TPP) has been chosen as the fluorophore in the present study. The nitroaromatic compounds used as quenchers are: 1,2-dinitrobenzene (*o*-DNB), 1,3-dinitrobenzene (*m*-DNB), 1,4-dinitrobenzene (*p*-DNB), 1,3,5-trinitrobenzene (TNB) and 2,4,6-trinitrotoluene, TNT. The reduction potentials of these acceptors vary over a range of potentials (−0.60 V to −0.91V) which can be used with advantage for studying the excited state electron transfer process[7]. In order to elucidate the mechanism of quenching, three types of surfactant solutions, viz. anionic sodium dodecyl sulphate (SDS), neutral Triton X-100, and cationic cetyltrimethylammonium bromide (CTAB) have been employed.

Materials and Methods

H_2TPP was prepared according to the method of Rothemund and Menotti[8] and purified using the procedure described by Barnett *et al.*[9] SDS(BDH) was purified by washing it with ether and recrystallising from ethanol. Triton X-100, (Aldrich Chemicals), CTAB (Sigma Chemicals) and *o*-DNB (Sigma Chemicals) were used as such. *m*-DNB was prepared and purified using the method described by Vogel[10]. *p*-DNB and TNT (Aldrich Chemicals) were recrystallised twice from hot water. TNB (BDH, AR) was recrystallised twice from benzene. Doubly distilled water was used to prepare aqueous solutions. A Hitachi (650.60) fluorescence spectrophotometer was used to monitor the fluorescence emission of porphyrin. A Beckmann model 25 UV-VIS spectrophotometer was used for the absorption spectral studies. A Sonics and Materials Ultrasonicator was used for sonicating the solutions.

H_2TPP was micellized using solvent evaporation method described earlier[11] and the method was found more convenient than the freeze-thaw method of Kano *et al.*[12]. In this method H_2TPP (1 mg) was dissolved in methylene chloride (100 ml). An aliquot (5 ml) of this solution was added to surfactant solution (2.5%, 75 ml). Purging the result-

Table 1—Binding and Quenching Constants of H_2TPP by Nitroaromatics in Micellar Media

Quencher	Surfactant	[Surfactant]	[Mic][a] ($M \times 10^4$)	$K_{SV}^{app} \times 10^{-3}$	$[Q]_{1/2}^{app}$[b] ($\times 10^4$ M)	Binding constant (K)	Range of n values	K_{SV}^{real}
		0.050	7.0	1.64	6.09			
o-DNB	SDS	0.035	4.5	2.00	5.00	2400 ± 100	0.10-0.30	1.88
		0.020	2.0	2.87	3.48			
		0.050	7.0	0.480	20.83			
m-DNB	SDS	0.035	4.5	0.665	15.04	2080 ± 10	0.60-1.60	0.617
		0.020	2.0	0.903	11.07			
		0.050	7.0	1.59	6.29			
p-DNB	SDS	0.035	4.5	1.98	5.06	2200 ± 50	0.10-0.60	1.83
		0.020	2.0	2.86	3.50			
		0.050	7.0	3.33	3.00			
TNB	SDS	0.035	4.5	3.83	2.61	1200 ± 100	0.05-015	5.00
		0.020	2.0	5.15	1.94			
		0.050	7.0	2.22	4.50			
TNT	SDS	0.035	4.5	2.66	3.76	2450 ± 30	0.08-0.17	2.90
		0.020	2.0	4.61	2.17			
		2.0% (v/v)	27.0	1.80	5.58			
TNB	Triton X-100	1.4% (v/v)	13.8	1.88	5.32	65 ± 10	0.01-0.04	57
		1.0% (v/v)	7.0	2.16	4.62			
		0.044	7.0	1.98	5.05			
TNB	CTAB	0.031	4.9	2.41	4.15	3900 ± 150	0.20-0.85	1.80
		0.018	2.7	3.87	2.58			

[a]Concentration of the micelles is calculated using Eq. (3). The values of 0.008 M, 0.001 M and 0.54% (v/v) are taken for cmc's for SDS, CTAB and Triton X-100, while values of 60, 61 and 10 are taken for the aggregation numbers respectively.
[b]$Q_{1/2}^{app}$ is the concentration of the quencher needed to reduce the original intensity to half of its value.

ing solution with oxygen-free nitrogen at 40°C ensured complete micellization of H_2TPP.

The nitroarenes were micellised by the following procedure: To a solution of nitroarene (10 mg) in dichloromethane (5 ml) was added the surfactant solution (25 ml) of the required concentration and the resultant solution allowed to evaporate with continuous purging of O_2-free N_2 gas. To ensure complete and uniform (micellization) the mixture was sonicated in pulses of 2 and 4 sec prior to recording the emission spectra.

Steady-state fluorescence quenching method was employed. The micellar solutions were excited at the soret band of H_2TPP (416 nm) and the emission intensity at 652 nm was monitored in all these studies. The changes in the emission intensity of the fluorophore on increasing addition of the micellized quenchers at ambient temperatures (25°C) were monitored.

Results and Discussion

Typical spectra of singlet emission quenching are shown in Fig. 1. Micellar solutions of the nitroaromatics do not show any absorption or fluorescence in the region of investigation. The absorption spectra of the micellar solutions containing H_2TPP and varying concentrations of nitroaromatic compounds do not show any significant change in the absorbance values of the soret and Q bands

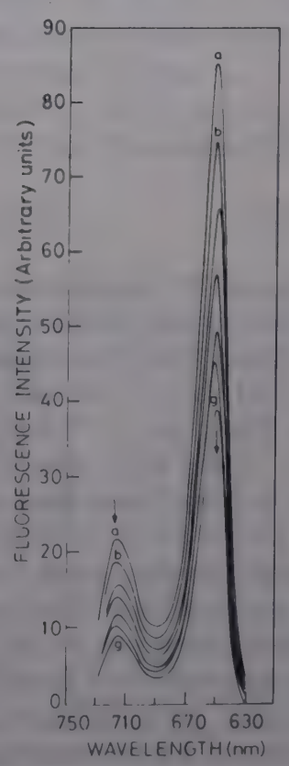

Fig. 1—Singlet emission spectra of (a) H_2TPP (4.2×10^{-8} M) in the presence of various concentrations of TNB (b to g: 4.0×10^{-5} M to 4.0×10^{-4} M) in SDS medium (0.05 M)

of the porphyrin, indicating possible absence of ground state complexes in these systems. Addition of acceptors to H_2TPP does not lead to any broadening of the fluorescence band of H_2TPP

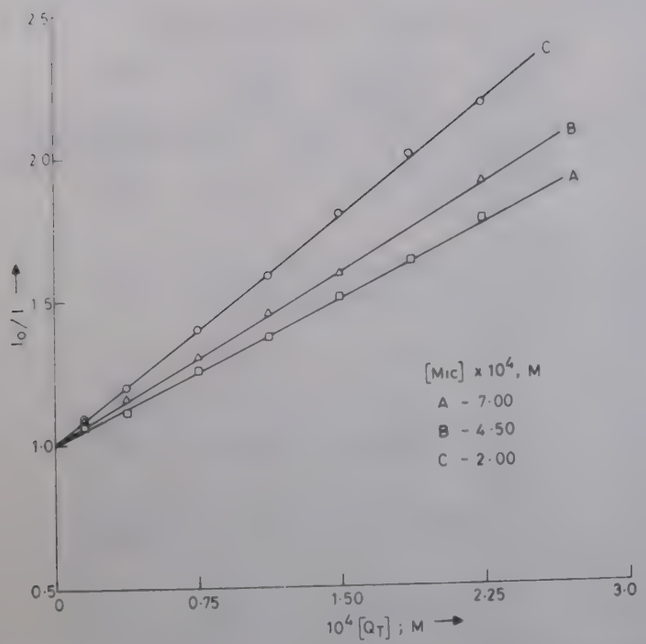

Fig. 2—Stern-Volmer plots of the singlet emission quenching of H_2TPP by TNB in SDS

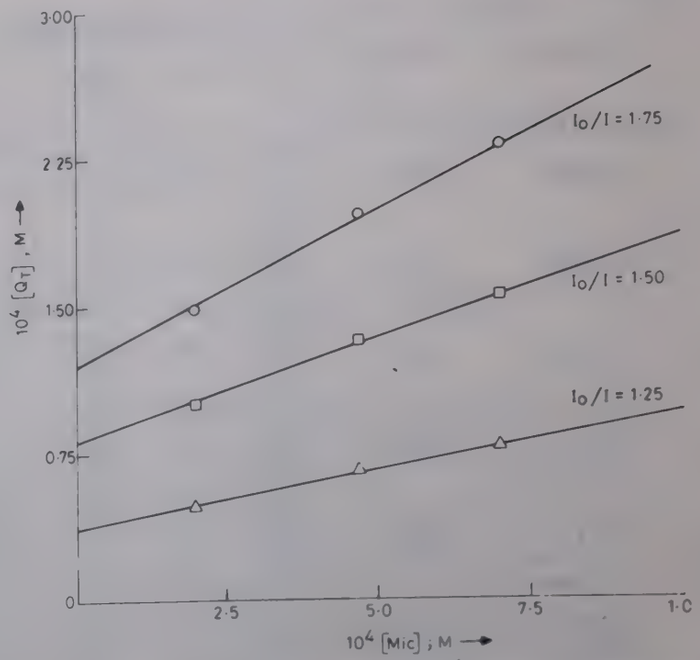

Fig. 3—Plots of $[Q]_T$ versus [Mic] at different I_0/I values for the singlet emission quenching of H_2TPP by TNB in SDS

showing the absence of formation of exciplexes. It seems reasonable to assume that the quenching of singlet emission of H_2TPP by nitroaromatic proceeds predominantly via electron transfer process (*vide infra*).

The process of quenching is found to follow the Stern-Volmer relation,

$$I_0/I = 1 + K_{SV}^{app}[Q]_T \qquad \ldots (1)$$

where I_0 and I are the steady state luminescence intensities in the absence and presence of acceptors respectively, K_{SV}^{app} is the apparent Stern-Volmer constant, and $[Q]_T$ is the analytical quencher concentration. The plots of I_0/I against the $[Q]_T$ are linear (Fig. 2) and K_{SV}^{app} values have been calculated (Table 1) from linear least square analysis of such plots. The linearity of these plots suggests negligible contribution from static quenching[13,14]. It is pertinent to mention here that the concentration of the quenchers employed in the present study does not lead to saturation. It is evident that an increase in micellar concentration decreases the K_{SV}^{app} values (Fig. 2). These data have been useful in the description of partition equilibria of the systems. The quenching constants obtained in the micellar systems are much larger (10^3) and are orders of magnitude higher than those obtained in homogeneous media[15]. The higher magnitudes of the quenching constants arise by the use of analytical quencher concentrations (Fig. 2) instead of using concentrations of the acceptors that are actually present in the micellar ensemble. The latter will be altogether different from the total concentrations, as the organized assemblies are known to partition the solubilizates. The solubilization dynamics in micellar systems can be represented according to Yeka *et al.*[16] by Scheme 1. It can be seen that the extent of quenching bears a relationship with the number of quencher molecules in the micelles[17]. A realistic estimate of quenching constants can be obtained using the true concentrations of the quenchers. The latter can be determined from the partition equilibria of the acceptor molecules distributed in aqueous phase and micellar pseudophase. In the present studies a concentration ratio, $[P]/[Mic] = 10^{-4}$ is employed. It is found that the emission intensity of micellized fluorophore reaches a maximum even at a lower concentration ratio of 10^{-4}. These two observations assure complete micellization of the fluorophore. The partition constants of the quencher molecules can be determined by a number of methods, viz. conductometry, elastic and quasi-

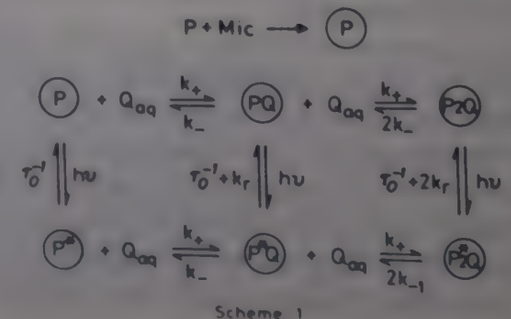

Scheme 1

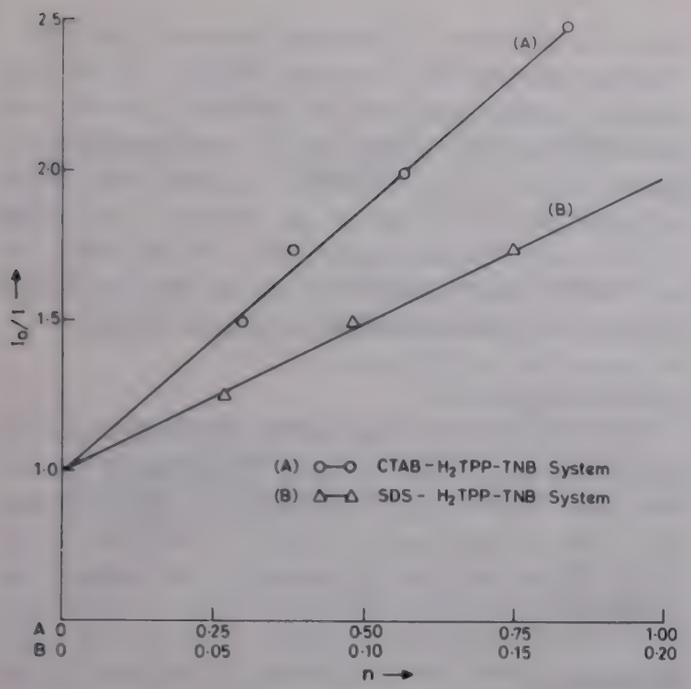

Fig. 4—Plots of fluorescence intensity ratio (I_0/I) versus average number of quencher molecules per micelle ($\bar{n}$)

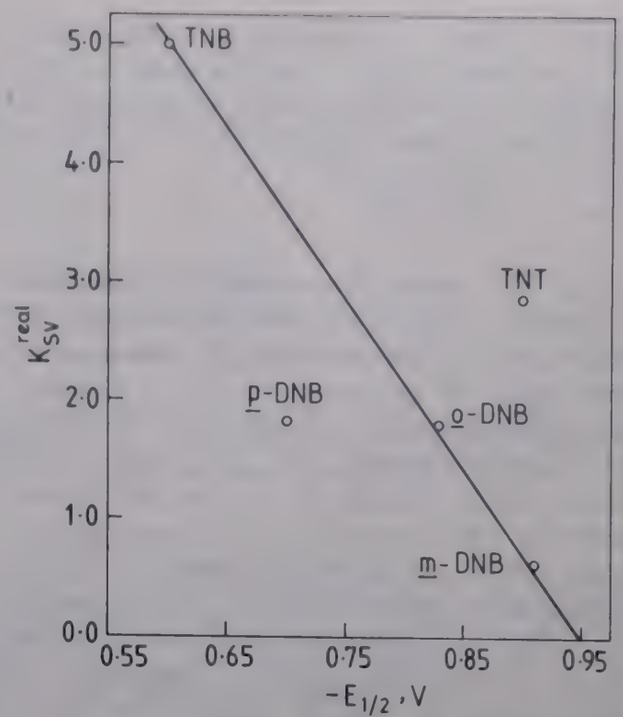

Fig. 5—Plot of K_{SV}^{real} values of singlet emission quenching of H_2TPP versus reduction potentials of the acceptors in SDS micelles

elastic light scatterings, gas chromatographic techniques, laser flash photolysis and life-time measurements. In the present study, we employed the fluorescence quenching method to obtain the partition constants of the quencher molecules since this method is independent of the fluoroprobe and does not require the life-time measurements[18–21] The quenching in micellar systems can be represented by Eq. (2).

$$Q_{aq} + Mic \rightarrow Q_{Mic} \quad \ldots (2)$$

where Q_{aq} and Q_{Mic} are the concentrations of the quencher in aqueous and micellar phases respectively, and the Mic is the concentration of the micelles. The latter can be calculated using Eq. (3).

$$[Mic] = \frac{[\text{Surfactant}]\text{-cmc (critical micelle concentration)}}{\text{Aggregation number (N)}} \quad \ldots (3)$$

The aggregation number (N) of the different surfactant, SDS, CTAB and Triton X-100, employed in the present studies was evaluated by Eq. (4) using the singlet emission quenching of H_2TPP by nitroaromatic acceptors.

$$\text{Ln}(I_0/I) = \frac{[Q]_T N}{([\text{Surfactant}]\text{-cmc})} \quad \ldots (4)$$

In Eq. (4) $[Q]_T$ is the total concentration of the quencher. The values calculated are found to be 60, 61 and 10 for SDS, CTAB and Triton X-100, respectively. These values are in close agreement with those reported by Fendler[3]. At present, it is difficult to assign any reason for low value of N for Triton X-100.

The constant K can be represented by Eq. (5)

$$K = [Q]_{Mic}/[Q]_{aq}[Mic] \quad \ldots (5)$$

The total concentration of the quencher that reduces the fluorescence intensity in a fixed proportion can be related to [Mic] by Eq. (6)

$$[Q]_T = \bar{n}/K + \bar{n}[Mic] \quad \ldots (6)$$

where $\bar{n}$ is the number of quencher molecules per micelle.

The K and $\bar{n}$ values, given in Table 1, are evaluated from the linear least square analysis of the linear plots of $[Q]_T$ versus [Mic] at different values of I_0/I (Fig. 3). It can be shown that the concentration of the micellized quencher is the product of $\bar{n}$ and [Mic]. It is observed that the values of K are independent of $\bar{n}$ values but are dependent on the nature of micelles and follow the order: CTAB > SDS > Triton X-100. This dependency of K on the nature of micelles can be rationalised in terms of ion-dipole interactions of the micellar phase with the quencher molecules. It is expected that cationic CTAB will enhance the binding of nitroaromatics since oxygens of the nitro groups bear partial

negative charge. It is possible to estimate the real S−V constants (K_{SV}^{real}) from the data, as K_{SV}^{real} is related to the average number of quencher molecules in the micelle by Eq. (7).

$$I_0/I = 1 + K_{SV}^{real}.\bar{n}[Mic] \quad \ldots (7)$$

The K_{SV}^{real} values, determined from the plots of I_0/I versus $\bar{n}$ (Fig. 4) are presented in Table 1. It is worthwhile to point out that K_{SV}^{real} values are of the same order of magnitude as those obtained in homogeneous media and are found to vary with the micellar system in the order: Triton X-100 > SDS > CTAB. In order to arrive at quenching rate constants, k_r, in these systems, we made use of the known life-times of H_2TPP in homogeneous medium, i.e. 15.7 ns in benzene[22]. The values of k_r obtained in this manner though are not strictly valid permit a comparison of the relative order of rates in different micelles. The magnitudes of k_r decrease in the order: Triton X-100 (3.64×10^9 s^{-1}) > SDS (0.32×10^9 s^{-1}) > CTAB (0.11×10^9 s^{-1}). An explanation for this could be traced to the different magnitudes of binding constants of quenchers to the micellar phase. An increase in binding constant should restrict the movement of quencher molecules to the micelles thereby decreasing the access of quencher molecules to fluorophore situated in the hydrophobic interior.

We examined the different mechanisms of quenching of the singlet emission of H_2TPP by nitroaromatic acceptors. The possibility of energy transfer as one of the mechanisms in these systems is ruled out, since (i) the narrow fluorescence bands of H_2TPP appear in the presence of varying amounts of nitroaromatic acceptors and (ii) the visible absorption band of the acceptors and the emission band of the H_2TPP are separated by more than 200 nm. Excited state electron transfer as a possible mechanism of singlet emission quenching in these systems is supported by the fact that K_{SV}^{real} values bear a linear dependence with reduction potentials of the acceptors (Fig. 5). It is possible to estimate oxidation potential of the couple $^1H_2TPP^*/H_2TPP^+$ in SDS micelles from the intercept on $E_{1/2}$ axis of Fig. 5. A value of 0.95 V (versus SCE) for the above couple is close to that of the computed value of 0.91 V. The latter is obtained from the $E_{1/2}$ values of the respective couples $P/P^{+\cdot}$ and $A/A^{-\cdot}$ and the singlet excitation energy in homogeneous medium.

The polarity of the medium is known to influence the efficiency of electron transfer reactions. It is observed that the emission maxima of the porphyrins remain unaltered in different micellar media implying that variation of micropolarities of the media has very little effect. Attempts to detect light-induced ESR signals in solutions containing H_2TPP and nitroaromatics have so far been unsuccessful which otherwise would have validated the electron transfer mechanism in the system.

Acknowledgement

The authors are thankful to the Department of Atomic Energy, Bombay and Department of Science and Technology, New Delhi for financial support. One of the authors (VHR) is thankful to the UGC, New Delhi for the award of a research associateship.

References

1 Kalyanasundaram K, *Photochemistry in microheterogeneous systems*, (Academic Press, New York) 1986.
2 Creed D & Caldwell R A, *Photochem Photobiol*, **41** (1985) 715.
3 Fendler J H, *Membrane mimetic chemistry* (Wiley, New York) 1982.
4 Fendler J H, *Ann Rev Phys Chem*, **35** (1984) 137.
5 Fendler J H, *J phys Chem*, **89** (1985) 2730.
6 Schemell R H & Whitten D G, *J phys Chem*, **85** (1981) 3473.
7 Droupadi P R & Krishnan V, *Photochem Photobiol*, **39** (1984) 161.
8 Rothemund P & Menotti A R, *J Am chem Soc*, **63** (1941) 267.
9 Barnett G H, Hudson M F & Smith K M, *Tetrahedron Lett*, (1973) 2887.
10 Vogel AI, *Practical organic chemistry* (Longmans Green & ELBS, London) 1968.
11 Hanumantha Rao V & Krishnan V, *Inorg Chem*, **24** (1985) 3538.
12 Kano K, Yoshiyuki Ueno, Keisuke Umakoshi, Shizunobu Hashimoto, Tasuo Ishibashi & Teiichiro Ogawa, *J Phys Chem*, **88** (1984) 5087.
13 Atik S S & Singer L A, *Chem Phys Lett*, **59** (1978) 519.
14 Zimiecki H W, Holland R & Cherry W R, *Chem Phys Lett*, **75** (1980) 145.
15 Chandrasekhar T K & Krishnan V, *Inorg Chem*, **20** (1981) 2782.
16 Yekta A, Aikawa M & Turro N J, *Chem Phys Lett*, **63** (1979) 543.
17 Almgren M & Loforth J E, *Coll Interface Sci*, **81** (1981) 486.
18 Encinas M V & Lissi E A, *Chem Phys Lett*, **91** (1982) 55.
19 Abuin E B & Lissi E A, *J Coll Interface Sci*, **95** (1983) 198.
20 Blatt E, Chatelier R C & Sawyer W H, *Chem Phys Lett*, **108** (1984) 397.
21 Blatt E, Chatelier R C & Sawyer W H, *Photochem Photobiol*, **39** (1984) 477.
22 Harriman A & Hosie R J, *J Chem Soc, Faraday Trans-2*, (1981) 1695.

Indian Journal of Chemistry
Vol. 27A, December 1988, pp. 1021-1024

Mechanism of Solidification of Binary Naphthalene-Benzoic Acid Eutectic System

P S BASSI*†, B L SHARMA, N K SHARMA & SHIV KUMAR
Department of Chemistry, University of Jammu, Jammu 180 004

Received 27 *July* 1987; *revised* 14 *March* 1988; *accepted* 30 *March* 1988

The nonideal character of binary naphthalene-benzoic acid eutectic system is ascertained from its ideal solid-liquid equilibrium data and the excess thermodynamic functions G^E and S^E. The behaviour of this system has been investigated by spontaneous crystallization, unidirectional velocity of solidification, viscosity measurements and microscopic studies.

The eutectic composites have considerable industrial importance[1]. While nonfaceted-nonfaceted (nf/nf) eutectic composites have been extensively investigated, the faceted-nonfacted (f/nf) class of eutectic composites have received comparatively lesser attention. But very little attention has been paid to the facted-faceted (f/f) eutectic composites. Presently, we have explored the nature, mechanism of solidification and structures both in the solid and liquid phases of f/f naphthalene-benzoic acid eutectic system.

Materials and Methods

Naphthalene (BDH) was purified by repeated sublimation (m.p. 353.5K). Benzoic acid (BDH, AR, m.p. 394.40K) was used as such. The solid-liquid equilibrium diagram for naphthalene-benzoic acid system and its spontaneous crystallization[2], linear velocity of crystallization[3] and the viscosities of the eutectic, pre-, post- and non-eutectic melts were measured by the methods reported earlier[4]. The microscopic studies were carried out using a polarising microscope.

Results and Discussion

The ideal liquidus temperatures (T's) at different compositions of naphthalene (x_i^l) were calculated from Eq. (1)[5], assuming that the naphthalene-benzoic acid system behaved ideally, i.e. activity coefficient, $\gamma_i^l = 1$. The value of heat of fusion, $\Delta_f H_i^0$ of component x_i^l ($i = 1,2$) used in the aforementioned calculation depends upon whether the mixture is rich in component x_1^l or x_2^l with the temperature of melt T_1^0 or T_2^0. Curve II in Fig. 1 represents the ideal phase diagram of this system and curves III and IV represent the temperatures of spontaneous crystallization and thaw points respectively. The eutectic composition is found at 0.6710 mol fraction of naphthalene with a temperature of melt 342.30 K. The excess thermodynamic functions, free energy and entropy of mixing at the temperature T and constant pressure were determined[6,7] using Eqs. (2) and (3) and the data are provided in Table 1.

$$-\ln x_i^l \gamma_i^l = \frac{\Delta_f H_i^0}{R}\left[\frac{1}{T} - \frac{1}{T_i^0}\right] \quad \ldots (1)$$

$$G^E = RT[x_1^l \ln \gamma_1^l + x_2^l \ln \gamma_2^l] \quad \ldots (2)$$

$$S^E = -R[x_1^l \ln \gamma_1^l + x_2^l \ln \gamma_2^l] \quad \ldots (3)$$

The ideal phase diagram (curve II, Fig. 1) and the excess thermodynamic functions G^E and S^E show that naphthalene-benzoic acid binary system deviates from the ideal behaviour. The excess free energy (G^E) is minimum for the mixture at the eutectic composition (Table 1) which is due to the reason that the eutectic composite has the lowest freezing point; whereas as expected, S^E is maximum at the eutectic composition, since at the eutectic composition there are three phases, viz. two solid phases and one liquid phase in equilibrium. Hence the molecular distribution at the eutectic composition is more probable than that in any other mixture of naphthalene-benzoic acid system.

As is evident from Table 2 the ΔS_m values of naphthalene and benzoic acid differ appreciably but for the mixtures these values should be higher by an amount contributed by the entropy of mixing (Table 1) in the melt, yet the ratio $\Delta T/T_m$ for the mixtures is nearly constant and also the crystallographic factor ξ approaches unity (Table 2). It follows that a definite relationship exists between

†Present address: Department of Chemistry, Guru Nanak Dev University, Amritsar

Table 1—Excess Thermodynamic Functions

Temp T_m(K)	Mol fr of naphthalene	$G^E \times 10^{-2}$ (kJ mol^{-1})	$S^E \times 10^{-4}$ (kJ mol^{-1} K^{-1})
390.50	0.1	28.73	−07.34
383.40	0.2	31.47	−08.20
376.40	0.3	34.25	−09.08
368.80	0.4	36.09	−09.80
358.20	0.5	31.64	−08.83
345.80	0.6	18.70	−05.44
342.30	0.6710(E)	12.67	−03.77
343.20	0.7	18.59	−05.44
347.30	0.8	38.35	−10.88
351.00	0.9	37.09	−10.47

E = Eutectic composition

Table 2—Heterogeneous Nucleation Data

Mol fr of naphthalene	$\Delta S_m \times 10^{-3}$ of nucleating phase (kJ mol^{-1} K^{-1})	$\xi = T_c/T_m$	$\Delta T/T_m$
0.0000	43.74	0.95	0.046
0.0963	43.74	0.95	0.046
0.1994	43.74	0.95	0.047
0.3003	43.74	0.95	0.053
0.3985	43.74	0.94	0.054
0.4887	43.74	0.94	0.057
0.5908	43.74	0.94	0.057
0.6968	54.04	0.96	0.036
0.7898	54.04	0.98	0.024
0.9029	54.04	0.98	0.022
1.0000	54.04	0.98	0.016

Table 3—Linear Velocity of Crystallization(V) at $\Delta T = 9.10$ K

Mol fr of naphthalene	$V \times 10^{-2}$ (cm s^{-1})
0.0000	87.50
0.5699	05.90
0.6710	192.30
0.7696	26.10
1.0000	15.70

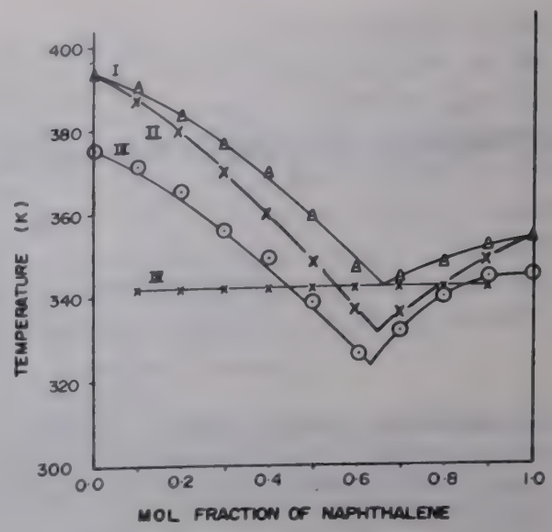

Fig. 1—Diagrams of state and undercooling for naphthalene-benzoic acid system [(I) Melting points; (II) ideal temperatures; (III) temperatures of spontaneous crystallisation; and (IV) thaw points]

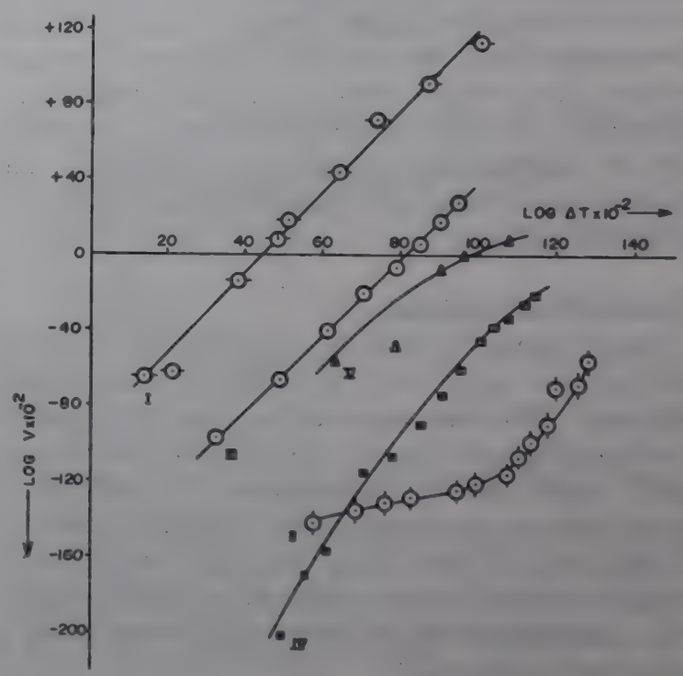

Fig. 2—Linear velocity of crystallisation for naphthalene-benzoic acid system at various degrees of undercooling [(I) Pure naphthalene; (II to IV) pre-eutectic, eutectic and post-eutectic samples containing 0.5699, 0.671 and 0.7696 mol fraction of naphthalene, respectively; and (V) pure benzoic acid]

nucleation (determined from the limit of undercooling) and the structure of the melt (determined from the entropy of fusion) and hence this observation verifies the nucleation theory.

The data for linear velocity of crystallization for eutectic, pre-, post-, and non-eutectic materials obey Eq. (4).

$$V = K(\Delta T)^n \qquad \ldots (4)$$

In Eq. (4), V is the velocity of crystallization and K and n are constants. The velocity of crystallization for the mixture at the eutectic composition shows anomalous behaviour (Fig. 2) which can be expected because of dimer character of benzoic acid. For the mixtures other than the eutectic, the velocity of crystallization decreases when one pure component is gradually added to the other. The data in Table 3 indicate that the velocity of crystallization of the eutectic composite is much higher than those of the pre-, post-, and non-eutectic materials for fixed undercooling ($\Delta T = 9.10$ K) indicating that the growth of the component is governed by a diffusion-controlled process[8].

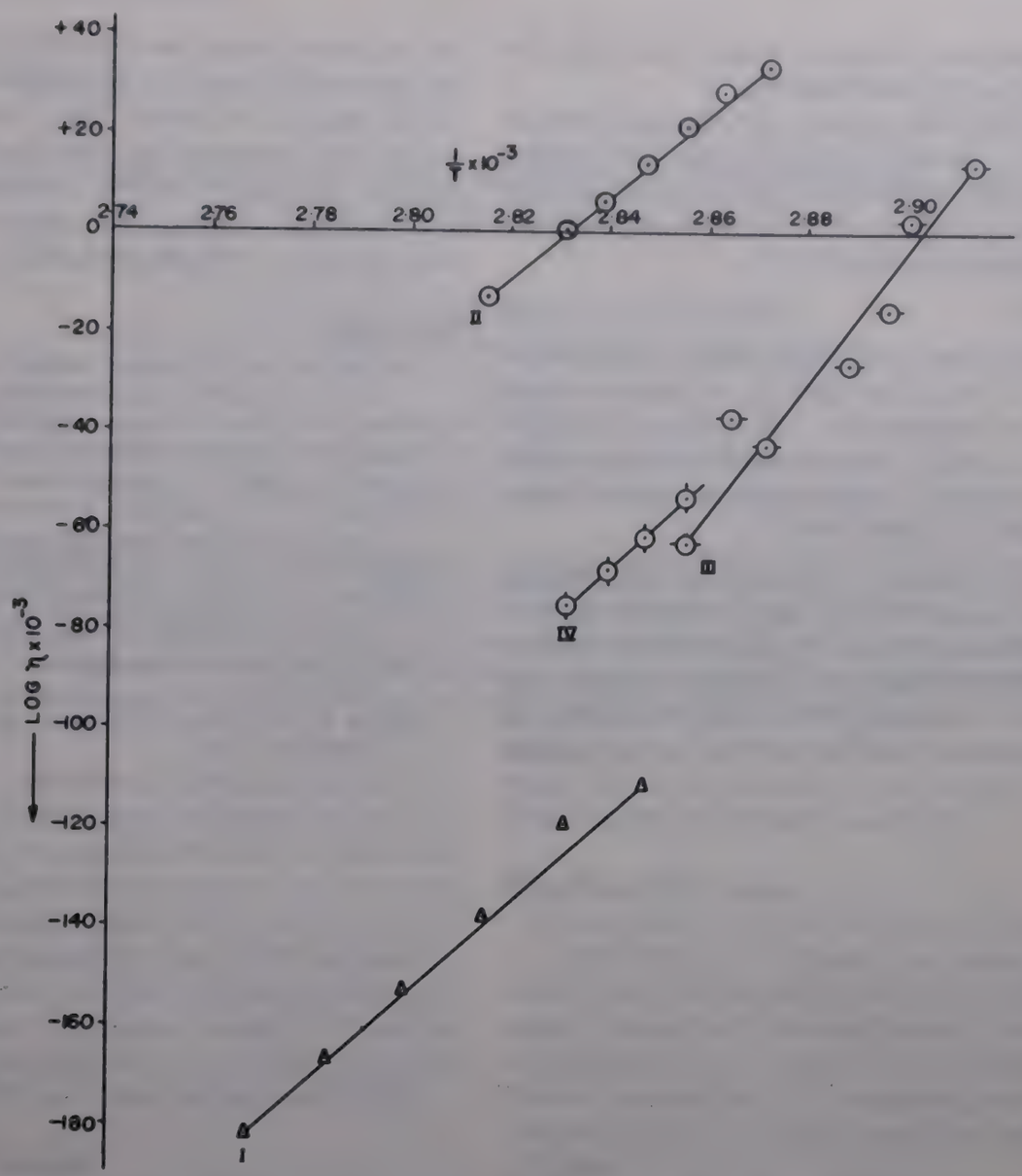

Fig. 3—Plots of log η versus 1/T for naphthalene-benzoic acid system [(I) Pure naphthalene; and (II to IV) pre-eutectic, eutectic and post-eutectic samples containing 0.5701, 0.6671 and 0.7678 mol fraction of naphthalene, respectively]

Though the velocity of crystallization for the eutectic melt is much higher, the components cannot escape the influence of each other while growing from the melt as has been observed in microstructure of solid eutectic.

Microscopic studies reveal that the solid separating out from the eutectic melt has entirely different structure from those of its constituent phases. The solid structures of the mixtures were found to be opaque. Growth of the two phases is quite interdependent and cross-diffusion, ahead of the interface, is required to sustain the growth process. Neither phase can escape the influence of the other and the normal dendrite growth is prevented. The microstructure of the eutectic composite of naphthalene-benzoic acid is faceted-faceted (f/f) which is in accordance with the Jackson and

Table 4—Activation Energy and Viscosity Data

Mol fr of naphthalene	Temp. (K)	Viscosity, η (cp)	$E_{vis} \times 10^{-6}$ (kJ mol^{-1})
1.0000	350.20	0.7850	
	353.20	0.7582	16.90
	357.20	0.7009	
	361.20	0.6568	
0.5701	348.20	1.0791	
	350.20	1.0509	16.76
	352.20	1.0148	
	354.20	0.9844	
0.6670(E)	344.20	1.0070	
	346.20	0.9388	25.54
	348.20	0.9036	
	350.20	0.8635	
0.7678	349.20	0.9152	
	350.20	0.8839	17.42
	352.20	0.8507	
	353.20	0.8392	

Hunt hypothesis[9]; since α values for both the components are greater than two.

At 350.20K, the viscosity is minimum (0.8635 cp) for the mixture at the eutectic composition (Table 4). The viscosities of pure components and various other mixtures were determined as a function of temperature using Eq. (5).

$$\eta = \eta_0 e^{E_{vis}/RT} \quad \ldots (5)$$

Log η values for any composition were plotted against 1/T (Fig. 3) to find the activation energy (E_{vis}) for that composition. The activation energies are given in Table 4. It is found that the activation energy is maximum for the mixture at the eutectic composition (25.5436 kJ mol^{-1}).

The lower value of viscosity at the eutectic composition indicates that the specific interactions are insignificant whereas the higher value of activation energy predicts the structural changes occurring in the eutectic melt, which may comprise of microregions or clusters rich in one component or the other. Hence two factors are contributing to the activation energy for the eutectic liquid: (i) activation energy for viscous flow, and (ii) energy required for breaking the clusters. The clustering number decreases with rise in temperature, and at a temperature when all the clusters have broken, only first factor will contribute to E_{vis}.

References

1 Paul Hagenmuller, *Preparative methods in solid state chemistry* (Academic Press, London) 1972, pp. 367.

2 Rastogi R P & Bassi P S, *J phys Chem*, **68** (1964) 2398.

3 Rastogi R P & Chatterji A C, *J phys Chem*, **59** (1955) 1.

4 Sharma B L & Bassi P S, *Indian J Chem*, **23A** (1984) 303.

5 Kirkwood J G & Oppenheim I, *Chemical thermodynamics* (McGraw-Hill, New York) 1961, pp. 120.

6 Nigam R K & Dhillon M S, *Indian J Chem*, **8** (1970) 614.

7 Prigogine I & Defay R, *Chemical thermodynamics* (Longmans Green, London) 1954, pp. 381.

8 Singh N B & Singh Narsing Bahadur, *J Crystal Growth*, **28** (1975) 267.

9 Jackson K A & Hunt J D, *Trans Met Soc AIME*, **236** (1966) 843, 1129.

Indian Journal of Chemistry
Vol. 27A, December 1988, pp. 1025-1027

Effect of *p*H, Urea, EDTA & Deoxycholate on Metachromasia Induced by Heteropolyanions

SHYAM NARAIN RAM, K D S YADAV* & B SHARMA
Department of Chemistry, University of Gorakhpur, Gorakhpur 273 009
and
CHANAN SINGH
Division of Biochemistry, Central Drug Research Institute, Lucknow 226 001

Received 21 *August* 1987; *revised* 18 *February* 1988; *accepted* 14 *March* 1988

Phosphomolybdic acid, phosphotungstic acid and silicotungstic acid as chromotropes, have been found to induce metachromatic effect in toluidine blue. These chromotropes produce stronger metachromatic effect than that by some well known chromotropes including isopolyacids excepting inorganic polyphosphates. The metachromatic effect increases with increasing [heteropolyanion]:[dye] ratio. The formation of the metachromatic complexes has been found to be suppressed by urea, EDTA and deoxycholate. Amongst these, EDTA is the most potent reagent followed by deoxycholate and urea. Effect of *p*H on the metachromatic effect has also been studied.

Metachromasia produced in toluidine blue by various types of chromotropes including inorganic isopolyacids and polyphosphates has been studied earlier[1-3]. Metachromatic property of this dye with heteropolyanions has been also reported[4]. The present investigation deals with the adverse effect of *p*H, urea, EDTA and deoxycholate on the metachromatic complexes formed by toluidine blue with phosphomolybdic acid (PMA), phosphotungstic acid (PTA) and silicotungstic acid (STA).

Materials and Methods

PTA, STA, PMA (E. Merck), urea (BDH), EDTA and deoxycholate (IDPL) were used as such without further purification. Toluidine blue (E. Merck) was purified by a known method[5] and its purity was checked chromatographically.

An aqueous solution containing a heteropolyanion (PTA, PMA or STA) was added to 3 ml of the dye solution (3.3×10^{-4} *M*). The total volumeof the solution was made up to 7.0 ml by the addition of doubly distilled water. At higher ratio of heteropolyanion to dye, the complex tended to change gradually from blue to pink-violet. All the observations were made immediately after preparing the solution and a fixed dye concentration was used in all the experiments. For studying the effect of *p*H, urea, EDTA and deoxycholate on metachromatic complex, the dye and heteropolyanion concentrations corresponding to maximum complex formation were taken. To this was added a definite amount of urea (0.05 *M*, 0.1 *M*) or EDTA (0.5 *M*) or deoxycholate (0.5 *M*) and the final volume was made upto 7.0 ml with doubly distilled water. The spectra were recorded using a Perkin-Elmer spectrophotometer model-24.

Results and Discussion

The visible spectra of the dye, STA-dye, PMA-dye and PTA-dye complexes are shown in Fig. 1. For a given dye concentration of 1.4×10^{-4} *M*, the concentrations of heteropolyanions mentioned in the caption to Fig. 1 give maximum spectral shifts. Further increase in the concentrations of heteropolyanions does not bring about any further spectral shifts.

It is evident that the heteropolyanions STA, PMA and PTA are effective in inducing metachromasia in toluidine blue, the effect being hypochromacity coupled with hypsochromic shifts[1,6,7].

The effect of *p*H on metachromasia induced by STA, PMA and PTA is presented in Table 1. It is evident that the maximum metachromatic effect for PTA and STA is induced at the *p*H 5.6 whereas the *p*H value of 4.6 induces maximum metachromatic effect in the case of PMA.

Fig. 2 shows the urea titration profiles of the metachromatic complexes of PMA, PTA and STA with toluidine blue. The metachromatic complexes with PTA and PMA are completely suppressed by 5×10^{-2} *M* and 4.2×10^{-3} *M* urea respectively whereas 5×10^{-2} *M* urea is not sufficient to suppress the metachromatic complex formed by STA. This indicates that STA-dye complex is the most stable against urea followed by PTA-dye and PMA-dye complexes in that order.

The urea titration curves in Fig. 2 depict three

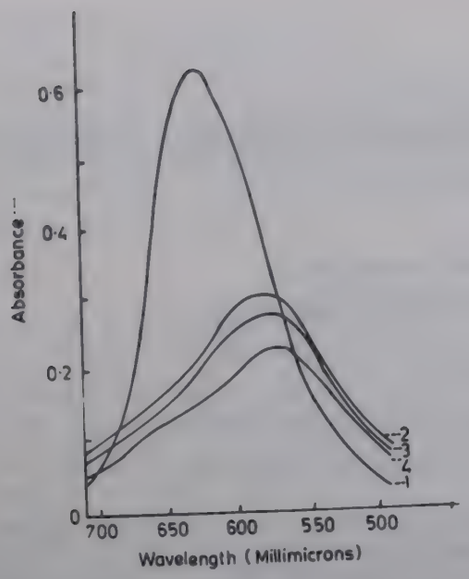

Fig. 1—Visible spectra of (1) toluidine blue in water (1.4×10^{-4} *M*), (2) STA (1×10^{-6} *M*) + toluidine blue, (3) PMA (1.5×10^{-5} *M*) + toluidine blue, (4) PTA (9.7×10^{-6} *M*) + toluidine blue

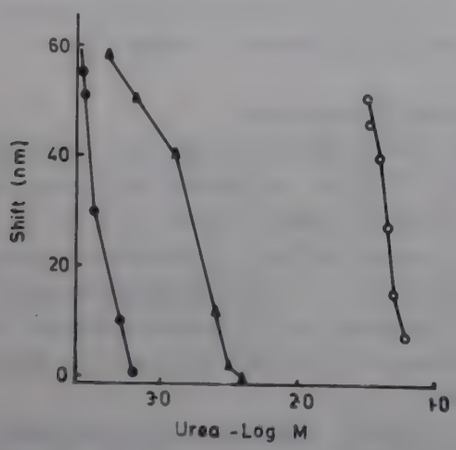

Fig. 2—Urea titration of metachromatic complexes of toluidine blue and heteropolyanions [–○– STA; –▲– PTA; –●–PMA]

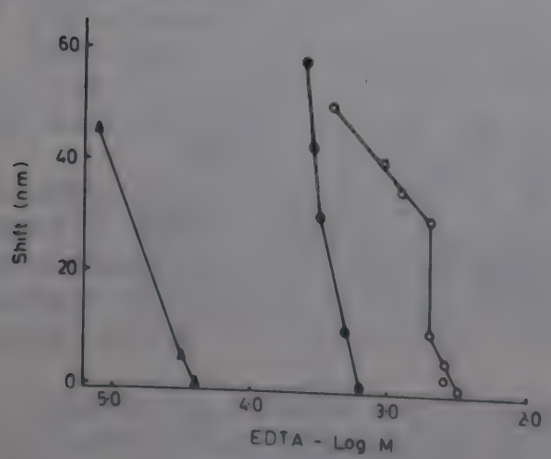

Fig. 3—EDTA titration of metachromatic complexes of toluidine blue and heteropolyanions [–○– STA; –●– PTA; –▲– PMA]

Table 1—Effect of *p*H on Toluidine Blue[b] Metachromasia Induced by Heteropolyanions[a] in the *p*H Range 3.6-7.0

Chromotropes	Conc. of chromotrope (*M*)	Buffer	*p*H	Shift (nm)
Phosphotungstic acid	9.7×10^{-6}	Acetate	3.6	40
		Acetate	4.6	42
		Acetate	5.6	48
		Phosphate	7.0	43
Silicotungstic acid	1.0×10^{-6}	Acetate	3.6	48
		Acetate	4.6	44
		Acetate	5.6	50
		Phosphate	7.0	40
Phosphomolybdic acid	1.5×10^{-5}	Acetate	3.6	35
		Acetate	4.6	43
		Acetate	5.6	40
		Phosphate	7.0	40

[a]Phosphotungstic acid, PTA; silicotungstic acid, STA; phosphomolybdic acid, PMA.
Acetate buffer: acetic acid/sodium acetate buffer = 0.01 *M*.
Phosphate buffer: disodium hydrogenphosphate/sodium hydrogen phosphate = 0.01 *M*.
[b][Toluidine blue] = 1.4×10^{-4} *M*.

sections in the case of STA-dye and PTA-dye complexes implying three types of bindings between the dye and the heteropolyanions. However, the metachromatic complex formed by the interactions of dye and PMA is too weak to demonstrate the three sections; only two sections are observed in this case.

Fig. 3 shows EDTA titration profiles of the metachromatic complexes of PMA, PTA and STA with toluidine blue. The EDTA titration profile of STA-dye complex depicts three sections implying three types of bindings between the heteropolyanion and the dye. PMA- and PTA-dye complexes are very sensitive towards the suppression by EDTA and only two sections are observed in the titration curves of their complexes.

The titration profiles of deoxycholate with PTA-dye and STA-dye complexes are shown in Fig. 4. In this case also, STA-dye complex exhibits three sections in the titration curve indicating three types of binding between the dye and the heteropolyanion. PTA-dye complex depicts only two sections indicating its sensitivity towards suppression by deoxycholate. PMA-dye metachromatic complex is too sensitive to demonstrate the titration curve.

The metachromatic shifts observed in these studies are of higher order than those previously reported for several other inducers[1-3,8,9].

The suppression of metachromatic reactions by

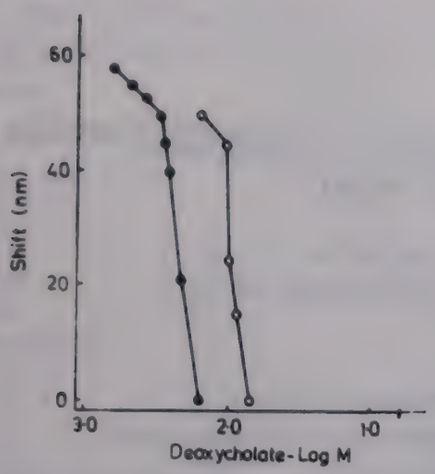

Fig. 4—Deoxycholate titration of metachromatic complexes of toluidine blue and heteropolyanions [—○— STA; —●— PTA]

urea is not due to disruption of the hydrogen bonds only which may or may not be involved in the formation of metachromatic complexes; the primary forces responsible for inducing metachromasia are electrostatic in nature[1-3,7]. The non-ionic/hydrophobic forces are likely to get involved in this phenomenon subsequently. The instability of these metachromatic complexes towards urea may be interpreted to mean that hydrophobic forces are playing a cardinal role in this phenomenon and once they get weakened by urea, the primary ionic forces are not able to maintain metachromasy.

EDTA dissociates the metachromatic complexes formed by the macroionic interactions of heteropolyanions and toluidine blue. It may be inferred, in analogy to behaviour of urea, that EDTA also acts by suppressing both ionic and hydrophobic forces involved. This property of EDTA is unrelated to its chelating action[10].

Deoxycholate also suppresses the metachromasia induced by heteropolyanions. This anionic detergent has already been shown[11] to dissociate a large variety of binary macroionic complexes including the suppression of metachromasia. It is more potent in comparison to urea. Such selective action against metachromasia has not been reported hitherto and such studies may have analytical potential of differentiating biomolecules.

Acknowledgement

The authors thank (late) Prof. S.C. Tripathi, Head of the Chemistry Department, University of Gorakhpur, Gorakhpur and Dr. M.M. Dhar, Director, CDRI, Lucknow for providing necessary facilities during the course of this investigation. Two of them (S N Ram, Senior Research Fellow and C Singh, Scientist Emeritus) are grateful to the CSIR, New Delhi for financial support.

References

1 Sylven B, *Quart J Micr Sci*, **95** (1954) 327.
2 Singh C, *Stain Technol*, **38** (1963) 103.
3 Kelly J W, *Stain Technol*, **31** (1956) 283; **33** (1958) 79.
4 Srivastava V K, Misra B B, Tripathi A M & Singh C, *Trans Met Chem*, **2** (1977) 106.
5 Pal M K & Schubert Maxwell, *J Am chem Soc*, **84** (1962) 4384.
6 Baker J R, *Principle of biological microtechniques: a study of fixation and dying* (Methuen, London), 1958, 243.
7 Bargeron J R & Singer M, *J Biophys Biochem Cytol*, **4** (1958) 433.
8 Singer M, *Internat Rev Cytol*, **1** (1952) 211.
9 Singh C, *Anal Biochem*, **38** (1970) 563.
10 Singh C, *Indian J Biochem Biophys*, **8** (1971) 45.
11 Singh C & Misra J, *Arzneim-Forsch*, **28** (1978) 1320.

Indian Journal of Chemistry
Vol. 27A, December 1988, pp. 1028-1030

Kinetics of Halogenation of Sulphacetamide & Sulphanilamide by Trichloroisocyanuric Acid

P S RADHAKRISHNAMURTI* & N K RATH
Department of Chemistry, Berhampur University, Berhampur 760 007
and
M YEDUKONDALU
College of Pharmaceutical Sciences, Berhampur 760 002

Received 25 *September* 1987; *revised* 19 *November* 1987; *accepted* 25 *January* 1988

Halogenation of sulphacetamide and sulphanilamide by trichloroisocyanuric acid (TCICA) in aqueous acetic acid-perchloric acid medium is pseudo-first order in [TCICA] and fractional order in $[H^+]$. The reaction is first order in [sulphanilamide] and fractional order in [sulphacetamide]. Change of dielectric constant of the medium has a marginal effect on the reaction rate. However, addition of NaCl enhances the rate in both the cases. A plausible mechanism has been suggested to account for the observed kinetics.

The kinetics of halogenation of substituted benzoic acids using a variety of halogenating agents like N-iodosuccinimide (NIS), chloramine-T (CAT) and trichloroisocyanuric acid (TCICA) have been studied in our laboratory[1-3]. In the present paper we report the results of investigations on the kinetics of chlorination of sulphacetamide and sulphanilamide by TCICA. To our knowledge this is the first systematic kinetic report on the use of TCICA as a chlorinating agent for sulpha drugs.

Materials and Methods

Sulphacetamide and sulphanilamide (Riedel) were recrystalised before use. TCICA (Fluka) was used as such. All other reagents used were of AR (BDH) grade, redistilled or recrystallised before use.

In the kinetic runs, disappearance of TCICA was followed iodometrically in acid medium. The rate constants computed were reproducible within $\pm 5\%$.

Stoichiometric runs employing $[TCICA] > [S]_0$ (e.g. $[TCICA] = 2 \times 10^{-3}$ to 4×10^{-2} mol dm^{-3}, $[S]_0 = 2 \times 10^{-4}$ to 5×10^{-4} mol dm^{-3} at $[HClO_4] = 0.5$ mol dm^{-3}) did not give meaningful results as the self-decomposition of TCICA under these conditions appreciably large.

Sulphacetamide gave 3-chlorosulphacetamide as the product and sulphanilamide gave 3-chlorosulphanilamide.

Results and Discussion

The salient features of the kinetic results are as follows:

(i) The reaction exhibits perfect pseudo-first order kinetics for more than four half-lives of TCICA disappearance as seen from the good linear plots of $\log [TCICA]_t$ versus time.

(ii) The pseudo-first order rate constant (k_{obs}) increases with increase in $[S]_0$ and $[H^+]$. The dependence of k_{obs} on [sulphacetamide] and $[H^+]$ is fractional each in the range studied; plots of $(k_{obs})^{-1}$ versus $[S]^{-1}$ or $(k_{obs}{}^{-1}$ versus $[H^+]^{-1}$ are linear with finite intercept on the $(k_{obs})^{-1}$-axis. However, the order in [sulphanilamide] is unity, probably due to the low equilibrium constant of the complex.

(iii) Increase in the percentage of acetic acid in the reaction medium (i.e. decreasing dielectric constant of the medium) has a marginal effect on the reaction rate at $[Cl^-]_{aq} = 0$. In the presence of Cl^-, k_{obs} increases significantly.

(iv) Increase in *p*H decreases the k_{obs} value in case of sulphanilamide. However, the reaction with sulphacetamide becomes very sluggish with increase in *p*H.

Structure and reactivity

Structural differences are responsible for the higher rate observed with sulphanilamide as compared to that with sulphacetamide (Tables 1 and 2). The pK_a values of sulphanilamide and sulphacetamide are 10.4 and 5.4 respectively and this clearly brings out the reasons for the higher reactivity of sulphanilamide. Application of Kendalls' treatment using the relation $\log B = H_0 - pK_a + \log B_0$ for these two substrates also shows higher reactivity for sulphanilamide. The relative acid independent rate constants computed are of the or-

Table 1 – Effect of Varying [TCICA], $[HClO_4]$, [S], Solvent, [NaCl] and Temperature on the Reaction Rate

Variations	$k_1 \times 10^2$ (min^{-1})	
	Sulphacetamide	Sulphanilamide
[TCICA] $\times 10^4$ (mol dm^{-3})		
1.25	2.77	8.75
2.50	2.49	7.63
5.00	2.12	7.60
[Substrate] $\times 10^2$ (mol dm^{-3})		
0.5	2.49	7.63
1.0	3.71	13.86
2.0	5.71	26.19
4.0	7.13	—
$[HClO_4] \times 10^2$ (mol dm^{-2})		
1.0	2.49	7.63
2.0	3.67	10.39
5.0	6.59	14.42
10.0	9.89	18.67
50.0	16.32	54.80
100.0	18.80	87.23
HOAc (v/v)		
40	2.99	9.29
50	2.49	7.63
60	2.44	7.96
70	3.77	7.046
Temperature (°C)		
35	2.49	7.63
40	3.90	9.19
45	5.00	14.70
[NaCl] $\times 10^4$ (mol dm^{-3})		
0.0	2.49	7.63
6.0	3.1	—
8.0	3.06	—
10.0	3.67	10.23
20.0	4.60	14.13

Table 2 – Arrhenius Activation Parameters at 308°K

	$E_a^{\neq}$ (kJ mol^{-1})	$\Delta H^{\neq}$ (kJ mol^{-1})	$\log_{10} A$	$\Delta S^{\neq}$ (J K^{-1} mol^{-1})
Sulphacetamide	99.0	96.5	12.18	4.89
Sulphanilamide	99.6	97.0	13.77	−2.45

der of 10^9 and 10^5 for sulphanilamide and sulphacetamide respectively.

Rate law and mechanism

The important steps in the present reactions are shown in Scheme 1.

Concentrations of monochloroisocyanuric acid (MCICA) and isocyanuric acid (ICA) would be negligible in acid medium as $(K_1K_2K_3)$ *and* (K_1K_2) are negligible as compared to K_1 (ref. 4). In the predominantly aqueous solution [HOCl],$[Cl^+]$ (ref. 5) and $[ClOOCCH_3]$ (ref. 6) would be negligible. If as a first approximation it is assumed that the TCICA species itself has a negligible contribution towards the overall halogenation rate and that the effective halogenating species are H_2OCl^+ in the absence of added Cl^- and $(H_2OCl^+ + Cl_2)$ in the presence of added Cl^-, then the rate laws (1) and (2), respectively can be derived from Scheme 1.

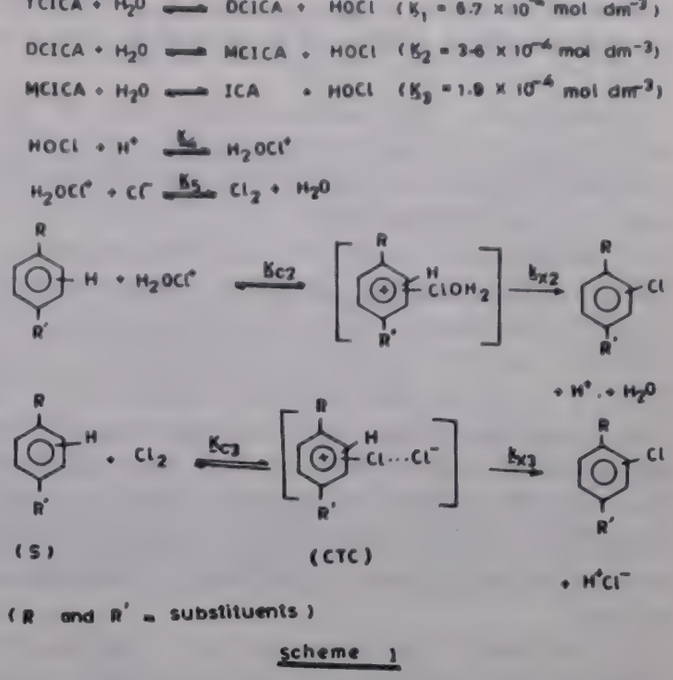
TCICA + H2O ⟶ DCICA + HOCl (K1 = 8.7 × 10⁻⁴ mol dm⁻³)
DCICA + H2O ⟶ MCICA + HOCl (K2 = 3.6 × 10⁻⁴ mol dm⁻³)
MCICA + H2O ⟶ ICA + HOCl (K3 = 1.8 × 10⁻⁴ mol dm⁻³)
HOCl + H⁺ ⟶ H2OCl⁺
H2OCl⁺ + Cl⁻ ⟶ Cl2 + H2O
+ H⁺ + H2O
+ H⁺Cl⁻
(S)
(CTC)
(R and R' = substituents)

Scheme 1

$$-\frac{d[TCICA]}{dt} = \text{Rate}$$

$$= \frac{k_{x2}K_{c2}K_1K_4[S][H^+][TCICA]}{([DCICA] + K_1 + K_1K_4[H^+])(1 + K_{c2}[S])} \quad \cdots (1)$$

$$= \frac{k_{x2}K_{c2}K_1K_4[S][H^+][TCICA]}{([DCICA] + K_1 + K_1K_4[H^+])(1 + K_{c2}[S])}$$

$$+ \frac{k_{x3}K_{c3}K_1K_4K_5[S][H^+][Cl^-][TCICA]}{([DCICA] + K_1 + K_1K_4K_5[H^+][Cl^-])(1 + K_{c3}[S])} \quad \cdots (2)$$

For the observed pseudo-first order disappearance of [TCICA] in the employed concentration range, if [DCICA] term in the denominator is small and negligible in comparison to other terms, Eqs (3) and (4) follow from Eqs (1) and (2) respectively.

$$k_{obs}(\text{at } [Cl^-]_{ad} = 0) = k_{H_2OCl^+}$$

$$= \frac{k_{x2}K_{c2}K_4[S][H^+]}{(1 + K_4[H^+])(1 + K_{c2}[S])} \quad \cdots (3)$$

$$k_{obs}(\text{at } [Cl^-]_{ad} = \text{finite}) - k_{obs}(\text{at } [Cl^-]_{ad} = 0) = k_{Cl_2}$$

$$\frac{k_{x3}K_{c3}K_4K_5[S][H^+][Cl^-]}{(1 + K_4K_5[H^+][Cl^-])(1 + K_{c3}[S])} \quad \cdots (4)$$

In Eqs)3) and (4) $k_{H_2OCl^+}$ and k_{Cl_2} represent the pseudo-first order rate constants due to H_2OCl^+ and Cl_2 respectively.

Although the mechanistic implications of observed kinetics of chlorination reaction using TCICA have been most plausibly explained, certain other factors need mention.

(a) Scheme 1 envisages the equilibrium interaction of (unprotonated) substrate(s) with the most effective chlorinating species in the medium, i.e. H_2OCl^+ in the absence of added Cl^- and $(H_2OCl^+ + Cl_2)$ in the presence of added Cl^-, to form a charge transfer (CT) complex which decomposes in a slow step to form the products. The formation of CT complexes of aromatic substrates with various electrophilic reagents in general, and with halogens in particular, is well documented[6].

(b) The amino derivatives might be significantly present in the protonated form in the $[H^+]$ range used. If the protonated form of the substrate (SH^+) were reactive the rate law (2) would have contained another $[H^+]$ term in the numerator and also the predominant product would have been a *meta*-chloro compound, but these are not observed experimentally. On the other hand if Scheme 2 (in which an N-chloro intermediate is formed[8] from SH^+ and the effective chlorinating species with the loss of H^+, as rapidly as it rearranges to a CT-complex) is considered as a representative sequence for the reaction of the amino derivative, rate law (5) could be derived by writing $[S]=[S]_0K_a/[H^+]$ where K_a is the proton dissociation constant of the conjugate acid (SH^+) of the amino derivative[9].

Scheme 2 leads to rate law (5).

$$k_{obs} = \frac{k_{x2}K'_{c2}K_rK_aK_4\,[H^+][S]_0}{(1+K_a[H^+])(1+[H^+]+K_aK_r[S]+K_aK_rK'_{c2}[S])} \quad \ldots(5)$$

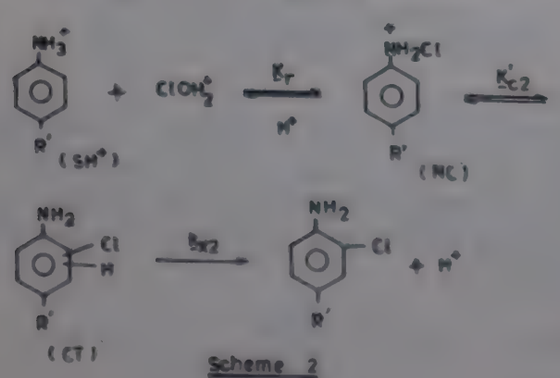

Scheme 2

Making an approximation that $([H^+]+K_aK_r[S]) << K_aK_rK'_{c2}[S] << 1$, ($K_r$ is a very small quantity in the $[H^+]$ and $[S]_0$ employed) Eq. (5) approximates to Eq. (3).

It is implied that these reactions pass through an activated state of CT complex arising essentially and effectively from the deprotonated SH^+ and the chlorinating species under consideration.

It is known that N-chloroanilines undergo rapid rearrangement[10], the N-chloro group attacking the nucleus leading to nuclear halogenated derivatives. Further the N-chloro intermediates would be very reactive under the conditions of the present study and would not have any built-in concentration, for Eq. (6) would operate otherwise,

$$R'C_6H_4NH(Cl) + 2I^- + H^+ \rightarrow R'C_6H_4NH_2 + I_2 + Cl^- \quad \ldots(6)$$

and the smooth kinetics could not have been followed by iodometry.

(d) The reactivity order for chlorination of these substrates is $Cl_2 > H_2OCl^+ >> HOCl$, which is more or less the general order observed for chlorination of aromatic substrates in aqueous acid media. The non-participation of Cl^+ (the unhydrated species) in chlorination reactions carried out in aqueous acid solutions has been discussed earlier[5].

References

1 Radhakrishnamurti P S & Panda B K, *Indian J Chem*, **22A** (1983) 770.

2 Radhakrishnamurti P S & Rath N K, *Indian J Chem*, **26A** (1987) 407-411.

3 Radhakrishnamurti P S & Mishra S A, Ph.D. Thesis (1983) Berhampur University.

4 Osaka Pharmaceutical Assoc. Osaka-Fu-Yaku Zasshi, **30** (1979) 39; Chem Abstr, **91** (1979) 157695g.

5 Swain C G & Crist D R, *J Am chem Soc*, **94** (1972) 3195.

6 *Comprehensive inorganic chemistry*, Vol 2, edited by J C Bailar, H J Emeleus, R Nyholm & A F T Dickenson (Pergamon, New York) 1973 Chap. 26.

7 Latimer W M, *Oxidation potentials* (Prentice Hall, New Jersey) (1961), p. 54.

8 Neale R S, Scheper R G & Walsh M R, *J org Chem*, **29** (1964) 3390; Haberfield P & Daxis Paul, *J Am chem Soc*, **87** (1965) 5502.

9 Meites L, *Hand book of analytical chemistry* (McGraw-Hill, London) 1963, Sec. 1, pp. 8, 20.

10 Haberfield P & Daxis Paul, *J org Chem*, **41** (1976) 3170; Gassman P G & Campbell G A, *J Am chem Soc*, **93** (1971) 2567; **94**, 3884, 3891.

Indian Journal of Chemistry
Vol. 27A, December 1988, pp. 1031-1034

Kinetics & Mechanism of Oxidation of Substituted Benzyl Alcohols by Sodium Bis[2-ethyl-2-hydroxybutanoato(2-)]oxochromate (V)

G SREELATHA, M PRASADA RAO, B SETHURAM* & T NAVANEETH RAO
Department of Chemistry, Osmania University, Hyderabad 500 007
Received 2 *November* 1987; *revised* 27 *February* 1988; *accepted* 21 *March* 1988

The kinetics of oxidation of benzyl alcohol and some substituted benzyl alcohols by sodium bis[2-ethyl-2-hydroxybutanoato(2-)]oxochromate (V) [Cr(V)] has been investigated in 25% (v/v) aq. acetic acid in the presence of perchloric acid. The order in [oxidant] and [substrate] is unity each. The rate of oxidation increases with increase in [2-ethyl-2-hydroxybutyric acid] (EHBA) and decreases with increase in percentage of HOAc and [H^+]. The order of reactivities is *p*-OMe > *m*-OMe > H > *p*-Br > *p*-Cl > *m*-Cl > *m*-NO_2. The Hammett's plot is linear with $\rho = -0.31$ ($r = 0.974$). A mechanism involving transfer of hydride ion from alcohol moiety to Cr(V) has been suggested to explain the kinetic results. Activation parameters have also been calculated and discussed.

It is well established that the most stable oxidation states of chromium are +3 and +6. Interest in the unusual and less stable oxidation states of various transition metal ions as oxidants, including chromium is of recent origin[1,2]. The preparation by Krumpolc and Rocek of several water soluble, air-stable carboxylato derivatives of chromium(V) has added yet another metal ion with unusual oxidation state. Sodium bis[2-ethyl-2-hydroxybutanoato(2-)]oxochromate (V) has been found to be the most stable of carboxylato derivatives[3], particularly in the *p*H range 2-4 and is found to act as one, two and also as a four-electron oxidant in the oxidation of vanadium(IV)[4], hydrazine[5] and hydroxylamine[6] respectively.

The present study is aimed at probing further the different aspects of Cr(V) oxidation of aromatic compounds, particularly those with hydroxyl function such as benzyl alcohols.

Materials and Methods

2-Ethyl-2-hydroxybutyric acid (EHBA, Aldrich) was recrystallized from benzene-hexane. Acetic acid was purified by the standard procedure. Benzyl alcohol (Fluka) and HClO4 (BDH) were used as such. Sodium bis[2-ethyl-2-hydroxybutanoato(2)]oxochromate(V) was prepared according to the reported method[3]. Stock solutions of Cr(V) were prepared in 1×10^{-3} mol dm^{-3} $HClO_4$ in the presence of 1×10^{-2} mol dm^{-3} EHBA, which formed a stable complex with Cr(V). Also EHBA did not undergo perceptible oxidation under the experimental conditions. Solutions were standardized iodometrically[7] as well as spectrophotometrically using the molar extinction coefficient of Cr(V) complex as 1.68×10^2 dm^3 mol^{-1} cm^{-1} at 510 nm (ref. 3). Since benzyl alcohols (BA) are insoluble in water, 25% (v/v) aq. acetic acid was used as the solvent. Acetic acid did not undergo any perceptible oxidation under the experimental conditions.

The reaction was initiated by the addition of requisite quantities of Cr(V) solution to the mixture of alcohol, acetic acid and $HClO_4$ after thermostating the two solutions separately for 30 min. The reaction was monitored by noting the absorbance of Cr(V) complex at 510 nm at regular time intervals using Carl-Zeiss VSU-2-P spectrophotometer. The *p*H of the solution within the range 2-4 was maintained by adding different amounts of $HClO_4$.

Under the conditions of [Cr(V)] ≫ [BA]in 25% (v/v) acetic acid medium, Cr(V) was allowed to react with benzyl alcohol and excess of oxidant was estimated. Values of Δ[Cr(V)]/Δ[BA] under different concentration ranges revealed 1:1 stoichiometry (substrate:oxidant). Benzaldehyde was characterised as the product of oxidation of benzyl alcohol. It was also noted that benzaldehyde did not undergo oxidation under the experimental conditions employed above.

No polymerisation was observed when acrylonitrile was added to the reaction mixture under nitrogen atmosphere indicating that free radicals were not formed during the course of the reaction.

Results and Discussion

Under the conditions of [alcohol] ≫ [Cr(V)] the plots of log $(a/a-x)$ versus time were linear, indicating first order dependence in [Cr(V)]. From the slopes of such plots the pseudo-first order rate constants (k_{obs}) were evaluated at different [Cr(V)] and were found to be non-variant. For example, under

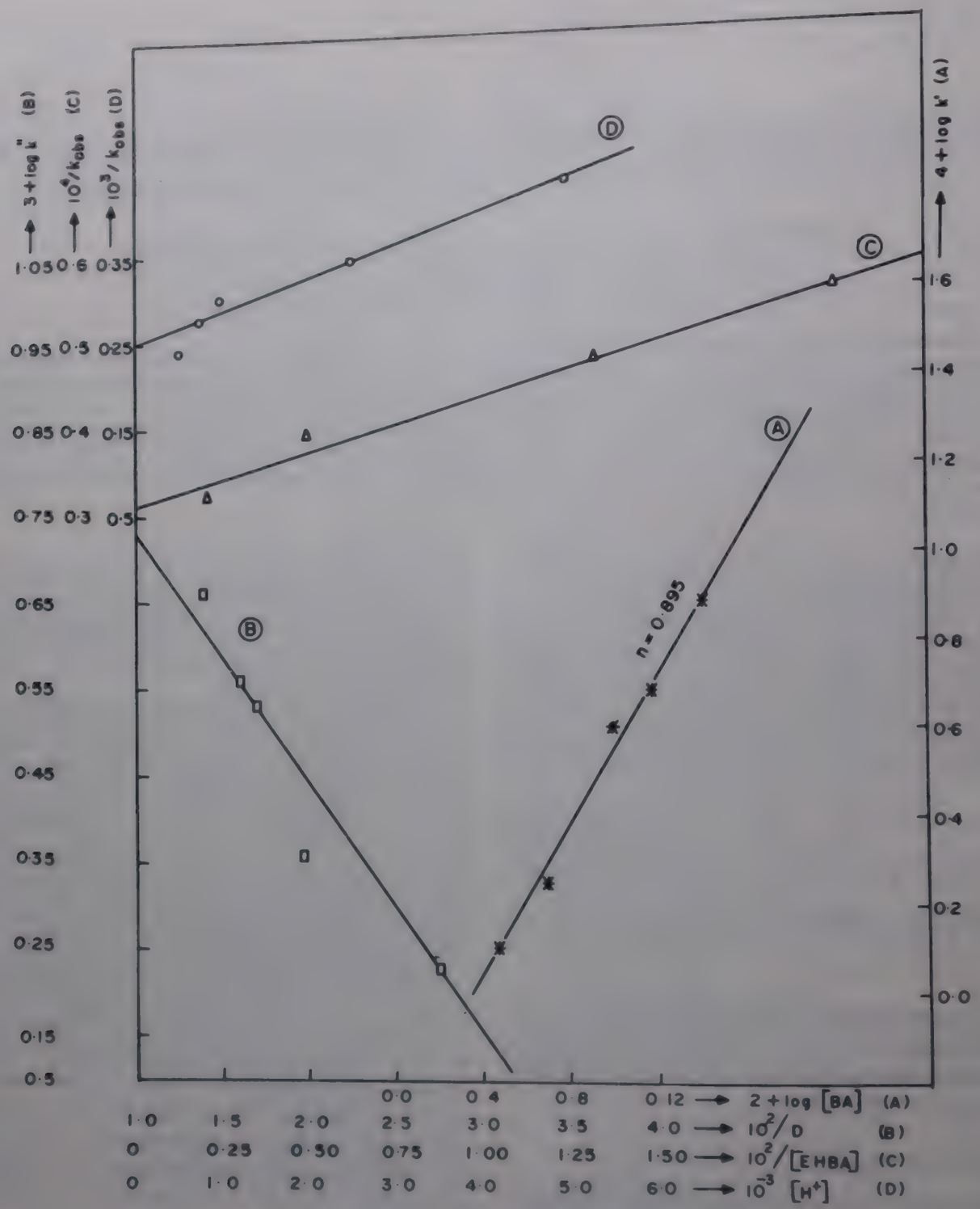

Fig. 1(A)—Plot of log k_{obs} versus log [BA] ([Cr(V)] = 3.00×10^{-3} mol dm^{-3}; [EHBA] = 1.00×10^{-2} mol dm^{-3}; [H$^+$] = 1.00×10^{-3} mol dm^{-3}, [AcOH] = 25.0% (v/v); temp = 303 K).

(B) Plot of log k'' versus 1/D ([Cr(V)] = 3.00×10^{-3} mol dm^{-3}; [BA] = 1.00×10^{-1} mol dm^{-3}; [H$^+$] = 1.00×10^{-3} mol dm^{-3}; [EHBA] = 1.00×10^{-2} mol dm^{-3}; temp = 303 K).

(C) Plot of $1/k_{obs}$ versus 1/[EHBA] ([Cr(V)] = 3.00×10^{-3} mol dm^{-3}; [BA] = 1.00×10^{-1} mol dm^{-3}; [H$^+$] = 1.00×10^{-3} mol dm^{-3}; [AcOH] = 25.0% (v/v); temp = 303 K).

(D) Plot of $1/k_{obs}$ versus 1/[H$^+$] ([Cr(V)] = 3.00×10^{-3} mol dm^{-3}; [BA] = 1.00×10^{-1} mol dm^{-3}; [EHBA] = 1.00×10^{-2} mol dm^{-3}; [AcOH] = 25.0% (v/v); temp = 303 K).

the conditions $[HClO_4] = 1.0 \times 10^{-3}$ mol dm^{-3}; $[EHBA] = 1.0 \times 10^{-2}$ mol dm^{-3}; $[BA] = 1.0 \times 10^{-1}$ mol dm^{-3}; temp. = 303 K and solvent = aq. acetic acid (25%, v/v), 10^4 k_{obs} remained constant at 3.64 ± 0.14 s^{-1} when 10^3 [Cr(V)] was varied form 3.0 to 10.0 mol dm^{-3}. The order in [alcohol] was nearly unity as obtained from the slope of the linear plot of log k' versus log [alcohol] (Fig. 1A). At fixed [Cr(V)], [alcohol] and [H$^+$] increase in [EHBA] increased the rate of oxidation (Fig. 1C). The rate of oxidation decreased with increase in [H$^+$] in the *p*H range of 2-4 (Fig. 1D). With increase in percentage of HOAc in the solvent medium (decrease in dielectric constant) the rate of oxidation increased. The plot of log k' versus 1/D was linear with a negative slope (Fig. 1B). The rate of oxidation was unaffected by the addition of salts like NaCl and $NaClO_4$. No reaction was observed between Cr(V) and tertiary butanol.

The Cr(V) complex, $[Cr^V(O)(EHBA)_2]^-$ was stable in the narrow *p*H range of 2-4 but below and above this range decomposition occurred. The possible species of Cr(V) present in the above *p*H region as suggested by Krumpolc and Rocek[8] are neutral species, i.e., $Cr^V(OH)(EHBA)_2$, monoanionic $Cr^VO(EHBA)_2^-$ and another species containing only one EHBA molecule. The species that absorbs at 510 nm is $Cr^VO(EHBA)_2^-$ and not any other species[4]. Alcohols predominantly exist in the neutral form even at very low *p*H[9]. In view of these observations a mechanism involving the reaction between $Cr^VO(EHBA)_2^-$ and alcohol is proposed in the present case (Scheme 1). This receives support from the solvent and ionic strength effect studies, unit dependence in [S] and absence of any kinetic evidence for complex formation (the pot of $1/k_{obs}$ versus 1/[S] is linear with negligible intercept on $1/k_{obs}$ axis).

$$Cr^V(OH)(EHBA)_2 \overset{K_1}{\rightleftharpoons} Cr^VO(EHBA)_2^- + H^+ \quad \ldots(1)$$

$$Cr^V(O)(EHBA)_2^- \overset{K_2}{\rightleftharpoons} Cr^VO(EHBA)^- + EHBA \ldots(2)$$

$$Cr^VO(EHBA)_2^- + Ph.CH_2OH \xrightarrow[\text{slow}]{k}$$

$$Ph-\underset{\underset{O}{\|}}{C}-H + Cr(III) + H^+ \quad \ldots(3)$$

(Scheme 1)

According to Eq. (1) if the monoanionic species is assumed to be the active species, the rate should decrease with increase in [H$^+$] which in fact was observed in the present study. The rate of oxidation increased with increase in [EHBA] further confirming that probably the monoanionic species, i.e. $Cr^VO(EHBA)_2^-$ is the most likely reactive species (Eq. 2). Scheme 1 leads to the rate law (4).

$$\frac{-d[Cr(V)]_t}{dt} = \frac{kK_1[EHBA][S][Cr(V)]_t}{[EHBA]\{[H^+] + K_1\} + K_1K_2} \quad \ldots(4)$$

$$\frac{-d\ln[Cr(V)]_t}{dt} = k_{obs}$$

$$= \frac{kK_1[EHBA][S]}{[EHBA]\{[H^+] + K_1\} + K_1K_2} \quad \ldots(5)$$

or

$$\frac{1}{k_{obs}} = \frac{[EHBA]\{[H^+] + K_1\} + K_1K_2}{kK_1[EHBA][S]} \quad \ldots(6)$$

As fixed [S] and [EHBA] Eq. (6) can be written as

$$\frac{1}{k_{obs}} = K_x[H^+] + K_y \quad \ldots(7)$$

where

$$K_x = \frac{1}{K_1k[S]};\ K_y = \frac{[EHBA] + K_2}{k[EHBA][S]}$$

According to Eq. (7) a plot $1/k_{obs}$ versus [H$^+$] should be linear with intercept which has been obtained in the present case (Fig. 1D).

As fixed [S] and [H$^+$] Eq. (6) reduces to Eq. (8)

$$\frac{1}{k_{obs}} = \frac{K_x'}{[EHBA]} + K_y' \quad \ldots(8)$$

where

$$K_x' = \frac{K_2}{k[S]} \text{ and } K_y' = \frac{K_1 + [H^+]}{kK_1[S]}$$

According to Eq. (8) a plot of $1/k_{obs}$ versus 1/[EHBA] should be linear with an intercept. This has been realised in the present study (Fig. 1C).

In order to calculate k, K_1 and K_2, the k_{obs} values were determined by varying [H$^+$] under different concentrations of EHBA and also by varying [EHBA] under different [H$^+$] by keeping [S] fixed. The plots of K_y versus 1/[EHBA] and K_y' versus [H$^+$] were linear with an intercept. From the values of slopes and intercepts of these plots k, K_1 and K_2 were evaluated to be 38.5×10^{-3} dm^3 mol^{-1} s^{-1}, 27.8×10^{-3} mol dm^{-3} and 2.10×10^{-3} mol dm^3 respectively confirming the proposed mechanism (see Scheme 1).

The effect of substituents on the reaction rate was studied using different substituted benzyl alcohols

Table 1—Effect of Substituent on Second Order Rate Constants and Activation Parameters

$[Cr(V)] = 3.00 \times 10^{-3}$ mol dm^{-3}; [HOAc] = 25% (v/v) [EHBA] = 1.00×10^{-2} mol dm^{-3}; $[HClO_4] = 1.00 \times 10^{-3}$ mol dm^{-3}; Temp = 308 K

Substituent	$10^3 k''$ dm^3 mol^{-1} s^{-1})	E_{exp}	$\Delta H^{\ddagger}$	$\Delta G^{\ddagger}$	$-\Delta S^{\ddagger}$ (J K^{-1} mol^{-1})
p-OMe	7.76	56.8	54.3	87.9	109
m-OMe	5.85	52.7	50.2	88.6	124
H	5.80	51.0	48.4	88.6	130
p-Br	5.75	50.0	47.4	88.7	134
p-Cl	5.08	46.6	44.0	89.0	146
m-Cl	4.60	43.9	41.3	89.3	155
m-NO_2	3.33	38.2	33.6	90.1	183

E_{exp}, $\Delta H''$ and $\Delta G''$ values in k J mol^{-1}

and the reactivities follow the order: *p*-OCH_3 > *m*-OCH_3 > H > *p*-Br > *p*-Cl > *m*-NO_2. The Hammett's plot is linear with $\rho = -0.31$ ($r = 0.974$). The negative ρ-value increases with increase in temperature. The ρ-values at temperatures 293, 298, 303, 308 K are -0.19, -0.23, -0.28 and -0.31 respectively.

In view of the negative test obtained for free radicals, negative slope for the Hammett's plot, and no reaction with *t*-butanol, a hydride ion transfer mechanism has been suggested despite the low value for ρ obtained. Such low values are not uncommon in hydride ion transfer mechanism[10].

The second order rate constants (k'') and the activation parameters, viz. E_a, $\Delta H^{\ddagger}$, $\Delta S^{\ddagger}$ and $\Delta G^{\ddagger}$ have been calculated and the values are listed in Table 1. The constancy in $\Delta G^{\ddagger}$ values suggest that a similar mechanism is operative with all the substrates used. The isokinetic temperature (β) obtained from the plot of $\Delta H^{\ddagger}$ versus $\Delta S^{\ddagger}$ is 285 K which is well below the experimental temperature range (293-308 K), suggesting that the reactions are entropy-controlled. The plots of log *k* versus 1/T also converge at 286 K which is nearly equal to the above value obtained by the above method.

Acknowledgement

One of the authors (GS) is thankful to the CSIR, New Delhi, for the award of a research fellowship.

References

1 William Levason & Mark D Spicer, *Coord Chem Rev*, **76** (1987) 45.

2 Audette R J, Quail J W & Smith P J, *Tetrahedron Lett*, **3** (1971) 279.

3 Krumpolc M & Rocek J, *J Am chem Soc*, **101** (1979) 3206.

4 Fanchiang Y T, Rathindra N Bose, Gelerinter E & Gould E S, *Inorg Chem*, **24** (1985) 4679.

5 Srinivasan V & Gould E S, *Inorg Chem*, **20** (1981) 3176.

6 Rajasekar N, Subramanian R & Gould E S, *Inorg Chem*, **21** (1982) 4111.

7 Kolthoff I M, Sandell E B, Meehan E J & Bruckenstein B, *Quantitative chemical analysis* (Macmillan, London), 1969, 861.

8 Krumpolc M & Rocek J, *Inorg Chem*, **24** (1985) 617.

9 Michael G, Hutchings & Johanu Gasteiger, *J chem Soc Perkin Trans*, **2** (1986) 455.

10 Harlan L, Goering & Robert R Jacobson, *J Am chem Soc*, **80** (1958) 3277.

Indian Journal of Chemistry
Vol. 27A, December 1988, pp. 1035-1039

Oxidation by Fe(VI): Kinetics of Fe(VI) Oxidation of Alcohols

K LAXMI VENKAT RAO, M PRASADA RAO, B SETHURAM* & T NAVANEETH RAO
Department of Chemistry, Osmania University, Hyderabad 500 007

Received 3 *November* 1987; *revised* 10 *March* 1988; *accepted* 4 *April* 1988

The kinetics of oxidation of methanol, ethanol, *n*-propanol, propan-2-ol and *n*-butanol by Fe(VI) has been studied at *p*H 10.8 using orthophosphate buffer in the presence of periodate. The self-decomposition of Fe(VI) under these conditions has been found to be the minimum. The order in [Fe(VI)] and [alcohol] is unity each. The rate of oxidation decreases with increase in *p*H, in the *p*H range of 9.8 to 11.9. Effect of [buffer] on the rate is negligible. Increase in [periodate] increases the rate slightly. A mechanism involving abstraction of a hydride ion from α-CH of alcohol has been suggested to explain the kinetic data.

Potassium ferrate(VI) is a powerful two-electron oxidant with an oxidation potential of 2.2 V in acid medium and 0.72 V in basic medium[1]. Only sporadic references are available in literature on the mechanistic details of ferrate(VI) oxidation, particularly the oxidation of organic compounds, probably due to its instability and difficulty in the preparation of a stable compound of Fe(VI). Bartzatt *et al.*[2] studied the kinetics of ferrate(VI) oxidation of some simple alcohols in the *p*H range of 8.12 to 9.02 in phosphate buffers and reported mixed order dependence of rate on [ferrate(VI)], i.e. first and second order in [Fe(VI)]. However under these conditions the self-decomposition of the oxidant was found to be considerable. Solutions containing Fe(VI) have been reported to be stabilized by periodate[3]. Schreyer and Ockerman[4] using phosphate buffers in the *p*H range of 7 to 8 reported marked retardation in the self-decomposition of Fe(VI) in water. In view of this the authors have tried to establish the conditions under which periodate and orthophosphate buffer stabilize Fe(VI) solution. Though periodate itself is a good oxidizing agent it is inactive towards monohydric alcohols[5]. In order to fulfil our objectives presently we have studied the kinetics and mechanism of oxidation of methanol, ethanol, *n*-propanol, propan-2-ol and *n*-butanol by Fe(VI) in the presence of orthophosphate and periodate mixtures under different conditions.

Materials and Methods

Potassium ferrate(VI) was prepared by the method of Thompson *et al.*[6] and assayed by both the chromite method[7] as well as by visible spectrophotometry. It was found to be 92% pure. All the chemicals used were of AR (BDH) grade and further purified wherever necessary by standard methods. Doubly distilled water was used throughout. Buffer solutions of required *p*H were prepared by mixing appropriate quantities of 0.2 mol dm^{-3} KH_2PO_4 and 0.2 mol dm^{-3} KOH.

The reactions were initiated by adding requisite amounts of solid potassium ferrate (K_2FeO_4) to a thermally equilibrated solution containing orthophosphate buffer, periodate and alcohol. The addition of potassium ferrate(VI) to the solution produced a purple colour which faded as K_2FeO_4 was reduced. The absorbance of ferrate(VI) was noted at regular intervals of time using Carl Zeiss spectrocolorimeter 'SPEKOL' at 505 nm at which the molar absorptivity of Fe(VI) is 1030 dm^3 mol^{-1} cm^{-1} (ref. 8).

Stoichiometry and product analysis

Under the conditions [Fe(VI)] ≫ [alcohol] in phosphate buffer-periodate medium, the change in absorbance of Fe(VI) was noted after an interval of 24 hr in the presence and absence (blank) of alcohol; one mole of Fe(VI) was found to react with 2 moles of alcohol indicating 1:2 stoichiometry.

The product of oxidation was characterised as corresponding aldehyde or ketone. Here Fe(VI) was reduced to Fe(II) which was then reoxidized to Fe(III) by dissolved oxygen in solution or by Fe(VI). The formation of Fe(II) as an intermediate during the reduction of Fe(VI) was detected by the addition of 1,10-phenanthroline[8]. Polymerisation of the monomer, acrylamide or methyl methacrylate did not occur when added to the reaction mixture even after a long time indicatlng absence of free radicals.

Results and Discussion

Self decomposition of ferrate(VI)

The self-decomposition of ferrate(VI) in the

absence and presence of periodate at different *p*H values has been investigated. In the absence of periodate self-decomposition of Fe(VI) was less at *p*H 9.8, but below and above this *p*H, decomposition rate markedly increased. However, in the presence of periodate, self-decomposition of Fe(VI) was markedly decreased with increase in *p*H, and was quite small at *p*H 10.8, compared to that in the absence of periodate at *p*H 9.8 (Table 1). The self-decomposition rate was found to be minimum at [periodate] $= 2.5 \times 10^{-4}$ mol dm^{-3}. The effect of varying [buffer] on self-decomposition rate was found to be negligible. Though the order in [Fe(VI)] was one as evidenced by the linear log [Fe(VI)] versus time plot, the rate decreased with the increase in [Fe(VI)]. This could be attributed to formation of unreactive dimerised form[8] of Fe(VI) as per equilibrium (1).

$$2FeO_4^{2-} + 2H^+ \rightleftharpoons Fe_2O_7^{2-} + H_2O \quad \ldots (1)$$

In the self-decomposition study it was suggested by earlier workers that the kinetic data best fit a rate equation that had a first and second order term in [Fe(VI)] and approximately first order in [H^+] as shown[2] by Eq. (2)

$$\text{Rate} = k_1^{H_2O}[FeO_4^{2-}][H^+]^x + k_2^{H_2O}[FeO_4^{2-}]^2[H^+]^y \quad \ldots (2)$$

where x and y are nearly equal to one.

In the present study also we have tried to find out the applicability of Eq. (2) when IO_4^- and phosphate buffers were employed as the medium. Equation (2) at constant *p*H may be rewritten as Eq. (3)

$$\text{Rate} = k_1[FeO_4^{2-}] + k_2[FeO_4^{2-}]^2$$

or

$$\frac{\text{Rate}}{[FeO_4^{2-}]^2} = \frac{k_1}{[FeO_4^{2-}]} + k_2 \quad \ldots (3)$$

Rate/$[FeO_4^{2-}]^2$ versus $1/[FeO_4^{2-}]$ plot was linear with an intercept nearly equal to zero ($k_2 = -0.0025$) and positive slope ($k_1 = 4.62 \times 10^{-3}$) indicating that the second order term is negligible.

Oxidation of alcohols

All the reactions were carried out in the absence and presence of alcohol at *p*H 10.8 in the presence of periodate under optimum concentration (2.5×10^{-4} mol dm^{-3}) at which self-decomposition of Fe(VI) was minimum. The rate of oxidation of alcohols was much greater than the rate of self-decomposition of Fe(VI) under the above conditions (Fig. 1A,A'). Under the conditions [alcohol] $\gg$ [Fe(VI)], plots of log (absorbance) versus time were linear indicating first order dependence in [Fe(VI)] which was also checked by initial rate method. The rate constants for true oxidation of alcohol was calculated by substracting the self-decomposition rate. The pseudo-first order rate constants (k_{obs}) at different [Fe(VI)] are given in Table 2.

Table 1—Effect of *p*H on Rate of Self-decomposition of K_2FeO_4

[K_2FeO_4] $= 6.30 \times 10^{-4}$ mol dm^{-3}; [IO_4^-] $= 2.50 \times 10^{-4}$ mol dm^{-3}
[Buffer] $= 0.133$ mol dm^{-3}; temp $= 298$ K

*p*H	$k_{obs} \times 10^3$ (s^{-1})	
	In absence of KIO_4	In presence of KIO_4
7.80	9.72	2.23
8.40	1.30	2.03
8.75	0.740	2.39
9.15	0.280	0.680
9.40	0.260	0.390
9.80	0.190	0.130
10.5	0.240	0.100
10.8	0.710	0.090
11.1	1.14	0.110

Table 2—Effect of Varying [K_2FeO_4] and [Propan-2-ol] on Rate of Oxidation of Propan-2-ol by K_2FeO_4

[IO_4^-] $= 2.50 \times 10^{-4}$ mol dm^{-3}; [buffer] $= 0.133$ mol dm^{-3}
temp $= 298$ K; *p*H $= 10.8$

$[K_2FeO_4] \times 10^4$ (mol dm^{-3})	[Propan-2-ol] (mol dm^{-3})	$k_{obs} \times 10^4$ (s^{-1})	$10^4 k'' = k_{obs}/[S]$ (dm^3 mol^{-1} s^{-1})
1.80	0.830	4.01	—
2.96	0.830	3.70	—
5.15	0.830	3.55	—
8.50	0.830	3.53	—
6.30	0.250	1.05	4.19
6.30	0.500	2.11	4.21
6.30	1.00	4.16	4.16
6.30	1.50	6.41	4.27
6.30	2.00	8.46	4.23

The combined rate equation which includes self-decomposition and oxidation of alcohols at a constant *p*H can be written as Eq. (4) which can be rewritten as Eq. (5)

$$\text{Rate} = k_1[FeO_4^{2-}] + k_s[FeO_4^{2-}][S] \quad \ldots (4)$$

$$k_{obs} = k_1 + k_s[S] \quad \ldots (5)$$

From the linear plots of k_{obs} versus [S], k_1 and k_s were calculated for different alcohols. The order in [alcohol] was nearly one (Table 2) (varying from 0.8-1.0 for different alcohols) as obtained from the slope of the linear plot of log ($k_{obs} - k_1$) against log[S]. The rate decreased with increase in *p*H in the *p*H range of 9.8-11.9. With propan-2-ol the order in [H^+] varied from 0.40 in the *p*H range of 9.8 to 10.5 to 0.12 in the *p*H range of 10.5 to 11.9. A similar trend was observed by Bartzatt[2] for the same substrate. The rate of oxidation

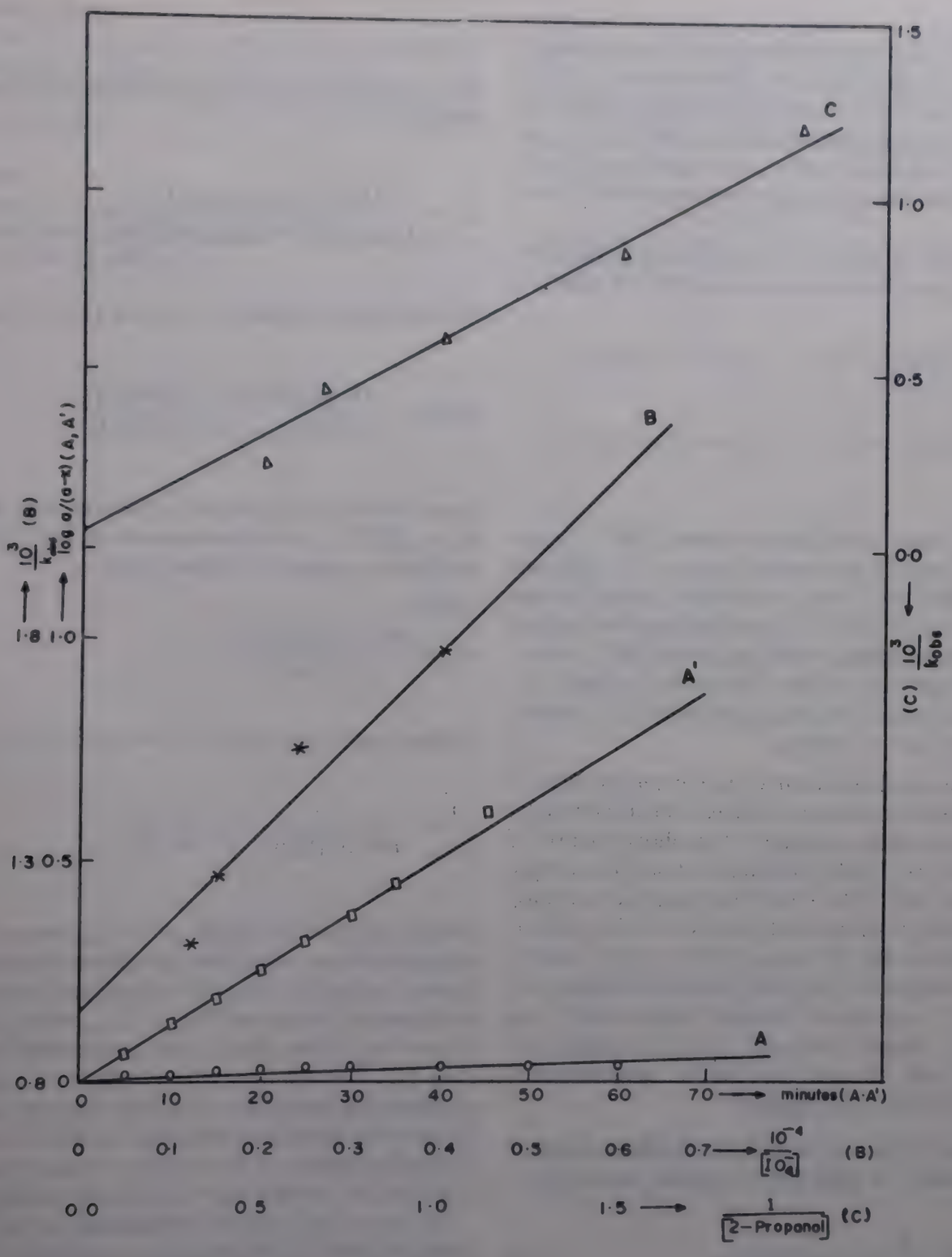

Fig. 1—(A) Plot of log $a/(a-x)$ versus time in the absence of propan-2-ol ($[K_2FeO_4] = 6.30 \times 10^{-4}$ mol dm^{-3}; $[IO_4^-] = 2.50 \times 10$ mol dm^{-3} [buffer] = 0.133 mol dm^{-3}; *p*H = 10.8; temp = 298 K)

(A') Plot of log $a/(a-x)$ versus time for oxidation of propan-2-ol by K_2FeO_4 ($[K_2FeO_4] = 6.30 \times 10^{-4}$ mol dm^{-3}; $[IO_4^-] = 2.50 \times 10^{-4}$ mol dm^{-3}; [propan-2-ol] = 0.833 mol dm^{-3}; [buffer] = 0.133 mol dm^{-3}; *p*H = 10.8; temp = 298 K)

(B) Plot of $1/k'$ versus $1/[IO_4^-]$ ($[K_2FeO_4] = 6.30 \times 10^{-4}$ mol dm^{-3}; [propan-2-ol] = 0.833 mol dm^{-3}; [buffer] = 3.33×10^{-2} mol dm^{-3}; *p*H = 10.8; temp = 298 K)

(C) Plot of $1/k_{obs}$ versus 1/[propan-2-ol] ($[K_2FeO_4] = 6.30 \times 10^{-4}$ mol dm^{-3}; [buffer] = 0.133 mol dm^{-3}; $[IO_4^-] = 2.5 \times 10^{-4}$ mol dm^{-3}; *p*H = 10.8; temp = 298 K)

slightly increased with increase in $[IO_4^-]$, and change in [buffer] had negligible effect. Also the order in $[IO_4^-]$ was fractional (0.43) as obtained from the slope of the linear plot of log k'' versus log $[IO_4^-]$. Plot of $1/k''$ versus $1/[IO_4^-]$ was linear with an intercept (Fig. 1B) indicating formation of a complex between Fe(VI) and IO_4^-.

Ferrate(VI) is known to exist in three different forms in aqueous solution (see equilibria[8] (6) and (7))

$$H_2FeO_4 \overset{K'}{\rightleftharpoons} HFeO_4^- + H^+ \quad ..(6)(K' = 3.16 \times 10^{-4})$$

$$HFeO_4^- \overset{K''}{\rightleftharpoons} FeO_4^{2-} + H^+ \; ..(7)(K'' = 1.58 \times 10^{-8})$$

Under the conditions of the experiment (pH > 7) equilibrium (6) may be assumed to lie far to the right and only equilibrium (7) is more probable as can be seen from K'' value. If $HFeO_4^-$ is to be the reactive species, the rate should increase with increase in $[H^+]$ or decrease with increase in pH. This infact has been observed in the present study suggesting $HFeO_4^-$ to be the most likely reactive species.

Alcohols are also known to exist in neutral form or as alkoxides depending upon the pH. But in view of the very low ionization constants of alcohols[9] (nearly of the order of 10^{-16}) alkoxide can exist only in strongly basic media (pH > 14). Therefore, it can be safely assumed that neutral form of alcohol is the only predominant species in the pH range of 9.8 to 12.0. Accordingly a mechanism involving reaction between an ion ($HFeO_4^-$) and dipole (alcohol) is proposed. This contention receives support from the studies of effect of ionic strength (or buffer concentration) on the rate which was negligible.

In the light of the results and observations recorded above Scheme 1 is suggested to explain the results.

$$HFeO_4^- + IO_4^- \overset{K_1}{\rightleftharpoons} C_1 \text{(Complex)} \qquad \ldots (8)$$

$$C_1 + S \overset{K_2}{\rightleftharpoons} C_2 \text{(Complex)} \qquad \ldots (9)$$

$$C_2 \overset{k}{\rightarrow} \text{products} \qquad \ldots (10)$$

Scheme 1

Since

$$[HFeO_4^-]_t = [HFeO_4^-] + C_1 + C_2$$

$$\text{Rate} = kC_2 \qquad \ldots (11)$$

The expression for the concentration of C_2 can be written as

$$C_2 = \frac{[HFeO_4^-]_t K_1 K_2 [S][IO_4^-]}{1 + K_1[IO_4^-] + K_1 K_2 [S][IO_4^-]}$$

Substituting the value of C_2 in rate Eq. (11) we get

$$\text{Rate} = \frac{kK_1 K_2 [HFeO_4^-]_t [S][IO_4^-]}{1 + K_1[IO_4^-] + K_1 K_2 [S][IO_4^-]} \qquad \ldots (12)$$

Since the order in [alcohol] is nearly one, the term $K_1 K_2 [S][IO_4^-]$ in the denominator of Eq. (2) may be neglected compared to other terms.

Hence,

$$k_{obs} = \frac{kK_1 K_2 [S][IO_4^-]}{1 + K_1[IO_4^-]} \qquad \ldots (13)$$

Taking reciprocal of Eq. (13) we get Eq. (14)

$$\frac{1}{k_{obs}} = \frac{1}{kK_1 K_2 [S][IO_4^-]} + \frac{1}{kK_2[S]} \qquad \ldots (14)$$

which predicts that the plot of $1/k_{obs}$ versus $1/[IO_4^-]$ should be linear. Such plots have been obtained in the present study (see Fig. 1B) supporting the proposed mechanism. At constant $[IO_4^-]$, $1/k_{obs}$ versus $1/[S]$ plot as per Eq. (14) was linear with a very small intercept (Fig. 1C). Though this cannot be taken as a clear cut evidence for formation of even an unstable complex, in view of intensification of colour of Fe(VI) on adding alcohol formation of an unstable complex during the reaction has been incorporated in the mechanism.

In view of the general applicability of the rate expressions derived, the mechanism suggested may be assumed to be operative in the present study.

The reactivities of alcohols followed the order: methanol < propan-2-ol < ethanol < n-propanol < n-butanol. Taft's plot was linear with $\rho^* = -1.05$ ($r = 0.98$). This indicates the formation of an electron-deficient centre in the transition state. In view of the above results it may be assumed that the complex (C_2) undergoes disproportionation with the elimination of a hydride ion from α-carbon of alcohol to give rise to the products. Removal of hydrogen from α-carbon receives further support from the absence of any reaction between Fe(VI) and t-butanol.

Acknowledgement

The authors are grateful to Prof B N Ananthan for suggesting the problem. One of the authors (K L V R) is thankful to the UGC, New Delhi, for the award of a teacher fellowship.

References

1 Wood R H, *J Am chem Soc*, **80** (1958) 2038.
2 Bartzatt R, Tabatabai Ali & James Carr D, *Synth react inorg met-org Chem*, **15** (1985) 1171.
3 Bailar J C, *Comprehensive inorganic chemistry*, **3** (1973) 1050.
4 Schreyer J M & Ockerman L T, *Anal Chem*, **23** (1951) 1312.
5 Fleury & Large J, *Compt rend*, **195** (1932) 1935.
6 Thompson G W, Ockerman L T & Schreyer J M, *J Am chem Soc*, **73** (1951) 1379.
7 Schreyer J M, Thompson G W & Ockerman L T, *Anal Chem*, **22** (1950) 1426.
8 James Carr D *et al.*, *Water chlorination chemistry environmental impact and health effects*, **5** (1984).
9 Michael G, Hutchings & Johann Gasteiger, *J chem Soc Perkin Trans*, **2** (1986) 455.

Indian Journal of Chemistry
Vol. 27A, December 1988, pp. 1040-1046

Characterization & Polymerization Studies on Silica-supported Titanium (IV) Complexes

G C OFUNNE*, B L BOOTH† & P J T TAIT†

Pure & Industrial Chemistry Department, University of Port Harcourt, Choba, Port Harcourt, Nigeria

Received 10 *September* 1987; *revised* 2 *February* 1988; *accepted* 14 *March* 1988

Polymerization of ethylene using silica-supported $[(MeO)_3Si(CH_2)_3C_5H_4]_2TiCl_2$ catalyst activated with diethylaluminium chloride has been investigated. The rate-time profiles obtained for room temperature polymerizations indicate a decay type behaviour. Although the rates obtained for the supported catalysts are higher than those of the homogeneous analogues, immobilisation of the complex on silica does not offer increased catalyst stability. Characterisation of the supported catalyst has shown that the interaction of $[(MeO)_3Si(CH_2)_3C_5H_4]_2TiCl_2$ with silica can result in two types of supported compounds: one in which the complex anchors to the silica surface with both $TiCl_2$ group and methoxy group and the other in which the methoxy group is anchored to the silica surface.

The use of transition metal complexes supported on silica, alumina or on other inorganic supports has been well known in Ziegler-Natta polymerisation ever since the development of silica supported chromium oxide catalyst for the polymerisation of ethylene[1]. The use of discrete, well characterized complexes supported on conventional supports offer some exciting possibilities for catalyst development and characterisation, and consequently it was decided to investigate the activity of the complex, $[(MeO)_3Si(CH_2)_3C_5H_4]_2TiCl_2$ supported on silica and activated with dialkylaluminium chloride, for ethylene polymerisation. This dichloro complex[2] has proved to be a very active and selective catalyst for terminal olefin hydrogenation, both in the homogeneous and in silica supported state.

Materials and Methods

All manipulations involving air-sensitive materials were performed under nitrogen atmosphere. The complexes, η^5-$(C_5H_5)_2TiCl_2$ (ref. 3), $(\eta^5$-$MeC_5H_4)_2TiCl_2$ (ref. 4), η^5-$C_5H_5TiCl_2$ (ref. 5) η^5-$MeC_5H_4TiCl_3$ (ref. 6) and $[\eta^5$-$(MeO)_3Si(CH_2)_3$-$C_5H_4]_2TiCl_2$ (ref. 2), were prepared as previously reported. All solvents were purified and dried by standard procedures.

Far infrared spectra were recorded using a Digilab model FTS-16 FT spectrophotometer. GLC analysis was carried out on a PYE 104 chromatograph using a 2m OV17 column.

Preparation of silica-supported $[(MeO)_3Si(CH_2)_3C_5H_4]_2TiCl_2$

Silica gel [Grace Davison, 929, surface area (BET, N_2) 281 $m^2\ g^{-1}$] was dried at 300°C for 12 hr *in vacuo* and cooled in a stream of nitrogen, before adding to degassed toluene (100 ml) which had been stirred with aqueous sodium hydroxide (0.2*M*, 1 ml). The silica was stirred at 80°C for 1 hr to equilibrate, filtered, washed several times with dried toluene, and dried at 300°C immediately before use. A solution of $[\eta^5$-$(MeO)_3Si(CH_2)_3$-$C_5H_4]_2TiCl_2$ in dried toluene was stirred with the silica at room temperature for 36 hr. Various loadings of the complex on silica were prepared by stirring at room temperature, except in the case of samples C and G, (Table 1) where refluxing was carried out for 16 hr. The silica was filtered, washed with dried diethyl ether, extracted with hot benzene, and dried *in vacuo* at 50°C.

Electron microprobe

The silica-supported catalysts were made into pellets and subjected to an electron microprobe X-ray fluorescence study for radial distributions titanium and chlorine. Samples D and G were investigated.

Radical profiles for Ti and Cl on the surface of the pellets were determined using an ARL-EMX/SN electron microprobe in the Metallurgy Department, UMIST. The microprobe conditions were as follows: 25 kV accelerating voltage; 0.01 μa sample current; and 1 μm beam width.

Fast atom bombardment mass spectroscopy (FAMBMS)

The silica gel, and samples A, D, and G (Table 1) were analysed as powders. For the fast

†Chemistry Department, UMIST, Manchester M60, 1QD, UK

atom bombardment the conventional ion source was replaced by an ion atom gun which allowed rapid switching from ion to atom mode and produced a pure mass, filtered particle beam having a current equivalent in the range 10^{-11} to 10^{-8} cm^{-2}.

The mass analyser used was a vacuum generator, MM12-12 quadrupole filter, with a mass range of 1-1200 daltons and unit resolution throughout the range. Secondary ion collection and energy selection was obtained by the modification of some of the optical equipments. A small, plasma discharge, neutral particle source was used for rapid profiling. All the samples were studied using fast argon atom bombardment. There were no problems for obtaining positive or the negative spectra from powders. The spectra were fully reproducible.

Polymerization procedure

In all the cases, the polymerization of ethylene was carried out in a polymerization reactor charged with dried toluene (500 ml), evacuated and purged three times with dried nitrogen. The temperature of the reactor was maintained by water pumped around the reactor from a thermostated bath. The catalyst was dispersed in dried and degassed toluene and carefully added to the reactor. The catalyst-toluene mixture in the reactor was stirred vigorously and ethylene was allowed to saturate the solution to a pressure of 1 atm. Then 2 ml of 15% $AlEt_2Cl$ in dried toluene were added by means of a hypodermic syringe. The solution immediately turned blue and the uptake of ethylene (with time) was recorded by an electronic counter system. The polymerization was allowed to continue for 100 min and was then quenched by the addition of ethanol. The polymer formed was precipitated with a mixture of methanol and HCl, filtered, washed and dried at 80°C *in vacuo*. The counts obtained were converted into rates using a conversion factor (C) obtained from Eq. (1).

$$C = \frac{\text{(Total yield of polymer at the end of polymerizaation)}}{\text{(Total number of counts at the end of the polymerization)}} \quad \ldots (1)$$

By multiplying this value with the number of counts on the print out, the weight of the polymer at any time in the reactor could be obtained.

Results and Discussion

Characterization of silica-support

In the present study, silica gel (Grace Davison 929) before use was heated at 300°C for 3 hr, and allowed to cool. Adsorption studies (BET) showed the surface area to be 281 m^2/g. IR spectrum of a 1 cm thick disc of pre-treated silica exhibited bands in the regions of 3650-3400 and 1300-960 cm^{-1} which are characteristic of surface Si−OH groups. Similarly, when examined with fast atom bombardment spectrometry (FABMS), fragments at *m/z* 45 and 28, corresponding to $[Si-OH]^{+\cdot}$ and $[Si]^{+\cdot}$ groups respectively, were obtained. Such results are in agreement with those reported by Vickerman *et al.*[7] when a similar technique was used to analyse glass and zeolite surfaces. Microanalysis of the silica did not detect any organic impurity.

Immobilization of $[(CH_3O)_3Si(CH_2)_3C_5H_4]_2TiCl_2$

The synthesis and characterization of $[(MeO)_3Si-(CH_2)_3C_5H_4]_2TiCl_2$ and other complexes have been reported previously[2]. Allum *et al.*[8] have detailed some possible methods of coupling unstable homogeneous catalysts of this type to silica supports. One possibility is to attach the precursor ligand to silica before complexing the attached ligand with the metal compound (see Eqs 2-4).

$$(CH_3O)_3Si(CH_2)_3C_5H_5 + -\underset{|}{\overset{|}{Si}}-OH \rightarrow \quad \ldots (1)$$

$$(Sil)-(CH_2)_3C_5H_5 + CH_3OH \quad \ldots (2)$$

$$(Sil)-(CH_2)_3C_5H_5 + Na \rightarrow (Sil)-(CH_2)_3C_5H_4^-Na^+ + H_2 \quad \ldots (3)$$

$$(Sil)-(CH_2)_3C_5H_4^-Na^+ + MCl_4 \rightarrow [(Sil)-CH_2C_5H_4]_2MCl_2 + NaCl \quad \ldots (4)$$

However, when using this method, the actual complex anchored to the surface cannot be characterized easily. In the present work, an alternative procedure has been employed. This procedure involves the synthesis of a well characterized discrete complex, and then the anchoring of this complex to a well charcterized silica support. $[(MeO)_3Si(CH_2)_2C_5H_4]_2TiCl_2$ was supported on pretreated silica by stirring in toluene, both at room temperature and also by refluxing at the boiling point of toluene.

In both the cases methanol was detected in the toluene by GLC. However when the reactants were refluxed at the boiling point of toluene HCl was also detected. These observations suggest that the surface silanol, apart from reacting with the methoxy group at reflux temperature, also reacts with the Ti−Cl group, thus displacing chlorine which is evolved as HCl. The possible reactions are illustrated in Eqs 5 and 6.

Table 1—Microanalytical Data for Immobilised Catalysts

Samples	Colour	Cl† (%)	Ti† (%)	Cl/Ti (Calc.)	Cl/Ti on surface	Approx area (nm^2) occupied by each Ti
A	Salmon red	3.85(1.08)	2.83(0.59)	2	1.83	0.79
B	Light pink	1.96(0.55)	1.33(0.28)	2	1.96	1.67
C*	Light brown	0.20(0.058)	0.35(0.073)	2	0.76	6.38
D	Salmon red	9.70(2.73)	6.00(1.26)	2	2.18	0.37
E	Dark brown	0.74(0.208)	0.82(0.17)	2	1.22	2.72
F	Salmon red	6.38(1.79)	3.75(0.78)	2	2.30	0.60
G*	Light bridge	0.04(0.004)	0.09(0.018)	2	0.20	24.96

*Prepared by refluxing in toluene.
†Values in parentheses are in mmol/g.

$$-\underset{|}{\overset{|}{Si}}-OH+[(CH_3O)_3Si(CH_2)_3C_5H_4]_2TiCl_2 \xrightarrow[\text{temp.}]{\text{room}}$$

$$(Sil)-[(CH_2)_3C_5H_4]_2TiCl_2+CH_3OH \quad \ldots(5)$$

$$-\underset{|}{\overset{|}{Si}}-OH+[(CH_3O)_3Si(CH_2)_3C_5H_4]_2TiCl_2 \xrightarrow[\text{temp}]{\text{reflux}}$$

$$(Sil)-Ti[C_5H_4(CH_2)_3]_2(Sil)+CH_3OH+HCl \quad \ldots(6)$$

Various loadings of the complex on silica were prepared by stirring in toluene at room temperature, except for sample C, and G for which the mixture was refluxed (see Table 1). This resulted in the evolution of HCl as well as the production of methanol indicating that the surface silanol groups had reacted with the Ti−Cl bonds. This conclusion is further substantiated by microanalyses for samples C and G which show a low Cl to Ti ratio (see Table 1).

Characterization of supported titanium complexes

Microanalytical results are summarised in Table 1. It is evident for Ti loadings >1.30% that chlorine:titanium ratios of about 2.0 are obtained. The data also show that various supported complexes with varying Ti loadings can be prepared depending on the conditions of preparation. Samples D and G have been selected for further studies. Analysis using IR spectroscopy gave bands at 468 (ν_{as} Ti−Cl), 434 (ν_2 − Ti − Cl), 190 ($\delta_s C_p$ − Ti − C_p), 100 (δ_s Cl − Ti − Cl) and 2900 (νC − H) cm^{-1}, for sample D. These bands are characteristic of the presence of a Cp_2TiCl_2 moiety on the surface. Furthermore, IR spectrum of sample G was complex and difficult to interpret. However, bands at 190 and 2900 cm^{-1} were observed.

In order to measure the degree of dispersion of the complex on silica surface, electron microprobe examination was used. Chandrasekharan *et al.*[8] have studied the dispersion of a Cp_2TiCl_2 immobilized on polystyrene beads and found a uniform distribution of Cp_2TiCl_2 on the polymer. Similarly, Dawan and Morel[9] have studied the dispersion of η^3-allylnickel(II) on a difluoroacetic terpolymer and reported that the metal atoms were attached to the matrix in such a way that there was a smooth cross-sectional distribution of nickel atoms throughout the polymer. In the present study sample D was examined by an electron microprobe technique and similar counts for titanium and chlorine atoms were obtained across the area studied (see Fig. 1). The intensities of the counts for chlorine, in sample D are about two times those for titanium. In addition the spectrum obtained for sample D is similar to those obtained for samples A and E. These results are consistent with an even distribution of the complex on silica surface. Examination of sample G by this technique, gave very low counts for chlorine, which is inconsistent with the expected Ti:Cl ratio and a uniform distribution on the support surface.

Further investigations of the catalyst surface were carried out using FABMS analysis. The spectrum of sample D displays fragment ions at *m/z* 27 $[C_2H_3]^{+\cdot}$, 41 $[C_3H_5]^{+\cdot}$, 65 $[C_5H_5]^{+\cdot}$, 77 $[C_6H_5]^{+\cdot}$ and 91 $[C_7H_7]^{+\cdot}$,

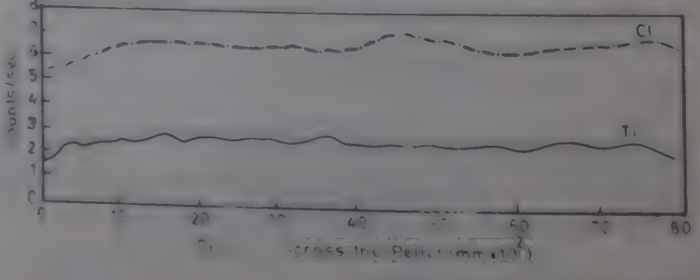

Fig. 1—X-ray fluorescene analysis of sample D [(———) Ti; (·····) Cl]

which are thought to have originated from the substituted cyclopentadienyl ring attached to the metal atom. Also, fragments associated with the titanium atom are observed at *m/z* 115 $[C_5H_6TiH]^+$, 119 $[TiCl_2]^+$, 127 $[CH_3C_5H_4Ti]^+$, 128 $[CH_3C_5H_4TiH]^+$, 147 $[C_5H_4TiCl]^+$, and 64 $[TiO]^+$. The intense peak observed at *m/z* 119 is a good indication that most of the Ti – Cl groups have not been hydrolysed (see Fig. 2). Sample G afforded a complicated FABMS spectrum and fragments containing $-TiCl_2$ group were not observed. In addition, the negative ion FABMS spectrum of sample D was studied (see Fig. 3). The main fragments observed were negative ions at *m/z* 35 $[Cl]^-$ and 37 $[Cl]^-$ with intense peaks. In contrast the spectrum obtained for sample G showed no significant fragments which could substantiate the existence of $-TiCl_2$ moieties on the surface.

The results from these analyses therefore indicate that the interaction of the present complex with the silica support can result in two types of supported compounds. In one of these the complex anchors to the silica surface with both the $TiCl_2$ and MeO-groups, as indicated in the analysis of sample G, while in the other, the methoxy group of the complex is anchored to the silica surface, as illustrated by the analytical observations for sample D.

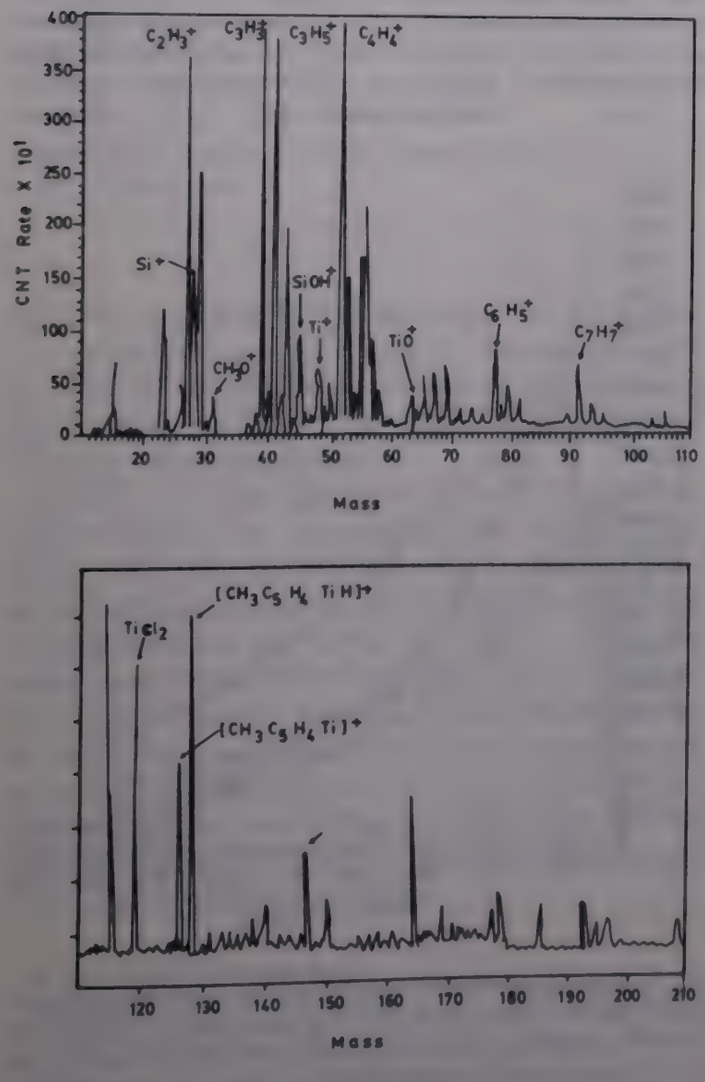

Fig. 2—FABMS spectrum of sample D

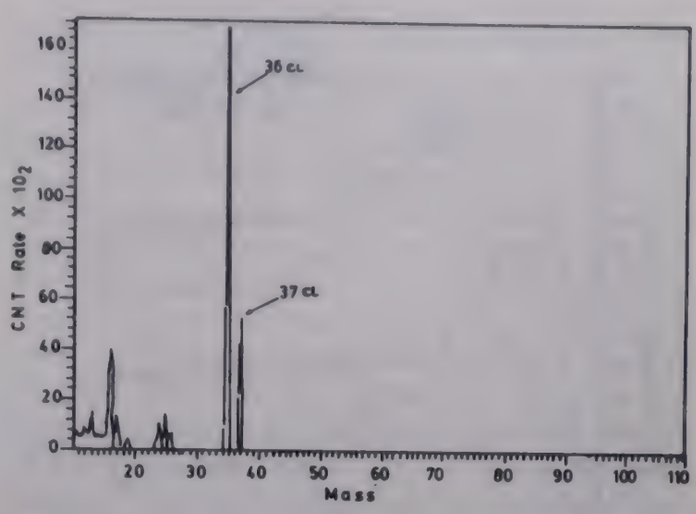

Fig. 3—Negative ion spectrum of sample D

Polymerization studies: Use of homogeneous catalysts

In order to compare the behaviour of homogeneous and supported polymerization systems, initially polymerization of ethylene was carried out using a number of homogeneous catalysts, viz. $(\eta^5\text{-}C_5H_5)_2TiCl_2$; $(\eta^5\text{-}MeC_5H_4)_2TiCl_2$; $\eta^5\text{-}C_5H_5TiCl_3$; $\eta^5\text{-}MeC_5H_4TiCl_3$ and $(\eta^5\text{-}(MeO)_3Si(CH_2)_3C_5H_4)_2TiCl_2$. All polymerizations were performed under similar conditions using $AlEt_2Cl$ as cocatalyst at an Al:Ti ratio of 3.64. Typical rate-time profiles are shown in Figs 4 and 5. It is evident from Fig. 6 that the catalyst systems $(\eta^5\text{-}MeC_5H_4)_2TiCl_2 - AlEt_2Cl$ and $[\eta^5\text{-}(MeO)_3Si(CH_2)_3C_5H_4]_2TiCl_2 - AlEt_2Cl$ all show settling periods, the maximum rates being attained within the first 15 min of polymerization after which the polymerization rates decrease gradually with time. The catalyst system $\eta^5\text{-}C_5H_5TiCl_3 - AlEt_2Cl$ and $\eta^5\text{-}MeC_5H_4TiCl_3 - AlEt_2Cl$ behave somewhat differently with higher maximum rates of polymerization being obtained within 10 min of the start of polymerization but showing a more rapid decrease in rate with time.

These catalyst systems are evidently more active but less stable. The significance of these rate-time profiles has been discussed elsewhere[10,11]. Values of maximum rates of polymerization together with corresponding rates after 60 min polymerization are presented in Table 2. The order of maximum activities of these homogeneous catalysts is as follows: $\eta^5\text{-}C_5H_5TiCl_3 > \eta^5\text{-}MeC_5H_4TiCl_3 > [\eta^5\text{-}(MeO)_3Si(CH_2)_3C_5H_4]_2TiCl_2 > (\eta^5\text{-}C_5H_5)_2TiCl_2 > (\eta^5\text{-}MeC_5H_4)_2TiCl_2$. While it is not easy to explain exactly

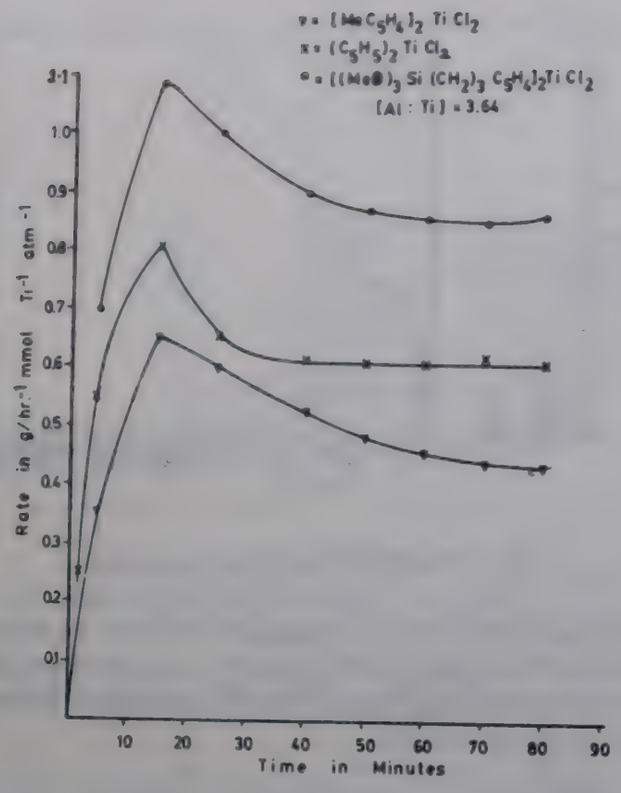

Fig. 4—Rate-time profiles for polymerization of ethylene with homogeneous catalysts using $AlEt_2Cl$ as cocatalyst [▲ = $(\eta^5$-$MeC_5H_4]_2TiCl_2$; X = $(\eta^5$-$C_5H_5)_2TiCl_2$; ● = $[\eta^5$-$(MeO)_3Si(CH_2)_3$-$C_5H_4]_2TiCl_2$. Polymerization condition: Al:Ti = 3.14:1; [Ti] = 0.55 mmol dm^{-3}; C_2H_4 = 1 atm; and temp. = 18°C]

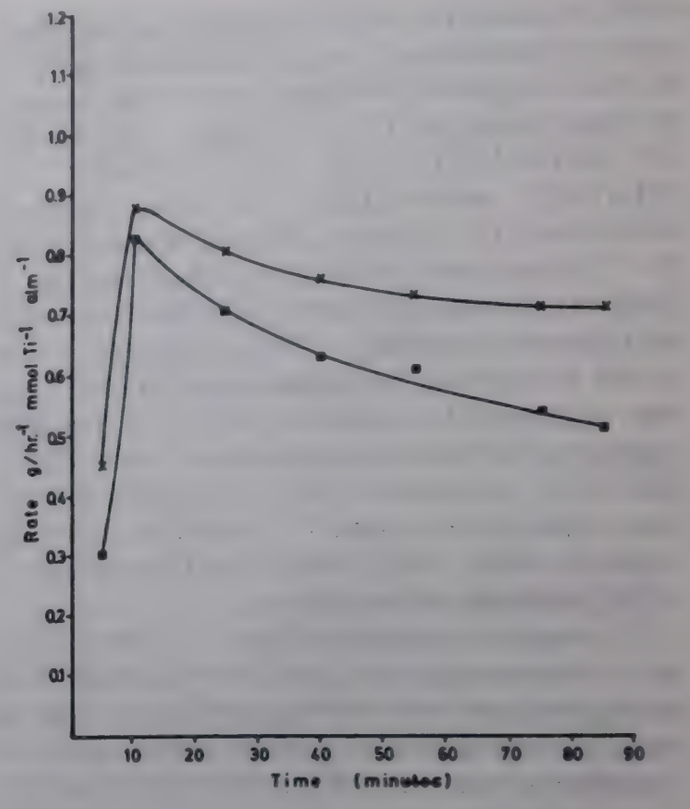

Fig. 6—Rate-time profile for polymerization of ethylene with homogeneous catalyst using $AlEt_2Cl$ as cocatalyst and with added water. [×, $(\eta^5$-$C_5H_5)_2TiCl_2 + H_2O$; ■, $[\eta^5$-$MeC_5H_4] + H_2O$. Polymerization conditions: Al:Ti = 3.61:1; [Ti] = mmol dm^{-3}; C_2H_4 = 1 atm.; and temp. = 18°C]

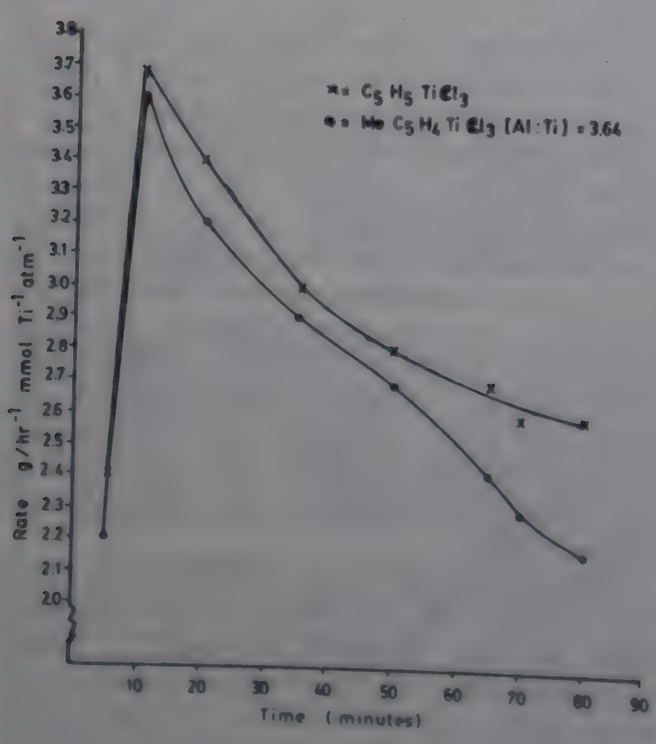

Fig. 5—Rate-time profile for polymerization of ethylene with homogeneous catalyst using $AlEt_2Cl$ as catalyst. ● η^5-C_5H_5-$TiCl_3$; X, η $MeC_5H_4TiCl_3$. Al:Ti = 3.64:1; Ti = 0.55 mmol dm^{-3}; C_2H_4 = 1 atm and temp. = 18°C]

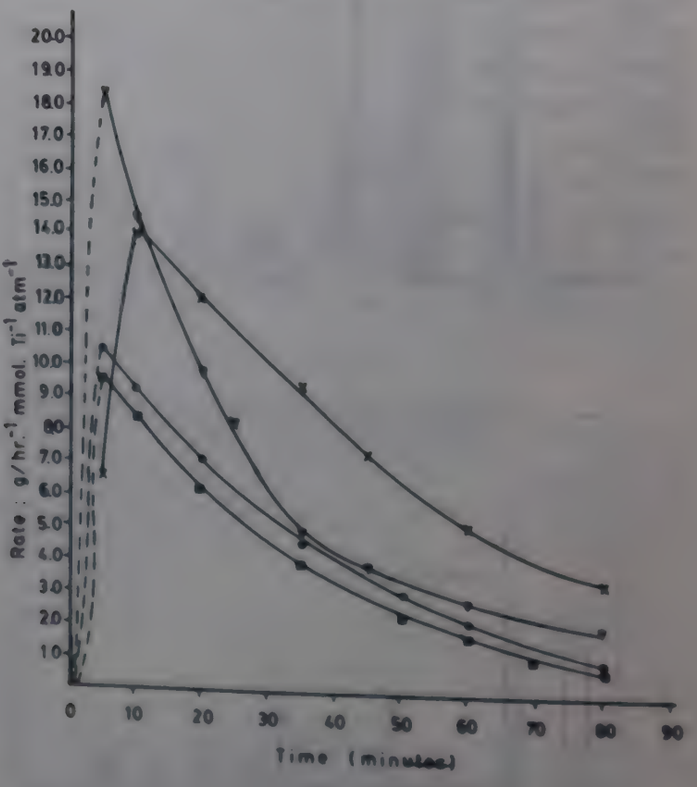

Fig. 7—Rate time profile for polymerization of ethylene with supported catalysts and using $AlEt_2Cl$ as cocatalyst [▲, sample D at 60°C; ●, sample A at 60°C; Δ, sample D at 18°C; O, sample A at 18°C. Polymerization condition: Al:Ti = 3.64:1; [Ti] = 0.55 mmol dm^{-3}; and C_2H_4 = 1 atm

Table 2—Rates of Ethylene Polymerization Using Various Homogeneous Catalysts

Catalyst	10^2 Rate/g (Polymer) (mmol Ti)$^{-1}$.hr^{-1} atm^{-1}	
	Maximum	At 80 min
η^5-$(C_5H_5)_2TiCl_2 - AlEt_2Cl$	81	81
$(\eta^5$-$MeC_5H_4)_2TiCl_2 - AlEt_2Cl$	65	44
$[\eta^5$-$(MeO)_3Si(CH_2)_3C_5H_4]_2TiCl_2 - AlEt_2Cl$	108	86
η^5-$C_5H_5TiCl_3 - AlEt_2Cl$	365	259
η^5-$MeC_5H_4TiCl_3 - AlEt_2Cl$	362	218
$(\eta^5$-$C_5H_5)_2TiCl_2 - AlEt_2Cl + H_2O$	87	70
$(\eta^5$-$CH_3C_5H_4)_2TiCl_2 - AlEt_2Cl + H_2O$	85	52

Polymerization condition: [Ti] = 0.55 mmol/dm^3; Al:Ti = 3.64: 1; C_2H_4 = 1 atmosphere; [H_2] = 0.01 mol/dm^3; temp = 18°C

Table 3—Rates of Ethylene Polymerization Using Supported Catalysts

Catalyst	Temp. °C	10 Rate/g (Polymer). (mmol Ti)$^{-1}$.hr^{-1}.atm^{-1}	
		Maximum	At 80 min
Sample D – $AlEt_2Cl$	18	1855	272
Sample D – $AlEt_2Cl$	60	1852	157
Sample A – $AlEt_2Cl$	18	1403	145
Sample A – $AlEt_2Cl$	60	1297	436

Polymerization condition: [Ti] = 0.55 mmol/dm^3; Al:Ti = 3.64: 1; C_2H_4 = 1 atmosphere

this order, it is clear that substitution of a methyl group in cyclopentadienyl ring decreases the catalyst activity. The $(\eta^5$-$RC_5H_4)TiCl_3$ complexes are invariably more active than the corresponding $(\eta^5$-$RC_5H_4)_2TiCl_2$ compounds.

Addition of small quantities of water (Fig. 6) increases slightly the maximum rates with $(C_5H_5)_2$-$TiCl_2 - AlEt_2Cl$ and $(MeC_5H_4)_2TiCl_2 - AlEt_2Cl$ systems, but does not alter the above order. The rate-time profiles obtained are similar in shape to those obtained under anhydrous conditions. Enhanced catalytic activities on the addition of small amounts of water to similar polymerization systems were first reported by Reichert and Meyer[12], who explained the phenomenon by postulating that the water reacted with the cocatalyst, $AlEt_2Cl$, to give an aluminoxane which acts as a better cocatalyst.

Use of supported complexes

Ethylene was polymerized using silica-supported silylated titanocene dichloride complexes. Three samples, A, D and G, of differing Ti loadings were studied.

Polymerizations were performed under conditions similar to those reported for the homogeneous systems. $AlEt_2Cl$ was used as cocatalyst and the Al:Ti ratio was maintained at 3.64:1. While samples A and D polymerized ethylene the low loading samples proved to be inactive. Typical rate-time profiles are shown in Fig. 7, and demonstrate that these polymerizations are basically of the decay type[13], in which the rate either shows a maximum initial value or increases quickly to reach a maximum value, and then decreases rapidly with time. This type of rate-time behaviour has been reported previously for many polymerization systems, including highly active supported catalysts $MgCl_2/EB/TiCl_4 - AlEt_3$ (ref. 13). It has also been observed in the polymerization of ethylene by catalyst systems derived from $TiCl_4$ and $AlEt_3$[14,15], and the homogeneous catalyst systems[16] such as $(\eta^5$-$C_5H_5)_2TiEtCl - AlEtCl_2$. Additionally some modified catalyst systems, e.g. $VOCl_2.2THF - AlR_3$ in vinyl chloride polymerization, behave in the same way[17]. All of the supported systems studied show maximum initial rates within 10 min of the start of polymerization, and these rates are higher than those for the corresponding soluble systems (see Tables 2 and 3). In all the cases the rates decrease significantly with time, showing that although these supported catalyst systems are more active than the corresponding homogeneous analogues, these are nevertheless somewhat unstable indicating that supporting the catalyst on an insoluble matrix has not achieved increased stability. And as in the case with the rates of many highly active $MgCl_2/EB/TiCl_4 - AlR_3$ catalyst systems the rate decay with time could be fitted to a second order decay pattern. Nevertheless it should not be concluded on the grounds of this evidence alone that the decay process is bimolecular, since the decay in the rate of polymerization of many highly active catalyst systems can be represented better by a modified multi-centre first order decay model[3].

References

1 Chien J C W & Hseih J T T, in *Cordination polymerization, A Memorial of K. Ziegler* edited by J C W Chien (Academic Press, New York) 1975, p. 305.

2 Booth B L, Ofunne G C, Stacey C & Tait P J T, *J organomet Chem*, **315** (1986) 143.

3 Tait P J T & Wang S (Under publication).

4 Wilkinson G & Birmingham J M, *J Am chem Soc*, **76** (1954) 4281.

5 Reynolds L T & Wilkinson G, *J inorg nucl Chem*, **8** (1959) 86.

6 Gorsich R D, *J Am chem Soc*, **82** (1960) 4211; Ethyl Corp., G. Pat. 1217952; *Chem Abst*, **61**, 3434.

7 Surman D J & Vickerman J C, *Applic Surface Sci*, **9** (1981), 108; Surman D J, Van den Berg J A & Vickerman J C, *Surf Inter Anal*, **4** (1982) 160.

8 Chandrasekharan E S, Grubbs R H & Brukaber C H, *J organomet Chem*, **120** (1976) 49.

9 Dawan F & Morel D, *J mol Catal*, **3** (1977) 403.

10 Bond W D, Brubaker C H, Chandrasekharan E S, Gibbon C, Grubbs R H & Kroll L C, *J Am chem Soc*, **97** (1975) 2128.
11 Chang B H, Grubbs R H & Brubaker C H, *J organomet Chem*, **172** (1972) 81.
12 Reichert K H & Meyer K R, *Makromol Chem*, **169** (1969) 163.
13 Tait P J T, *Catalytic polymerization of olefins* – Proceedings of the International Symposium on Future Aspects of olefin polymerization, Tokyo, (1986).
14 Burnett G M & Tait P J T, (Unpublished data); Tait P J T, Ph.D. Thesis, University of Aberdeen, 1959.
15 Danusso F, Sianesi D & Calcagno B, *Chim & Ind*, **40** (1959) 628.
16 Borisovia L F, Fushman E A, Vizen E I & Chivkov N M, *Europ Polymer J*, **9** (1973) 953.
17 Chesworth A C, Haszeldine R N & Tait P J T, *Polymer*, (1973) 224.

Indian Journal of Chemistry
Vol. 27A, December 1988, pp. 1047-1049

Synthesis of Carbene Complexes of Iron from gem-Dichlorocyclopropylcycloalkanes

S S ALAM, M A HASHEM* & S S ULLAH
Department of Chemistry, jahangirnagar University, Savar, Dhaka, Bangladesh

Received 21 *September* 1987; *revised and accepted* 7 *March* 1988

The carbene complex 7-irontetracarbonylbicyclo[4.1.0]heptane(**2**) has been prepared by reacting 7,7-dichlorobicyclo[4.1.0]heptane (**1**) with $Na_2Fe(CO)_4$, whereas 5,10,10-trichloro-5-sodiumirontetracarbonyltricyclo[7.1.0.0^{4,6}] decane (**4**) and 10,10-dichloro-5-irontetracarbonyltricyclo[7, 1.0.0$^{4\,6}$]decane (**5**) have been synthesized by the reaction of disodium tetracarbonylferrate, with 5, 5, 10, 10-tetrachlorotricyclo[7, 1.0.0.$^{4\,6}$]decane (**3**). The complex(**4**) on thermal decomposition affords 5,6,10,10-tetrachlorobicyclo[7.1.0] dec-4-ene(**6**) whereas on irradition it gives 5, 5′-di(5, 10, 10-trichlorotricyclo[7.1.0.0$^{4.6}$]decanyl) (**7**).

Since the first planned synthesis and characterization of a stable transition metal carbene complex by Fischer and Maasböl[1], a series of new preparative routes has been developed. Carbene complexes can now be obtained either from non-carbene complex precursors or by a modification of pre-existing carbene complexes. The reaction of anionic metal complexes with certain organic salts or neutral compounds having highly ionic bonds has been used in several cases for the preparation of carbene complexes[2].

Carbene complexes of iron have been obtained employing similar methods[3]. Herein we report the synthesis and characterisation of carbene complexes of iron starting from simple *gem*-dichlorocyclopropylcycloalkanes. The stability of the formed carbene complexes has also been investigated[4].

Materials and Methods

All reactions and isolation procedures were performed under dry nitrogen atmosphere. IR spectra were recorded on a Beckman IR-4220 spectrophotometer, PMR spectra on Bruker WH-4000MHz and Varian EM-360 (200 MHz) instruments and mass spectra on DS-55 and Varian MAT-711 spectrometers (70 V); only ^{35}Cl values are given. Solvents were distilled under dry nitrogen and kept over molecular sieves prior to use. THF was distilled over sodium and benzophenone.

7,7-Dichlorobicyclo[4.1.0]heptane (**1**) and *cis*-5, 5, 10, 10-tetrachlorotricyclo[7.1.0.0$^{4.6}$]decane (**3**) were prepared by phase transfer catalysis method[5]. Disodium tetracarbonylferrate[6], $Na_2Fe(CO)_4$ was prepared by reacting pentacarbonyliron with sodium amalga in THF.

Reaction of disodium tetracarbonylferrate with 7,7-*dichlorobicyclo*[4.1.0]*heptane*(**1**).

To a suspension of $Na_2Fe(CO)_4$ (5.43 g, 25.4 mmol) in THF (50 ml) was added **1** (1g, 6.1 mmol) in THF (40 ml) with vigorous stirring at $-40°$. Stirring was continued for 3 hr more at $-40°$C and THF removed *in vacuo* to give a reddish brown mass. This was extracted with petroleum ether (40-60°) (2 × 80 ml) and filtered through kieselguhr. Removal of solvent from the filtrate gave light brown liquid, which was chromatographed over a column of silica gel (60-120 mesh) under N_2 atmosphere. Elution with petroleum ether (40-60°) led to two distinct bands, which were collected separately. The removal of solvent from the first fraction gave a light brown viscous compound **2** (1.5 g, 23%), b.p. 192°-94°. IR (cyclohexane): 2050(s), 2020(w), 2005(s) and 1978(w)(ν_{CO})cm^{-1}; PMR (200 MHz, $CDCl_3$): δ0, 9-1.4 (*m*, 4H), 1.5-1.70(*m*, 4H), 1.72-2.10(*m*, 2H); MS: *m/z* 262(M^+, 40%), 234(M − CO, 8), 206 (M − 2CO, 6), 178(M − 3CO, 10), 150(m − 4CO, 15), 94(M − 4CO—Fe, 50), 82(55), 70(65), 57(100). The second fraction gave $Fe_3(CO)_{12}$.

Reaction of cis-5, 5, 10, 10-*tetrachlorotricyclo*[7.1.0.0$^{4.6}$]*decane*(**3**) *with disodium tetracarbonylferrate in THF*

Ligand **3** (1.59g.5.5 mmol) in THF (40 ml) was added dropwise to a suspension of $Na_2Fe(CO)_4$ (5.43 g. 25.4 mmol) in THF at $-40°$. After 2.5 hr THF was removed *in vacuo* to furnish a reddish brown mass which was extracted with petroleum ether (40-60°) (2 × 80 ml) and filtered through kieselguhr. Removal of solvent from the filtrate gave a reddish-brown crystalline mass, which was chromatographed over silica gel (60-120 mesh) column. Elution with petroleum ether gave two distinct bands. The light brown band upon removal of solvent *in vacuo* afforded a light brown crystalline substance **4** (1.1 g, 17%), m.p. 138-40°; IR)cyclohexane): 2255(s), 2043(vs) and 2025(s) (νCO)cm^{-1}; PMR (400 MHz, $CDCl_3$): δ0.85-0.90(*m*

6 – H), 1.20-1.30 (*m*, 7 – H), 1.56-1.67 (*m*, 3, 4—H), 1.67-1.80(*m*, 2.8—H), 2.10-2.25(*m*, 1,9—H); MS: *m/z* 428(M^+, chlorine isotopic pattern, 1), 405 (M – Na, 1), 400(M-CO, 1), 372(M—2CO, 1), 364(M—HCl—CO, 1), 349(M—Na—2CO, 1), 344(M—3CO, 1), 336(M—HCl—2CO, 1), 321(M—Na—3CO, 1), 316(M—4CO, 1), 308(M—HCl—3CO, 1)293(M—Na—4CO, 1) 280(M—HCl-4HCO, 1), 257(M—Na—4CO—HCl, 1), 249(N—Na—2HCl—3CO, 1), 237 [M—Na—$Fe(CO)_4$, 4], 201(M—Na—$Fe(CO)_4$—HCl, 8], 189[M—Na—$Fe(CO)_4$—HCl—C, 10], 165[M—2HCl—Na—$Fe(CO)_4$, 12], 129[M—3HCl—Na—$Fe(CO)_4$, 20], 109(100). The green band was identical with $Fe_3(CO)_{12}$.

The same reaction was repeated for 3.5 hr when another light brown crystalline compound **5** (1.8 g, 19%), m.p. 145-47° was isolated; IR (cyclohexane): 2260(s), 2040(vs), 2015(s, (νCO)cm^{-1}; PMR (200 MHz, C_6D_6), δ0.65-1.25 (m, 8H), and 1.26-1.63(m, 4H), MS: *m/z* No M^+, 334(M—HCl, Cl— isotopic pattern, < 1), 306(M—HCl—CO, 1), 278(M—HCl—2CO,1), 272(M—2Cl—CO, 1), 250(M—HCl—3CO, 1); 222(M—HCl—4CO, 1) 187(M—HCl—Cl—4CO, 1) 166[M—HCl—$Fe(CO)_4$, 2], 131[M—HCl—Cl—$Fe(CO)_4$, 6], 130[M—2HCl—Fe(!CO)$_4$, 6], 127(30), 109(100), 101(30), 91(64), C, H-analysis (Found: C, 45.1; H, 3.03, $C_{10}H_{12}Fe(CO)_4Cl_2$ requires C, 45.4; H, 3.2%).

Thermal decomposition of complex **4** *into complex* **6**

Complex **4** (0.45 g, 1.05 mmol) dissolved in cyclohexane was refluxed with continuous stirring for 2 hr. The solvent was removed under reduced pressure when a pure white crystalline substance **6** (0.18 g, 63%), m.p. 150-52° was obtained; IR (nujol mull): 1605(vs) ($\nu_{C=C}$)cm^{-1}; PMR(200 MHz, CD_2Cl_2): δ1.10-1.30(*m*, 2H), 1.40-1.80(*m*, 6H), 2.0-2.31(*m*, 2H), 3.30-3.50(*m*, 6-H) and 5.7-5.8(*m*, 4-H); MS: *m/z* no M^+, 237(M-Cl, Cl-isotopic pattern, 4%), 202(M-2Cl, 12), 167(m-3Cl, 10), 132(M-4HCl, 8), 109(100), 91(100), and 77(55).

Photochemical conversion of complex **4** *into* **7**.

A degassed solution of **4** (0.4 g, 1.05 mmol) in benzene (50 ml) was irradiated with a medium pressure mercury lamp for 1.25 hr. After completion of irradiation the reaction mixture was filtered through kieselguhr under N_2 atmosphere to give colourless filtrate, which upon concentration under reduced pressure, gave **7** as a pure white crystalline solid (0.19 g, 39%), m.p. 158-60°; PMR (200 MHz, CD_2Cl_2): δ1.2-1.3(*m*, 2H), 1.50-1.82(*m*, 16H), 2.05-2.40 (m, 6H); MS: *m/z* no M^+, 237(M^+/2, isotopic pattern of chlorine atom, 6%), 202(M/2—Cl, 18), 167(M/2-2Cl, 8), 132(M/2-3Cl, 6), 109(80), 91(100) and 77(48). (Found: C, 49.1; H, 4.9 $C_{20}H_{24}Cl_2$ requires C, 50.6; H, 5.1%).

Results and Dsicussion

The reaction of $Na_2Fe(CO)_4$ with the ligand (**1**) in 4:1 molar ratio at – 40°C gave the light brown complex **2** (22%) (Scheme 1) which was not stable when exposed to atmosphere. The IR spectrum at **2** exhibited four sharp νC = O modes at 2050, 2020, 2005 and 1978 cm^{-1}. The upward shift in the νC = O modes in comparison to that of $Na_2Fe(CO)_4$ at 1790 cm^{-1} indicated the formation of the complex. The IR spectrum of **2** also indicated that an $Fe(CO)_4$ moiety was attached to the ligand **1** via iron-carbon double bond. The PMR spectrum of **2** displayed a four-proton multiplet at δ1.50-1.70 due to 2, 2, 5, 5-methylene protons. The low field multiplet at δ1.75-2.10 could be assigned to H-1 as H-6. The upfield shift of 3, 3, 4, 4-protons(4H) at δ0.9-1.4 is believed to be due to the anisotropic effect of the carbonyl group and metal-carbon double bond. Therefore, the PMR spectrum of **2** also indicates that $Fe(CO)_4$ moiety is attached through C-7 of the organic ligand. In the mass spectrum the molecular ion peak at *m/z* 262 was compatible with the composition of **2** as $C_7H_{10}Fe(CO)_4$. Successive loss of four carbon monoxide units gave the peaks at *m/z* 234, 206, 178, 150. The peak at 94 was due to the loss of $Fe(CO)_4$ moiety from the molecular ion (M^+).

The reaction of $Na_2Fe(CO)_4$ with the ligand(**3**) in 4:1 molar ratio at – 40° for 2.5 hr led to the complex **4**. The IR spectrum of **4** exhibited the three/νC = O modes at 2255, 2043 and 2025 cm^{-1} in comparison to that at 1790 cm^{-1} in $Na_2Fe(CO)_4$ indicating the formation of a complex. In the PMR spectrum the low field multiplet at δ2.10-2.25 was assigned to H-1 and H-9, with multiplet at 1.67-1.80 and 1.56-1.67 to H-2, H-8 and H-3, H-4 respectively. The H-6 and H-7 appeared as multiplets at δ0.85-0.90 and 1.20-1.30 respectively. Mass spectrum of **4** gave the parent molecular ion (M^+) peak at *m/z* 428 with isotopic

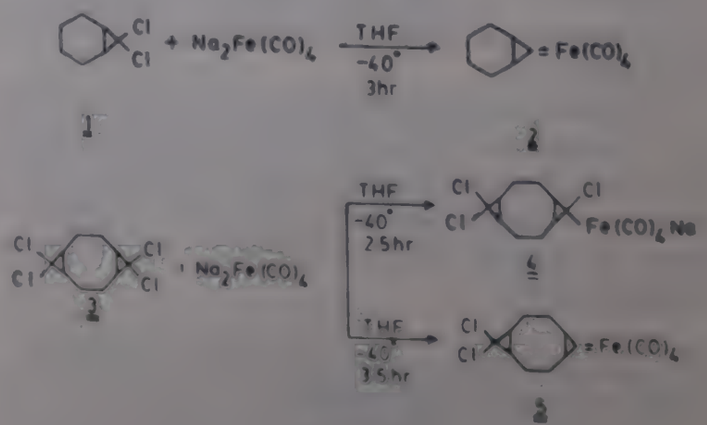

Scheme 1

mass of chlorine atoms, which favourably fitted the proposed molecular formula $C_{10}H_{12}Cl_3Fe(CO)_4Na$. Apart from the parent molecular ion peak it also exhibited peaks at 400, 372, 344 and 316 corresponding to the successive loss of four carbon monoxide units. The peak at 237 was due to the loss of $NaFe(CO)_4$ moiety. The same reaction when repeated for a little longer time (3.5 hr) led to another crystalline solid **5**. The IR spectrum of **5** exhibited three $\nu C=O$ modes at 2260, 2040 and 2015 cm^{-1} indicating it to be different from **4**. In its PMR spectrum the broad multiplet at δ0.65-1.25 was assigned to 2, 2, 3, 3, 7, 7, 8, 8-H and that at 1.26-1.64 due to 1, 4, 6, 9-H. In mass spectrum there was no molecular ion (M^+) peak. The peaks at *m/z* 334, 336 with intensity for chlorine isotopic pattern, were due to the loss of HCl unit from M^+. The peaks at 306, 278, 250, 222 were due to the successive loss of four CO units from *m/z* 334. The peak at *m/z* 166 was due to the loss of $Fe(CO)_4$ moiety from *m/z* 334. On the above fragmentation pattern, it can be assumed that the molecular ion should be at *m/z* 370, which corresponded to the molecular formula $C_{10}H_{12}Cl_2Fe(CO)_4$ for the complex **5**.

Thermal decomposition of **4** in cyclohexane for 2 hr resulted a white crystalline compound **6**, m.p. 150-52° (Scheme 2). The compound **6** decomposed very slowly in air. This compound was unsaturated and contained chlorine atom. The IR spectrum of **6** did not exhibit any $\nu C=O$ modes but displayed a band at 1605 cm^{-1} assignable to $\nu C=C$ mode. This clearly indicated the formation of an unsaturated compound. The low field one-proton multiplet at δ5.7-5.8 was assigned to unsaturated proton H-4 and the one-proton multiplet at 3.30-3.50 was assigned to C_6-H in which chlorine atom was attached. The two-proton multiplet at δ2.0-2.30 could be due to H-1 and H-9. The mass spectrum of **6** did not show the parent molecular ion(M^+) peak but the peaks appearing at *m/z* 237 202, 167 and 132 were due to the successive loss of four chlorine atoms. On the above fragmentation pattern, it can be assumed that the molecular ion (M^+) peak should be at *m/z* 272 which corresponded to the molecular formula $C_{10}H_{12}Cl_4$ for **6**. The formation of **6** has been rationalised in Scheme 2.

Photochemical irradiation of **4** in benzene for 1.25 hr gave **7** as a white crystalline solid m.p. 158-60° (Scheme 2). It is a stable compound. The IR spectrum of **7** was devoid of $\nu C=O$ modes and in the PMR spectrum the high field multiplet at δ1.2-1.3 could be assigned to H-9, 9′ and the sixteen-proton multiplet at 1.5-1.82 was assigned to H-2, 2′, 3, 3′, 7, 7′- and 8, 8′.

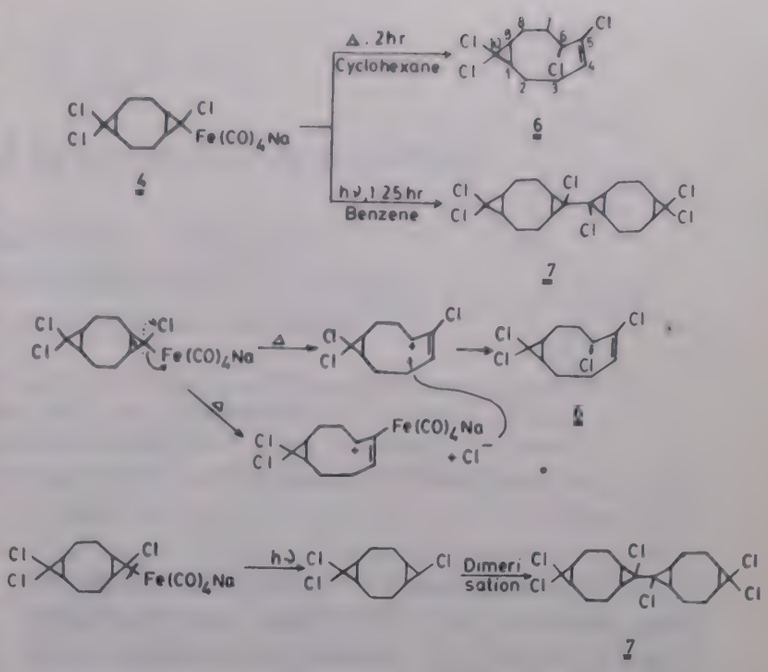

Scheme 2

The low field six-proton multiplet at δ2.05-2.40 could be assigned to H-4, 4′, 6, 6′ and 1, 1′. Mass spectrum of **7** did not show the parent molecular ion (M^+) peak, but was cleaved into two equal fragments to give peaks at *m/z* 237, 239, 241, 243 showing the isotopic patterns of chlorine atoms. The peaks at *m/z* 202, 167 and 132 were due to the successive loss of three chlorine atoms from the half part. From the spectroscopic analysis it is assumed that the **7** was a dimer of molecular weight 237. The intermediate monomeric radical was formed pherhaps through the homolytic fission of carbon-metal bond (Scheme 2).

Acknowledgement

We thank the Institute of Organic Chemistry, Technical University, Berlin, West Germany and Department of Chemistry, Australian National University, Canberra, for the spectral analyses.

References

1 Fischer E O & Maasböl A, *Angew Chem*, **76** (1964) 645; *Angew Chem (Int Ed Engl)*, **3** (1964) 580.
2 Öfele K, *Angew Chem*, **80** (1968) 1032; *Angew Chem (Int Ed Engl)*, **7** (1968) 950.
3 Gompper R & Bartmann E, *Angew Chem*, **90** (1978) 490; *Angew Chem (Int Ed Engl)*, **17** (1978) 457.
4 Huheey J E, *Inorganic chemistry, Principles of structure and reactivity* (Harpot, New York) 404.
5 (a) Makosza M & Warzynicwicz M, *Tetrhedron Lett*, (1969) 4659.
(b) Dehmlow E V, *Angew Chem*, **86** (1974) 187; *Angew Chem (Int Ed Engl)*, **13** (1974) 170.
6 Collman J P, *Acc chem Res*, **8** (1975) 342.

Indian Journal of Chemistry
Vol. 27A, December 1988, pp. 1050-1052

Synthesis & Reactions of Isotetralenetricarbonyliron

M N ABSER, M A HASHEM, S E KABIR & S S ULLAH*
Department of Chemistry, Jahangirnagar University, Savar, Dhaka, Bangladesh

Received 23 *November* 1987; *revised and accepted* 14 *March* 1988

The complex isotetralenetricarbonyliron (I) has been synthesized by the photochemical reaction of isotetralene with $Fe(CO)_5$. Complex(I) on reaction with $Ph_3C^+BF_4^-$ affords the trienyl salt $[C_{10}H_{11}Fe(CO)_3]BF_4$ (II) via hydride abstraction. Complex(II) reacts with $NaBH_4$ to give back complex (I). The complexes have been characterized on basis of IR, PMR and mass spectra and elemental analyses.

Photochemical synthesis of metal-olefin complexes using $Fe(CO)_5$ and cycloolefins precursors has been the subject of considerable research mainly because this method operates under considerably milder conditions than the conventional thermal method[1-5]. In such complexes the bonding of an organic group to a transition metal can be used to modify the reactivity and regiospecificity[6] and this property is particularly useful in organic synthesis. The synthesis and hydride abstraction reactions of *trans, trans, trans*-1,5,9-cyclododecatrienetricarbonyl-iron[4], *trans*-1,4,9-decatrienetricarbonyliron[7] and limonenetricarbonyliron[5] have been recently reported from our laboratory. Iron carbonyl derivatives of polycyclic polyenes are, however, rare. Herein we report the photochemical synthesis of the title compound (I) and its reaction with triphenylmethyltetrafluoroborate.

Materials and Methods

All operations were carried out *in vacuo* or under N_2 atmosphere. Infrared spectra were recorded on a PE 983 spectrophotometer, PMR spectra on Bruker WH 360 and Varian XL 200 instruments and mass spectra on a high resolution MS-12 spectrophotometer. Photochemical reactions were carried out in sealed glass tubes by irradiating with a 125 watt medium pressure mercury lamp. Solvents were distilled under nitrogen and kept over molecular sieves prior to use.

Triphenylmethyltetrafluoroborate was prepared according to the published method[8]. Isotetralene (Aldrich) was used as received.

Photochemical reaction of isotetralene with $Fe(CO)_5$: Formation of isotetralenetricarbonyliron(I)

A mixture of pentacarbonyliron (0.9 g, 4.5 mmol) and isotetralene (0.6 g, 4.5 mmol) in benzene (30 ml) was irradiated in a sealed tube for 10 hr and filtered through kieselguhr. Removal of solvent *in vacuo* afforded a yellow oil, which was subjected to column chromatography over silica employing pet. ether (40-60°) as an eluent. Removal of solvent under reduced pressure afforded I as yellow oil in 73% yield; IR(cyclohexane): νCO 2040 and 1956 cm^{-1}; PMR($CDCl_3$): δ 5.0-6.0 (*m*, 2H) and 0.8-3.6 (*m*, 10H); MS: *m/z* 272 (M^+), 244 ($M^+ - CO$), 216 ($M^+ - 2CO$) and 188 ($M^+ - 3CO$). (Found: C, 57.9; H, 4.8. $C_{13}H_{12}O_3Fe$ requires C, 57.4; H, 4.5%).

A similar reaction using excess pentacarbonyliron (2.7 g, 13.5 mmol) and isotetralene (0.6 g, 4.5 mmol) followed by similar work-up also afforded the same complex (I); no other product was isolated.

Reaction of complex-I with triphenylmethyltetrafluoroborate: Formation of complex-II

To a dry dichloromethane solution (5 ml) of complex-I (0.5 g, 1.4 mmol), was added a solution of triphenylmethyltetrafluoroborate (0.60 g, 1.8 mmol) in the same solvent. The mixture was stirred at room temperature for 1 hr under nitrogen when a pale yellow precipitate began to appear. Dry ether was added for complete precipitation. The product was separated by decantation of the supernatant liquid, washed with dry ether and dried under reduced pressure to afford the fairly air-stable pale yellow crystalline trienyl salt, $[C_{10}H_{11}Fe(CO)_3]BF_4$(II) (0.42 g, 63%), which crystallized from dichloromethane/ether, m.p. 271-73°(d); IR(nujol): νCO 2120 and 2070 cm^{-1}; PMR(CD_3CN): δ 7.87 (*dd*, 1H, *J*=6.0, 4.0 Hz), 7.45 (*dd*, 1H, *J*=6.0, 4.0 Hz), 6.90 (*d*, 1H, *J*=6.0 Hz), 5.6-6.0 (*m*, 2H), 3.95-4.35 (*m*, 2H) and 2.6-3.4 (*m*, 4H); MS: *m/z* 271 (M^+), 243 ($M^+ - CO$), 215 ($M^+ - 2CO$) and 187 ($M^+ - 3CO$) (Found:

C,44.0; H, 3.6. $C_{13}H_{11}FeO_3BF_4$ requires C, 43.6; H, 3.1%).

Reaction of complex-II with $NaBH_4$: Formation of complex-I

To an aqueous suspension (10 ml) of II (0.1 g, 0.3 mmol) was added sodium borohydride (0.03 g, 0.3 mmol) in water (5 ml). The mixture was stirred for 1 hr, extracted with ether, dried ($MgSO_4$) and the solvent removed under reduced pressure. The yellow oil obtained was purified by column chromatography over silica, eluting with pet. ether (40-60°). Removal of solvent *in vacuo* afforded a yellow liquid, identical (IR, PMR, mass) with complex-I.

Results and Discussion

The structure of complex-I, in which isotetralene is bonded to $Fe(CO)_3$ moiety through two of its non-conjugated double bonds, has been confirmed as follows: The lowfield PMR signals at δ 5.02-6.0 have been assigned to the free olefinic protons and these at higher field at δ 0.66-3.4 are attributable to the olefinic protons coordinated to $Fe(CO)_3$ moiety and the methylene protons bonded to sp^3 carbon atoms. The mass spectrum shows the molecular ion peak at *m/z* 272 (M^+) and other peaks at *m/z* 244, 216, 188 and 132 indicate successive loss of three CO units and Fe; the presence of $Fe(CO)_3$ moiety in the complex is thus evident[9].

A common tendency in tricarbonyl(diene or triene)iron complexes is the formation of cations by hydride abstraction when treated with triphenylmethyltetrafluoroborate[4-7,10-13]. Accordingly the trienyl salt (II) obtained by reacting complex-I with $Ph_3C^+BF_4^-$ exhibits in its IR ν(CO) bands at 2120 and 2070 cm^{-1} which are of similar pattern but shifted to higher frequencies than those of the corresponding neutral complex (2048 and 1956 cm^{-1}) indicating that I and II have similar structures but with greater positive charge at the metal atom of complex-II. Similar observations were reported for a number of dienyl- or trienyl-tricarbonyl-iron complexes[4,10]. The structure of salt (II) is further supported by PMR and mass spectra and elemental analyses. The low field PMR signals at δ 6.90 (*d*, 1H, $J_{AB}=6$ Hz), 7.45 (*dd*, 1H, $J_{AB}=6$ Hz, $J_{BC}=4.0$ Hz) and 7.87 (*dd*, 1H, $J_{CD}=6$ Hz, $J_{BC}=4.0$ Hz) have been assigned to allylic protons H_A, H_B and H_C respectively (Scheme 1). The signals at δ 5.6-6.0 (*m*, 2H) and 2.6-3.4 (*m*, 4H) have been assigned to the free olefinic protons and the methylene protons of the same ring respectively and those at δ 3.95-4.35 (*m*, 2H) to the

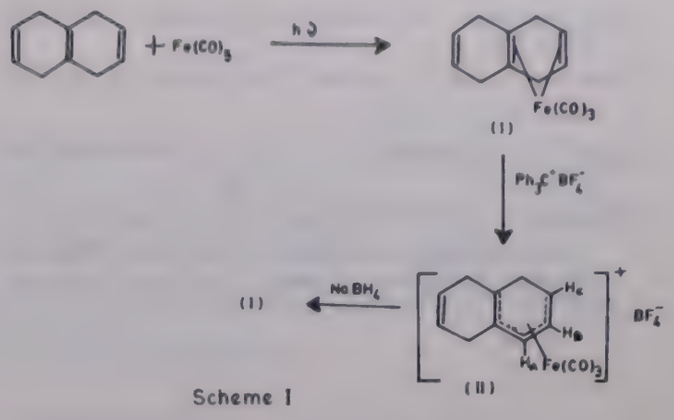

Scheme 1

methylene protons adjacent to the allylic system. This assignment is in contrast to our previous observations according to which the central carbon atom of an allylic group bonded to an $Fe(CO)_3$ moiety is particularly electronegative and consequently the proton attached to it resonate at higher field. In complex-II the H_A proton is more shielded than H_B and H_C protons and hence appears as a doublet at higher field (δ 6.90) showing coupling to H_B. A plausible explanation for this may be that the stereochemical arrangement of H_A is such that it is more closer to the metal than H_B and H_C.

The mass spectrum of II showed the highest peak at *m/z* 271 corresponding to the cationic part $[C_{10}H_{11}Fe(CO)_3]^+$ of the complex-II. Other peaks at 243, 215 and 187 indicate successive loss of three CO units from $[C_{10}H_{11}Fe(CO)_3]^+$. Elemental analyses are also in agreement with the formula proposed for complex II, which also satisfies the 18-electron rule.

Treatment of the trienyl salt(II) with $NaBH_4$ leads to I. It is suggested that H^- attack on II leads to the reformation of the original neutral complex-I. Similar observations have been reported in literature[10,14,15].

Acknowledgement

The PMR and mass spectra were obtained through the courtesy of the Department of Chemistry, Tasmania University, Australia, Technical University, Berlin, West Germany and University College, London.

References

1 Lewis J & Parkins A W, *J chem Soc (A)*, (1967) 1150.
2 Rosenblum M, North B, Wells D & Giering W P, *J Am chem Soc*, **94** (1972) 1239.
3 Grubbs R H & Pancoast T A, *Synth react inorg Metal org chem*, **8** (1978) 1.
4 Ullah S S, Kabir S E, Molla M E & Wahiduzzaman S M, *Indian J Chem*, **23A** (1984) 180.
5 Ullah S S, Molla M E & Begum N, *Indian J Chem*, **23A** (1984) 992.
6 Pearson A J, *Transition Met Chem*, **6** (1981) 67.

7 Ullah S S, Molla M E & Molla A H, *Indian J Chem*, **23A** (1984) 995.

8 Dauben H J, Lewis J, Homen R & Marmon K M, *J org Chem*, **25** (1960) 1442.

9 Victor R, Ben-Shoshan R & Sarel S, *Tetrahedron Lett*, (1970) 4259.

10 Deeming A J, Ullah S S, Domingos A J P, Johnson B F G & Lewis J, *J chem Soc Dalton*, (1974) 2093; Ullah S S, *Synthesis & reactions of some* 1,5-*cyclooctadiene complexes of iron & osmium*, Ph D Thesis, University College, London, 1971.

11 Pettit R, *J organometal Chem*, **100** (1975) 205.

12 Birch A J & Jenkins I D, *Transition metal organometallics in organic synthesis*, Vol 1 (Academic Press, New York) 1976 pp. 1.

13 Pearson A J, *Acc chem Res*, **13** (1980) 463.

14 Fischer E O & Fischer R D, *Angew Chem*, **72** (1960) 719.

15 Khand I U, Pauson P L & Watts W E, *J chem Soc (C)*, (1969) 2024.

Indian Journal of Chemistry
Vol. 27A, December 1988, pp. 1053-1055

Alkoxy Boron-bridged Macrocyclic Compounds of Nickel(II) with 1,1′,8,8′-Tetraalkoxy-1,8-dibora-4,5,11,12-tetraphenyl-3,6,10,13-tetraaza-2,7,9,14-tetraoxatetradecacyclo-3,5,10,12-tetraene & 1,1′,9,9′-Tetraalkoxy-1,9-dibora-4,6,12,14-tetramethyl-3,7,11,15-tetraaza-2,8,10,16-tetraoxa-cyclohexadeca-3,6,11,14-tetraene

H C RAI*, JAYA TIWARY & REKHA KUMARI
Department of Chemistry, L S College, University of Bihar, Muzaffarpur

Received 31 *August* 1987; *revised* 23 *February* 1988; *accepted* 29 *March* 1988

A series of 14- and 16-membered alkoxyboron-bridged macrocyclic complexes of nickel(II) of the type $NiL^{1,2}$ where L^1 = 1,1′,8,8′-tetraalkoxy-1,8-dibora-4,5,11,12-tetraphenyl-3,6,10,12-tetraaza-2,7,9,14-tetraoxatetradecacyclo-3,5,10,10-12-tetraene and L^2 = 1,1′,9,9′-tetraalkoxy-1,9-dibora-4,6,12,14-tetramethyl-3,7,11,15-tetraaza-2,8,10,16-tetraoxacyclohexadeca-3,6,11,14-tetraene have been prepared by adopting an '*in situ*' procedure using nickel(II) chloride, dioxime and boric acid. The hydroxy or alkoxy groups have been derived from the solvent molecules. All the compounds are spin-paired, crystalline and intensely coloured solids. Infrared and electronic spectra show that they are isotructural and possess a nearly square planar configuration.

Recently, a series of clathrochelates of iron(II) with pentan-2,4-dione dioxime and 1,2-diphenylethane-1,2-dione dioxime have been reported[1]. It has also been reported that bis(dimethylglyoximato)copper(II) and bis(acetylacetonedioximato)copper(II) complexes yield trinuclear cluster complexes with copper(II) salts, having the stoichiometries $Cu_3L_2X_4(NO_3)_2$ (L=DMG)[2]. The nickel(II) and cobalt(II) analogues with pentane-2,4-dione dioxime have been reported[3].

Sahoo *et al.*[4] have reported a number of 14- and 16-membered macrocyclic complexes of nickel(II) and cobalt(II) of the types $NiL_2(BF_2)_2$ and $CoL_2(BF_2)_2.2H_2O$ (H_2L=pentane-2,4-dione dioxime, 1,2-diphenylethane-1,2-dione dioxime or 1,2-difurylethane-1,2-dione dioxime) alongwith a copper(II) macrocyclic complex, $CuL_2(BF_2)_2$, where L represents the dianion of 1,2-diphenylethane-1,2-dione dioxime[4].

In the present paper, we report a series of complexes of nickel(II) of the type, $NiL^{1,2}$, with the title ligands L^1 and L^2 (structures I, II).

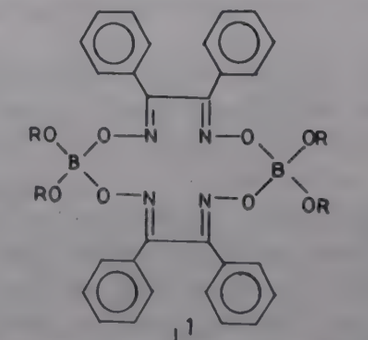

L^1

R=-H,-CH_3,C_2H_5,-C_3H_7,-C_4H_9

(I)

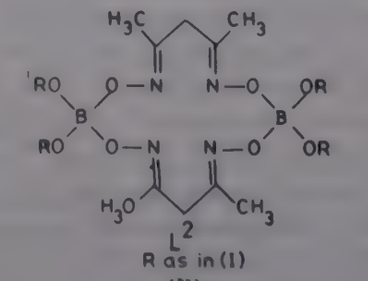

L^2

R as in (I)

(II)

Materials and Methods

All the chemicals used were BDH, E. Merck or S. Merck reagents. Pentane-2,4-dione dioxime and 1,2-diphenylethane-1,2-dione dioxime were prepared following literature procedures and their melting points agreed well with the reported values[5,6]. All the compounds have been prepared under similar experimental conditions and the preparation of one of the compounds is described here as an example.

1,1′,9,9′-Tetraethoxy-19,dibora-4,6,12,14-tetramethyl-3,7,11,15-tetraaza-2,8,10,16-tetraoxacyclohexadeca-3,6,11,14-tetraene-nickel(II)

A mixture of $NiCl_2 \cdot 6H_2O$ (2.4 g, 0.01 mol), pentane-2,4-dione dioxime (2.6 g, 0.02 mol), boric acid (1.24 g, 0.02 mol) and 40 ml of dry ethanol was stirred and refluxed for about 30 min on a water bath whereupon the solution gradually

Table 1—Analytical, Colour and Electronic Spectral Data of $NiL^{1,2}$

Complexes	Colours	Found (Calc.)%				λ_{max} (cm^{-1})*
		Ni	C	H	N	
NiL^1, R = H	Red	9.39 (9.44)	53.81 (53.76)	3.82 (3.84)	8.92 (8.96)	20,800b, 30,400s
NiL^1, R = CH_3	Pink	9.46 (9.50)	56.42 (56.38)	4.67 (4.69)	8.17 (8.22)	20,350b, 30,000s
NiL^1, R = C_2H_5	Orange yellow	7.98 (8.00)	58.55 (58.61)	5.37 (5.42)	7.56 (7.59)	20,400b, 30,700s
NiL^1, R = i-C_3H_7	Reddish brown	7.39 (7.44)	60.49 (60.53)	6.00 (6.05)	7.02 (7.06)	20,500b, 30,500s
NiL^1, R = n-C_4H_9	Violet	6.98 (6.94)	62.16 (62.19)	6.61 (6.59)	6.48 (6.59)	20,200b, 30,300s
NiL^2, R = H	Yellow	14.32 (14.56)	29.95 (29.62)	4.84 (4.93)	13.78 (13.82)	20,700b, 30,200s
NiL^2, R = CH_3	Deep brown	12.81 (12.79)	35.98 (36.44)	6.10 (6.07)	12.08 (12.14)	20,400b, 30,100s
NiL^2, R = C_2H_5	Yellow	11.39 (11.41)	41.69 (41.77)	6.88 (6.96)	10.80 (10.83)	20,600b, 31,000s
NiL^2, R = i-C_3H_7	Orange	10.18 (10.29)	46.11 (46.07)	7.72 (7.67)	9.74 (9.77)	20,500b, 30,700s
NiL^2, R = n-C_4H_9	Violet	9.33 (9.38)	49.59 (49.60)	8.19 (8.26)	8.85 (8.90)	20,300b, 30,500s

*The molar extinction coefficients have been found to be of the order of 10^3.

turned yellow and the colour deepened on slow addition of about 2.0 g of borax in small quantities during reflux. The solution thus obtained was allowed to concentrate by slow evaporation at room temperature over a period of several hours when an yellow crystalline product was obtained. It was filtered off, washed with small quantities of ethanol and recrystallized from acetonitrile. Yield was nearly 50%. Hydroxy, methoxy, isopropoxy and *n*-butoxy boron compounds were prepared using water, methanol, *iso*-propanol and *n*-butanol respectively as the solvents. Nickel in the complexes (Table 1) was analysed at our laboratory using the standard procedure[7]. C, H and N analyses were done at CDRI, Lucknow. The analytical data are in good agreement with the reported formulae, $NiL^{1,2}$. IR spectra of the complexes were recorded in the range 4000-250 cm^{-1} on a Beckman spectrophotometer.

Results and Discussion

Preparation of the compounds

The reaction taking place in the synthesis of alkoxy boron-bridged macrocyclic compounds using nickel II chloride, pentane-2,4-dione dioxime of 1,2diphenylethane-1,2-dione dioxime and boric acid involves a high degree of molecular re-arrangement in which two dioxime molecules, two boric acid molecules, one nickel II ion and four solvent molecules participate and it can be represented by the equation:

$$NiCl_2 + 2H_2L + 2H_3BO_3 + 4ROH = NiL_2[B(OR)_2]_2 + 6H_2O + 2HCl$$

where H_2L = pentane-2,4-dione dioxime, or 1,2-diphenylethane-1,2-dione dioxime; R = $-H$, $-CH_3$, $-C_6H_5$, $-i-C_3H_7$ or $-n-C_4H_9$.

Both hydrogen ion and water, which are formed during the reaction, besides the macrocyclic compound, have a considerable effect on the reaction. The concentration of water has to be kept at the minimum by using dry alcohols in order to prevent contamination of one compound with another which may be formed on account of the *trans*-esterification reaction. It is also essential to maintain an optimum acidity in the reaction mixture for effective cyclisation. This has been achieved by adding small amounts of borax, so that the progress of the reaction is controlled by the addition of borax or sodium acetate. The metal ions undoubtedly play a pivotal role in the reaction process by binding the dioxime moieties in an *anti*-configuration and place the oxygen atoms of the oxime groups in suitable geometrical positions for reaction with the boron containing molecules.

Infrared spectra

Some striking differences between the IR spectra of the ligands (pentane-2,4-dione dioxime and 1,2-diphenylethane-1,2-dione dioxime) and their nickel II

macrocyclic compounds have been observed with regard to sharpness, intensity and positions of important vibrational bands such as $\nu C{=}N$, $\nu N-O$ and $\nu B-O$, which provide valuable information for elucidation of the structures. However, it is significant to note that there is an overall similarity in the spectra of all the macrocyclic compounds with minor variations arising due to $-CH_2$ or $-CH_3$ deformation vibrations in the case of pentane-2,4-dione dioxime and phenyl ring vibrations in the case of 1,2-diphenylethane-1,2-dione dioxime. This indicates that the compounds possess similar structures.

The oximes and the bis(dioximato)nickel(II) complexes exhibit a broad and smooth band at 3200 cm^{-1} which is assigned to $\nu O-H$ mode of the hydrogen bonded oximes. In the macrocyclic compounds, this band completely disappears clearly implying the breakdown of $O-H$ bonds during the reaction of the oximes with boric esters; however, the hydroxy compounds show characteristic band due to $\nu O-H$. A sharp and intense band in the region 1660-1580 cm^{-1} is observed for all the compounds which has been assigned to $\nu C{=}N$. It is observed that the $\nu C{=}N$ mode in all the compounds appears at a higher frequency with reduced intensity as compared to that in the free oximes[2-4].

All the compounds show two intense and sharp bands in the regions 1240-1225 and 1100-1060 cm^{-1} which have been attributed to $\nu N-O$ vibrations. These bands, like the $\nu C{=}N$ vibration, also appear at higher frequencies in the complexes compared to their positions in the free oximes and these results are consistent with the earlier findings[3].

Besides the above mentioned general similarity between the spectra of complexes of the two series with those of the ligand L^1 and L^2, an additional group of four bands appears in the spectra of the ligand L^1 and its complexes which have been assigned to the phenyl ring vibrations. They appear at ~1590, ~1570, ~1500 and ~1440 cm^{-1}.

The most striking feature in the spectra of the compounds is the appearance of intense, sharp and clearly identifiable bands in the region 1200-780 cm^{-1} which are absent in the spectra of the free oximes and bis-dioximato metal complexes. The bands appear at ~1190, ~1000 and ~790 cm^{-1} and have been assigned to the $B-O$ stretching vibrations.

The ligands L^1 and L^2 are coordinated to the nickel(II) ion in a tetradentate manner through the nitrogen atoms so as to fully encircle the metal ion. The electronic spectra and magnetic moments, which are described in the following paragraphs, are consistent with the planar structure(III) of the compounds.

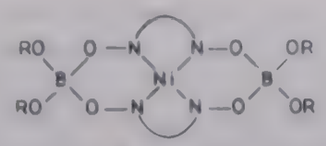

R as in (I)

(III)

Magnetic susceptibility measurements were carried out by the Gouy method using $Hg[Co(CNS)_4]$ as a calibrant. All the compounds were found to be diamagnetic with the spin singlet, $^1A_{1g}$, as the ground state. Their electronic spectra, recorded using a Beckman spectrophotometer, are dominated by intense bands in the visible and UV regions. The spectra consist of a broad band in the region 20,000-22,000 cm^{-1} and can be interpreted in terms of a planar structure(III). The width of the spectral band manifests[8] that the band represents a group of two to three transitions, the overlapping transitions being $^1A_{2g} \leftarrow {}^1A_{1g}$, $^1B_{2g} \leftarrow {}^1A_{1g}$ and $^1E_g \leftarrow {}^1A_{1g}$. The more intense bands observed beyond 30,000 cm^{-1} are believed to arise from $M \rightarrow L(\pi^*)$ charge-transfer transitions.

Acknowledgement

The authors express their gratitude to Prof. T. Sharma, Head, University Department of Chemistry, University of Bihar, Muzaffarpur for providing laboratory facilities. They also thank Dr. L.K. Mishra, Department of Chemistry, Patna University, Patna for help in analytical and magnetic measurements. One of the authors (J.T.) is thankful to the authorities of the University of Bihar, Muzaffarpur for financial support.

References

1 Rai H C, Jena A K & Sahoo B, *Inorg chim Acta*, **35** (1979) 29.
2 Singh C B & Sahoo B, *J inorg nucl Chem*, **36** (1974) 1259.
3 Singh C B, Rai H C & Sahoo B, *Indian J Chem*, **15A** (1977) 691.
4 Chakrabarti J & Sahoo B, *Indian J Chem*, **21A** (1982) 48.
5 Wild F, *Characterization of organic compounds*, (Cambridge Univ Press, London) 1962, 119.
6 *Beilstein's hand buch der organischen chemie*, Band VII, (Verlag Von Julius Springer, Berlin) 1937, 700.
7 Vogel A I, *A text book of quantitative inorganic analysis*, 2nd edn (Longmans Green, London) 1957.
8 Gray H B in *Transition metal chemistry*, Vol. I, edited by R L Carlin (Marcel Dekker, New York) 1965.

Indian Journal of Chemistry
Vol. 27A, December 1988, pp. 1056-1059

Intercalated Compounds of Cu(II) Montmorillonite Clay with 1,2-Diaminoethane & 1,2-Diaminopropane

NITIN LABHASETWAR & O P SHRIVASTAVA*
Department of Chemistry, Dr. H.S. Gour Vishwavidyalaya, Sagar, 470 003

Received 27 *July* 1987; *revised* 27 *February* 1988; *accepted* 22 *March* 1988

Synthesis and characterisation of two intercalated compounds are reported in which the Cu(II)-exchanged montmorillonite clay behaves as a host compound for 1,2-diaminoethane and 1,2-diaminopropane. Chemical analyses and infrared spectra of these compounds reveal that Cu(II) present inside the interlayer spacings of the clay channels forms coordination compounds with 1,2-diaminoethane and 1,2-diaminopropane. The lattice expansion in the clay has been confirmed by IR spectra and X-ray powder diffraction patterns of the intercalated compounds. It has been observed that the silicate layer lattice expands on chelation along the *c* axis. In view of the nitrogen retaining property of the clay framework through coordination, these compounds show promise as nitrogen immobilizing agents in clays.

Ion exchange capacity of clay minerals has been thoroughly investigated by several workers. The montmorillonite group of clays, having the general formula $(Al, Mg)_{2-3}(Si, Al_4)O_{10}(OH)_2nH_2O$[1], can take up water between the structural layers and show cation exchange properties[2]. Several workers have investigated the typical layered silicate lattice compounds and demonstrated their remarkable ion exchange capacities[3-7]. Many attempts have been made to prepare macromolecules in the interspaces between the silicate layers of clay minerals[8,9]. Intercalation behaviour of montmorillonite is of much interest because it can act as a host compound having several types of inclusion spaces such as three dimensional cages, parallel channels and layers[2,10,11]. In this paper physicochemical data on intercalated compounds of Cu(II) montmorillonite clay with 1,2-diaminoethane and 1,2-diaminopropane have been reported.

Materials and Methods

Cu(II) montmorillonite was prepared[7,12] by soaking the USGS mineral sample in 1.0 *M* copper sulphate solution at 25°C for 10 days. The cation exchanged clay was thoroughly washed with distilled water and dried at 80°C for 3 hr. The inclusion behaviour of amines was examined by shaking the Cu(II) montmorillonite clay with 0.1 *M* AR grade amine solution in 100 ml acetone for 7 days. The Cu(II) montmorillonite clay yielded a single phase after 4-5 days with change in colour from light green to pink. The products were throughly washed with acetone and dried at 50°C before analysis. Copper was estimated spectrophotometrically[13]. The percentage of nitrogen was determined at the RSIC Nagpur by Duma's method. The IR absorption spectra of the compounds were recorded on a Perkin-Elmer-397 IR spectrophotometer in KBr pallets. The room temperature magnetic susceptibilities of the prepared compounds were determined by Gouy's method using $Hg[Co(NCS)_4]$ as the standard. All the chemicals used were of AR grade. The X-ray powder diffraction patterns of the compounds were recorded at RSIC Nagpur on a Phillips X-ray machine having an attached microprocessor PW 1700 diffractometry system. The diffraction data were recorded between 10 and 60° (2θ) in the case of Cu(II) montmorillonite and 1,2-diaminopropane-Cu(II) montmorillonite and between 10 and 100° (2θ) in the case of 1,2-diaminoethane-Cu(II) montmorillonite. The X-ray diffraction data were obtained using $Cu-K_\alpha$ radiation of wave length 1.542 Å.

Results and Discussion

The clay mineral montmorillonite is made up of negatively charged silicate layers and has a typical composition $(Al, Mg)_{2-3}(Si,Al)_4O_{10}(OH)_2 \cdot nH_2O$ with interlayer cations compensating the positive charge deficiency of silicate layers. The chemical composition of this clay is variable due to considerable atomic substitution possible in this clay but the major constituents are always Si, Al, Mg and water along with considerable amounts of exchangeable cations. These exchangeable cations are present alongwith water molecules inside the interlayer spacings of the clay framework[14]

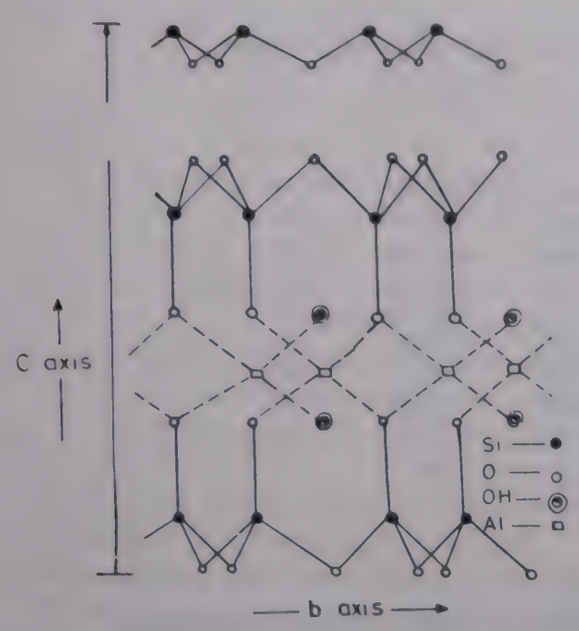

Fig. 1—Structure of montmorillonite

(Fig. 1). The interlayer space in montmorillonite clay is substantial, permitting it to act as a host compound and, therefore, it is possible to prepare coordination compounds of exchangeable cations present in the interlayer spacings of the clay mineral[15].

The pink colour which developed on treating Cu(II) montmorillonite with amines indicated the formation of Cu-amine complex and this was confirmed by chemical analysis (Table 1) and IR absorption spectra. The significant 1,2-diaminoethane and 1,2-diaminopropane contents (Table 1) indicate the formation of coordination compounds of Cu(II) with amines. The amine: Cu molar ratio works out to be 1.9:1 indicating the formation of $Cu(amine)_2$ complexes. The IR absorption spectra of these intercalated compounds show some clear changes when compared with those of free ligands. Bands observed around 3310-3320 cm^{-1} and 1575 cm^{-1} are due to $\nu N-H$ and δNH_2 vibrations respectively of amines. [Bands occurring at 2955 and 1450 cm^{-1} are due to C–H stretching and C–H bending vibrations[16-18]]. In comparison to the IR spectra of the free ligands, these compounds show negative shift (10-30 cm^{-1}) in the stretching and bending vibrations of the amine molecules corroborating the coordination of Cu(II) with amines through 'N' atom. Farmer[19] has observed O–H bending in montmorillonite clay at ~1630 cm^{-1}. This absorption occurs at 1605-1645 cm^{-1} as a broad band in the IR spectra of the Cu(II) montmorillonite clay. In 1,2-diaminoethane and 1,2-diaminopropane intercalated compounds the O–H bending appears at 1635-1655 and 1600-1640 cm^{-1} respectively (Table 2). A comparison of IR spectra with that of Cu(II) montmorillonite clay clearly indicates the broadening of the Si–O stretching region around 1000 cm^{-1} (ref. 19). This suggests that expansion in the silicate layer of the clay mineral takes place due to the formation of complexes of Cu(II) with amine within the interlayer spacings of the clay framework[12,20].

Table 1—Analytical and Magnetic Susceptibility Data of Cu(II) Montmorillonite Clay and Intercalated Compounds

Compound (colour)	Chemical Analysis			Magnetic susceptibility $\chi_g \times 10^{-6}$ (308 K)
	Cu (mmol/100g)	N (wt %)	Ligand (mmol/100g)	
Montmorillonite clay (Light yellow)	—	—	—	2.6866
Cu(II) montmorillonite (Light green)	54.1	—	—	3.4216
1,2-Diaminoethane-Cu(II) montmorillonite (Pink)	53.62	2.8	100	3.2948
1,2-Diaminopropane-Cu(II) montmorillonite (Pink)	52.36	2.78	99.28	3.2457

Table 2—Principal Infrared Frequencies (cm^{-1}) and Their Assignments

Compound	νC–H	νN–H	δN–H	δC–H	νO–H	δO–H
1,2-Diaminoethane	2958	3330s	1590m	1450	—	—
1,2-Diaminopropane	2962	3335s	1590m	1452	—	—
Cu(II) montmorillonite	—	—	—	—	3600s	1605-1645b
1,2-Diaminoethane-Cu(II) montmorillonite	2955w	3320vw	1575sh	1450w	3600vs	1635-1655m
1,2-Diaminopropane-Cu(II) montmorillonite	2960s	3310w	1575vw	1450m	3595vs	1600-1640sh

Table 3—X-Ray Powder Diffraction Data for Cu(II) Montmorillonite

Peak No.	*d*-spacings (Å)	Relative Intensity I/I_{max}, %	Obs. $\sin^2\theta$	Calc. $\sin^2\theta$	(*h k l*)
1	7.3129	11.66	0.0110	0.0114	011
2	6.0621	6.77	0.0161	0.0160	002
3	4.4702	100.00	0.0296	0.0296	020
4	4.0749	23.80	0.0357	0.0360	003
5	3.3406	17.87	0.0531	0.0520	120
6	3.0798	22.24	0.0625	0.0640	004
7	2.5717	29.67	0.0897	0.0896	200
8	2.1996	16.52	0.1226	0.1224	041
9	1.6715	8.57	0.2120	0.2120	311

$A = 0.0224$, $a = 5.242$ Å
$B = 0.0074$, $b = 8.9976$ Å
$C = 0.0040$, $c = 12.411$ Å

Table 4—X-Ray Powder Diffraction Data for 1,2-Diaminoethane-Cu(II) Montmorillonite

Peak No.	*d*-spacings (Å)	Relative Intensity I/I_{max}, %	Obs. $\sin^2\theta$	Calc. $\sin^2\theta$	(*h k l*)
1	5.0873	9.28	0.0226	0.0229	100
2	4.4724	100.00	0.0296	0.0296	020
3	3.1949	21.97	0.0581	0.0593	104
4	2.8684	21.25	0.0721	0.0728	123
5	2.5687	25.79	0.0899	0.0902	016
6	2.4824	14.65	0.0962	0.0978	210
7	2.2333	6.25	0.1189	0.1184	040
8	1.6986	10.77	0.2056	0.2056	301
9	1.4996	25.00	0.2638	0.2662	245
10	1.2830	12.36	0.3604	0.3616	400
11	1.2436	6.25	0.3836	0.3833	073
12	1.0982	19.14	0.4919	0.4977	177

$A = 0.0226$, $a = 5.2200$ Å
$B = 0.0074$, $b = 8.9976$ Å
$C = 0.0023$, $c = 16.3609$ Å

Table 5—X-Ray Powder Diffraction Data for 1,2-Diaminopropane Cu(II) Montmorillonite

Peak No.	*d*-spacings (Å)	Relative intensity I/I_{max}, %	Obs. $\sin^2\theta$	Calc. $\sin^2\theta$	(*h k l*)
1	6.4972	5.88	0.0140	0.0163	0.12
2	4.4841	100.00	0.0295	0.0296	020
3	3.3486	10.61	0.0521	0.0522	120
4	3.1151	5.88	0.0611	0.0611	122
5	2.5589	28.93	0.0928	0.0926	201
6	1.6955	10.61	0.2064	0.2055	301

$A = 0.02260$, $a = 5.1287$ Å
$B = 0.00740$, $b = 8.9976$ Å
$C = 0.00223$, $c = 16.6200$ Å

Tables 3,4 and 5 report the X-ray powder diffraction data on Cu-exchanged clay and two intercalated compounds. The X-ray powder diffraction patterns of intercalated compounds show several changes including appearance of some new peaks and change in the *d*-spacings and intensities. This can be attributed to the formation of complexes of 1,2-diaminoethane and 1,2-diaminopropane with copper of Cu(II) montmorillonite clay and consequent structural changes brought about in the silicate layer of the clay[21]. Reflection of the (001) plane of the monoclinic cell of this clay is not ob-

servable due to its occurrence at low angle ($2\theta < 10°$) in the X-ray powder diffraction patterns but the calculated values of (001) plane are expected to show expansion in case of intercalated compounds. The calculated[22-25] and observed values of $\sin^2\theta$ are in good agreement within the limits of experimental error. This further suggests that the crystallinity remains intact on chelation. The complete indexing has been summarised in Tables 3,4 and 5. The amine:Cu molar ratio and other spectral data lead us to propose tetracoordinated Cu(II) in the $Cu(amine)_2$ type of complexes formed in the interlayer space of the clay. The magnetic susceptibility values of the clay significantly change on cation exchange but remain almost unchanged on chelation with amines. Thus, this study indicates that the absorption of amine on Cu(II) montmorillonite clay results in the formation of complexes located on the interlameller surface of the clay and the symmetry axis of the complex is oriented perpendicular to the silicate layer[26]. This behaviour of clay could make Cu(II)-exchanged montmorillonite useful as micro-encapsulating agent for unstable substances such as insecticides, herbisides and soil disinfectants. The study of thermal behaviour of such compounds is still in progress.

Acknowledgement

We thank the M.P. Council of Science and Technology for financial assistance. Thanks are also due to the Head, Dept. of Chemistry, Dr. H.S. Gour Vishwavidyalaya, Sagar (M.P.) for providing necessary facilities.

References

1 Theng B K G, *The chemistry of clay organic reactions*, (Adam-Hilger, London), 1974, Chapter 1.

2 Mason B & Moore C B, *Principles of geochemistry* (Wiley Eastern, New Delhi) 4th Edn, 1985, 156.

3 Barrer R M, *Zeolites and clay minerals as sorbents and molecular sieves* (Academic Press London, New York) 1978, 497.

4 Shrivastava O P & Glasser F P, *J mat Sci Lett*, **4** (1985) 1122.

5 Shrivastava O P & Glasser F P, *J react Solids*, **2** (1986) 261.

6 Komarnani S & Roy D M, *Science*, **221** (1983) 647.

7 Rees L V C, *The properties and applications of zeolites*, (Chemical Society Special Publication) No. 33, London, 1979, 218.

8 Blumstein A, Herz J, Sinn J & Sardron C, *C R Acad Sci*, **246** (1958) 1856.

9 Blumstein A, *Bull Soc chim Fr*, (1961) 899.

10 Takemoto K, *Chemistry of inclusion compounds* (Tokyo-Kagaku Dojin, Tokyo), 1969, Chapter 2.

11 Brown G, *The X-ray identification and crystal structure of clay minerals* (Min Soc, London) 1961.

12 Kijima T, Tanaka J, Goto M & Matsui Y, *Nature*, **310** (1984) 45.

13 Vogel A I, *A text book of quantitative inorganic analysis*, (ELBS, London) 4th Edn, 1978, 740.

14 Eitel W, *Silicate sciences* (Academic Press, New York) **1** (1964) 234.

15 Bodenheimer W, Kirson B & Yariv S H, *Israel J Chem*, **1** (1963) 69.

16 Cotton F A, Leihr H D & Wilkinson G, *J inorg nucl Chem*, **2** (1956) 141.

17 Califano S & Murcia R, *Gazz chim ital*, **80** (1956) 1014.

18 Nakamoto A, *Infrared spectra of inorganic & coordination compounds* (Wiley, New York) 1963, part 3.

19 Farmer V C, *Clay Mineralogy*, **7** (1968) 373.

20 Farmer V C & Russell J D, *Spectrochim Acta*, **20** (1984) 1149.

21 Banerjee S P, *J Indian chem Soc*, **61** (1984) 547.

22 Henry N F M, Lipson H & Wooster W A, *Interpretation of X-ray diffraction photographs* (McMillan, London) 1951, 179.

23 Buerger, *X-ray crystallography* (Wiley, New York) 1953, 100.

24 Peiser H S, Rooksby H P & Wilson A J C, *X-ray diffraction by polycrystalline materials* (The Institute of Physics, London) 1955, 344.

25 Woolfson, *An introduction to X-ray crystallography* (Cambridge University Press, Cambridge) 1980, 125.

26 Son S, Uada S, Kanamaru F & Kolzumi M, *J phys Chem*, **80** (1976) 1780.

Indian Journal of Chemistry
Vol. 27A, December 1988, pp. 1060-1063

Synthesis & Characterisation of Imidodi(thiocarbonic acid O-alkyl ester) Derivatives of Triphenylphosphine Complexes of Rhodium(I) & Ruthenium(II)

S SUMATHY, S AYYAVOO, V CHINNUSAMY & K NATARAJAN*
Department of Chemistry, Bharathiar University, Coimbatore 641 046

Received 19 *October* 1987; *revised* 19 *February* 1988; *accepted* 29 *February* 1988

Rhodium(I) complexes of the types $[Rh(CO)(LL)(PPh_3)_2]$ and $[Rh(LL)(PPh_3)_3]$ have been synthesised by the replacement of H or Cl and a PPh_3 by a bidentate chelate ligand, imidodi(thiocarbonic acid O-alkyl ester) from $[RhCl(CO)(PPh_3)_3]$ and $[RhH(PPh_3)_4]$ respectively. Ruthenium(II) complexes of the types $[RuCl(CO)(LL)(PPh_3)_2$ and $[RuH(CO)(LL)(PPh_3)_2]$ have been prepared by the replacement of H or Cl and a PPh_3 group from $[RuHCl(CO)(PPh_3)_3]$ and $[RuH_2(CO)(PPh)_3]$ respectively. All the complexes have been characterised and structures proposed on the basis of elemental analyses, IR, ^{31}P NMR, and electronic spectral measurements.

Although the complexes of β-diketones have been investigated with virtually every metal and metalloid, the analogous thio-β-diketonate derivatives have received little attention[1] owing to the difficulty in preparing dithio-β-diketone ligands. Only a few thio-β-diketonate derivatives have been prepared by replacing oxygen atoms in metal-β-diketonates by sulphur atoms. In the recent past, numerous complexes[2-5] with ligands containing the moiety $-C(=S)-NH-CO-$ have been prepared, but those with the ligands containing $-CS-NH-CS-$ group do not appear to have been reported. Hence we have studied the interactions of imidodi(thiocarbonic acid O-alkyl ester) derivatives with triphenylphosphine complexes of Rh(I) and Ru(II). The complexes thus prepared have been characterised and structures proposed on the basis of spectral (IR, ^{31}P NMR, electronic) and analytical data.

Materials and Methods

All the reagents used were of CP or AR grade. All the solvents were freshly distilled before use. IR spectra were recorded in KBr or in chloroform on a Perkin-Elmer 597 IR grating spectrophotometer in the range 4000-250 cm^{-1}; electronic spectra in chloroform on a Hitachi-Perkin-Elmer 10/100 recording spectrophotometer; and ^{31}P NMR spectra on a Bruker WP-80FT instrument. The starting complexes $[RuHCl(CO)(PPh_3)_3]$[6], $[RuH_2(CO)(PPh_3)_3]$[7], $[RhCl(CO)(PPh_3)_3]$[8], $[RhH(PPh_3)_4]$[8] and imidodi(thiocarbonic acid O-alkyl ester)[9] derivatives were prepared by the literature procedures.

The ligands used were of the type $[Ro-CS-NH-CS-OR]$ $[R=CH_3, C_2H_5$ and $CH(CH_3)_2]$ and are represented as L−L.

Preparation of complexes:

(i) *Complexes of type* $[Rh(CO)(L-L)(PPh_3)_2]$

To a solution of $[RhCl(CO)(PPh_3)_3]$ (250 mg; 1 mol) in benzene (2 ml) was added the appropriate ligand (58 to 64 mg; 1 mol) and the solution refluxed for 2 hr. It was concentrated on a water-bath to almost dryness and the residue dissolved in minimum amount of dichloromethane. On the addition of methanol a yellow compound separated out, which was filtered, washed several times with methanol and finally with ether and dried; yield, 60-70%.

The brown isomers of the same formula were prepared similarly by taking the rhodium complex and the appropriate ligand in 1:2 ratio; yield, 65-75%.

(ii) *Complexes of type* $[Rh(L-L)(PPh_3)_3]$

These complexes were prepared as above by taking $[RhH(PPh_3)_4]$ and the appropriate ligand in 1:1 ratio; yield, 64-72%.

(iii) *Complexes of type* $[RuCl(CO)(L-L)(PPh_3)_2]$

To a solution of $[RhHCl(CO)(PPh_3)_3]$ (250 mg; 1 mol) in benzene (20 ml) as added the appropriate ligand (36-48 mg; 1 mol) and refluxed for 1 hr. The solvent was evaporated and the residue dissolved in minimum amount of dichloromethane. On the addition of methanol a solid separated out, which was filtered, washed with methanol and finally with ether and dried; yield, 64-72%.

(iv) *Complexes of type* $[RuH)co)(L-L)(PPh_3)_2]$

These complexes were prepared as described

Table 1—Analytical Data for Rh(I) and Ru(II) Complexes

Complex	Colour	m.p. (°C)	Found (Calc), %		
			C	H	S
$Rh(CO)(C_4H_6O_2S_2N)(PPh_3)_2$	Yellow	80-82	60.22 (60.08)	4.46 (4.39)	7.66 (7.81)
$Rh(CO)(C_6H_{10}O_2S_2N)(PPh_3)_2$	do	173	60.86 (60.92)	4.67 (4.72)	7.45 (7.55)
$Rh(CO)(C_8H_{14}O_2S_2N)(PPh_3)_2$	do	177	61.84 (61.72)	5.21 (5.03)	7.30 (7.31)
$Rh(CO)(C_4H_6O_2S_2N)(PPh_3)_2$	Brown	130	60.14 (60.08)	4.36 (4.39)	7.58 (7.81)
$Rh(CO)(C_6H_{10}O_2S_2N)(PPh_3)_2$	do	135	60.78 (60.92)	4.75 (4.72)	7.38 (7.55)
$Rh(CO)(C_8H_{14}O_2S_2N)(PPh_3)_2$	do	110	61.79 (61.72)	5.13 (5.03)	7.20 (7.31)
$Rh(C_4H_6O_2S_2N)(PPh_3)_2$	do	123-26	66.03 (66.10)	4.79 (4.84)	6.02 (6.07)
$Rh(C_6H_{10}O_2S_2N)(PPh_3)_2$	do	125-27	66.48 (66.55)	5.13 (5.08)	6.00 (5.91)
$Rh(C_8H_{14}O_2S_2N)(PPh_3)_2$	do	285-87	66.85 (66.97)	5.34 (5.31)	5.61 (5.76)
$RuCl(CO)(C_4H_6O_2S_2N)(PPh_3)_2$	Yellow	164-66	57.80 (57.71)	4.19 (4.22)	7.60 (7.50)
$RuCl(CO)(C_6H_{10}O_2S_2N)(PPh_3)_2$	do	153-56	58.49 (58.53)	4.61 (4.53)	7.03 (7.26)
$RuCl(CO)(C_8H_{14}O_2S_2N)(PPh_3)_2$	do	82	59.37 (59.31)	4.88 (4.83)	6.98 (7.03)
$RuH(CO)(C_4H_6O_2S_2N)(PPh_3)_2$	do	145-47	60.19 (60.14)	4.58 (4.52)	7.93 (7.82)
$RuH(CO)(C_6H_{10}O_2S_2N)(PPh_3)_2$	do	148-50	60.88 (60.92)	4.82 (4.84)	7.62 (7.56)
$RuH(CO)(C_8H_{14}O_2S_2N)(PPh_3)_2$	do	144	61.61 (61.64)	5.18 (5.14)	7.21 (7.30)

*Sulphur was estimated as given by A.I. Vogel, in *A textbook of inorganic quantitative analysis* (English Language Society, London), 1978.

above taking $[RuH_2(CO)(PPh_3)_3]$, and the appropriate ligand in 1:1 ratio; yield, 60-68%.

Results and Discussion

Rhodium(I) complexes of type $[Rh(CO)(LL)(PPh_3)_2]$

The yellow and brown complexes of imidodi(thiocarbonic acid-O-methyl/ethyl/isopropyl ester) of the general formula $[Rh(CO)(LL)(PPh_3)_2]$ were obtained by the reaction of $[RhCl(CO)(PPh_3)_3]$ and imidodithio ester in 1:1 and 1:2 molar ratios, respectively. In all the reactions the ligands could replace one of the PPh_3 group and the chloride ligand giving the products. The analytical data of these complexes summarised in Table 1, confirmed the molecular formuloa $[Rh(CO)(LL)(PPh_3)_2]$. In the IR spectra of all the compounds, the thioamide bands were present with little shift in their absorptions compared to those of the free ligands indicating coordination of the ligands with the metal ion. Evidence for the presence of S,S′ coordination of the ligands has been provided by the presence of IR absorptions around 1180 cm^{-1} (assignable to $\nu C=S$ modes), with a shift of around 20 cm^{-1} compared to those of the free ligand. All the compounds exhibited $\nu C=O$ modes around 1955 cm^{-1} indicating the coordinated carbon monoxide ligand[10]. In addition to these bands, absorptions due to triphenylphosphine ligand appeared in the expected regions.

Since both the yellow and brown compounds analysed for the same molecular formula $[Rh(CO)(LL)(PPh_3)_2]$, we assume that they are two different isomers. In order to decide on the geometry of the two type of compounds, ^{31}P NMR spectra of $[Rh(CO)(C_4H_6O_2S_2N)(PPh_3)_2]$ (yellow) and $[Rh(CO)(C_4H_6O_2S_2N)(PPh_3)_2]$(brown) were taken in toluene. The yellow compound showed two singlets at 35.65 and 31.70 ppm. The brown compound showed only one singlet at 48.40 ppm. This observation leads to three possible structures (I-III) for

these isomeric compounds. Of these I and II should give two singlets and the III should give only one singlet. Hence the brown isomer can be assigned the structure III. The yellow isomer can have either structure I or II. Generally Rh(I) and Co(I) form trigonal bipyramidal compounds rather than the square pyramidal one[11]. Hence, structure II is assigned to the yellow isomer. Moreover, the relative *trans* influence sequence which shifts ^{31}P signal to the high field lies in the order $Cl < P < C < H$[11]. Based on this, we tentatively assign the signal at 31.7 ppm to the phosphine *trans* to the carbonyl group and the signal at 35.65 ppm to the other phosphine group. In the brown isomer, the low field signal around 48.40 ppm is due to the two phosphines *trans* to each other. Based on the above data, we assign structure II for all the yellow isomers and structure III to all the brown isomers of the molecular formula $[Rh(CO)(LL)(PPh_3)_2]$. In all these complexes, the ligand coordinates in the conventional fashion, viz. through two sulphur atoms from the *enol* form of the ligands.

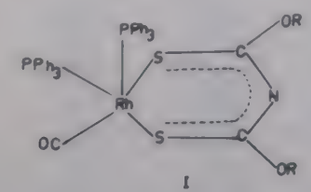

I

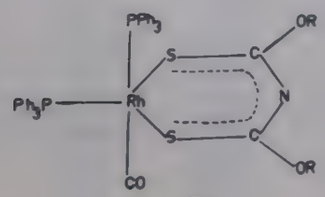

II

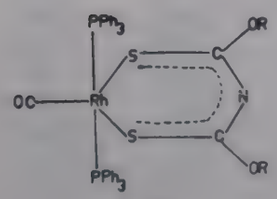

III

Rhodium(I) complexes of type $[Rh(LL)(PPh_3)_2]$

In the preparation of the compounds of the type $[Rh(LL)(PPh_3)_2]$ (LL = imidodi(thiocarbonic O-alkyl ester), the ligand replaces one of the PPh_3 group an a hydride to give the product of the molecular formula $[Rh(LL)(PPh_3)_2]$. The analytical data of these complexes are also given in Table 1. In the IR spectra of these complexes thioamide bands are present with little shifts in their absorptions compared to those of the free ligands indicating their coordination to the metal ion. Evidence for the presence of S,S'-coordinated ligand has been provided by the presence of peaks in the region 1190-1180 cm^{-1}, assignable to $\nu C=S$. The absence of a band at 2156 cm^{-1} due to $\nu Rh-H$ in all the complexes shows that the hydride ligand in the starting material has been replaced by the coordinated bidentate ligand. The striking feature of the IR spectra of the complexes is the absence of bands in the region 3350-3175 cm^{-1} which could be assigned to ν_{as} and $\nu_s - NH$ modes. .This indicates that the ligand is coordinated as an enolate ion. In addition to these, bands due to triphenylphosphine appeared in the expected regions.

The five-coordinate Rh(I) complexes present a problem that is not encountered with four- or six-coordinate complexes[12]. Hence, the ^{31}P NMR spectra of one complex was studied in order to decide on their geometries. The ^{31}P NMR spectra of $[Rh(C_8H_{14}O_2S_2N)(PPh_3)_3]$ exhibited two singlets at 48.4 and 35.47 ppm with an intensity ratio of 1:2. Phosphorus-31 NMR studies on ML_3-trialkylphosphite compelxes of Fe(O), Ru(O), Os(O), Co(I), Rh(I), Ir(I), Ni(II), Pd(II) and Pt(II) showed the structures of these molecules to be trigonal bipyramidal and not square pyramidal[13-16]. Hence, tentatively a trigonal bipyramidal structure has been proposed for all the compounds of the type $[Rh(LL)(PPh_3)_3)]$.

Ruthenium(II) complexes $[RuX(CO)(LL)(PPh_3)_2]$ *[X = Cl or H; LL = imidodi-(thiocarbonic acid O-methyl/ethyl/isopropyl esters]*

All the compounds were prepared by the reaction of either $[RuHCl(CO)(PPh_3)_3)]$ or $[RuH_2(CO)(PPh_3)_3]$ with the appropriate ligands. Under ordinary conditions, the ligand could replace one of the triphenylphosphines and a hydride ligand from the complex giving the product $[RuX(CO)(LL)(PPh_3)_2]$. The analytical data given in Table 1 fit very well with the molecular formula. In the IR spectra of these complexes the thioamide bands are present with little shifts in their absorptions as compared to those of the free ligands. The IR peaks in the region 1190-1175 cm^{-1} (due to $\nu C=S$ mode) clearly indicate the presence of S,S'-coordination of the ligands in the complexes. The $\nu C=O$ modes in the complexes appear in the region 1940-1920 cm^{-1} showing the presence of coordinated carbon monoxide[10].

All the compounds are diamagnetic which corroborates oxidation state of +2 for ruthenium. The electronic spectra of the complexes in chloroform exhibit two to three bands in the region 600-400 nm. The week band in the region 440-425 nm can be tentatively assigned to the transition $^1A_{1g} \rightarrow {}^1T_{1g}$

(ref. 16). This and the other band positions indicate an octahedral geometry for all the ruthenium(II) complexes[17,18].

References

1 Mehrotra R C, Bohra R & Gaur D P, *Metal β-diketonates and allied derivatives* (Academic press, New York), 1978.
2 Singh T & Agarwala U, *Indian J Chem*, **19A** (1980) 755.
3 Singh T & Agarwala U, *Indian J Chem*, **19A** (1980) 750.
4 Satpathy K C & Mishra H P, *Indian J Chem*, **20A** (1981 1035.
5 Saheed R & Agarwala U, *Indian J Chem*, **20A** (1981) 1196.
6 Ahmad N, Levison J J, Robinson S D & Uttley M F, *Inorg Syn*, **15** (1974) 48.
7 Boniface S M, Clark G R, Collins T J & Roper W R, *J organometal Chem*, **206** (1981) 106.
8 Ahmad N, Levison J J, Robinson S D & Uttley M F, *Inorg Syn*, **15** (1974) 58.
9 Bunnenberg R & Jochims J C, *Chem Ber*, **114** (1981) 1132.
10 Nakamoto K, *Infrared spectra of inorganic and coordination compounds* (John Wiley, New York), 1972.
11 Meek D W & Mazanec T J, *Acc chem Res*, **14** (1981) 266.
12 Rossi A R & Hoffman R, *Inorg Chem*, **14** (1975) 365.
13 English A D, Ittel S D, Tolman C A, Meakin P & Jesson J P, *J Am chem Soc*, **99** (1977) 117.
14 Jesson J P & Meakin P, *J Am chem Soc*, **95** (1973) 1344.
15 Jesson J P & Meakin P, *J Am chem Soc*, **96** (1974) 5760.
16 Meakin P & Jesson J P, *J Am chem Soc*, **96** (1974) 5751.
17 Lever A B P, *Inorganic electronic spectroscopy* (Elsevier, New York), 1984.
18 Natarajan K & Agarwala U, *Inorg nucl chem Lett*, **14** (1978) 7.

Indian Journal of Chemistry
Vol. 27A, December 1988, pp. 1064-1067

Synthesis, Characterization & Antifungal Properties of Some Four-coordinate Nickel(II) & Four- & Five-coordinate Copper(II) Complexes Containing Tridentate Thiosemicarbazones & Heterocyclic Bases

M AKBAR ALI*, M H KABIR, M NAZIMUDDIN & S M M H MAJUMDER
Department of Chemistry, University of Chittagong, Bangladesh
M T H TARAFDER
Department of Chemistry, Rajshahi University, Bangladesh
and
M A KHAIR
Department of Botany, University of Chittagong, Bangladesh

Received 29 *October* 1987; *revised and accepted* 10 *March* 1988

Schiff bases (ONS donors) obtained by the reaction of salicylaldehyde and 5-bromosalicylaldehyde with thiosemicarbazide form 1:1 metal-ligand complexes with Ni(II) and Cu(II). Magnetic, spectral and mass spectroscopic evidences support a dimeric structure for Ni(ONS) complexes. The Cu(ONS) complexes are antiferromagnetic in nature with sub-normal room temperature magnetic moments. An oxygen-bridged binuclear structure is proposed for these complexes. In the presence of heterocyclic bases such as pyridine, 2,2'-bipyridine and 1,10-phenanthroline, adducts of the type Cu(ONS)B (B = py, bipy, phen) have been isolated. Conductivity, magnetic data and spectral evidences support a square-planar structure for Cu(ONS)Py complexes and five-coordinate, presumably trigonal-bipyramidal structure for the Cu(ONS)Bipy and Cu(ONS)Phen complexes. Antifungal activities of the schiff bases and their metal complexes against three plant pathogens, viz. *A. alternata*, *F. moniliforme* and *D. orezae* have been studied. All the compounds studied display marked fungitoxicity against these fungi. The metal complexes are more fungitoxic than the free ligands.

As a part of our general investigation of metal complexes of sulphur-nitrogen chelating agents, we report herein the results of studies on the synthesis, characterization and antifungal properties of some nickel(II) and copper(II) complexes of two ONS tridentate thiosemicarbazone ligands. The ligands were obtained by the condensation of 2-hydroxybenzaldehyde and 5-bromo-2-hydroxybenzaldehyde with thiosemicarbazide. Although some metal complexes of these two ligands have been reported[1], to the best of our knowledge the complexes presently studied are new.

Materials and Methods

The IR spectra were recorded in KBr on a Pye-Unicam model SP3-300 infrared spectrophotometer, PMR spectra on a Bruker WH-200 spectrometer in DMSO using TMS as an internal standard and electronic spectra in nujol on a Shimadzu UV-120(02) spectrophotometer. Magnetic measurements were made by the Gouy method using $HgCo(NCS)_4$ as the standard. All other measurements and corrections were done as described before[2].

Preparation of ligands

Both the schiff bases were prepared by the following general procedure: To a boiling solution of thiosemicarbazide (1.8 g; 0.02 mol) in ethanol (200 ml) was added salicylaldehyde or 5-bromosalicylaldehyde (0.02 mol), the mixture heated for 30 min and left aside for 1 hr when a brownish white crystalline product separated out. The product was filtered, washed with ethanol and recrystallized from abs. ethanol and dried over P_4O_{10} in a vacuum desiccator, m.p. of the schiff base derived from salicylaldehyde, 225° (Found: C, 48.46; H, 4.69; N, 21.13; $C_8H_9N_3OS$ requires: C, 49.23; H, 4.61;N, 31.53%); m.p. of the schiff base derived from 5-bromosalicylaldehyde, 236° (Found: C, 34.96; H, 2.96; N, 13.08; $C_8H_8N_3OSBr$ requires: C, 35.06; H, 2.92; N, 13.33%).

General method for preparation of ML_1 and ML_2 complexes (M = Ni(II) and Cu(II); H_2L_1 and H_2L_2 are the schiff bases derived from salicylaldehyde and 5-bromosalicylaldehyde)

A solution of metal(II) acetate (1 mmol) in methanol (40 ml) was mixed with a solution of the

appropriate ligand (1 mmol) in abs. ethanol (50 ml) and heated on a water-bath for 15 min. The reaction mixture was cooled slowly and the solid product formed was filtered, washed several times with ethanol and dried in a desiccator over P_4O_{10}.

General method preparation of complexes ML_1X and ML_2X[M= Ni(II) and Cu(II); X= Py)]

A solution of the ligand (1 mmol) in ethanol (50 ml) was mixed with a solution of nickel or copper acetate (1 mmol) in methanol (50 ml). Pyridine (0.5 ml) was added and the mixture heated for 30 min. The volume of the solution was reduced to10 ml. On standing for 1 hr a solid product separated out which was filtered, washed thoroughly with ethanol and dried *in vacuo* over P_4O_{10}.

General method for preparation of CuL_1X and CuL_2X (X= 2,2'-dipyridyl or 1,10-phenanthroline)

A solution of copper(II) acetate (1 mmol) in methanol (40 ml) was mixed with a solution of 2,2'-dipyridyl or 1,10-phenanthroline (2 mmol) in ethanol (10 ml). A deep blue solution resulted to which was added a solution of the appropriate schiff base (1 mmol) in absolute ethanol (50 ml). The mixture was heated under reflux for 5-8 hr and cooled. The solid product obtained was filtered, washed with ethanol and dried *in vacuo* over P_4O_{10}.

Antifungal and phytotoxic tests

The compounds were incorporated in PDA medium previously inoculated with either of *Alternaria alternata*, *Fusarium moniliforme* or *Drechslera orezae*. Dimethyl sulphoxide was used as a solvent for the compounds and the concentration of each was adjusted to 0.1% in a volume of 20 ml of culture medium poured in sterilized petri dishes. The percent growth inhibition was calculated on the basis of average diameter of the fungal colony.

Rice seeds were used to evaluate the phytotoxic effects of the compounds on seed germination and seedling vigour. The test compounds were dissolved separately in dimethyl sulphoxide so as to maintain a concentration of 0.1%. Rice seeds (10 g) were then soaked in solutions (20 ml) of the compounds for 30 min, whereas soaking the same amount of seeds in dimethyl sulphoxide alone served as reference. Two hundred seeds after treatment including the untreated ones were sown in four replications in sterile sand medium. After 10 days the germination was counted and 25 seedlings from each replication were removed at random and the root and shoot lengths were measured. The vigour index (V I) of the seedlings was calculated.

Results and Discussion

The schiff bases, L_1 and L_2 derived from salicylaldehyde and 5-bromosalicylaldehyde, respectively are expected to exist in thioketo (IA) and thioenol (IB) forms.

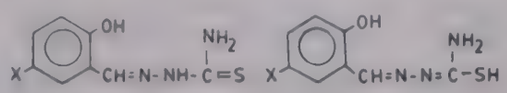

(IA) (IB)

The IR spectra of these compounds do not display the νS−H mode at about 2600 cm^{-1} indicating that in the solid state these two ligands remain in the thioketo form (IA). The PMR spectra of the schiff bases in DMSO-d_6 display resonances at δ 11.50, 9.90,7.20 and 6.86-7.90 attributable to the −OH, −NH, $-NH_2$ and aromatic ring protons, respectively. The absence of any peak attributable to the S−H protons imply that in solution the schiff bases remain predominantly in the thioketo(IA) form. However, in solution and in the presence of nickel(II) and copper(II) ions, these compounds exist in tautomeric equilibrium: IA⇌IB. The tautomer (IB) by loss of both phenolic and thiol protons react with metal ions as dinegatively charged chelating agents producing crystalline compounds. This is supported by the disappearance of νOH/νNH modes of the free ligands around 3300-2850 cm^{-1} in the IR spectra of the complexes indicating coordination to metal ions via deprotonation. The PMR spectra of Ni(ONS) complexes do not contain signals due to the −OH and −NH protons of free ligands supporting that the ligands are deprotonated during complexation. The bands at 3455 and 3250 cm^{-1} in the IR spectra of H_2L_1 and H_2L_2 are assigned to the $\nu_{as}NH_2$ modes and the one at 3160 cm^{-1} to the ν_sNH_2, which do not undergo any perceptible shifts suggesting that there is no interaction between NH_2 groups and metal ions. The azomethine nitrogen atom also participates in coordination as shown by the shift of νC=N mode of the free ligands around 1595 cm^{-1} to lower wavenumbers. The coordination of azomethine nitrogen is further supported by the displacement of νN−N modes of the ligands (H_2L_1 1060 cm^{-1} and H_2L_2, 1080 cm^{-1}) to lower wavenumber (1030 cm^{-1} for the complexes of H_2L_1 and 1070 cm^{-1} for the complexes of H_2L_2)[3,4].

Since the schiff bases are coordinated as dinegatively charged tridentate ligands and microanaly-

Table 1—Colour, Conductivity, Magnetic Moments and Analytical Data of the Complexes

Compound	Colour	m.p. (°C)	μ_{eff} (B.M.) (at 303K)	Found (Calc.) (%)				Λ^a (ohm^{-1} cm^2 mol^{-1})
				C	H	N	M	
NiL_1	Orange	350	Diam.	38.13 (38.14)	3.13 (2.80)	16.05 (16.68)	23.01 (23.30)	1.95
$NiL_2 \cdot H_2O$	Orange-red	350	Diam.	27.15 (27.54)	1.98 (2.31)	12.05 (12.04)	16.23 (16.83)	1.90
$NiL_1 \cdot py$	Orange-red	340	Diam.	46.97 (47.17)	3.65 (3.65)	16.81 (16.92)	17.89 (17.74)	1.20
$NiL_2 \cdot py$	Yellow-red	259	Diam.	37.91 (38.09)	2.70 (2.70)	14.14 (13.67)	14.80 (14.32)	1.0
CuL_1	Chocolate	214	Diam.	37.15 (37.40)	3.29 (2.75)	16.27 (16.35)	24.84 (24.73)	2.30
CuL_2	Brown	244	1.02	28.50 (28.62)	1.91 (1.80)	12.21 (12.51)	18.41 (18.92)	1.8
$CuL_1 \cdot py$	Brown	201	1.82	46.01 (46.49)	3.64 (3.60)	16.39 (16.68)	18.70 (19.01)	0.6
$CuL_2 \cdot py$	Dark-green	201	1.90	37.58 (37.65)	2.65 (2.67)	13.60 (13.51)	15.98 (15.32)	1.45
$CuL_1 dipy$	Dark-green	196	1.91	52.16 (52.35)	3.90 (3.66)	16.21 (16.95)	15.64 (15.39)	1.0
$CuL_2 dipy$	Dark-green	247	1.87	43.87 (43.96)	2.98 (2.87)	14.13 (14.24)	12.99 (12.92)	0.5
$CuL_1 phen$	Black-green	197	1.89	46.27 (46.67)	3.08 (2.55)	13.53 (13.60)	12.44 (12.34)	1.3

[a]Molar conductivity of 10^{-3} *M* solutions in dimethyl sulphoxide

tical data (Table 1) conform to the metal-ligand ratio as 1:1, both the NiL and CuL complexes appear to contain three-coordinate metal ions. However, the diamagnetism of the nickel(II) complexes suggests that they have four-coordinate square-planar structure. The electronic spectra of Ni(II) complexes also support square-planar structure. The spectra display shoulders around 520 nm and no other bands in the *d-d* transition region. Such spectra are quite similar to those exhibited by square-planar nickel(II) complexes of sulphur-nitrogen ligands[5]. The molecular weights of the complexes could not be determined because of poor solubilities of the complexes in most of the non-coordinating organic solvents. However, the electron impact mass spectrum of NiL_1 shows a peak at m/z 502 due to the dimeric molecular ion, besides showing another peak at m/z 251 corresponding to the monomeric unit. Based on this evidence a dimeric four-coordinate square-planar structure for NiL_1 and NiL_2 complexes is suggested. The mono-ligand copper(II) complex of H_2L_2 complex of H_2L_2 has a room temperature magnetic moment of 1.02 B.M., which is much lower than that observed for normal copper(II) complexes. This low magnetic moment suggests strong antiferromagnetic interactions between copper(II) ions in an oxygen-bridged binuclear structure. A sulphur-bridged dimeric structure seems unlikely since sulphur-bridging leads to very strong antiferromagnetic interactions resulting in complete diamagnetism in copper(II) complexes[5].

The room temperature magnetic moment of CuL_2 (1.02 B.M.) suggests that a mercapto sulphur-bridged dimeric structure seems unlikely. The mass spectrum of CuL_1 is different from that of NiL_1 suggesting that the nickel and copper complexes have different structures. The mass spectrum of CuL_1 does not show any peak attributable to the $Cu_2(ONS)_2$ dimer nor does it show a peak corresponding to the monomer Cu(ONS). This is a strong evidence that metal-ligand bonding for the CuL_1 complexes is different from that in the NiL_1 complexes.

Reaction of the schiff bases with copper(II) acetate in the presence of heterocyclic bases such as pyridine, 2,2′-bipyridine and 1,10-phenanthroline produces crystalline compounds of empirical formula, Cu(ONS)B. The molar conductance data of the complexes (Table 1) are in keeping with their non-electrolytic nature. The ligands, therefore, must be behaving as dinegatively charged species. The IR spectra of Cu(ONS)B display bands characteristic of the coordinated heterocyclic bases[6-8].

The colours of Cu(ONS)B are green in contrast

to the red-brown colour of the Cu(ONS) complexes for which dimeric structures have been proposed. The room temperature magnetic moments (Table 1) of these copper complexes suggest that the complexes have normal magnetic moments of 3*d* ion. The electronic spectrum of CuL_1Py displays a *d-d* band at around 590 nm which is similar to those displayed by other copper(II) complexes for which square-planar structure has been proposed[9]. Therefore, a square-planar structure is proposed for the Cu(ONS)Py complexes. A comparison of the electronic spectra of Cu(ONS)Py with those of Cu(ONS)Bipy and Cu(ONS)Phen shows that the structure of the latter compounds is different than that of the former complex. The tendency of 1,10-phenanthroline and 2,2′-bipyridine to act as bidentate chelating agents and the schiff bases as ONS tridentate ligands is expected to impose a five-coordinate configuration in these complexes. An oxygen-bridged or a sulphur-bridged dimeric or polymeric structure will be very unlikely since such bridging arrangements generally lead to antiferromagnetic interactions causing a reduction in the room temperature magnetic moment[5,6]. The Cu(ONS)Bipy and Cu(ONS)Phen complexes most probably have a five-coordinate geometry. The electronic spectrum of Cu(ONS)Bipy contains two incompletely resolved bands around 630 nm. Similar incompletely resolved bands in the same region have also been observed in the electronic spectrum of bis(N-methylsalicylaldiminato)copper(II) for which a trigonal-bipyramidal structure has been proposed[9]. Based on magnetic, conductivity, IR and electronic spectral data, the Cu(ONS)B (B = Bipy, Phen) complexes are, therefore, assigned the five-coordinate trigonal-bipyramidal geometry. Attempts to synthesize similar five-coordinate nickel(II) complexes of the type Ni(ONS)B did not meet with success.

Fungicidal and phytotoxic activities of the ligands and their metal complexes

Results of antifungal screening experiments indicate that the metal complexes are more fungitoxic than the free ligands. The copper(II) complexes display better fungitoxicity than the nickel(II) complexes. Among the three fugni *A. alternata* shows the highest susceptibility compared to the other two. The mixed-ligand complexes, have antifungal activities comparable with those of the mono-ligand metal complexes. Metal complexes of H_2L_1 are slightly more active than the complexes of H_2L_2. Tests for phytotoxicity based on germination and vigour index of rice seedlings show that there is slight reduction in germination and seedling vigour in all the treatments including DMSO. Treatment with solvent (DMSO) alone does not differ significantly from the complexes used in combination with it. However, in some of the treatments, the vigour index is found to be lower than the treatment by the solvent alone.

Acknowledgement

We gratefully acknowledge Dr M Ekramul Haque of Kanazawa University, Japan for microanalytical data, Mr Swapan K Chowdhury of Chemistry Department, Alberta University, Canada for PMR and mass spectra and Miss Tapashi Ghosh Roy of Chemistry Department, Roorkee University, India for variable-temperature magnetic data. One of us (MAA) thanks the UGC, Bangladesh for financial support.

References

1 Ablov A V, Goldanskii V I, Turta K I, Stukan R A, Zelentsov V V, Ivanov E V & Gerbeleu N V, *Dokl acad nauk USSR*, **196** (1971) 1101.
2 Akbar Ali M & Bose R N, *Polyhedron*, **3** (1984) 517.
3 Burns G R, *Inorg Chem*, **7** (1968) 277.
4 Mohan M, Sharma P, Kumar M & Jha N K, *Inorg chim Acta*, **125** (1986) 9.
5 Nyholm R S, *Proc chem Soc*, (1964) 273.
6 Inskeep R G, *J inorg nucl Chem*, **24** (1962) 763.
7 Schilt A A & Taylor R C, *J inorg nucl Chem*, **9** (1959) 217.
8 Monoyama M, *Inorg chim Acta*, **13** (1975) 5.
9 Sacconi L, Ciampolini M & Speroni G, *J am chem Soc*, **87** (1965) 3102.

Indian Journal of Chemistry
Vol. 27A, December 1988, pp. 1068-1072

Tetrad Effect in the Solution Stabilities of Mixed Ligand Complexes of Lanthanides

SANGEETA VERMA & M C SAXENA*
Department of Chemistry, Dr. Harisingh Gour Vishwavidyalaya, Sagar (M.P.) 470003

Received 11 *September* 1987; *revised and accepted* 14 *March* 1988

The occurrence of tetrad effect in the solution stabilities of mixed ligand complexes of lanthanides has been studied for the ternary systems of the type [Ln(III).A.L], where Ln(III) = La^{3+}, Ce^{3+}, Pr^{3+}, Nd^{3+}, Eu^{3+}, Gd^{3+}, Tb^{3+} or Dy^{3+}; A = HEDTA, CDTA or DTPA; and L = IMDA. The formation constants $\log K^{MA}_{MAL}$, $\log K^{M}_{ML}$ and $\log K^{ML}_{ML_2}$ have been determined by potentiometric *p*H-titrations using Irving-Rossotti approach at 25°C and at ionic strength, $I = 0.2$ (mol dm^{-3}, $NaClO_4$). The formation constants of the mixed ligand complexes follow the sequence: HEDTA > CDTA > DTPA, reflecting mainly the electrostatic effect. The $\Delta \log K$ values are negative. The stability data indicate the occurrence of tetrad effect at Gd(III). A differential plot method has been used to locate the occurrence of tetrad effect at the one-fourth and three-fourths filled 4*f*-shells also. The so-called inclined −W plots have been obtained on correlating the formation constants with the total orbital angular momentum quantum number, L_{Ln}, of the lanthanides. The implications of periodicity in L_{Ln} have been discussed with reference to the inclined-W plots.

Some properties of tervalent lanthanides, when studied as a function of 4*f* electrons ($4f^n$), have been found to show a discontinuity at Gd(III) corresponding to the half-filled 4*f*-shell. These properties are separation coefficients[1], free energy changes of binary complex formation[2] and extraction[3], enthalpies and entropies of extraction[4,5], free energies of crystallisation[6] and hydration of lanthanide ions[7], unit cell volumes of lanthanide compounds[8], IR stretching frequencies[9], deprotonation constants of lanthanide complexes[10] and Racah parameters of lanthanide(III) ions[11]. The discontinuity which may be observed less prominently at the $4f^0 - 4f^7$ (quarter filled 4*f*-shell) and $4f^{0} - 4f^{1}$ (three-fourths filled 4*f*-shell) stages also, has been variously termed as Gd-break[12], double-double effect[13,14] and tetrad effect[15].

The present work aims at studying the possible occurrence of tetrad effect in the solution stabilities of mixed ligand Ln(III) complexes. The ternary systems investigated are of the type [Ln(III).A.L], where Ln(III) = La^{3+}, Ce^{3+}, Pr^{3+}, Nd^{3+}, Sm^{3+}, Eu^{3+}, Gd^{3+}, Tb^{3+} or Dy^{3+}; A = N′-(2-hydroxyethyl)ethylenediamine NNN′-triacetate (HEDTA), 1,2-diaminocyclohexane NNN′N′-tetraacetate (CDTA) or diethylenetriamine NNN′N″N″-pentaacetate (DTPA), and L = iminodiacetic acid (IMDA).

Materials and Methods

The Ln(III) nitrates (99.9% purity) were supplied by M/s Indian Rare Earths Ltd. Other chemicals used were standard reagents (Sigma/Merck GR/B D H Analar). The Ln(III) solutions were standardised by EDTA titrations[16]. The final metal and ligand concentrations were maintained at $[M] = [A] = [L] = 1 \times 10^{-3}$ mol dm^{-3}. The metal-ligand formation constants $\log K^{M}_{ML}$, $\log K^{MA}_{MAL}$, and $\log K^{ML}_{ML_2}$ (in which case the secondary ligand concentration was kept at five-fold excess) were determined by potentiometric *p*H-titrations using the Irving-Rossotti approach[17,18] at 25°C and at an ionic strength, $I = 0.2$ (mol dm^{-3}, $NaClO_4$). An Elico digital *p*H-meter (model LI-120) with an accuracy of 0.01 *p*H units, a micro-burette reading upto 0.02 ml and a carbonate-free (0.2 mol dm^{-3}) NaOH solution were used for the *p*H titrations. Reproducibility of *p*H data was ascertained by repeating the titrations. The values of formation constants were refined by the method of linear plots[19] and were subjected to statistical refinement also using 'Q-test'[20], which is a powerful tool for testing a statistically suspect observed value. The refined formation constant values are presented in Table 1. Figures in parentheses indicate standard deviations. The values of $\Delta \log K_1$ ($= \log K^{MA}_{MAL} - \log K^{M}_{ML}$), $\Delta \log K_2$ ($= \log K^{MA}_{MAL} - \log K^{ML}_{ML_2}$) and $\Delta \log K_1$ ($= \log K^{M}_{ML} - \log K^{ML}_{ML_2}$), as derived from the formation constants, are recorded in Table 2.

Results and Discussion

A representative set of *p*H titration curves for the ternary system [Tb(III).CDTA.IMDA] is repro-

Table 1 – Formation Constants of Binary ($\log K^{M}_{ML}$ & $\log K^{ML}_{ML_2}$) and Ternary ($\log K^{MA}_{MAL}$) Lanthanide(III) Complexes [Temp. = 25°C; ionic strength, I = 0.2 (mol dm^{-3}, $NaClO_4$)]

Formation constant	La ($4f^0$)	Ce ($4f^1$)	Pr ($4f^2$)	Nd ($4f^3$)	Sm ($4f^5$)	Ev ($4f^6$)	Gd ($4f^7$)	Tb ($4f^8$)	Dy ($4f^9$)
$\log K^{M}_{ML}$ (L= IMDA)	6.30 (±0.03)	6.41 (±0.02)	6.55 (±0.02)	6.70 (±0.03)	6.86 (±0.03)	6.91 (±0.03)	6.78 (±0.02)	7.06 (±0.04)	7.16 (±0.04)
$\log K^{ML}_{ML_2}$	4.80 (±0.03)	4.88 (±0.01)	4.91 (±0.01)	5.09 (±0.03)	5.53 (±0.03)	5.58 (±0.02)	5.53 (±0.02)	5.68 (±0.02)	5.74 (±0.02)
$\log K^{MA}_{MAL}$ (A= HEDTA)	4.37 (±0.02)	4.42 (±0.01)	4.44 (±0.02)	5.06 (±0.02)	5.65 (±0.01)	5.76 (±0.01)	5.68 (±0.01)	5.86 (±0.02)	6.15 (±0.02)
$\log K^{MA}_{MAL}$ (A= CDTA)	4.17 (±0.04)	4.27 (±0.03)	4.33 (±0.02)	4.47 (±0.04)	4.68 (±0.03)	4.78 (±0.02)	4.65 (±0.01)	4.84 (±0.01)	5.11 (±0.03)
$\log K^{MA}_{MAL}$ (A= DTPA)	3.60 (±0.03)	3.72 (±0.03)	3.80 (±0.03)	4.09 (±0.03)	4.27 (±0.03)	4.43 (±0.03)	4.19 (±0.02)	4.50 (±0.02)	4.63 (±0.02)

Values in parentheses indicate standard deviations.

Table 2 – Calculated Values of $\Delta \log K_1$ ($= \log K^{MA}_{MAL} - \log K^{M}_{ML}$), $\Delta \log K_2 = (\log K^{MA}_{MAL} - \log K^{ML}_{ML_2})$, and $\Delta \log K_L$ ($= \log K^{M}_{ML} - \log K^{ML}_{ML_2}$)

$\Delta \log K$	La ($4f^0$)	Ce ($4f^1$)	Pr ($4f^2$)	Nd ($4f^3$)	Sm ($4f^5$)	Eu ($4f^6$)	Gd ($4f^7$)	Tb ($4f^8$)	Dy ($4f^9$)
$\Delta \log K_1$ (HEDTA)	−1.93	−1.99	−2.11	−1.64	−1.21	−1.15	−1.10	−1.20	−1.01
$\Delta \log K_1$ (CDTA)	−2.13	−2.14	−2.22	−2.23	−2.18	−2.13	−2.23	−2.22	−2.05
$\Delta \log K_1$ (DTPA)	−3.00	−2.69	−2.75	−2.61	−2.59	−2.48	−2.59	−2.56	−2.53
$\Delta \log K_2$ (HEDTA)	−0.43	−0.46	−0.47	−0.03	+0.12	+0.18	+0.15	+0.18	+0.41
$\Delta \log K_2$ (CDTA)	−0.63	−0.61	−0.58	−0.62	−0.85	−0.80	−0.88	−0.84	−0.63
$\Delta \log K_2$ (DTPA)	−1.20	−1.16	−1.11	−1.00	−1.26	−1.15	−1.34	−1.18	−1.11
$\Delta \log K_L$	+1.50	+1.53	+1.64	+1.61	+1.33	+1.33	+1.25	+1.38	+1.42

duced in Fig. 1. An analysis of the nature of the *p*H titration curves shows that the present mixed ligand complexes are formed in two steps: M + A ⇌ MA, and MA + L ⇌ MAL. The formation of MA chelates is over in the *p*H range 2-3. The secondary ligand L gets bound to MA in the *p*H region ~ 5.5-6.5. The formation of the MAL complexes is also evident from the non-superimposable nature of the theoretical composite curve[21] and from the horizontal distances between the various curves[22]. No precipitation was observed in the MAL systems upto *p*H 10-12.

The $\log K^{MA}_{MAL}$ values with different 'A' lie in the sequence HEDTA > CDTA > DTPA, which is opposite to the known order[23] (DTPA > CDTA > HEDTA) with respect to these ligands for their MA chelates. The reversal seems to be brought about mainly by the electrostatic factor. The MA species formed with HEDTA, CDTA and DTPA are neutral, mono-negative and binegative, respectively. Their combination with IMDA (L^{2-}) evidently involves increasing coulombic repulsion. The stepwise complexation is shown in Eqs 1-3.

$$Ln(III) + HEDTA^{3-} \rightleftharpoons [Ln(III).HEDTA];$$
$$[Ln(III).HEDTA] + IMDA^{2-} \rightleftharpoons [Ln(III).HEDTA.IMDA]^{2-} \quad \ldots (1)$$

$$Ln(III) + CDTA^{4-} \rightleftharpoons [Ln(III).CDTA]^{-};$$
$$[Ln(III).CDTA]^{-} + IMDA^{2-} \rightleftharpoons [Ln(III).CDTA.IMDA]^{3-} \quad \ldots (2)$$

$$Ln(III) + DTPA^{5-} \rightleftharpoons [Ln(III).DTPA]^{2-};$$
$$[Ln(III).DTPA]^{2-} + IMDA^{2-} \rightleftharpoons [Ln(III).DTPA.IMDA]^{4-} \quad \ldots (3)$$

The electrostatic repulsion involved in the second step in each case leads to the sequence $\log K^{MA}_{MAL} < \log K^{M}_{ML}$ and, hence, the $\Delta \log K$ values are negative. Gradually increasing negative charge on the MA species, as shown in Eqs (1) to (3), enhances the electrostatic repulsion involved in

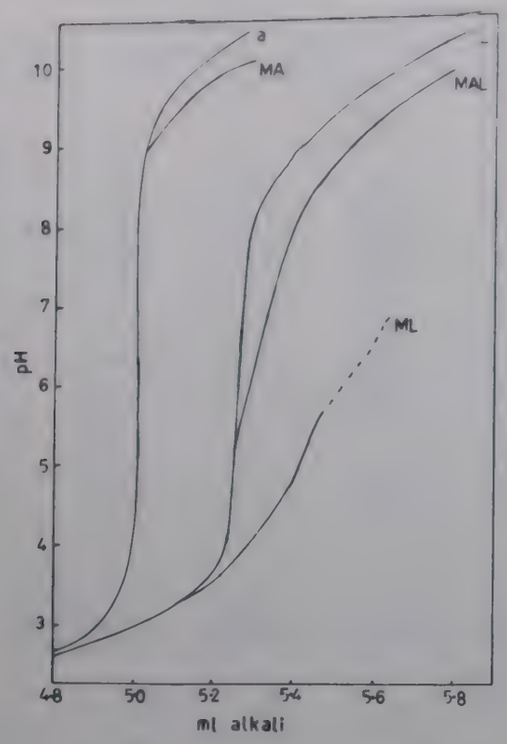

Fig. 1 – Representative *p*H titration plots for the system [Tb(III). CDTA.IMDA] [Curves A: reference acid, MA: primary complex, L: secondary ligand, ML: binary complex, MAL: ternary complex.]

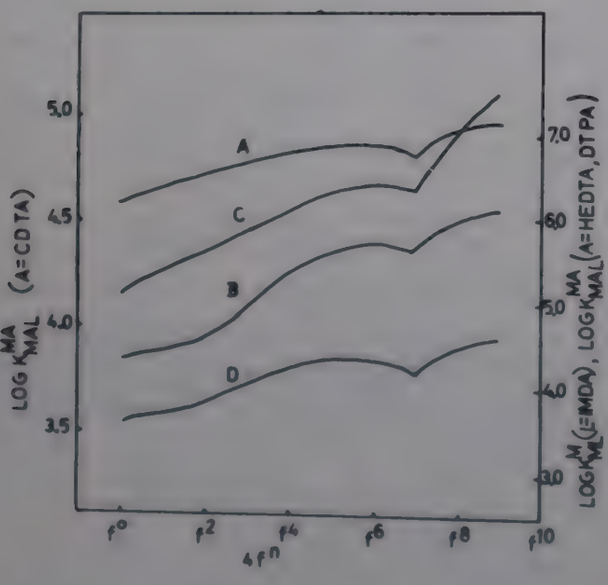

Fig. 2 – Variation in the formation constants with the No. of 4*f*-electrons ($4f^n$) of the Ln(III) ions. [Curve A: $\log K^{M}_{ML}$ (L = IMDA), curve B: $\log K^{MA}_{MAL}$ (A = HEDTA), curve C: $\log K^{MA}_{MAL}$ (A = CDTA), curve D: $\log K^{MA}_{MAL}$ (A = DTPA)].

the formation of the mixed ligand complexes. This is reflected by the observed trend in $\Delta \log K$ values (Table 2). The $\Delta \log K_1$ values are found to be comparatively less negative or even positive in some cases. This is so due to the observed sequence, $\log K^{M}_{ML} > > \log K^{MA}_{ML} \geq \log K^{MA}_{MAL}$. A marked lowering of $\log K^{MA}_{ML}$ values seems to be a consequence of significant statistical and steric effects

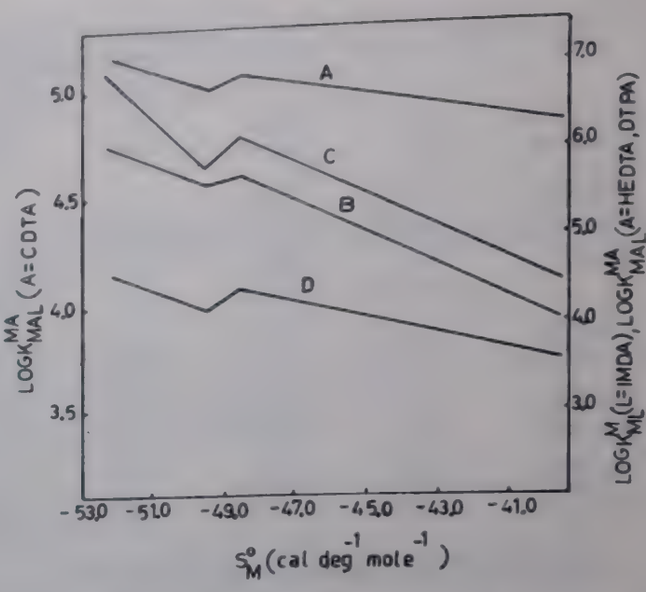

Fig. 3 – Variation in the formation constants with the standard entropies, S°_{M} of the lanthanides. [Curve A: $\log K^{M}_{ML}$ (L = IMDA), curve B: $\log K^{MA}_{MAL}$ (A = HEDTA), curve C: $\log K^{MA}_{MAL}$ (A = CDTA), curve D: $\log K^{MA}_{MAL}$ (A = DTPA)].

involved in the complexation (second step, i.e., $ML + L \rightleftharpoons ML_2$) with IMDA, due to its fairly large size and tridentate character. All $\Delta \log K_L$ values ($\Delta \log K_L = \Delta \log K_2 - \Delta \log K_1$) are observed to be positive due to the sequence $\Delta \log K_2 > \Delta \log K_1$. It has been suggested[24] that such a trend indicates a greater contribution from nonstatistical factors (presently, electrostatic factor) during the formation of mixed ligand complexes.

The primary and secondary ligands used in the present work are similar with imino nitrogen(s) and carboxylate oxygens as the binding sites (denticities : IMDA : 3, HEDTA : 5, CDTA : 6, DTPA : 8). Assuming the usual coordination number of Ln(III) ions to be eight or nine, an expansion of coordination sphere is indicated in the formation of mixed ligand complexes with DTPA.

The $\log K^{MA}_{MAL}$ (or $\log K^{M}_{ML}$) vs $4f^n$ plots, as shown in Fig. 2, indicate a marked depression at Gd(III) which is manifestation of tetrad effect. A possible minor discontinuity at the $4f^3 - 4f^4$ stage is, however, not clearly seen except with HEDTA. Plots of $\log K^{MA}_{MAL}$ (or $\log K^{M}_{ML}$) vs S°_{M} (standard entropy of Ln(III) ions in cal deg^{-1} mol^{-1}) also show (Fig. 3) a prominent break at Gd(III). A general linear increase (in two segments due to the 'Gd-break') in the formation constants with the standard entropies of the Ln(III) ions may be interpreted as an evidence of entropy stabilisation[26] of these mixed ligand complexes. A 'differential plot method' has been suggested here for locating two possible minor breaks at the $4f^3 - 4f^4$ and $4f^{10} - 4f^{11}$ stages. These plots have been drawn between $(\Delta \log K/\Delta r)$ vs $(r + \frac{1}{2}\Delta r)$ or $4f^n$.

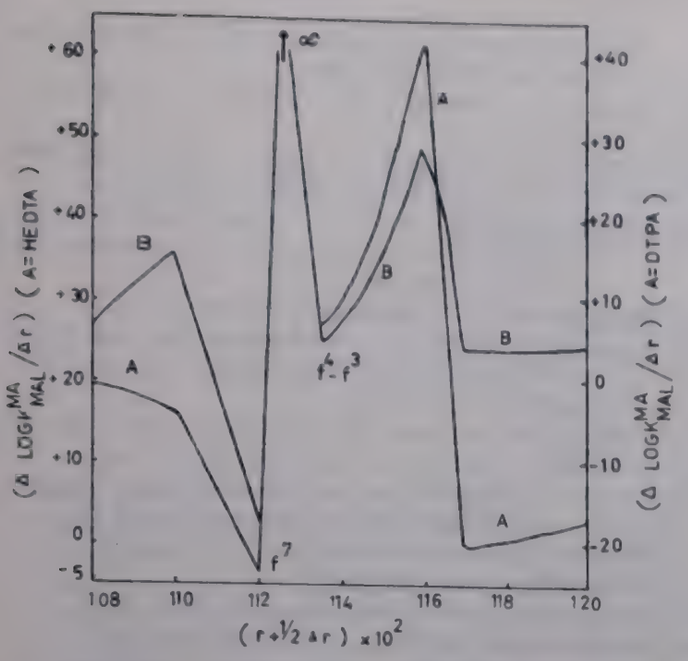

Fig. 4 – Differential plots showing variation in $(\Delta \log K^{MA}_{MAL}/\Delta r)$ with $(r+\frac{1}{2}\Delta r)\times 10^2$. [Curve A: HEDTA, curve B: DTPA].

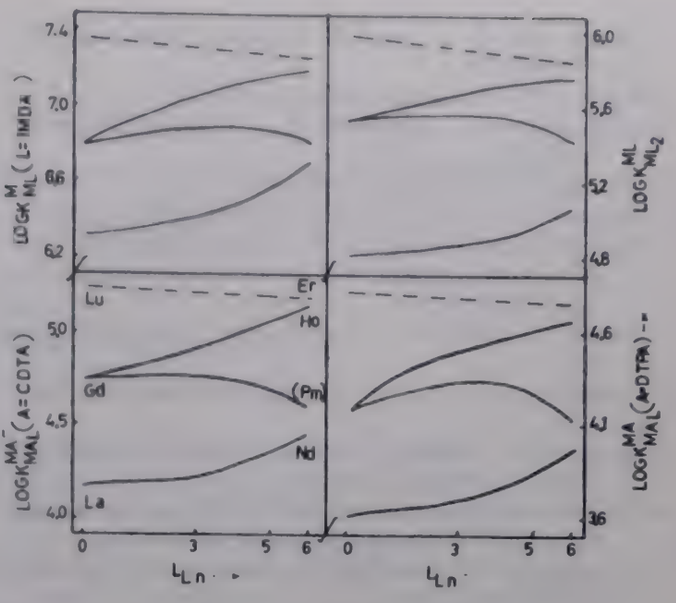

Fig. 5 – Inclined-W plots showing variation in the formation constants with the total orbital angular momentum (L_{Ln}) of the lanthanides.

where $\Delta \log K$ stands for the difference between the formation constants (or a Ln(III) property, in general) of two successive Ln(III) ions, and Δr for the corresponding difference between the ionic radii (Goldschmidt values[27]). The present set of representative plots (Fig. 4) show a clear dip at the $4f^3-4f^4$ stage also besides the much more prominent minima at the $4f^7$ stage which indicates the occurrence of tetrad effect at the ends of the first and second tetrads.

The dependence of the properties of lanthanides on their total orbital angular momentum, L_{Ln} has been proposed by Sinha[28] (the so called 'inclined-W hypothesis'). Fig. 5 shows plots of $\log K^{MA}_{MAL}$ (or $\log K^{M}_{ML}$) vs L_{Ln} for the present set of formation constant values. All the plots are of inclined-W type but are devoid of symmetry, and, in some cases, linearity within the segments. It is evident that the curvature in the second segment is caused by the tetrad effect. Since the L_{Ln} values themselves exhibit periodicity, plots of smoothly increasing/decreasing properties over the Ln(III) series are expected to yield the so called inclined-W. Thus, on correlating $4f^n$, ionic potential, polarising power (properties increasing gradually across the Ln(III)-series), and ionic radius, standard entropy and standard oxidation potential (properties decreasing over the Ln(III)-series) inclined-W plots (figures not shown) are obtained. The only difference in these two sets of plots is that the positions of the Ln(III) ions get reversed. In either case the three vertices of the inclined-W coincide with the configurations $4f^3-4f^4$, $4f^7$ and $4f^{10}-4f^{11}$, i.e., the ends of first, second and third tetrad, respectively.

Siekierski[11,29] and Dzhurinskii[30,31] are of the opinion that the inclined-W plots are accidental. The total dependence of the properties (showing tetrad effect) on the L_{Ln} quantum number is questionable[32]. But it may be emphasised[33] that all the $4f$ electrons in the lanthanides have the same energy and their ground terms are characterised by L_{Ln}. Splitting of the terms occurs as a consequence of L–S coupling. The magnitude of splitting appears to vary periodically with the number of $4f$ electrons. It is also observed that properties (here $\log K^{MA}_{MAL}$) vary rather smoothly for the terms S ($L_{Ln}=0$) and I ($L_{Ln}=6$), but discontinuity occurs corresponding to the terms F ($L_{Ln}=3$) and H ($L_{Ln}=5$).

Acknowledgement

The authors are thankful to the Head, Department of Chemistry, Dr H.S. Gour Vishwavidyalaya, for providing laboratory facilities and to the UGC, New Delhi for the financial support.

References

1 Preobrazhenskii B K, *Khim Nauka i Prom*, **4** (1959) 521.
2 Fidelis I & Siekierski S, *J inorg nucl Chem*, **28** (1966) 185.
3 Siekierski S, *J inorg nucl Chem*, **32** (1970) 519.
4 Fidelis I & Siekierski S, *J inorg nucl Chem*, **29** (1967) 2629.
5 Fidelis I, *J inorg nucl Chem*, **32** (1970) 997.
6 Mioduski T & Siekierski S, *J inorg nucl Chem*, **37** (1975) 1647.

7 Guillaumont R & David F, *Radiochem Radioanal Lett*, **17** (1974) 25.
8 Siekierski S, *J inorg nucl Chem*, **33** (1971) 377.
9 Janowski A & Lewandowski W, *J inorg nucl Chem*, **42** (1980) 561.
10 Mioduski T, *J Radioanal Chem*, **53** (1979) 25.
11 Siekierski S, *J inorg nucl Chem*, **43** (1981) 3381.
12 Ashcroft S J & Mortimer C T, *Thermochemistry of transition metal complexes*, (Academic Press, London, New York) 1970, 386.
13 Fidelis I & Siekierski S, *J inorg nucl Chem*, **28** (1966) 185.
14 Fidelis I & Siekierski S, *J inorg nucl Chem*, **33** (1971) 3191.
15 Peppard D F, Mason G W & Lewey S, *J inorg nucl Chem*, **31** (1969) 2271.
16 West T S, *Complexometry with EDTA and related reagents*, (BDH Chemicals Ltd, Poole) 1969, 188.
17 Irving H M & Rossotti H S, *J chem Soc*, (1953) 3397; (1954) 2904.
18 Chidambaram M V & Bhattacharya P K, *J inorg nucl Chem*, **32** (1970) 3271.
19 Rossotti F J C & Rossotti H S, *Acta chem scand*, **9** (1955) 1166.
20 Pecsok R L, Shields L D, Cairns T & McWilliams I G, *Modern methods of chemical analysis*, 2nd Edn (John Wiley, New York) 1976, 491.
21 Carey G H & Martell A E, *J Am chem Soc*, **88** (1967) 2859.
22 Katkar V S & Munshi K N, *J Indian chem Soc*, **18** (1986) 948.
23 Ashcroft S J & Mortimer C T, *Thermochemistry of transition metal complexes*, (Academic Press, London, New York) 1970, 391 & 394.
24 Bhattacharya P K, *J scient ind Res*, **40** (1981) 382.
25 Bagnall K W, *Inorganic chemistry*, Series two, Vol 7, *Lanthanides and actinides* (Butterworths, London), 1975, Chapters 2 & 3.
26 Limaye S N & Saxena M C, *J Indian chem Soc*, **62** (1985) 576.
27 Lurie Ju, *Handbook of analytical chemistry* (English Translation), (MIR Publishers, Moscow) 1975, 22.
28 Sinha S P, *Helv chim Acta*, **58** (Fasc 7) (1975) 1978.
29 Siekierski S, *Kemia-Kemi*, **6** (1979) 5.
30 Dzhurinskii B F, *Russ J inorg Chem*, **25** (1980) 41.
31 Dzhurinskii B F, *Russ J inorg Chem*, **28** (1983) 617.
32 Williams R J P, *Structure and Bonding*, **50** (1982) 81.
33 Sinha S P, *Systematics and the properties of the lanthanides*, (D Reidel Publishing Company, Dordrecht, Holland) 1983, 71.

Indian Journal of Chemistry
Vol. 27A, December 1988, pp. 1073-1079

Conductance Studies of Tetraalkylammonium Iodides in Dimethyl Sulphoxide-Water Mixtures

S DAS & D K HAZRA*
Department of Chemistry, North Bengal University, Darjeeling 734 430

Received 12 *November* 1987; *revised and accepted* 14 *March* 1988

Molar conductances of Me_4NI, Et_4NI, Pr_4NI, Bu_4NI, NaI and $NaBPh_4$ have been measured at 298 ± 0.01 K in the concentration range 0.005-0.08 mol dm^{-3} in dimethyl sulphoxide (DMSO) + water mixtures containing 20, 40, 60 and 80 wt% DMSO. The data have been analysed by the 1978 Fuoss conductance equation and the characteristic parameters Λ°, K_A and R have been evaluated. The Λ° values have been split into limiting ion conductances using the 'reference electrolyte' method and the corresponding Walden products evaluated. The association constants (K_A) have been found to be negligible for these salts over the entire range of solvent composition studied. The Walden product ($\Lambda^\circ\eta_0$) varies with solvent composition and the maximum observed is different for different electrolytes. Variation in $\lambda^\circ_+ \eta_0$ values of the tetraalkylammonium ions with solvent composition has been explained in terms of ion-solvent interactions and structural changes in solvent mixtures.

Arrington *et al.*[1] and Das *et al.*[2] respectively reported the conductances and viscosities of tetraalkylammonium halides in pure dimethyl sulphoxide (DMSO). Evans and Kay[3] reported the conductances of these salts in water and drew useful inferences regarding the effects of interactions of water with the hydrophobic side chains of these electrolytes. However, such studies in DMSO-water mixtures do not appear to have been attempted and hence the title investigation.

Materials and Methods

Dimethyl sulphoxide (Baker analysed) and tetraalkylammonium iodides (Fluka, purum) were further purified as described earlier[2]. Sodium tetraphenylborate (Fluka, puriss) was recrystallized from acetone and dried *in vacuo* at 353K. Sodium iodide (GR, E Merck) was used as such after drying at 400 K. Triply distilled water was used for preparing DMSO-water mixtures, which were pre-

(accuracy ± 0.1%) at 298 ± 0.01 K and a frequency

Stock solutions (0.1 *M*) of various salts were prepared by weight and the working solutions were obtained by weight dilution. The molar concentrations of the solutions were calculated from molality and density values. The concentrations varied between 0.005 and 0.08 *M*.

The viscosity of solvent mixtures were taken from our earlier works[4] and the densities were determined using an Ostwald-Sprengal type pycnometer. Dielectric constants of the solvent mixtures were taken from the literature[5].

A Pye-Unicam conductivity bridge (model 9509) was used for measuring the conductances (accuracy ± 0.1%) at 298 ± 0.01K and a frequency of 2 kHz with a dip-type cell (cell constant = 0.730 cm^{-1}).

Results and Discussion

The equivalent conductances and the corresponding molarities at different percentages of DMSO + H_2O mixtures are given in Table 1. The data have been first analysed by Shedlovsky's method[6] using Eqs (1-6):

$$\frac{1}{S\Lambda} = \frac{1}{\Lambda^0} + \frac{C\Lambda S f_\pm^2 \pm K_A}{\Lambda_0^2} \quad \ldots (1)$$

$$S = \left[\frac{B\sqrt{C\Lambda}}{2\Lambda_0^{3/2}} + \sqrt{\left(1 + \frac{\beta^2 C\Lambda}{4\Lambda_0^3}\right)}\right]^2 \quad \ldots (2)$$

$$\beta = \frac{8.204 \times 10^5 \Lambda_0}{(\varepsilon T)^{3/2}} + \frac{82.5}{\eta(\varepsilon T)^{1/2}} \quad \ldots (3)$$

$$\log f_\pm = -\frac{1.8246 \times 10^6 (C\alpha)^{1/2}/(\varepsilon T)^{3/2}}{1 + 50.29 \times 10^8 R\,(C\alpha)^{1/2}/(\varepsilon T)^{1/2}} \quad \ldots (4)$$

$$\alpha = \frac{S\Lambda}{\Lambda^\circ} \quad \ldots (5)$$

$$q = \text{Bjerrum critical distance} = \frac{e^2}{2\varepsilon kT} \quad \ldots (6)$$

The association constant, K_A, and the limiting equivalent conductance (Λ°) were iteratively calculated and the values thus obtained are given in Table 2. The standard deviations in Λ° were $< \pm 0.1\%$.

Table 1—Equivalent Conductances of Tetraalkylammonium Iodides in DMSO + Water Mixtures at 25°C

[C in mol lit^{-1} & Λ in Ω^{-1} cm^2 mol^{-1}]

20% (w/w) DMSO

Me_4NI		Et_4NI		Pr_4NI	
10^4C	Λ	10^4C	Λ	10^4C	Λ
73.1	78.22	73.2	68.85	73.2	60.03
102.6	75.05	102.7	67.93	102.8	59.23
		310.2	63.97	309.1	55.57
309.6	72.25	414.7	62.64	519.7	53.19
414.1	81.01	626.1	60.56	625.4	52.29
624.4	64.06	732.8	59.71	731.8	51.50
730.5	62.97				

Bu_4NI		NaI		$NaBPh_4$	
10^4C	Λ	10^4C	Λ	10^4C	Λ
73.8	55.51	73.2	73.05	73.7	53.14
102.8	54.66	102.8	72.96	102.8	52.30
311.1	44.37	309.1	67.94	310.8	43.92
522.9	44.27	517.3	67.51	522.2	41.94
630.2	43.29	622.1	65.73	629.3	41.95
738.4	41.98	727.4	63.24	737.1	41.94

40% (w/w) DMSO

Me_4NI		Et_4NI		Pr_4NI	
10^4C	Λ	10^4C	Λ	10^4C	Λ
74.9	47.88	75.4	39.47	76.7	34.49
105.6	47.35	105.7	38.92	105.7	33.95
211.6	45.37	212.2	36.32	212.1	31.31
425.1	43.05	319.1	34.78	319.5	30.99
532.5	41.88	426.2	33.10	427.6	29.64
640.4	40.49	644.4	32.59	646.2	29.02
748.9	39.82	754.3	32.21	756.8	28.54

Bu_4NI		NaI		$NaBPh_4$	
10^4C	Λ	10^4C	Λ	10^4C	Λ
76.1	31.83	75.1	49.28	75.8	30.85
105.8	31.08	105.6	49.24	105.7	30.75
212.5	28.12	318.3	45.24	319.6	29.57
320.1	27.77	533.2	44.17	536.9	27.94
528.1	26.21	641.5	43.65	640.8	27.68
648.6	25.65	750.3	42.38	757.6	27.32
760.2	24.47				

60% (w/w) DMSO

Me_4NI		Et_4NI		Pr_4NI	
10^4C	Λ	10^4C	Λ	10^4C	Λ
77.1	28.31	77.1	28.24	78.2	24.57
108.5	27.62	108.6	27.62	108.7	24.01
327.1	25.02	438.4	23.27	328.3	22.54
547.4	22.90	549.8	21.83	557.2	19.88
658.5	22.64	661.8	21.07	663.9	19.59
769.8	20.89	774.5	20.53	777.4	19.30

(*Contd.*)

Table 1—Equivalent Conductances of Tetraalkylammonium Iodides in DMSO + Water Mixtures at 25°C—*Cont.*

[C in mol lit^{-1} & Λ in Ω^{-1} cm^2 mol^{-1}]

20% (w/w) DMSO

Bu_4NI		NaI		$NaBPh_4$	
10^4C	Λ	10^4C	Λ	10^4C	Λ
55.1	21.74	65.9	29.96	66.4	22.83
108.7	21.67	108.5	29.49	108.7	21.39
218.3	19.47	327.1	28.18	328.4	20.43
328.7	19.31	547.9	27.38	551.3	19.05
440.1	19.19	659.1	26.49	664.1	18.98
552.3	17.93	770.7	26.25	777.5	18.14

80% (w/w) DMSO

Me_4NI		Et_4NI		Pr_4NI	
10^4C	Λ	10^4C	Λ	10^4C	Λ
57.1	25.44	55.8	24.28	55.9	22.70
83.5	25.03	84.1	23.85	84.7	22.25
110.1	24.55	110.2	23.52	110.1	21.96
332.2	24.10	332.1	21.59	333.4	20.06
557.1	23.55	558.4	20.28	559.1	18.73

Bu_4NI		NaI		$NaBPh_4$	
10^4C	Λ	10^4C	Λ	10^4C	Λ
56.1	21.58	56.2	25.18	56.1	18.41
82.2	21.20	82.3	24.38	82.3	18.04
110.1	20.86	110.4	24.55	110.2	18.00
333.5	19.13	332.2	23.04	333.1	16.22
560.2	16.61	560.1	22.94	560.2	14.73

Table 2—Limiting Conductances (Λ°) and Association Constants (K_A) of Tetraalkylammonium Iodides in DMSO + Water Mixtures at 298 K (Calculations based on Shedlovsky's Method)

Salt	20%		40%		60%		80%	
	Λ°	K_A	Λ°	K_A	Λ°	K_A	Λ°	K_A
Me_4NI	83.74	2.14	51.58	2.02	31.42	5.99	26.79	−2.24
Et_4NI	73.57	0.43	42.31	2.35	31.74	8.44	26.26	1.98
Pr_4NI	64.62	0.47	36.91	1.10	28.98	7.15	24.66	2.29
Bu_4NI	59.74	4.21	35.45	4.68	23.48	1.79	23.78	7.72
NaI	77.96	0.12	52.70	0.91	31.91	−4.04	27.66	3.43
$NaBPh_4$	57.32	3.38	33.33	−1.58	24.31	1.39	20.41	2.99

The low values of association constant ($K_A < 10$) suggests that the electrolytes are present as free ions in these solvent mixtures. This is reasonable in view of the high dielectric constants of the mixtures ($46.7 \leq D \leq 78$).

The conductance data were also analysed by Fuoss-Onsager equation[7] for unassociated electrolytes (see Eq. 7)

$$\Lambda = \Lambda^\circ - SC^{1/2} + EC \log C + (J - B\Lambda^\circ)C = \Lambda^\circ + J'C \quad \ldots (7)$$

The Λ°-values previously determined were used to calculate E and S values by the iteration procedure. The Λ°-values thus calculated are recorded in Table 3.

The recent computation method proposed by Fuoss[8] was used to calculate the conductance parameters from the measured equivalent conductances of the salts at 298 K. For a set of conductance data ($C_j\Lambda_j$, $J = 1 \ldots n$), three adjustable parameters Λ°, K_A and R (cosphere diameter) were obtained by solving Eqs (8-13):

$$\Lambda = P[\Lambda^\circ(1 + RX) + EL] \quad \ldots (8)$$

$$P = [1 - \alpha(1 - \gamma)] \quad \ldots (9)$$

Table 3—Limiting Conductances ($\Delta°$) of Tetraalkylammonium Iodides in DMSO + Water Mixtures at 298 ± 0.01 K

[Values obtained from Fuoss-Onsager Equation]

Salt	20%	40%	60%	80%
Me_4NI	83.97(±0.33)	51.46(±0.21)	31.77(±0.39)	27.08(±0.36)
Et_4NI	73.82(±0.02)	42.19(±0.43)	30.75(±0.32)	26.28(±0.04)
Pr_4NI	64.82(±0.04)	36.99(±0.34)	26.86(±0.26)	24.65(±0.31)
Bu_4NI	59.44(±0.20)	35.02(±0.26)	23.52(±0.38)	23.75(±0.17)
NaI	78.38(±0.22)	52.83(±0.34)	32.12(±0.22)	27.55(±0.21)
$NaBPh_4$	57.11(±0.36)	33.73(±0.11)	24.35(±0.34)	20.35(±0.24)
Bu_4NBPh_4	38.17	15.92	15.75	16.55

$$\gamma = 1 - K_A C\gamma^2 f^2 \quad \ldots(10)$$

$$-\ln f = \beta\kappa/2(\dot{1} + \kappa R) \quad \ldots(11)$$

$$\beta = e^2/DkT \quad \ldots(12)$$

$$K_A = K_R/(1-\alpha) = K_R(1+K_S) \quad \ldots(13)$$

where RX and EL are relaxation and hydrodynamic terms respectively and other terms have their usual significance. The calculations were performed on a Wipro Z-650 computer using the programme furnished by Prof R M Fuoss. Initial $\Lambda°$ values for the iteration procedure were obtained from Shedlovsky extrapolations of the data.

Calculations were made by finding the values of $\Lambda°$ and α which minimize

$$\sigma^2 = \sum[\Lambda_j(\text{cal}) - \Lambda_j(\text{obs})]^2/(n-2) \quad \ldots(14)$$

for a sequence of R values and then plotting $\sigma\% = 1000\ \sigma/\Lambda°$ against R, the best fit R corresponding to the maximum in the $\sigma\%$ versus R curve. First a course scan for all the salts was done from R = 4 to R = 15 with increment of one unit in R values. But no significant minimum was found and the computations were done by fixing R at $\beta/2$.

The values of $\Lambda°$, K_A and R obtained by this procedure are recorded in Table 4. The corresponding $\Lambda°$-values in water and DMSO taken from literature[1,3] are also included for comparison.

The limiting conductance values obtained from Shedlovsky's method, Fuoss-Onsager method for unassociated electrolytes and the recent (1978) Fuoss method show reasonably good agreement with each other. It is apparent that the improvement in the values is only marginal in most cases. The $\Lambda°$-values decrease continuously and the minima in the $\Lambda°$-values are observed in the region of 60 wt% DMSO.

The splitting of $\Lambda°$ into single ion values was made using Bu_4NBPh_4 as the reference electrolyte[9-11] using the relationship[12] (15)

$$\frac{\lambda°_{Bu_4N^+}}{\lambda°_{Ph_4B^-}} = \frac{r_{Ph_4B^-}}{r_{Bu_4N^+}} = \frac{5.35}{5.00} = 1.07 \quad \ldots(15)$$

The ionic radii of Bu_4N^+ and Ph_4N^- were taken from the works of Gill *et al.*[13,14]. The limiting ionic conductances are given in Table 5. The Walden products of the ions are recorded in Table 6.

The viscosity (η_0) of the solvent mixture (DMSO + H_2O) increases rapidly to reach a maximum at about 33 mol % or 68 wt % DMSO. At this stage the η_0 is nearly four times the viscosity of water and thereafter decreases comparatively slowly[5]. The addition of DMSO to water first enhances the three dimensional structure of water; subsequent addition of DMSO leads to breakdown of water structure but with concomittant formation of DMSO − H_2O complex. The maximum structuredness seems to occur at ~33 mol % DMSO due to the formation of DMSO·$2H_2O$ complex[15-17] and thereafter cleavage of the complex takes place. The continuous increase in η_0 and decrease in $\Lambda°$ values of salts with a maximum and minimum around 33 mol% DMSO respectively suggest that the hydrodynamic entity increases continuously upto 33 mol% DMSO but decreases thereafter. Tetraalkylammonium ions are expected to be strongly solvated by water. Addition of DMSO increases the size of the hydrodynamic entity which becomes maximum at 33 mol% DMSO ($\Lambda°$-minimum), thereafter the dehydration of ions occurs. However, the nature of solvation will vary from ion to ion. Thus the differences in values of a particular electrolyte in different solvent mixtures must be due to difference in mobilities of the ions at infinite dilution.

The data in Table 4 show that the limiting equivalent conductances decrease with increase in alkyl chain length of the tetraalkylammonium iodide. This is in agreement with the earlier findings in several pure and mixed solvents[18] and can be attributed with the size and structure-forming ef-

Table 4—Conductance Parameters of Tetraalkylammonium Iodides, NaI and $NaBPh_4$ in DMSO + H_2O Mixtures at 298 K

Wt% DMSO	Λ° (Ω^{-1} cm^2 mol^{-1})	K_A (dm^{-3} mol^{-3})	$\beta/2$	σ%	Walden product
		Me_4NI			
0	121.38	—	—	—	1.081
20	84.40(±0.41)	3.36	3.62	0.32	1.131
40	51.44(±0.29)	3.39	3.69	0.21	1.151
60	32.24(±0.17)	7.58	3.87	0.38	1.102
80	27.53(±0.31)	5.18	4.29	0.25	0.925
100	42.40				0.848
		Et_4NI			
0	109.28	—	—	—	0.972
20	72.72(±0.52)	1.59	3.62	0.11	0.990
40	42.13(±0.34)	4.27	3.69	0.34	0.953
60	31.44(±0.39)	9.36	3.87	0.36	1.088
80	26.57(±0.21)	4.06	4.29	0.23	0.911
100	40.80	—	—	—	0.808
		Pr_4NI			
0	100.18	—	—	—	0.892
20	63.94(±0.45)	1.68	3.62	0.16	0.870
40	38.32(±0.47)	3.65	3.69	0.22	0.834
60	26.49(±0.25)	5.67	3.87	0.37	0.942
80	25.12(±0.37)	4.44	4.29	0.32	0.856
100	37.20				0.744
		Bu_4NI			
0	96.27	—	—	—	0.856
20	61.48(±0.17)	7.26	3.62	0.20	0.823
40	36.23(±0.33)	7.36	3.69	0.32	0.804
60	23.69(±0.28)	7.56	3.87	0.23	0.814
80	24.23(±0.31)	8.60	4.29	0.25	0.835
100	35.39	—	—	—	0.704
		NaI			
0	127.11	—	—	—	1.132
20	78.35(±0.55)	1.26	3.62	0.33	1.050
40	52.99(±0.61)	2.13	3.69	0.31	1.176
60	31.94(±0.49)	5.11	3.87	0.36	1.104
80	27.72(±0.24)	3.21	4.29	0.22	0.956
100	37.95	—	—	—	0.753
		$NaBPh_4$			
20	58.64(±0.34)	3.96	3.62	0.37	0.786
40	33.40(±0.49)	4.28	3.69	0.26	0.744
60	24.37(±0.46)	5.70	3.87	0.39	0.841
80	20.49(±0.21)	5.18	4.29	0.17	0.707
100	24.76	—	—	—	0.488

Table 5—Limiting Ionic Conductances in DMSO-Water Mixtures at 298K

Wt% DMSO	λ°_+ (Ohm^{-1} cm^2 mol^{-1})						
	Me_4N^+	Et_4N^+	Pr_4N^+	Bu_4N^+	Na^+	I^-	BPh_4^-
0	44.42	32.32	23.22	19.31	50.15	76.96	—
20	44.51	32.83	24.05	21.59	38.46	39.89	20.18
40	23.86	14.55	10.74	8.65	25.41	27.58	8.08
60	16.83	16.06	11.21	8.31	16.61	15.38	7.76
80	12.09	11.13	9.68	8.79	12.28	15.44	8.21
100	18.60	17.06	13.42	11.59	14.15	23.80	10.61

Table 6—Ionic Walden Products at Infinite Dilution in DMSO-Water

Wt% DMSO	η_0 (cp)	$\lambda^\circ_\pm\eta_0$ (ohm^{-1} cm^2 mol^{-1} p)						
		Me_4N^+	Et_4N^+	Pr_4N^+	Bu_4N^+	Na^+	I^-	BPh_4^-
0	0.890	0.395	0.287	0.207	0.172	0.446	0.685	—
20	1.341	0.597	0.440	0.322	0.289	0.516	0.535	0.271
40	2.221	0.530	0.323	0.238	0.192	0.564	0.612	0.179
60	3.454	0.581	0.555	0.387	0.287	0.574	0.531	0.268
80	3.446	0.416	0.383	0.333	0.303	0.423	0.532	0.283
100	2.000	0.372	0.341	0.268	0.232	0.283	0.476	0.212

fect of the cations[19] (anions being the same). Size and structure-forming effect decrease as the alkyl chain length increases and so the mobility is in the reverse order.

The Λ°-values decrease with the increase in viscosity of the solvent mixtures but the Walden products ($\Lambda^\circ\eta_0$) are found tobe different. However, the maximum in η_0 almost coincides with observed minimum in Λ°. The results suggest that the hydrodynamic entity is of importance in both the cases but the difference in solvation of ions is responsible for the change in mobility of the ions and hence Λ°.

Water molecules tend to form cage-like structure around R_4N^+ ions and the alkyl chains of R_4N^+ ions are partially hidden in these cages resulting in tighter packing but the size of the clathrate-like structure formed about the hydrocarbon portions of the ions increases as the length of the side chain increases[20]. The volume decrease results in a comparatively small hydrodynamic entity leading to increased Λ°-values. The introduction of DMSO initially causes a slight increase in Λ°-values due to increased structure formation in water. The Λ°-values subsequently decrease with further addition of DMSO due to solvation of ions by DMSO or DMSO·$2H_2O$ complexes leading to an increase in hydrodynamic entity. However, dehydration and solvation by DMSO at higher percentage cause Λ° to increase.

The hydrodynamic entity around the tetraalkylammonium ion should be greater in water than that in DMSO but the increased values of Λ° in water may be due to greater free movement of ions through the polar H-bonded solvent system having high dielectric constant. The three dimensional water structure have 'holes' which facilitate the transference of ions. The transfer process is obviously difficult in DMSO-water mixtures as the holes may be blocked by DMSO or DMSO·$2H_2O$ complex[17].

From Table 4 we find that the association constants, K_A, are low for all the electrolytes and pass through a maximum around 60 wt% DMSO. This may be ascribed to the selective solvation of cations and anions by DMSO in mixed solvent, preventing cations and anions approaching each and hence lowering K_A values.

The λ°_+ values decrease as we go from Me_4N^+ to Bu_4N^+ in pure as well as in the mixed solvents (Table 5). The trend is similar to that observed in water. The change in λ°_+ is only marginal initially, then sharply decreases to pass through a minimum at about 80 wt% DMSO (except for Bu_4N^+ where the minimum is observed at 60 wt% DMSO). The size and hydrophobic solvation in water and binary mixtures increase in the sequence $Me_4N^+ < Et_4N^+ < Pr_4N^+ < Bu_4N^+$, so that the λ°_+ should be in the reverse order. The cation solvation is usually pronounced in DMSO and the solvated sizes also follow the above order. The λ°_+ of Na^+, which is highly solvated by water, decreases and passes through a minimum at 80 wt% DMSO while minimum in λ°_- of I^- is obtained in 60 wt % DMSO. The iodide ion is a strong structure breaker in water and is also poorly solvated by DMSO due to steric factor[20].

The ionic Walden products, $\lambda^\circ_+\eta_0$, for the tetraalkylammonium ions show two maxima at 20 and 60 wt% DMSO (at 20 and 80 wt% for Bu_4N^+). For Na^+ ion, the maximum in $\lambda^\circ_+\eta_0$ occurs at 60 wt%. The Walden product of I^- show a maximum around 40 wt% DMSO and thereafter it decreases. Though the variation of the Walden product with solvent composition is difficult to quantify, it can be suggested from the results that these ions are solvated to different extents in these solvent mixtures.

Acknowledgement

The authors are thankful to Prof S C Lahiri for helpful discussion. One of the authors (S D) thanks the UGC, New Delhi for the award of a research fellowship.

References

1 Arrington D E & Griswold E, *J phys Chem*, **74** (1970) 123.

2 Das S, Hazra D K & Lahiri S C, *Z phys Chem (Frankfurt)*, **138** (1983) 185.

3 Evans D F & Kay R L, *J phys Chem*, **70** (1966) 366.

4 Das S & Hazra D K, Unpublished data.

5 Covington A K & Dickinson T, in *Physical chemistry of organic solvent systems*, edited by A K Covington & T Dickinson (Plenum Press, New York) 1973, p. 19.

6 Fuoss R M & Shedlovsky T, *J Am chem Soc*, **71** (1949) 1496.

7 Fuoss R M & Onsager L, *J phys Chem*, **61** (1957) 668.

8 Fuoss R M, *J phys Chem*, **82** (1978) 2427.

9 Krumgalz B S, *J chem Soc Faraday Trans* 1, **79** (1983) 571.

10 Fuoss R M & Hirsch E, *J Am chem Soc*, **82** (1960) 1013.

11 Coetzee J F & McGuire D K, *J phys Chem*, **67** (1963) 1810.

12 Krumgalz B S, *J chem Soc Faraday Trans I*, **76** (1980) 1275.

13 Gill D S, *Electrochim Acta*, **24** (1979) 701.

14 Gill D S & Sekhri M B, *J chem Soc Faraday Trans I*, **79** (1982) 119.

15 Macdonald D D & Hyne J B, *Can J Chem*, **49** (1971) 611.

16 Macdonald D D, Hyne J B & Swinton F L, *J Am chem Soc*, **92** (1970) 6355.

17 Lindberg J J & Kenttamma J, Soumen Kem, **B33** (1960) 104.

18 Fernandez-Prini R, in *Physical chemistry of organic solvent systems*, edited by A K Covington & T Dickinson (Plenum Press, New York), 1973, Chapter 5.

19 Bahadur Lal & Murti M V R, *J chem Soc Faraday Trans I*, **79** (1980) 1409.

20 Yang-Wen W, in *Structure and transport processes in water and aqueous solutions*, edited by R A Horne (Wiley-Interscience, New York) 1971 Chapter 15 pp. 639.

Indian Journal of Chemistry
Vol. 27A, December 1988, pp. 1080-1083

Spectrophotometric Study of Acid-Base Equilibria of Sudan Green in Mixed Water-Organic Solvent Media

M M SELEIM, K A IDRISS*, MAGDA S SALEH & H SEDAIRA

Department of Chemistry, Faculty of Science, University of Assiut, Assiut, Egypt

Received 21 *October* 1987; *revised and accepted* 25 *February* 1988

The visible absorption spectra of 1,4-bis(4'-methylanilino)-8-hydroxyanthraquinone (Sudan Green or SG) have been recorded in water-organic solvent mixtures in the *p*H range 0.2-11.5. The organic solvents used are ethanol, dimethylformamide and acetone. The spectral changes have been explained in terms of shifts in equilibria amongst different molecular and ionic species of SG existing in solution. The pK_a values corresponding to the different ionisation steps have been determined at 25°C and $I = 0.1$ mol dm^{-3} ($NaClO_4$) by graphical analysis of the absorbance-*p*H curves. The elimination of proton from the α-OH group of the nonionised species of SG occurs below *p*H 4.5 as a result of mesomeric interaction between the imino nitrogen and the C = O group. The results obtained are discussed in terms of molecular structure of the reagent and the nature of the organic cosolvent used.

Our continued interest in the solution equilibria of arylaminoanthraquinones[1-5], led us to undertake the title study. The main objectives have been to study *p*H-dependence of the spectral changes and to obtain a desirable level of control over the various acid-base equilibria existing in solution. The values of the acid dissociation constants have also been determined whenever possible from the graphical analysis of the spectral data.

Materials and Methods

Stock solution of Sudan Green (SG) (2×10^{-4} mol dm^{-3}) was prepared by dissolving accurately weighed amount of the purified reagent in spectrograde ethanol, dimethylformamide or acetone. Other chemicals used were of AR grade. Standard carbonate-free NaOH and perchloric acid solutions were prepared. Deionized water was used throughout the present study. The working solutions were prepared by accurate dilution. The acidity of the solutions was adjusted by adding dilute $HClO_4$ or NaOH solution. The ionic strength was maintained constant at $I = 0.1$ mol dm^{-3} ($NaClO_4$). The absorption spectra were recorded on a Pye-Unicam SP 8000 spectrophotometer at 25°C using 1 cm matched stoppered quartz cells. *p*H measurements were made using a Radiometer *p*H-meter (model M63) equipped with Radiometer combined glass electrode. The *p*H values in mixed media were corrected as described by Douheret[6].

Results and Discussion

Depending on the acidity of the medium, the solution of SG contains four different acid-base forms, viz., LH_5^{2+}, LH_4^+, LH_3^0 and LH_2^-. The diprotonated species LH_5^{2+} (520 nm) is present in strong acid medium (*p*H < 0.3). In the *p*H range of 0.5-1.2 the solution contains the purple monoprotonated LH_4^+ form (550 and 630 nm) together with the neutral LH_3^0 form (*p*H > 1.5). Above *p*H 2, the spectrum of SG exhibits a new absorption band in the region 440-460 nm. The longer wavelength band appears as split bands with λ_{max} at 590 and 640 nm. The intensity of 440 nm band increases rapidly with rise in *p*H whereas that of 550 nm band decreases gradually until it vanishes completely at *p*H ~ 4.5. These spectral changes are assumed to accompany the transformation of the neutral form LH_3^0 to the monoanionic species LH_2^-. The red LH_3^-. The red LH_3^0 species existing in the *p*H range of 2-3.5 is converted into the pale green monoanionic LH_2^- at *p*H ~ 4.0, above which the spectrum of the solution exhibits no band shift or intensity changes.

The acid-base equilibria of SG have been studied in media containing 20%, 50% and 75% of the organic cosolvent (ethanol, DMF or acetone). The absorbance of 4×10^{-5} mol dm^{-3} SG solution in the presence of various concentrations of $HClO_4$ or NaOH was recorded. The spectral changes of SG with *p*H (Fig. 1 as a representative case) show three isosbestic points (near 575, 560 and 495 nm) indicating the presence of different equilibria in solution.

The dissociation constants of SG in various media were evaluated from the individual formation regions of the absorbance-*p*H curves by graphical analysis. The principles of the graphical treatment of data have been given elsewhere[7-9]. For the sake of brevity we shall give only the final equations. The transformations are derived from the equation for the equilibrium constant and mass balance equations, combined

with the equation for total absorbancy of the solution (assuming the validity of Beer's law). After simple rearrangement one obtains for the eqilibrium (A) the transformations (1-4)

$$LH_x \overset{K_a}{\rightleftharpoons} HL_{x-1} + H^+ \; ; K_{a_x} \qquad \ldots(A)$$

$\varepsilon 1 \qquad\qquad \varepsilon 2$

$$A = \varepsilon_1 C_L + K_{a_x}(\varepsilon_2 C_L - A)/[H^+] = A_{01} + F_1 K_{a_x}$$

$$\ldots(1)$$

$$A = \varepsilon_2 C_L - (A - \varepsilon_1 C_L) K_{a_x}^{-1}[H^+] = A_{02} - F_2 K_{a_x}^{-1}$$

$$\ldots(2)$$

$$C_{L/A} = 1/\varepsilon_1 - (C_L \varepsilon_2 - A)[H^+]^{-1} A^{-1} \varepsilon_1^{-1} K_{a_x}$$
$$= \varepsilon_1^{-1} - Q_1[H^+]^{-1} \qquad \ldots(3)$$

$$C_{L/A} = 1/\varepsilon_2 + (A - C_L \varepsilon_1)[H^+] A^{-1} \varepsilon_2^{-1} K_{a_x}^{-1}$$
$$= \varepsilon_2^{-1} + Q_2[H^+] \qquad \ldots(4)$$

where A is the absorbance, C_L is the total reagent concentration, ε_1 and ε_2 are molar absorption coefficients, K_a is the equilibrium constant of the reaction (A), and the other symbols are self-explanatory. The plots of A[= f (F_1 or F_2)] versus $C_L/A = (f(Q_1[H^+]^{-1}$ or $Q_2[H^+])$ were linear. The values of the dissociation constants were obtained from the slopes of these linear plots. More precise values of K could be evaluated using "the graphical logarithmic analysis". The corresponding Eq. (5) can be derived from any one of the Eqs (1)-(4).

$$\log \frac{A - \varepsilon_1 C_L}{\varepsilon_2 C_L - A} = q\, pH - pK_{a_x} \qquad \ldots(5)$$

The slope of the plot $\log [(A - A_{01})/(A_{02} - A)]$ versus f (pH) gives the number of protons (q) liberated in the acid-base equilibrium (q = 1 for reaction A). The value of pH at which $\log [(A - A_{01})/(A_{02} - A)]$ is equal to zero determines the value of pK_{a_x}/q.

The procedure described above was applied separately to each wavelength and from the series of pK_{a_x} values mean values were calculated. Deviation from the mean pK values were evaluated using Eq. (6).

$$\sigma(pK) = \left[\frac{1}{N_\lambda} \sum_{n=1}^{N_\lambda} (p\bar{K} - pK_n)^2\right] \qquad \ldots(6)$$

where $p\bar{K}$ is the mean value calculated from pK values obtained from curves for individual wavelength n; N_λ is the number of wavelengths used. The acid-base and spectral characteristics of SG are given in Table 1.

Below pH 0.4, the spectrum of SG consists mainly of a symmetrical band with λ_{max} at ~ 520 nm. This band undergoes red shift and an apparent decrease in intensity on decreasing the acidity of the medium. At pH 2.5-4, the spectra of the reagent display an absorption at ~ 460 nm which is blue shifted with rise in pH. In addition, two overlapped bands are well defined at 590 and 640 nm. The latter band makes its first appearance at pH ~ 1.2.

The appearance of only one absorption band at lower pH values can be ascribed to the localisation of the π-electrons of the imino nitrogen whereas the separation into two bands is due to the interaction of these electrons with the π-electrons of the aromatic system. The band at ~ 460 nm can be assigned to π-π^* intramolecular charge transfer associated with the charge migration from the substituents to the an-

Table 1 — Acid-Base and Spectral Characteristics of SG in Various Media.

% of organic solvent	pK_a^+		$\lambda_{isosbestic}$			λ_{max}, nm; ($10^{-4}\varepsilon_{max}$) mmol^{-1}cm^2		
	(LH_4^+/LH_3^0)	(LH_3^0/LH_2^-)	LH_5^{2+}/LH_4^+	LH_4^+/LH_3^0	LH_3^0/LH_2^-	LH_4^+	LH_3^0	LH_2^-
			Ethanol-water media					
20	1.85 ± 0.03	3.72 ± 0.01	573	560	498	548(1.5)	633(1.05)	453(2.25)
50	2.33 ± 0.01	3.75 + 0.01	570	562	497	545(1.55)	638(1.35)	456(2.38)
75	2.45 ± 0.02	3.85 ± 0.03	570	560	596	545(1.6)	636(1.42)	455(2.38)
			DMF-water media					
20	1.75 ± 0.02	3.67 ± 0.03	570	560	498	544(1.63)	635(1.25)	458(2.33)
50	2.18 ± 0.01	3.65 + 0.01	574	560	495	545(1.63)	638(1.30)	453(2.45)
75	2.38 ± 0.02	3.55 ± 0.02	576	562	492	546(1.45)	637(1.13)	450(2.23)
			Acetone-water media					
20	2.04 ± 0.03	3.74 ± 0.01	575	560	494	540(2.25)	635(1.70)	455(2.23)
50	2.34 ± 0.03	3.85 + 0.02	575	562	495	542(2.50)	638(1.70)	456(2.43)
75	....	3.88 + 0.01	572	564	498	542(2.55)	636(1.70)	458(2.35)

† Mean value obtained from the values calculated for each wavelength using Eq. (5).

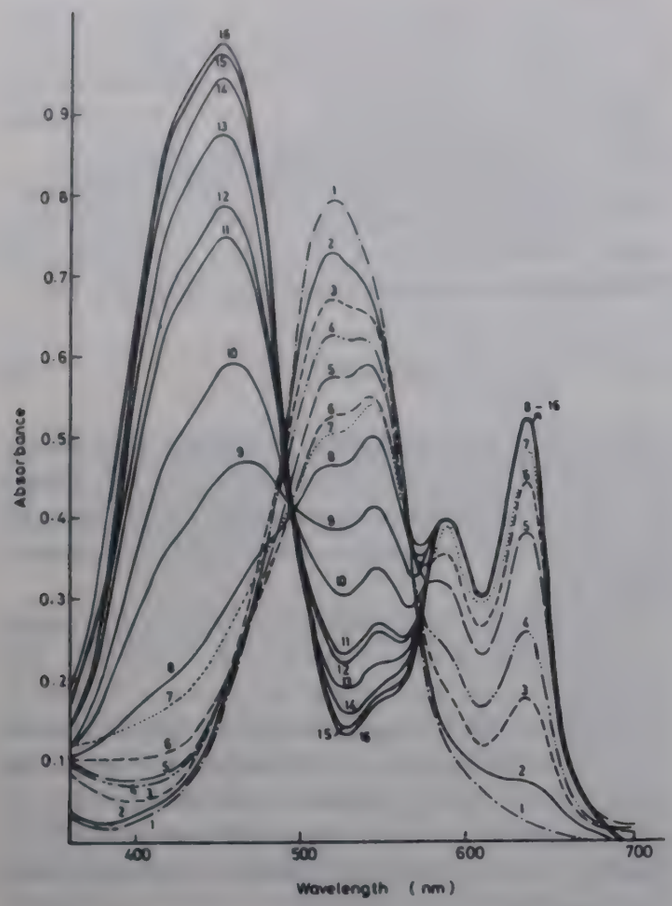

Fig. 1—Dependence of absorption spectra of SG on acidity [$C_L = 4 \times 10^{-5}$ mol dm^{-3}; 50% DMF. Curves 1-16 at *p*H values 0.3, 0.8, 1.85, 2.02, 2.22, 2.50, 2.78, 2.95, 3.30, 3.60, 3.80, 3.90, 4.15, 4.55, 5.95 and 7.90 respectively]

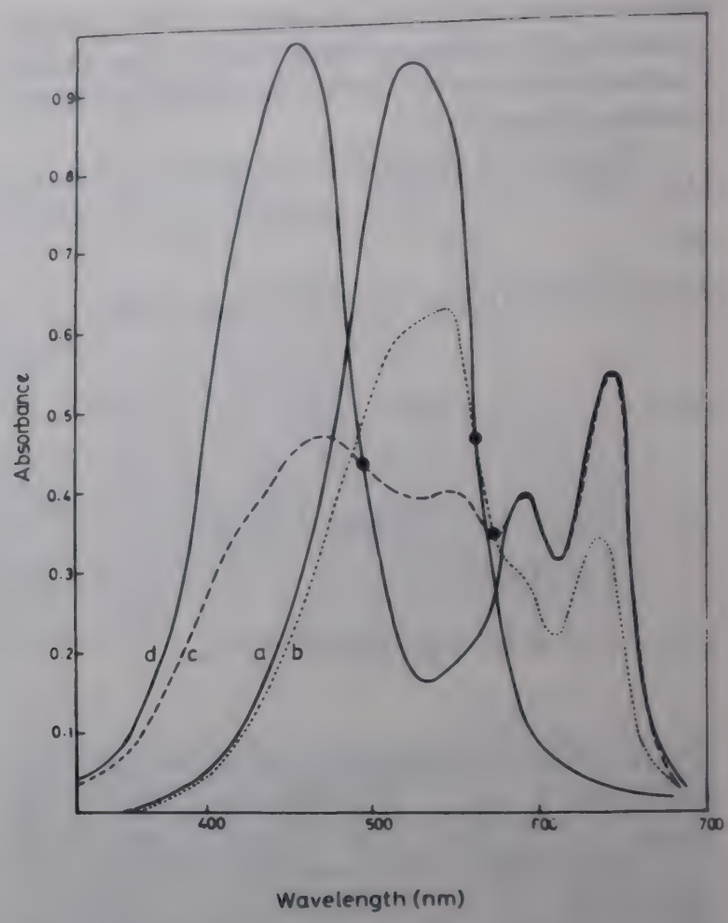

Fig. 2—Absorbance versus wavelength-curves for individual acid-base forms of SG [$C_L = 4 \times 10^{-5}$ mol dm^{-3}; 50% ethanol; $I = 0.1$ ($NaClO_4$), curves a-d for the forms LH_5^{2+}, LH_4^+, LH_3^0 and LH_2^- at *p*H 0.2, 1.10, 3.05 and 5.0 respectively.]

thraquinone moiety. The blue shift of this band with increase in *p*H is due to blocking of the lone pair of electrons of N atom, leading to hindrance of the charge transfer resulting in higher excitation energy.

As referred elsewhere in the paper, the appearance of three distinct isosbestic points (Figs 1 and 2) indicates the existence of different equilibria. These equilibria can be represented as shown in Scheme 1.

The appearance of the two overlapped bands on the longer wavelength side at *p*H ~ 1.2 and the obvious decrease in intensity of the π-π^* transition band at 280 nm corresponding to the quinonoid system suggest that SG in its monocationic form (LH_4^+) is involved in a resonance interaction of the type I ⇌ II. Such equilibrium seems to be shifted to the right at *p*H 2. This assumption provides evidence for the spectral changes accompanying liberation of a proton from the α-(OH) group, which takes place in the *p*H range of 3.5 to 4.0. The band at 520 nm becomes ill-defined at *p*H ~ 4 presumably due to the transformation of LH_3^0 to LH_2^-. The removal of the proton from the α-(OH) group hinders the ionisation of the mesomeric form (II) of SG. This is evidenced by the non-existence of spectral changes above *p*H ~ 5.

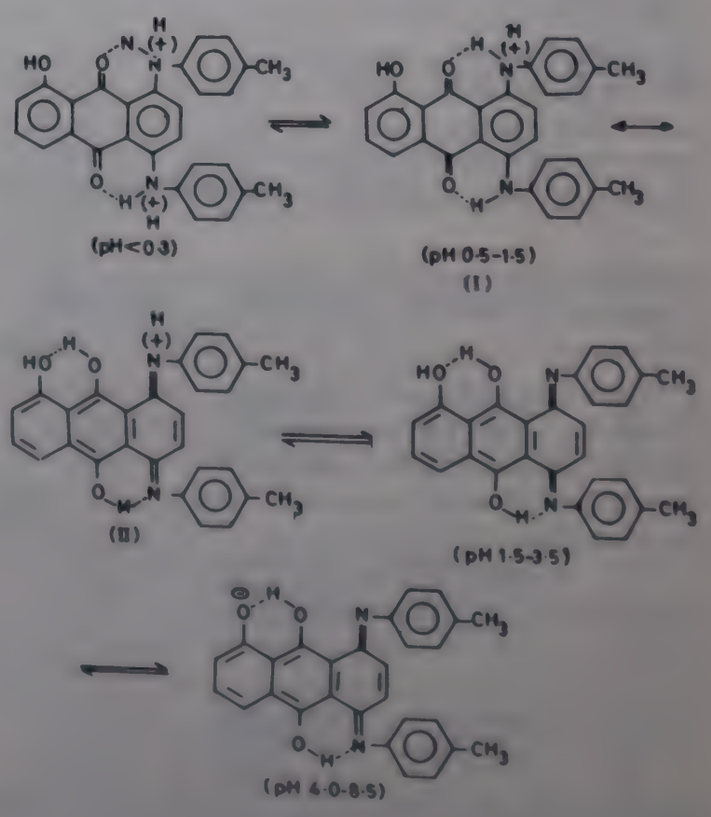

Scheme 1

An attempt was made to ascertain the ability of proton dissociation from the LH_2^- species *p*H-metrically. Titration of $HClO_4$ (50 ml, 2.5×10^{-3} mol dm^{-3}) at $I = 100$ mmol dm^{-3} ($NaClO_4$) was performed in 50% (v/v) ethanol, DMF or acetone-water medium. The *p*H-titration curves of SG in its monoanionic form (LH_2^-) gives only one steep inflection at $C_{OH}/C_L = 1$, where C_{OH} is the equivalent base added and C_L is the total initial concentration of SG. Multi-titrations were carried out in the media investigated. The inflection obtained was always found to start at *p*H 8-8.5. This inflection was unambiguously due to dissociation of the proton from LH_2^- species and the production of doubly ionised form (LH^{2-}) of the compound.

It is therefore not surprising that the LH_2^- species in the prevalent form of SG in the *p*H range of 4.5-8. In this respect, it is worthy of mentioning that the last proton elimination is not accompanied by measurable changes in the spectra of SG in different media (cf. Figs. 1 and 2). This behaviour can be explained on the basis that the N-phenyl moiety is twisted out-of-plane of the rest of the molecule[10,11], resulting in a weak interaction of the N-phenyl group with the anthraquinone nucleus. Accordingly one can assume that the acid dissociation occurring at $pH > 8.5$ is due to liberation of proton from the anilino group. The above conclusion may give us an insight into the complex forming ability of SG when present in its divalent anionic form.

The pK_a values obtained in solutions containing the same percentage of the different organic solvents follow the order: DMF (9.35) < ethanol (9.5) < acetone (9.79). This is presumably due to a decrease in the tendency of the solvent to associate with the solute through H-bond. Acetone is characterized by a very weak tendency to donate hydrogen bond[12]. The lowest pK_a value in DMF is because of its high basic character facilitating the ionisation process.

References

1 Idriss K A, Issa I M & Seleim M M, *J appl Chem Biotechnol*, **27** (1977) 549.
2 Idriss K A & Seleim M M, *Indian J Chem*, **19(A)** (1980) 771.
3 Idriss K A & Seleim M M, *J Chem Tech & Biotechnol*, **30** (1980) 136.
4 Idriss K A, Awad A, Seleim M M & Abu-Bakr M S, *Bull Soc chim Fr*, (1981) 180.
5 Idriss K A, Hassan M K, Abu-Bakr M S & Sedaira H, *Analyst*, **109** (1984) 1389.
6 Douheret G, *Bull Soc chim Fr*, (1967) p 1412.
7 Sommer L, Kuban V & Havel J, *Folia fac Sci nat Univ Brno Chemia*, 7 (1970) part 1, p. 33-62.
8 Rossotti F J C & Rossotti H, *The determination of stability constants* (McGraw-Hill, New York) 1961.
9 Kuban V, summer L & Havel J, *colln Czech chem Commun*, **40** (1975) 604.
10 Brocklehurst P, *Tetrahedron*, **18** (1962) 299.
11 Smith W F, *Tetrahedron*, **19** (1963) 445.
12 Coetzee J F & Richie C D, *Solute-solvent interactions* (Marcel Dekker, New York) 1969.

Indian Journal of Chemistry
Vol. 27A, December 1988, pp. 1084-1086

Notes

On the Counting of Conjugated Circuits in Benzenoid Hydrocarbons

I GUTMAN†
Division of Physical Chemistry, The University of Trondheim,
N-7034 Trondheim-NTH, Norway

Received 26 *July* 1988; *accepted* 18 *August* 1988

The importance of distinguishing between linearly independent and linearly dependent conjugated circuits is pointed out. In Randić's conjugated circuit model only independent conjugated circuits are considered. A class of benzenoid hydrocarbons is described which possesses no linearly independent conjugated circuits of size greater than 14.

In 1982 El-Basil proposed a method[1] for counting conjugated circuits in catacondensed benzenoid hydrocarbons. Whereas the correctness of El-Basil's method is not disputed, we wish to point out that not the number of conjugated circuits, but the number of independent conjugated circuits is the quantity needed in theoretical chemistry[2-5]. For instance, in ref. 1 the Randić resonance energy (RRE) of pentaphene was claimed to be given by the relation (1)

RRE (pentaphene) =

$$(26\,R_1 + 16\,R_2 + 6\,R_3 + 4\,R_4 + 2\,R_5)/10 \qquad \ldots (1)$$

whereas if one takes into account the linear dependency of some of the conjugated circuits, it is given by the relation (2).

RRE (pentaphene) =

$$(26\,R_1 + 16\,R_2 + 5\,R_3 + 2\,R_4 + R_5)/10 \qquad \ldots (2)$$

The aim of the present note is to clarify this discrepancy.

The precise definition of linear dependency of conjugated circuits can be found in the first paper[2] on the conjugated circuit model. We illustrate this concept by taking the example of a Kekulé structure (k) of pentaphene; structure (k) contains nine conjugated circuits which are depicted in Fig. 1.

If a conjugated circuit can be obtained by adding or subtracting the edges of conjugated circuits of smaller size (contained in the same Kekulé structure), then this circuit is considered as linearly dependent and is disregarded[2-4].

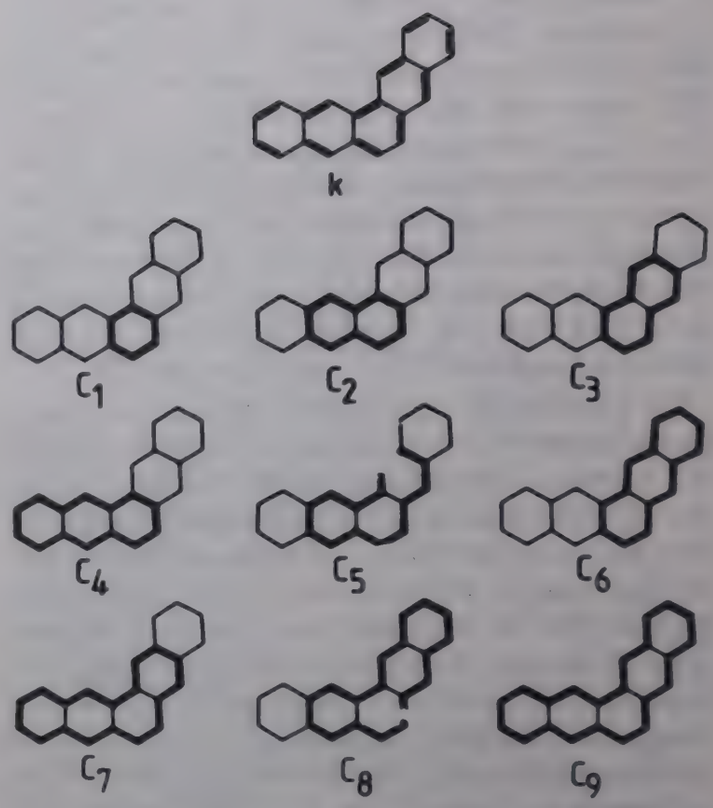

Fig. 1 – A Kekulé structure of pentaphene and the 9 conjugated circuits which it contains. Since $C_5 = C_2 + C_3 - C_1$, $C_7 = C_4 + C_3 - C_1$, $C_8 = C_2 + C_6 - C_1$ and $C_9 = C_4 + C_6 - C_1$, only 5 of the these conjugated circuits are linearly independent.

For example, the circuit C_5 of the Kekulé structure (k) is linearly dependent because of the relation: $C_5 = C_2 + C_3 - C_1$.

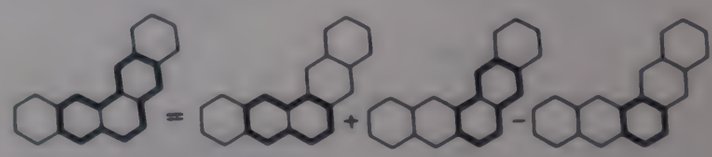

In Fig. 1 is indicated that a total of four conjugated circuits of structure (k) are linearly dependent. Thus the conjugated circuit decomposition of structure (k) is $R_1 + 2\,R_2 + 2\,R_3$, and not $R_1 + 2\,R_2 + 3\,R_3 + 2\,R_4 + R_5$ as would be obtained by neglecting the independence requirement. (Here and later R_i stands for a conjugated circuit of size $4i + 2$, the notation usual in the conjugated circuit theory[2-5].)

If one performs such a circuit decomposition for all the ten Kekulé structures of pentaphene and adds the results, the total circuit decomposition of pentaphene is found to be $26\,R_1 + 16$

†Permanent address: Faculty of Science, University of Kragujevac, P.O. Box 60, YU-34000 Kragujevac, Yugoslavia

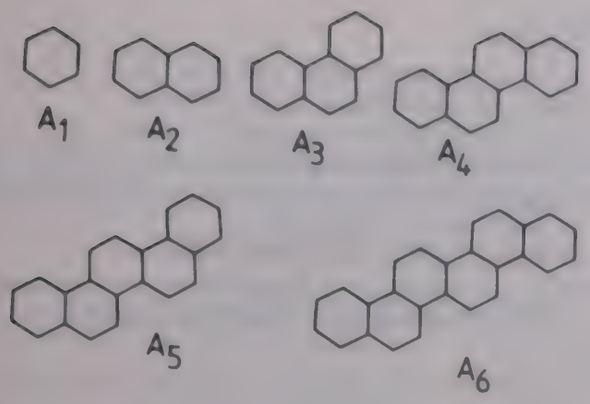

Fig. 2 – Class of zig-zag polyacenes.

$R_2 + 5\ R_3 + 2\ R_4 + R_5$, from which the previously given expression (2) for RRE follows immediately.

As seen from the above example, the numbers of conjugated circuits which play role in Randić's theory[2–4] are not equal to (and are always smaller than) the numbers computed by El-Basil's method[1]. In the following we wish to point out an interesting case, namely the class of zig-zag polyacenes. For these benzenoid hydrocarbons (see Fig. 2) all conjugated circuits of size greater than 14 are linearly dependent.

Denote the zig-zag polyacene with h hexagons by A_h. Recall than A_1, A_2, A_3, A_4, A_5, A_6 are benzene, naphthalene, phenanthrene, chrysene, picene and fulminene, respectively. In the terminology of El-Basil[6] A_h is the acene whose generating graph has h vertices and only two-vertex linear subgraphs.

Denote further by $\rho_i\ (A_h)$ and $\eta_i\ (A_h)$ the number of independent conjugated circuits of size $4i + 2$ and the total number of conjugated circuits of size $4i + 2$, respectively, of the molecule A_h.

It is well known[7] that the number of Kekulé structures of A_h is equal to F_{h+1}, the $(h+1)$-th Fibonacci number. (Recall that $F_0 = F_1 = 1$, $F_2 = 2$, $F_3 = 3$, $F_4 = 5$, ..., $F_{h+1} = F_h + F_{h-1}$.) From this, using El-Basil's method[1] one easily obtains the relation (3)

$$\eta_i(A_h) = 2 \sum_{j=0}^{h-i} F_j F_{h-i-j} \quad (i = 1,2,....,h) \qquad \ldots (3)$$

On the other hand, $\rho_1\ (A_h) = \eta_1\ (A_h)$, $\rho_2\ (A_h) = \eta_2\ (A_h)$, but $\rho_3\ (A_h) = \frac{1}{2}\eta_3\ (A_h)$ and $\rho_4\ (A_h) = \rho_5\ (A_h) = ... = \rho_h\ (A_h) = 0$.

We first show that $\rho_3\ (A_h) = \frac{1}{2}\eta_3\ (A_h)$. In order to do this observe that all conjugated circuits of size $4 \times 3 + 2 = 14$ in A_h must have the shape of phenanthrene. Two arrangements, α and β of double and single bonds are possible:

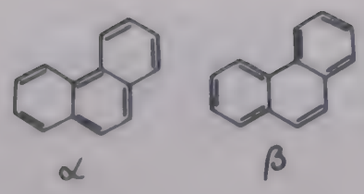

Now, the arrangement α implies the existence of three further conjugated circuits α_1, α_2, α_3 of size 10, 10 and 6, respectively:

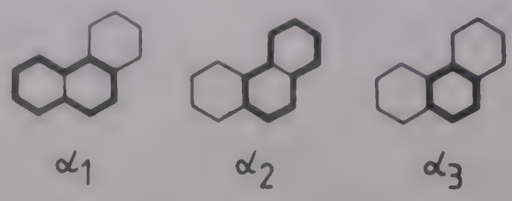

It is easily seen that: $\alpha = \alpha_1 + \alpha_2 - a_3$, and thus α is linearly dependent.

The examination of β shows that this conjugated circuit is linearly independent. This means that only every second conjugated circuit of size 14 is independent in A_4, which is exactly the statement we wanted to prove.

In order to veryfy that $\rho_4\ (A_h) = 0$ we apply a similar argument. All conjugated circuits in A_h having size $4 \times 4 + 2 = 18$ have the shape of chrysene. The arrangement of the double and single bonds is either γ or δ:

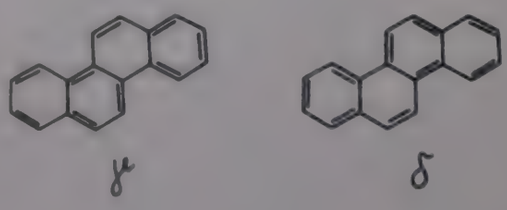

Since γ and δ are symmetry equivalent, whatever holds for γ, the same is true for δ.

The arrangement γ implies the existence of the conjugated circuits γ_1, γ_2 and γ_3 of size 10, 14 and 6, respectively:

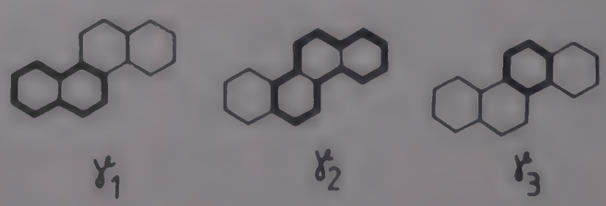

One immediately has $\gamma = \gamma_1 + \gamma_2 - \gamma_3$, which means that neither γ nor δ are linearly independent. Consequently, there are no linearly independent conjugated circuits of size 18 in A_h.

The result that $\rho_i(A_h) = 0$ for $i = 5$, $i = 6$ etc. can be deduced in a fully analogous manner.

Hence we have shown that in the case of zig-zag polyacenes the RRE is given by the expression (4)

$$RRE(A_h) = (\eta_1 R_1 + \eta_2 R_2 + \tfrac{1}{2}\eta_3 R_3)/F_{h+1} \quad \ldots (4)$$

and is completely independent of the actual choice of the parameters R_4, R_5 etc.

References

1 El-Basil S, *Indian J Chem*, **21B** (1982) 561.
2 Randić M, *Chem Phys Lett*, **38** (1976) 68.
3 Randić M, *J Am chem Soc*, **99** (1977) 444.
4 Randić M, *Tetrahedron*, **33** (1977) 1905.
5 Trinajstić N, *Chemical graph theory*, Vol II (CRC Press, Boca Raton) 1983, Chapter 1.
6 El-Basil S, *Indian J Chem*, **20B** (1981) 586.
7 Cyvin S J & Gutman I, *Kekulé structure in benzenoid hydrocarbons* (Springer-Verlag, Berlin) 1988.

Indian Journal of Chemistry
Vol. 27A, December 1988, pp. 1087-1088

Dimerization & Subsequent Complexation of 1,5,9-Cyclododecatriene with Hexacarbonyltungsten

K A AZAM, M B H HOWLADER, S E KABIR & S S ULLAH*

Department of Chemistry, Jahangirnagar University, Savar, Dhaka, Bangladesh

Received 10 *December* 1987; *accepted* 14 *January* 1988

The photochemical reaction of *trans, trans,cis*-1,5,9-cyclododecatriene with $W(CO)_6$ affords tricyclo[12.10.0.0^{2,13}] tetracicos-5,9,17-21-tetraene-η^4-bis[tetracarbonyltungsten]] (IV) which has been characterized by IR, PMR and mass spectra and elemental analyses.

Dimerization and subsequent complexation of cycloolefinic ligands during reaction of iron[1,2] and ruthenium[3] carbonyls have been reported and the results have been explained in terms of catalytic behaviour of metal carbonyls. Under mild conditions isomerization of *trans,trans,cis*-1,5,9-cyclododecatriene (I) to all *trans*-1,5,9-cyclododecatriene (II) and subsequent complexation with iron carbonyl has been observed by us[4] during the photochemical reaction between $Fe(CO)_5$ and I. Under more forcing conditions, I undergoes dimerization via isomerization to II and leads to the formation of $[C_{24}H_{36}Fe(CO)_3]$ (V) on reaction with $Fe(CO)_5$ (ref. 5). We have presently studied the photochemical reaction between I and $W(CO)_6$ in order to see if I undergoes isomerization, dimerization as well as complexation.

All operations were carried out under nitrogen atmosphere. Infrared spectra were recorded on a PE 983 spectrophotometer, PMR spectra on a Varian XL-200 spectrophotometer and mass spectra on a high resolution VG ZAB F-1 spectrometer. Molecular weights were determined by cryoscopy in benzene using a Kanuer cryoscopic unit autorecorder.

Photochemical reaction of trans,trans,cis-1,5,9-cyclododecatriene (I) with $W(CO)_6$

A mixture of $W(CO)_6$ (3.52 g) and I (4.86 g) in dry ether (200 ml) was irradiated with a 400 watt medium pressure mercury lamp in an immersion well quartz apparatus for 1 hr. The colour of the solution turned pale yellow and then deep yellow. The solvent was removed under reduced pressure and the residue purified by chromatography over

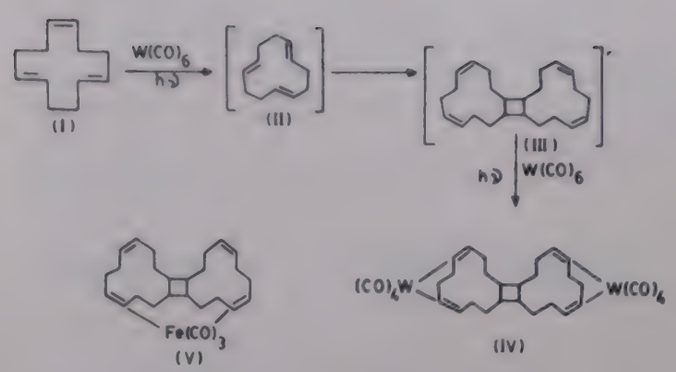

Scheme 1

silica. Elution with pet. ether (40-60°)-ethyl acetate (10:1, v/v) afforded a yellow crystalline complex $[C_{24}H_{36}W_2(CO)_8]$ (IV) (Found: C, 42.5; H, 4.4. $C_{32}H_{36}O_8W_2$ requires C, 42.0; H, 4.0%).

The IR spectrum of IV (in cyclohexane) exhibits νCO modes at 1980, 1957, 1939 and 1896 cm^{-1}. The PMR spectrum of IV in $CDCl_3$ exhibits an eight-proton multiplet at δ 5.0-5.45 appearing upfield in comparison to free olefinic protons, which has been assigned to the coordinated olefinic protons. The multiplet in the region δ 1.8-2.75 (24H) has been attributed to methylene protons whereas that at δ 1.0-1.3 (4H) to the protons attached to the cyclobutane ring. The appearance of this four-proton multiplet has been taken as one of the evidences for the dimerization of II during the course of the reaction to afford the dimer (III). The mass spectrum of IV shows molecular ion peak at *m/z* 916 with other peaks arising by the successive loss of six CO groups from M^+. Molecular weight (898) determined by cryoscopic method in benzene is in good agreement with the expected molecular weight. In our previous publication[5], the reaction of $Fe(CO)_5$ with I gave *trans,trans,cis*-1,5,9-cyclododecatrienetricarbonyliron, *trans,trans, trans*-1,5,9-cyclododecatrienecarbonyliron and $[C_{24}H_{36}Fe(CO)_3]$, a complex arising by the isomerisation of I to II followed by dimerization of II and complexation with $Fe(CO)_5$ moiety. In contrast reaction of I with $W(CO)_6$ leads to only complex (IV). We believe that formation of compound (IV) takes place according to Scheme 1.

The authors are thankful to the Department of Chemistry, University College London, London School of Pharmacy and Australian National University, Australia for IR, PMR and mass spectra and elemental analyses.

References

1 Edward R, Howel J A S, Johnson B F G & Lewis J, *J chem Soc Dalton*, (1974) 2110.

2 Connelly N G, Kelly R I, Kitchen M D, Mills R M, Stansfield R F D, Whitelay M W, Whiting S M & Woodward P, *J chem Soc Dalton*, (1981) 1317.

3 Goddardand R & Woodward P, *J chem Soc Dalton*, (1979) 661.

4 Ullah S S, Kabir S E, Molla M E & Wahiduzzaman S M, *Indian J Chem*, **23A** (1984) 180.

5 Ullah S S, Kabir S E, Molla M E & Wahiduzzaman S M, *Indian J Chem*, **24A** (1985) 45.

Indian Journal of Chemistry
Vol. 27A, December 1988, pp. 1089-1091

Linear Free Energy Correlation in Substitution Reactions of Octahedral Cobalt(III) Complexes

ANADI C DASH* & AJAYA K PATNAIK†
Department of Chemistry, Utkal University,
Bhubaneswar 751 004

Received 14 *September* 1987; *revised and accepted* 15 *January* 1988

Linear free energy correlation between log k_{aq} and log K_{eq} for the aquation of the carboxylatopentaamminecobalt(III) complexes,

$$(NH_3)_5CoO_2CR^{2+} \underset{k_{an}}{\overset{k_{aq}}{\rightleftharpoons}} (NH_3)_5CoOH_2^{3+} + RCO_2^- \quad (K_{eq} = k_{an}/k_{aq})$$

is satisfied for a variety of carboxylate ligands including the amino acidate betaines, $^-O_2C(CH_2)_xNH_3^+$. The rate-equilibrium data for a wide variety of ligands fit the linear plot with slope = 1.0, indicating the validity of the dissociative interchange mechanism (I_d). Extension of linear free energy correlation to the aquation of the binuclear complexes of oxalatopentaamminecobalt(III), $(NH_3)_5CoC_2O_4M^{(n+1)+}$ ($M^{n+} = Mn^{2+}$, Co^{2+}, Ni^{2+}, Cu^{2+}, Zn^{2+}, Al^{3+}, Ga^{3+}, In^{3+} and Fe^{3+}), however, indicates that possibility of acyl cleavage mechanism for the metal ion catalysed path cannot be completely ruled out.

While attempting to elucidate the mechanism of substitution reactions of cobalt(III) complexes of pentaammine class, Langford[1] noted that the plot of log k_{aq} versus log K_{eq} (see Eq. 1; $K_{eq} = k_{an}/k_{aq}$) was linear with unit slope for a limited number of leaving groups, X^-;

$$(NH_3)_5CoOH_2^{3+} + X^{n-} \underset{k_{aq}}{\overset{k_{an}}{\rightleftharpoons}} (NH_3)_5CoX^{(3-n)+} \quad \ldots (1)$$

The linear free energy correlation between ΔG^* and ΔG° (overall reaction) with unit slope was taken to indicate that transition state of the reaction was very similar to the products[2]. The activation volume measurements for the aquation of $(NH_3)_5CoX^{(3-n)+}$ ($X = Cl^-, Br^-, NO_3^-, SO_4^{2-}$, DMSO and H_2O) led to the computation of the molar volume of the D-transition state[3] which turned out to be independent of the leaving group, X^{n-}. From such studies Palmer and Kelm[3] concluded that the transition state was very much like a five-coordinate intermediate thus reinforcing the dissociative interchange mechanism (I_d).

The overall reaction represented by Eq. (1), infact, proceeds via two stages: (i) diffusion-controlled ion-pair formation (outer sphere complex) (Eq. 2); and (ii) slow outer sphere-inner sphere interconversion reaction (Eq. 3)

$$(NH_3)_5CoOH_2^{3+} + X^{n-} \overset{Q_0}{\rightleftharpoons} (NH_3)_5CoOH_2^{3+}, X^{2-} \quad \ldots (2)$$

$$(NH_3)_5CoOH_2^{3+} + X^{n-} \underset{k_{aq}}{\overset{k_{ex}}{\rightleftharpoons}} (NH_3)_5CoX^{(3-n)+} \quad \ldots (3)$$

Setting

$$K_{eq} = (Q_0 k_{ex}/k_{aq}) \quad \ldots (4)$$

we obtain

$$\log k_{aq} = \log (Q_0 k_{ex}) - \log K_{eq} \quad \ldots (5)$$

where Q_0 is the equilibrium constant of ion-pair formation and k_{ex} is the outer sphere-inner sphere interchange rate constant of ion-pair. It is interesting to note that spontaneous aquation of carboxylatoamminecobalt(III) complexes fit the linear free energy correlation satisfactorily[4,5]. This is an additional evidence in support of the operation of dissociative interchange mechanism (I_d) in the aquation of the carboxylatopentaamminecobalt(III) complexes. In other words the validity of LFER suggests that Co − O bond heterolysis occurs in the spontaneous aquation of $(NH_3)_5CoO_2CR^{n+}$. This is in support of the oxygen exchange experiments reported on the spontaneous aquation of $(NH_3)_5CoO_2CCH_3^{2+}$, and $(NH_3)_5CoO_2CCO_2H^{2+}$ (ref. 6,7). Contrastingly LFER for the aquation of $(OH_2)_5CrX^{(3-n)+}$ ($X = Cl^-, Br^-, I^-, NCS^-, SCN^-$) yielded 0.56 as the slope of the analogous plot[8]. The mechanism for these cases has been assigned to be I_a.

LFER for metal ion catalysed aquation of oxalatopentaamminecobalt(III)

The metal ion catalysed aquation of oxalatopentaamminecobalt(III) and *cis*-oxalato(ammine)-bis(ethylenediamine)cobalt(III) have been investigated by us earlier[9,10]. Recently Monk *et al*[11] have reinvestigated the kinetics of metal ion catalysed aquation of oxalatopentaamminecobalt(III). Agreement between our results and those of Monk *et al*[11] is satisfactory.

Herein an attempt has been made to elucidate the intimate mechanism of aquation of binuclear spe-

†Present address: Lecturer in Chemistry, D.A.V. College, Koraput 764 020, Koraput, Orissa.

cies, $(NH_3)_5CoC_2O_4M^{(n+1)+}$ through relevant linear free energy relationship. The rate-equilibrium relationship for the reactions stated in Eq. (6) may be given as in Eq. (7)

$$(NH_3)_5CoC_2O_4M^{(n+1)+} \underset{k_{an}^{MOX}}{\overset{k_{aq}^{M}}{\rightleftharpoons}} (NH_3)_5CoOH_2^{3+} + C_2O_4M^{(n-2)+} \quad \ldots (6)$$

$$K_{eq} = k_{aq}^{M}/k_{an}^{MOX}$$

$$\log k_{an}^{MOX} + \log K_{eq} \quad \ldots (7)$$

The overall equilibrium constant,

$$K_{eq} = [ROH_2^{3+}][C_2O_4M^{(n-2)+}]/[RC_2O_4M^{(n+1)+}] \quad \ldots (8)$$

$(R = (NH_3)_5Co^{3+})$ may be redefined as

$$K_{eq} = K_{MOX}/(K_M Q) \quad \ldots (9)$$

where K_{MOX}, K_M and Q are forward equilibrium constants for the reactions (10-12), respectively

$$C_2O_4^{2-} + M^{n+} \overset{K_{MOX}}{\rightleftharpoons} C_2O_4M^{(n-2)+} \quad \ldots (10)$$

$$RC_2O_4^{+} + M^{n+} \overset{K_M}{\rightleftharpoons} RC_2O_4M^{(n+1)+} \quad \ldots (11)$$

$$ROH_2^{3+} + C_2O_4^{2-} \overset{Q_{ox}}{\rightleftharpoons} RC_2O_4^{+} \quad \ldots (12)$$

Combining Eqs (7) and (9) we obtain the linear free energy relationship, given by Eq. (13)

$$\log k_{aq}^{M} = \log (k_{an}^{MOX}/Q_{ox}) + \log (K_{MOX}/K_M) \quad \ldots (13)$$

The values of k_{aq}^{M} at 25°C for different metal ions were calculated by extrapolation ($\log k_{aq}^{M}$ versus 1/T plot) of our earlier data[9]. The stability constants of monoxalato complexes of metal ions (K_{MOX}) at zero ionic strength at 25°C are available for Mn(II), Co(II), Ni(II), Cu(II), Zn(II) and Fe(III)[12,13]. The values of $\log K_{MOX}$ at $I = 1$ mol dm^{-3} and 25°C are available for Al^{3+}, In^{3+}; the same for Ga^{3+} is available at $I = 1.0$ mol dm^{-3} and 20°C (ref. 12). The temperature effect was disregarded and the $\log K_{MOX}$ values of these metal ions were corrected to $I = 0$ using the relationship (14)

$$\log K_{MOX}\,(I=0) = \log K_{MOX}\,(I = 1 \text{ mol dm}^{-3}) + 1.8 \quad \ldots (14)$$

as it is noted[12,13] that $\log K_{FeOX}$ at $I = 0$ is 1.8 unit higher than the same at $I = 1.0$ mol dm^{-3} (25°C).

Table 1—Rate and Equilibrium Constant Data for Aquation of Binuclear Complexes, $(NH_3)_5CoC_2O_4M^{(n+1)+}$

M^{n+}	$\log (K_M)^a$ (dm^3 mol^{-1})	$\log (K_{MOX})^b$ (dm^3 mol^{-1})	$\log (k_{aq}^{M})^d$ (s^{-1})	$\log (K_{MOX}/K_M)$
Mn^{2+}	1.2	3.97	−7.14	2.77
Co^{2+}	1.7	4.79	−6.72	3.09
Ni^{2+}	2.1	5.16	−6.68	3.06
Cu^{2+}	2.7	6.2	−5.28	3.50
Zn^{2+}	1.8	4.89	−6.89	3.09
Fe^{3+}	3.2	9.4	−4.62	6.2
Al^{3+}	1.7	7.9	−5.10	6.2
Ga^{3+}	2.7	8.25[c]	−5.03	5.55
In^{3+}	2.4	7.1	−5.75	4.7

(a) $I = 0.3$ mol dm^{-3}, 30°C ref (14)
(b) $I = 0$, 25°C, ref (12, 13) and see discussion part
(c) $I = 0$, 20°C ref (12)
(d) $I = 0.3$ mol dm^{-3}, 25°C ref (9)

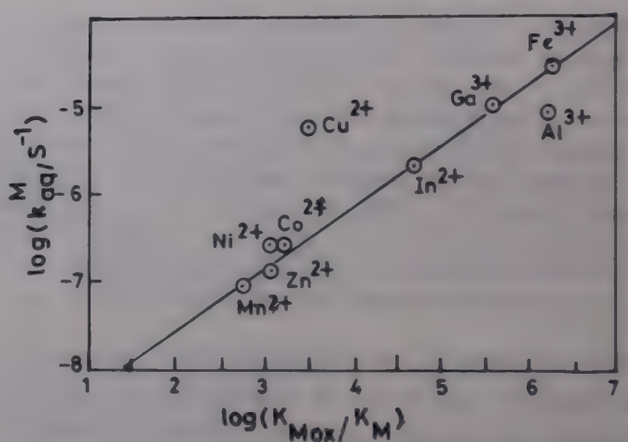

Fig. 1—$\log (k_{aq}^{M}/s^{-1})$ versus $\log (K_{MOX}/K_M)$ plot for aquation of $(NH_3)_5CoC_2O_4M^{(n+1)+}$ at 25°C.

The values of K_M at $I = 0.3$ mol dm^{-3} (30°C) as reported earlier from equilibrium measurements[14] were used as such. Relevant data are collected in Table 1. The plot of $\log k_{aq}^{M}$ versus $\log (K_{MOX}/K_M)$ is shown in Fig. 1. Only the data point for Cu_{aq}^{2+} deviates significantly from the linear plot. The higher reactivity of the binuclear complex of Cu^{2+} relative to that predicted by the LFER is a stereochemical consequence; Cu_{aq}^{2+} being strongly tetragonal, exhibits much higher reactivity than other octahedral bivalent aquo actions $M(OH_2)_6^{2+}$ of the first transition series. The effect of the tetragonal distortion on $\log (K_{CuOX}/K_{Cu})$ is presumably annuled to a great extent while it is not so on $\log k_{aq}^{Cu}$.

It is to be noted that the slope of LFER (Fig. 1) is 0.7. This is indicative of the fact that the mechanism of aquation of binuclear species is predominantly I_d involving a transition state in which $C_2O_4M^{(n-2)+}$ species, at the most, is weakly bound to the cobalt(III) centre (i.e. heterolysis of Co − O bond is

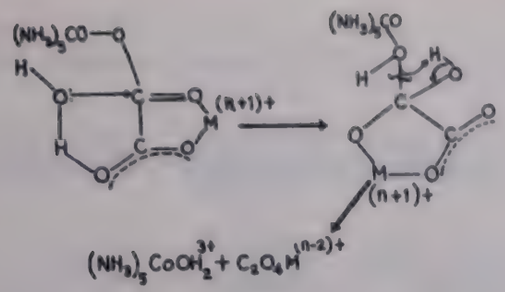

SCHEME 1

rate-determining). The intercept of the plot yields $k_{an}^{MOX} = 2.1 \times 10^{-6}$ dm^3 mol^{-1} s^{-1} at 25°C [based on $Q_{OX} = 2138$ dm^3 mol^{-1}, see Eq. (12)] which agrees satisfactorily with the anation rate constant for $(NH_3)_5CoOH_2^{3+}$ with a wide variety of anating ligands[4,5], further supporting the I_d mechanism of aquation of the binuclear complexes. The alternative path of reaction involving metal ion promoted hydration of the acyl carbonyl (see Scheme 1) of the carboxyl group bridging cobalt(III) and M^{n+} followed by C−O bond cleavage (ester cleavage) though appears to be less important cannot be completely ruled out as the slope of LFER is less than 1. The oxygen exchange experiments have demonstrated that the acyl cleavage mechanism operates in the H^+-catalysed path of aquation $(NH_3)_5CoC_2O_4H^{2+}$ and $(NH_3)_5CoO_2CCF_3^{2+}$, the carboxylatocobalt(III) complexes possessing activated carboxyl groups[7]. It is not unreasonable to expect that the acyl cleavage (C − O) mechanism might be operative not as a substitute for I_d mechanism but as an additional one, in the aquation of binuclear compexes of trivalent metal ions since the bridging carboxyl group is likely to be prone to hydration under the activating influence of the M^{3+} ions.

Further work is necessary to elucidate this aspect of the metal ion catalysed aquation of the oxalato complexes.

References

1 Langford C H, *Inorg Chem*, **4** (1965) 265.

2 Pross A in *Adv phys org Chem*, edited by V Gold & D Bethell (Academic Press) **Vol 14** (1977) 71; Hammond G S, *J Am chem Soc*, **77** (1955) 334; Leffler J E & Grunwald E, *Rates and equilibria of organic reactions* (Wiley, New York) 1963, pp 163.

3 Palmer D A & Kelm H, *Coord chem Rev*, **36** (1981) 89.

4 Haim A, *Inorg Chem*, **9** (1970) 426.

5 House D A, *Coord chem Rev*, **23** (1977) 223; Dash A C & Nanda R K, *Inorg Chem*, **12** (1973) 2024; Dash A C & Nanda R K, *J inorg nucl chem*, **38** (1976) 119; Dash A C & Dash M S, *J coord Chem*, **6** (1976) 1; ibid, **10** (1980) 79; Dash A C & Mohanty B, *Indian J Chem*, **17A** (1979) 296; Dash A C & Ray N, *Indian J Chem*, **14A** (1976) 78.

6 Bunton C A & Llewellyn D R, *J chem Soc*, (1953)1692.

7 Andrade C, Jordan R B & Taube H, *Inorg Chem*, **9** (1970) 711.

8 Swaddle T W, *Coord chem Rev*, **14** (1974) 217.

9 Dash A C & Nanda R K, *Inorg Chem*, **13** (1974) 655.

10 Dash A C & Nanda R K, *J Indian chem Soc*, **52** (1975) 289.

11 Abdullah P B & Monk C B, *J chem Soc Dalton Trans*, (1983) 1175.

12 Martell A E & Smith R M, *Critical stability constants*, Vol 3 (Plenum, New York) 1977, pp 94.

13 *Stability constants*: Part I, Special Publication No 6, (The Chemical Society, London) 1957.

14 Dash A C & Nanda R K, *J inorg nucl Chem*, **36** (1974) 1595.

Indian Journal of Chemistry
Vol. 27A, December 1988, pp. 1092-1094

Enthalpies of Mixing of Polyoxypropyleneglycols with Benzene, Ethanol & Water at 321.35 K

R PARASHAR* & S C SHARMA

Department of Chemistry, Panjab University, Chandigarh 160 014

Received 27 *January* 1988; *revised and accepted* 18 *March* 1988

The enthalpies of mixing of polyoxypropyleneglycols of molecular weights 150, 425 and 2025 with benzene, ethanol and water have been determined at 321.35 K. Specific interaction exists in polyglycol-benzene systems. There is an evidence of lesser interaction energy for formation of dissimilar contacts as compared to that for similar contacts in ethanol solutions. Water forms intermolecular hydrogen bonds with polyglycol molecules. The interchange energy for formation of H-bonds is calculated to be -6.694 kJ mol^{-1}.

As an extension of earlier works[1-5] from our laboratory on enthalpies of mixing of polyoxyethyleneglycols (PEG) and polyoxypropyleneglycols (PPG), presently we have determined enthalpies of mixing of PPG fractions in benzene, ethanol and water at 321.35 K.

The liquid PPGs having molecular weights of 150, 425 and 2025 were procured from Union Carbide Canada and were evacuated for 6-8 hr before use. All the solvents were purified by the usual techniques and were tested for purity by comparing their densities and refractive indices with the literature values.

The enthalpies of mixing were determined using an isothermal phase-change calorimeter with cetylalcohol[6] as the dilatometric fluid, which was filled in the jacket of the calorimeter (surrounding the reaction vessel) under reduced pressure.

The values of enthalpy of solution per mol of polymer (H_s) and enthalpy of mixing per mol of solution (H_m) for the PPG-solvent systems are reported in Tables 1-3.

PPG-benzene systems

It is found that H_m is positive for PPG-150 and PPG-425 over the entire concentration range. For PPG-2025, the H_m values are positive at low polymer concentrations but become negative at high concentrations passing through a minimum at $w_2 \simeq 0.14$. The results are similar to those reported by Lakhanpal *et al.*[1,7] for PEG-benzene systems and Sharma *et al.*[8,9] for polytetramethylene oxide-benzene systems. Sharma *et al.* have explained the dependence of H_m on polymer molecular weight on the basis of end group effect[9]. Our results can also be explained on the same basis. Since PPG

Table 1 — Enthalpies of Mixing for PPG-Benzene Systems at 321.35K

Polymer weight fraction (w_2)	H_s mol^{-1} of polymer (kJ)	H_m mol^{-1} of solution (J)
	PPG-150	
0.004051	30.7	64.85
0.01217	24.2	153.9
0.03221	18.2	309.6
0.05549	12.9	382.4
0.08811	10.5	504.2
0.1265	7.92	556.9
0.2323	5.20	706.7
0.3139	4.13	794.1
0.3795	3.54	855.2
0.4326	3.02	859.8
0.5539	2.15	846.0
0.6435	1.70	824.7
0.7548	1.15	705.8
0.8899	0.484	393.3
0.9692	0.115	107.5
	PPG-425	
0.005546	33.3	34.00
0.01413	28.2	73.64
0.02678	18.7	93.72
0.07014	10.9	148.5
0.09204	8.93	163.2
0.1239	8.03	207.5
0.1730	6.13	226.8
0.1955	6.04	258.2
0.2437	4.90	304.2
0.3467	3.71	329.7
0.4100	3.21	364.0
0.5149	2.59	421.7
0.6018	1.82	395.0
0.7233	1.05	341.0
0.8719	0.402	239.3
0.9662	0.083	70.3
0.9796	-0.112	-100.8
0.9917	-0.054	-51.88
	PPG-2025	
0.005587	87.8	19.24
0.01437	63.6	35.56
0.03147	42.6	53.13
0.06114	22.6	56.90
0.09846	12.3	51.04
0.1311	-5.85	-29.70
0.2273	-6.65	-74.47
0.3043	-6.20	-102.9
0.3716	-5.58	-124.3
0.4245	-5.15	-150.6
0.5072	-5.97	-228.0
0.5968	-5.47	-294.9
0.7199	-3.61	-325.5
0.8669	-1.75	-351.0
0.9684	-0.494	-267.4

Table 2—Enthalpies of Mixing for PPG-Ethanol Systems at 321.35 K

Polymer weight fraction (w_2)	H_s mol^{-1} of polymer (kJ)	H_m mol^{-1} of solution (J)
	PPG-150	
0.006579	6.44	13.10
0.01516	3.32	15.56
0.03037	1.23	12.13
0.06095	1.49	29.29
0.1044	0.807	28.45
0.1711	0.765	40.15
0.2827	0.199	21.50
0.3811	0.325	50.20
0.4509	0.250	50.20
0.5079	0.156	37.66
0.5915	−0.0138	−4.184
0.7137	−0.218	−94.56
0.8717	−0.183	−123.4
0.9647	−0.00581	−46.86
	PPG-425	
0.006561	26.9	19.25
0.01580	15.6	27.15
0.03050	4.68	15.77
0.06366	0.486	3.565
0.1120	−0.749	−10.13
0.1792	−0.740	−17.15
0.2979	−0.205	−9.245
0.3830	0.0502	3.185
0.4497	0.120	9.842
0.5101	0.185	18.79
0.5993	0.227	31.72
0.7188	0.318	69.04
0.8643	0.250	100.8
0.9668	0.061	46.02
	PPG-2025	
0.006360	132.6	18.83
0.01618	67.8	25.52
0.03149	22.6	16.74
0.06831	19.8	38.49
0.1124	12.7	36.40
0.1692	11.8	54.40
0.2902	13.8	127.2
0.3794	14.9	204.6
0.4476	15.2	275.7
0.5117	15.6	362.3
0.5990	15.3	503.3
0.7102	14.4	757.7
0.8548	12.3	1447
0.9647	4.53	1732

Table 3—Enthalpies of Mixing for PPG-Water Systems at 321.35 K

Polymer weight fraction (w_2)	H_s mol^{-1} of polymer (kJ)	H_m mol^{-1} of solution (J)
	PPG-150	
0.003250	−13.7	−5.424
0.01104	−17.9	−24.12
0.02217	−22.3	−61.04
0.05288	−19.1	−132.5
0.08175	−17.6	−197.1
0.1543	−17.6	−377.0
0.2663	−15.7	−631.8
0.3511	−13.4	−820.5
0.4784	−10.3	−1020
0.5503	−8.68	−1112
0.6373	−6.95	−1205
0.7558	−4.59	−1242
0.8890	−2.04	−998.7
0.9755	−414.6	−0.500
	PPG-425	
0.005353	−39.9	−9.082
0.01405	−46.2	−27.74
0.02872	−46.2	−57.74
0.06428	−51.7	−150.2
0.1060	−49.6	−248.1
0.1369	−46.9	−313.4
0.1832	−45.7	−430.1
0.2885	−35.5	−599.2
0.3715	−29.0	−709.6
0.4399	−21.7	−794.5
0.4963	−23.7	−950.6
0.5784	−19.8	−1084
0.7016	−14.3	−1296
0.8879	−4.84	−1217
0.9700	−1.13	−755.6

fractions are H-bonded due to the presence of −OH groups at the chain ends, these bonds are broken on addition of benzene leading to positive values of H_m. At the same time benzene molecules enter into a specific interaction with the chain oxygen atoms of PPG molecules leading to negative H_m values for PPG-2025-benzene system, since the end group effect decreases with increase in PPG molecular weight. The end group effect dominates H_m values for low molecular weight PPG and at low concentrations of PPG-2025.

PPG-ethanol systems

The H_m values in ethanol have small magnitudes for low molecular weight fractions. These become highly positive for PPG-2025. This is in conformity with the results reported earlier for the liquid PEGs[1]. The interaction energy in polyglycol-ethanol systems is essentially due to H-bonding. The molecules of ethanol are also known to be H-bonded. The interactions between dissimilar molecules in alcoholic solutions of PPG are on account of formation of H-bonds. The positive values of H_m indicate that the interaction energy for the establishment of dissimilar contacts is numerically smaller than the average value of the interac-

tion energies of similar molecules. It may be observed that H_m becomes more endothermic for PPG-2025 at high polymer concentrations. This may be attributed to rupture of intermolecular H-bonds in the solvent, which may not be possible at low PPG concentrations and also for low molecular weight fractions.

PPG-water systems

The H_m values are negative and almost independent of molecular weight of the polymer fraction. The PPG-2025 is only partially soluble in water. The results of the present systems are similar to those for PEG-water systems[2]. As in PEGs, highly negative values of H_m for the present systems suggest the formation of H-bonds between water and PPG molecules. Since polyglycol and water molecules are both expected to be associated in their pure states, the negative values of H_m suggest a much stronger interaction between water and PPG molecules as compared to water-water and glycol-glycol interactions. As the major interaction in the present systems involves H-bonding, the interchange energy for the formation of H-bonds may be calculated from the values of H_s. Since PPG contains Avogadro number of oxygen atoms per 58 g of the polymer, it is possible to represent H_s by Eq. (1)

$$H_s = WM/58 \qquad \ldots (1)$$

where W is the interchange energy for one mole of hydrogen bonds in these aqueous solutions and M is the molecular weight of the PPG. From the known values of H_s for a solution at any particular polymer concentration, the values of W can be calculated. These values were calculated for w_2 ranging from 0 to 0.20. The average of these values for PPG-150 and 425 are found to be -6.360 and -7.029 kJ mol^{-1} respectively.

Lakhanpal *et al.* calculated the average values of interchange energy (W) for PEGs[2,10] at 321.35 K and 300.05 K as -6.020 and -6.721 kJ mol^{-1} respectively. Singh[11] calculated $W = -7.750$ kJ mol^{-1} for PPGs at 300.05 K. The average value of $W = -6.694$ kJ mol^{-1} has been calculated presently at 321.35 K.

It is observed that values of W are numerically higher for aqueous solutions of PPG. The higher negative values may be attributed to the electron repelling character of $-CH_3$ group adjacent to the chain-oxygen atoms and this may be responsible for the increased strength of H-bonds in PPG. The temperature dependence of W is also seen to be fairly marked, its values increasing with decrease in temperature.

It has been reported by Singh[11] that excess entropy of mixing for PPG-water system is negative which suggests a high degree of order in aqueous solutions. It is quite likely that increase in temperature may weaken this order in solution and thus decrease 1-type of contacts leading to lower value of W.

References

1 Lakhanpal M L, Sharma S C, Bal Krishan & Parashar R, *Indian J Chem*, **14A** (1976) 642.

2 Lakhanpal M L & Parashar R, *Indian J Chem*, **22A** (1983) 48.

3 Lakhanpal M L, Singh H G, Singh H & Sharma S C, *Indian J Chem*, **6** (1968) 95.

4 Lakhanpal M L & Conway B E, *J Polym Sci*, **46** (1960) 75.

5 Kershaw R W & Malcolm G N, *Trans Faraday Soc*, **64** (1968) 323.

6 Lakhanpal M L & Parashar R, *Indian J Chem*, **8** (1970) 368.

7 Lakhanpal M L, Taneja H L & Sharma R K, *Indian J Chem*, **4** (1966) 12.

8 Sharma S C, Mahajan R, Sharma V K & Lakhanpal M L, *Indian J Chem*, **21A** (1982) 685.

9 Sharma S C & Sharma V K, *Indian J Chem*, **24A** (1985) 292.

10 Lakhanpal M L, Kapoor V, Sharma R K & Sharma S C, *Indian J Chem*, **4** (1966) 59.

11 Singh H G, *Ph D Thesis*, Faculty of Science, Panjab University, Chandigarh, India (1970).

Indian Journal of Chemistry
Vol. 27A, December 1988, pp. 1095-1096

Electroreduction of Samarium(III) in Calcium Nitrate Tetrahydrate Melt

C K BHASKARE*
Department of Chemistry, Shivaji University, Kolhapur 416 004
and
K N GANAGE
Department of Chemistry, S S G M College, Kopargaon 423 601

Received 29 *June* 1987; *revised* 15 *March* 1988; *accepted* 4 *April* 1988

Polarographic behaviour of Sm(III)/Sm(II) redox system in calcium nitrate tetrahydrate melt at 55°C using rotating platinum microelectrode is reported. The reversibility of the system has been used successfully for coulometric generation of Sm(II) and its biamperometric titration with potassium dichromate.

The molten hydrated salts are interesting solvent systems for electrochemical studies because they form an intermediate group of solvents between anhydrous fused salts and water. Braunstein *et al.*[1] studied polarographic reduction of Cd(II) ions in the molten calcium nitrate tetrahydrate and its mixture with potassium nitrate. Moynihan and Angell[2] reported the diffusion coefficients of Ag(I), Cd(II) and Tl(I) by chronopotentiometric technique in this hydrate melt. Lovering[3], Shillina *et al.*[4] and Plambeck *et al.*[5] reported polarographic half-wave potentials and diffusion coefficients of a number of common ions in the melts of hydrated salts. The polarographic reduction of samarium(III) to samarium(II) and its coulometric determination in aqueous medium were reported by Feldman and Purdy[6], Wise[7] and Saxena[8].

However, there is no report on electroreduction of Sm(III) in the fused hydrated salts. Presently we have studied the polarographic reduction of Sm(III) in calcium nitrate tetrahydrate melt. The reversibility of the system has been used successfully for coulometric generation of Sm(II) and its biamperometric determination in this melt.

The rotating platinum microelectrode assembly was fabricated in our laboratory (speed 600 rpm). A double walled, borosilicate glass cell was used for the polarographic measurement and coulometric generation. Hot water from a thermostat was circulated around the cell to maintain the temperature at 55 ± 1°C. The reference electrode system for polarographic reduction was Ag/Ag(I) in $Ca(NO_3)_2$ $4H_2O$ melt/Ag(S). The reference electrode was kept in a side tube connected to the cell through a frit disc.

Other details regarding the instrumentation were same as those reported in our earlier communication[9].

Samarium solution (5 mg/ml) was prepared by dissolving samarium nitrate (1.205 g) in calcium nitrate tetrahydrate melt and diluted to 100 ml with the melt. The solution was standardized by literature procedure[10].

The dichromate solution (0.0016 *M*) was prepared using potassium dichromate (AR, BDH).

The solution were kept in a thermostat at 55°C.

Polarograms of Sm(III) were recorded on a Sargent-Welch model XVI polarograph with a low scan rate. Since the solubility of oxygen in the calcium nitrate tetrahydrate melt was negligible[2], no special precautions were taken to exclude air from the system, except for tightly capping the cell to avoid loss of water due to evaporation. Calcium nitrate tetrahydrate is thermally stable upto 90°C. Beyond this temperature it gets dehydrated slowly upto 160°C (ref. 11).

Samarium(II) was generated coulometrically by passing a constant current (10 mA) for a known interval of time. The contents of the outer vessel were titrated with 0.0016 *M* dichromate ion biamperometrically. The experiment was repeated for larger duration till constant titre was obtained which was indicated by an L shaped biamperometric curve. From the constant titre value of potassium dichromate, the quantity of Sm(III) could be calculated from the relation,

1.00 ml of 0.0016 *M* dichromate = 1.50 mg of Sm(III)

Samarium(III) in calcium nitrate tetrahydrate melt gives a half-wave potential of 2.1 V [versus Ag/Ag(I)]. The reversibility of Sm(III)/Sm(II) redox system is observed in the Sm(III) concentration range of 2.0×10^{-4} to 6.00×10^{-4} *M*. The Levich equation and not Ilkovic equation is found to be applicable when rotating platinum microelectrode is used[12].

Samarium(II) in aqueous system has low stability whereas it is quite stable in calcium nitrate tetrahydrate melt. Hence electroreduction in this medium is of analytical importance. Samarium(III) can successfully be determined by coulometric generation of Sm(II) followed by the biamperometric titration of Sm(II) against dichromate due to reversibility of Sm(III)/Sm(II) redox system in the

calcium nitrate tetrahydrate melt. The current efficiency was found to be 100% in constant current coulometry. The results of the biamperometric titration are reproducible with a standard deviation of 0.35%.

This method is applicable to the determination of Sm(III) in lanthanide samples free from europium, ytterbium and uranium.

The titrimetric determination of Sm(II) in aqueous media are not feasible because of the low stability of Sm(II) ions; however these ions are found to be stable in calcium nitrate tetrahydrate melt, hence the present method can be applied for the routine estimation of samarium provided the quantity of samarium is 2 to 6 mg/ml. We do not claim to have presented a method that supercedes the existing methods.

One of the authors (KNG) is thankful to the CSIR, New Delhi for the award of a junior research fellowship.

References

1 Braunstein J, Orr L, Alvarex-Funes A R & Braunstein H, *J electroanal Chem*, **15** (1967) 337.

2 Moynihan C T & Angell C A, *J phys Chem*, **74** (1970) 736.

3 Lovering D G, *Colln Czech chem Commun*, **38** (1973) 1719.

4 Shillina G V & Delimarskii Yu K, *Ukr Khim Zh*, **36** (1970) 781.

5 Bansal N P & Plamback J A, *J electrochem Soc*, **124** (1977) 1036; *Electrochim Acta*, **23** (1978) 1053.

6 Feldman F J & Purdy W C, *J Polarogr Soc*, **13** (1967) 116.

7 Wise E N, *US Atomic Energy Comm TID* (1964) 20548.

8 Saxena O C, *Chim Anal*, **50** (1968) 638.

9 Bhaskare C K & Ganage K N, *Indian J Chem*, **27A** (1988) 350.

10 Pribil R, *Talanta*, **22** (1975) 688.

11 Duval C, *Inorganic thermogravimetric analysis* (Elsevier, Amsterdam) 1963 pp. 274.

12 Meites L & Thomas H, *Advanced analytical chemistry* (McGraw Hill, New York) 1958.

Indian Journal of Chemistry
Vol. 27A, December 1988, pp. 1097-1099

Compounds of Vanadium(IV) with Imidazoles & Piperidines

TANKESWAR BORA* & (Mrs) MEENA DEVI
Department of Chemistry, Dibrugarh University, Dibrugarh 786 004

Received 23 *September* 1987; *revised* 29 *February* 1988; *accepted* 28 *March* 1988

Vanadyl sulphate and vanadyl chloride react with imidazole, substituted imidazoles and piperidines to yield products of the types $[VOL_3(H_2O)]SO_4$ (L = Im), $VOL(H_2O)SO_4$ (L = 1-MeIm, 1-VIm), $V_2O_3L(H_2O)SO_4$ (L = 1,2-Me_2Im, 2-MeIm, 4-MeIm, 2-*i*-PrIm, 2-EtIm, 2-Et-4(5)-MeIm, 2-Me-1-VIm, 2-PhIm, 1-EtPip, 2-EtPip and 1-MePipz), $V_2O_4(L)(H_2O)$ (L = Im 1,2-Me_2Im, 2-MeIm, 4-MeIm, 2-EtIm, 2-*i*-PrIm) and $V_3O_6(L)(H_2O_2)$ (L = 2-Me-1-VIm, 2-PhIm, 2-PhIm and 1-EtPip). The compounds have been characterized on the basis of elemental analyses, molar conductivity, IR and electronic spectral studies. The compounds $[VOL_3(H_2O)]SO_4$ (L = Im) and $VOL(H_2O)SO_4$ (L = 1-MeIm, 1-VIm) are six coordinate with $\mu_{eff.} = 1.8$-2.1 B.M. while the others are pentacoordinate with $\mu_{eff.} = 1.01$-1.4 B.M. The low values of magnetic moments indicate polymeric nature of the complexes and presence of antiferromagnetic interaction. Broad ESR spectral bands in most of the compounds with *g* values 1.98-1.99 reveal considerable anisotropy.

Vanadium(IV) complexes with pyridines[1] and vanadium(II) complexes with pyrazole[2] and imidazole[2] are known. Mixed ligand complexes of oxovanadium(IV) with some nitrogen donor ligands have also been reported[3,4]. But no oxovanadium (IV) compounds of imidazoles, piperidines and piperazines have so far been reported. In this note, we report compounds of vanadium(IV) with some N-donor ligands such as imidazole(Im), 1-methylimidazole (1-MeIm), 1-vinylimidazole(1-VIm), 1,2-dimethylimidazole(1,2-Me_2Im), 2-methylimidazole(2-MeIm), 4-methylimidazole(4-MeIm), 2-isopropylimidazole(2-*i*-PrIm),2-ethylimidazole(2-EtIm), 2-ethyl-4(5)-methylimidazole(2-Et-4(5)-MeIm), 2-methyl-1-vinylimidazole(2-Me-1-VIm), 2-phenylimidazole(2-PhIm),1-ethylpiperidine(1-Etpip), 2-ethylpiperidine(2-Etpip) and 1-methylpiperazine(1-Mepipz).

Vanadyl sulphate (Loba), vanadyl chloride (Fluka), imidazoles (BASF, TCI or Fluka), piperidines (Fluka) and piperazine (Fluka) were used as such. Molar conductances of the compounds in H_2O, DMF or DMSO were determined with a direct reading Systronics conductivity bridge. IR and ESR spectra were recorded on instruments as reported earlier[5]. C, H and N were estimated at RSIC, CDRI, Lucknow. Magnetic moments were determined with a Gouy balance. Reflectance spectra of the compounds were recorded with a Shimadzu UV-240 spectrophotometer using barium sulphate as the reference material. Sulphur was estimated gravimetrically as barium sulphate.

Preparation of complexes: (*i*) *compounds with* $VOSO_4 \cdot 5H_2O$

$VOSO_4 \cdot 5H_2O$ (0.5 g) was dissolved in ~3 ml of H_2O. To it was added 5 ml of EtOH and one drop of conc. H_2SO_4. Nitrogen was passed through the solution for 5 min, followed by addition of the corresponding bases. Passing of nitrogen under reflux was continued for 30 min. Most of the compounds were precipitated immediately. The mixture was then concentrated followed by filtration of the precipitated complexes. However, V_2O_3(1-Etpip)$(H_2O)SO_4$, V_2O_3(2-Etpip)$(H_2O)SO_4$ and V_2O_3(1-MePipz)$(H_2O)SO_4$ precipitated only on concentration. V_2O_3(2-EtPip)$(H_2O)SO_4$ was obtained on extraction of the concentrated syrupy mass with water. $[VO(Im)_3(H_2O)]SO_4$ is brown in colour while all the other complexes are dark green. Excepting $[VO(Im)_3(H_2O)]SO_4$ and V_2O_3(1-MePipz)$(H_2O)SO_4$, most of the compounds are soluble in H_2O and DMF.

(*ii*) *Compounds with* $VOCl_3$

To $VOCl_3$ (0.5 ml), were added the corresponding bases in excess EtOH. The compounds precipitated immediately. The compounds are yellow, brown or green in colour. Most of the compounds are soluble in DMSO and partially so in DMF.

The compounds do not dissociate in DMF or DMSO indicating their undissociative nature. On standing they, however, slowly dissociate as shown by increased conductivity. Dissociation also takes place in H_2O in the case of the compounds $VOL(H_2O)SO_4$ (L = 1-MeIm, 1-VIm) and $V_2O_3L(H_2O)SO_4$ (L = 1,2-Me_2Im, 2-MeIm, 4-MeIm, 2-*i*-PrIm, 2-EtIm, 2-Et-4(5)-MeIm, 2-Me-1-VIm, 2-PhIm, 1-EtPip, 2-EtPip and 1-MePipz). All the compounds have high melting points. Analytical data of the compounds are tabulated in Table 1. The compounds exhibit a sharp band at ~980 cm^{-1} which may be attributed to $\nu V{=}O$[1]. The splitting of this band indicates its terminal nature. The bands at ~400 cm^{-1} indicate the coordination of the bases to oxovanadium(IV) species[1]. In addition to these bands the usual ligand bands appear which are found to shift

Table 1—Analytical and Electronic Spectral Data (cm^{-1}) of Some Oxovanadium(IV) Compounds with Imidazoles and Piperidines

Compound	Found (Calc) %				Electronic transitions	
	C	H	N	S	$b_2 - e_\pi^*$	$b_2 - b_1$
$[VO(Im)_3H_2O]SO_4$	28.30 (28.06)	4.31 (3.66)	20.49 (21.82)	8.19 (8.31)		17,241
$VO(1\text{-MeIm})(H_2O)SO_4$	17.95 (18.26)	2.51 (3.07)	10.03 (10.55)	11.55 (12.16)		20,000
$VO(1\text{-VIm})(H_2O)SO_4$	21.05 (21.83)	2.78 (2.93)	10.18 (10.19)	10.85 (11.63)		19,084
$V_2O_3(1,2\text{-Me}_2\text{Im})(H_2O)SO_4$	16.80 (16.67)	2.80 (2.79)	6.97 (7.78)	8.45 (8.89)	14,706 sh	19,841
$V_2O_3(2\text{-MeIm})(H_2O)SO_4$	13.30 (13.88)	2.50 (2.33)		8.89 (9.24)	14,663	18,587
$V_2O_3(4\text{-MeIm})(H_2O)SO_4$	14.75 (13.88)	2.42 (2.33)	7.07 (7.49)	8.94 (9.24)		
$V_2O_3(2\text{-}i\text{-PrIm})(H_2O)SO_4$	19.75 (19.26)	3.28 (3.23)	7.19 (7.49)	8.16 (8.36)	14,837 sh	19,231
$V_2O_3(2\text{-EtIm})(H_2O)SO_4$	17.70 (16.67)	3.19 (2.79)	7.61 (7.78)	8.47 (8.89)		17,422
$V_2O_3(2\text{-Et-4(5)-MeIm})(H_2O)SO_4$	19.80 (19.26)	3.01 (3.23)	7.29 (7.49)	8.22 (8.55)	14,706 sh	20,492
$V_2O_3(2\text{-Me-1-VIm})(H_2O)SO_4$	19.20 (19.36)	2.66 (2.71)	7.13 (7.53)	8.34 (8.60)		20,000
$V_2O_3(2\text{-PhIm})(H_2O)SO_4$	27.50 (26.49)	2.65 (2.47)	6.53 (6.87)	7.55 (7.84)		18,519
$V_2O_3(1\text{-EtPip})(H_2O)SO_4$	22.40 (22.29)	4.01 (4.54)	3.63 (3.72)	8.20 (8.49)	14,793 sh	19,011 22,124*
$V_2O_3(2\text{-EtPip})(H_2O)SO_4$	22.85 (22.29)	4.54 (4.54)	3.34 (3.72)	8.36 (8.49)	15,244 sh	19,380
$V_2O_3(1\text{-MePipz})(H_2O)SO_4$	15.55 (16.49)	4.20 (3.88)	7.43 (7.69)	7.99 (8.78)	14,286 sh	18,587
$V_2O_4(Im)(H_2O)$	13.7 (14.3)	2.62 (2.40)	10.23 (11.11)			17,361
$V_2O_4(1,2\text{-Me}_2\text{Im})(H_2O)$	20.60 (21.44)	3.20 (3.59)	9.71 (10.01)		13,405 sh	18,248
$V_2O_4(2\text{-MeIm})(H_2O)$	17.9 (18.06)	2.76 (3.03)	10.40 (10.53)			
$V_2O_4(4\text{-MeIm})(H_2O)$	18.0 (18.06)	3.02 (3.03)	10.31 (10.53)		13,405 sh	18,248
$V_2O_4(2\text{-}i\text{-PrIm})(H_2O)$	23.8 (24.5)	4.21 (4.11)	9.36 (9.52)			
$V_2O_4(2\text{-EtIm})(H_2O)$	21.55 (21.44)	3.72 (3.6)	9.91 (10.01)		14,706	17,794
$V_3O_6(2\text{-Me-1-VIm})(H_2O)_2$	18.80 (18.34)	2.44 (2.75)	7.57 (7.64)		14,620 sh	18,797
$V_3O_6(2\text{-PhIm})(H_2O)_2$	26.0 (25.2)	2.9 (2.8)	6.76 (6.53)		14,749 sh	18,182
$V_3O_6(1\text{-EtPip})(H_2O)_2$	20.60 (21.12)	4.5 (4.81)	3.45 (3.52)		14,749 sh	18,519

*$b_2 - a_1$ transition

slightly ($\Delta\nu = 5\text{-}50$ cm^{-1}) on coordination. On the basis of analytical data and IR spectra, the tentative structures of the compounds may be represented as shown below.

The magnetic moments of the compounds $[VO(Im)_3H_2O]SO_4$, $VO(1\text{-MeIm})(H_2O)SO_4$ and $VO(1\text{-VIm})(H_2O)SO_4$ are in the range 1.71 to 1.81 B.M. and are very close to the spin-only value. The magnetic moments of the other compounds are quite low (1.01-1.14 B.M.). These lower values of magnetic moments indicate presence of antiferromagnetic interaction and polymeric nature[1] of the complexes. Spin-spin interaction between two vanadium atoms in a dimeric/polymeric structure

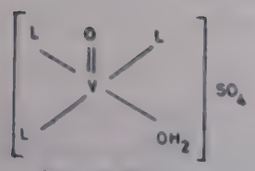

$[VOL_3(H_2O)]SO_4$
(L=Im)

$V_2O_3L(H_2O)SO_4$
(L=1, 2-Me_2Im, 2-MeIm, 4-MeIm, 2-i-PrIm, 2-EtIm, 2-Et-4(5)-MeIm, 2-Me-1-VIm, 2-PhIm, 1-Et Pip, 1-MePipz)

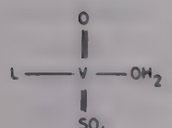

$VOL(H_2O)SO_4$
(L=1-MeIm, 1-VIm)

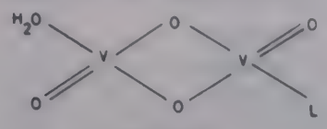

$V_2O_4L(H_2O)$
(L=Im, 1,2-Me_2 Im, 2-MeIm, 4-MeIm, 2-Et Im, 2-i-Pr Im)

$V_3O_6L(H_2O)_2$
(L=2 Me-1-V Im, 2-Ph Im, 1-Et Pip)

may also contribute to the low values of magnetic moments.

The powder ESR spectra of the compounds exhibit one prominent peak both at 198 K and 298 K with g values ranging from 1.95 to 1.99. In a few compounds, the signals are found to be split. In V_2O_3(1-MePipz)$(H_2O)SO_4$, the signals split into 16 components with $g_\perp$ and $g_\parallel$ values of 1.917 and 1.94 respectively. The splitting of the signals reveals considerable anisotropy around the vanadium atom.

The electronic spectra and magnetic moments of the compounds $[VO(Im)_3(H_2O)]SO_4$, and $VOL(H_2O)SO_4$ (L=1-MeIm, 1-VIm) reveal that they are structurally different from the others. These compounds exhibit only a single strong sharp peak at ~17,240 cm^{-1} (Table 1) whereas the other compounds exhibit normally two peaks, one at 13,405-15,244 cm^{-1} and the other at 17,241-20,000 cm^{-1} (Table 1) and the bands are comparatively broad. Highly distorted oxovanadium(IV) compounds normally exhibit three spin-allowed transitions[6-8] $b_2 \rightarrow e\pi^*(^2B_2 \rightarrow {}^2E)$, $b_2 \rightarrow b_1(^2B_2 \rightarrow {}^2B_1)$ and $b_2 \rightarrow a_1(^2B_2) \rightarrow {}^2A_1)$. For oxovanadium(IV) complexes of carboxyhydrazones, these bands occur at 12,100-14,500, 15,00-17,300 and 22,800-24,900 cm^{-1} (ref. 9). Appearance of a shoulder at ~13,000 cm^{-1} with a broad strong band at ~18,000 cm^{-1} in most of the compounds indicates that they exhibit Jahn-Teller distortion.

The authors are thankful to RSIC, CDRI, Lucknow for C,H,N analyses and IR, to RSIC, IIT, Bombay for ESR spectra and to the UGC, New Delhi for a fellowship to one of the authors (M.D.).

References

1 Paul R C, Sharma N C, Verma R D & Sharma A K, *Indian J Chem*, **14A** (1979) 705.
2 Mani F, *Inorg nucl Chem Lett*, **12** (1976) 271.
3 Prasad K M, Pandey B & Sahay S, *Indian J Chem*, **25A** (1986) 970.
4 Nath P K & Dash K C, *Indian J Chem*, **25A** (1986) 968.
5 Bora T, Devi M & Gogoi P K, *Transition Met Chem*, **11** (1986) 467.
6 Ballhausen C J & Gray H B, *Inorg Chem*, **1** (1962) 111.
7 Selbin J, *Chem Rev*, **65** (1965) 153; *Coord Chem Rev*, **1** (1966) 293.
8 Lever A B P, *Inorganic electronic spectroscopy* (Elsevier, Amsterdam) 1986.
9 Pandey O P, *Polyhedron*, **5** (1986) 1587.

Indian Journal of Chemistry
Vol. 27A, December 1988, pp. 1100-1101

Ternary Complexes of Copper(II) Involving Barbituric Acid and Some of Its Derivatives

ROHITASHVA M TRIPATHI, (Mrs) RANJANA GHOSE & ANIMESH K GHOSE*

Department of Chemistry, Faculty of Science, Banaras Hindu University, Varanasi 221 005

Received 15 *December* 1987; *revised and accepted* 21 *March* 1988

Stability constants of ternary complexes of Cu(II) with 2,2′-bipyridyl as primary ligand and barbituric acid or its 5,5-substituted derivatives as secondary ligand in 50% (v/v) aq. ethanol have been determined *p*H-metrically at $\mu = 0.1$ *M* ($NaNO_3$) and temp = 30° ± 1°C. The equilibrium constants of ternary species follow the acidity order of barbiturates.

Barbiturates, which are widely used in medicine[1], are among the most frequently encountered drugs in the field of toxicology. Moreover, barbiturates are weak acids and can form metal complexes[2-4]. The study of stabilities of mixed complexes are important in biological systems as many metabolic and toxicological functions are to a large extent dependent upon them.

In the present note the stability constants of mixed ligand complexes of barbituric acid (BBA), 5,5-diethylbarbituric acid (BABL), 5-ethyl-5-phenylbarbituric acid (PHEN BABL), 5,5-diallylbarbituric acid (ALLOBABL) and with Cu(II) in the presence of 2,2 -bipyridyl are reported.

All chemicals used were of AR grade and doubly distilled, CO_2-free water was used for preparing solutions.

The following five mixtures were prepared in 50% (v/v) aqueous ethanol medium (total volume 50 ml), and titrated individually against standard alkali using Global digital *p*H meter (DPH 500) with a glass calomel electrode assembly: (i) Nitric acid; (ii) nitric acid + bipy; (iii) nitric acid + bipy + metal ion; (iv) nitric acid + secondary ligand; and (v) nitric acid + bipy + secondary ligand + metal ion. The final concentrations of nitric acid, metal ion and bipy or secondary ligand in all these mixtures were 2.0×10^{-3} *M*, 1.0×10^{-3} *M* and 1.0×10^{-3} *M* respectively.

The electrode system was calibrated by direct titration with HNO_3 and the observed *p*H in 50% (v/v) aq. ethanol medium was corrected for actual $[H^+]$ following the procedures of Uitert *et al.*[5].

The calculation of stability constants of proton-liand and mixed ligand complexes were according to Martell[6] and Thompson *et al.*[7] respectively.

Table 1—Stability Constants of Ternary Complexes in 50% (v/v) Aq Ethanol $\mu = 0.10$ M $NaNO_3$; temp. = 30° ± 1°C

[Ionic strength = 0.1 *M* ($NaNO_3$); temp. = 30° ± 1°C]

Barbituric acid	pK_1	pK_2	log K_{cu} bipy L
Parent acid	12.39	4.69	9.40
5,5-Diethyl	12.84	9.30	9.86
5,5-Diallyl	12.53	9.20	9.83
5-Ethyl-5-phenyl	12.29	8.76	9.80

In acid medium barbituric acid is present in the trioxo form, the three O-atoms and the two N-atoms have lone electron pairs. So the molecule could act as a good complexing agent.

The higher pK_a values of substituted barbituric acids over that of parent compound (vide Table 1) are due to the fact that 5,5′-disubstitution forces the substituted compounds to exist in 2,4,6-triketo form.

The titration of a solution containing Cu(II)-bipy in equimolar quantities gives one inflexion in the lower *p*H region indicating the formation of a 1:1 complex. Turbidity appears during the later part of the titration where probably a hydroxo complex is formed.

Although bipy is relatively weak base, it forms chelates with metal ions in which there are presumably strong σ donor bonds, supplemented by some moderate degree of π bonding. The resulting complexes have a high order of stability and the complexes are formed at lower *p*H. Thus bipy behaves as a suitable primary ligand. Therefore, when 1:1 (M:A) mixtures are taken, obviously bipy occupies two of the coordination positions around the metal ion leaving the other positions to be occupied by H_2O molecules. Interactions with barbiturates would result in the replacement of H_2O by L.

In the titration of 1:1:1 system, Cu(II)-bipy BBA, two inflextions are observed. In the lower *p*H region the curve for the mixed systems overlaps the curve for the 1:1 Cu(II)-bipy system upto *p*H ~ 3.5. It indicates that initially 1:1 Cu(II)-primary ligand (bipy) complex is formed prior to the addition of the secondary ligand. Further addition of alkali neutralizes the protons liberated from the secondary ligand due to ternary complex formation.

The values of the stability constants of the ternary complexes studied are given in Table 1.

Inspite of the fact electrometric studies cannot establish coordination site conclusively, from the literature reports[8,9], it is presumed that metal ion is bonded through the nitrogen of the barbiturate anion in the ternary complexes.

The stabilities of the ternary complexes follow the increasing order of protonation constant (pK_2) of the barbiturates.

The authors are thankful to the Bureau of Police Research & Development, Ministry of Home Affairs, Government of India, New Delhi for a fellowship to one of them (RMT).

References

1 Litter M, *Farmacologia experimentally clinica*, 5th Edn (El Ateneo, Buenos Aires) 1975.
2 Doornbos D A, *Pharm Weekblad*, **102** (1967) 269.
3 Jimenez H, Borras J & Ortiz R, *J Indian Chem Soc*, **LXI** (1984) 128.
4 Tabassum S, Siddiqi K S, Khan N H, Kureshy R I & Zaidi S A A, *Indian J Chem*, **26A** (1987) 489, 523.
5 Van Uitert L G & Haas C G, *J Am Chem Soc*, **75** (1953) 451.
6 Chaberek (Jr.) S & Martell A E, *J Am Chem Soc*, **74** (1952), 5052; **77** (1955) 1477.
7 Thompson L C & Loraas J A, *Inorg Chem*, **2** (1963) 89.
8 Caira M R, Fazakerley G V, Linder P W & Nassimbeni L R, *Inorg Nucl Chem Lett*, **9** (1973) 1101.
9 Fazakerley G V, Linder P W, Nassimbeni L R & Rodgers A L, *Inorg Chem Acta*, **9** (1974) 193.

Indian Journal of Chemistry
Vol. 27A, December 1988, pp. 1102-1104

Synthesis, Characterisation & Antimicrobial Studies of Co(II) & Ni(II) Complexes with Some Pyrazoles

ZAHID HUSSAIN CHOHAN*, MISBAHUL AIN KHAN & MOHAMMAD MOAZZAM

Department of Chemistry, Islamia University, Bahawalpur, Pakistan

Received 23 *February* 1987; *revised and accepted* 6 *April* 1988

A number of new complexes of nickel(II) and cobalt(II) with pyrazole-derived ligands have been synthesized and characterized. These complexes have been tested against various bacteria such as *Staphylococcus aureus, Escheria coli* and *Pseudomonas aeruginosa.* The complexes show significant antimicrobial activity compared to that of parent compound.

A large number of metal ions, particularly transition metals, are known to display antimicrobial activity[1-3]. As a part of our research programme in the same area, we have synthesized some new biologically important metal-diazole complexes of the type ML_2X_2 where M = Ni(II) and Co(II); L = 2-(pyrazo-1-yl)-pyridine (I), 2-(3,5-diphenyl-pyrazol-1-yl)-pyridine (II), 2-(3,5-diphenylpyrazo-1-yl)-pyridine(III) and 2-(3,5-diphenylpyrazol-1-yl)-5-nitropyridine (IV); and X = Cl. We have also studied their spectroscopic characteristics and antimicrobial effect on various bacteria.

The ligands used in this work were prepared by the method reported by Khan *et al.*[4].

Elemental analyses of C, H and N were carried out on a coleman automatic analyser. The magnetic measurements were done on solid complexes using the Gouy method.

The electronic spectra were studied with a Beckman spectrophotometer model DU using glass cells of 1cm thickness. Infrared spectra were recorded on a Perkin-Elmer 521 spectrophotometer.

Metal contents of the complexes were determined by first treating the complexes with boiling conc. nitric acid and then evaporating to dryness repeatedly till the organic matter was destroyed. The residue was dissolved in water and filtered. The filtrate was used for estimation of cobalt and nickel by the pyridine method[5].

Melting points were recorded on a Gallenkamp melting point apparatus and are uncorrected.

General method of preparation of metal complexes

To an ethanolic solution (30 ml) of the ligand (2 mmol) was added with stirring an ethanolic solution (20 ml) of the metal chloride salt (1 mmol). The contents were refluxed for 3 hr. The resulting mixture was then cooled, washed with ether (2 × 20 ml) and later reduced to a small volume (15 ml). The concentrated solution was left overnight at room temperature and the product thus formed was separated. It was recrystallized from water to get fine crystals (70% yield).

Table 1—Physical and Analytical Data of the Complexes

Complex No. (Molec. formula)	m.p. (°C)	Mag. moment (B.M.)	Found (Calc.), %		
			C	H	N
1 ($C_{16}H_{17}N_6NiCl_2$)	142-145	2.92	45.43 (45.48)	4.02 (4.51)	19.87 (19.91)
2 ($C_{20}H_{20}N_8O_4NiCl_2$)	170-173	2.85	42.43 (42.46)	3.53 (3.52)	19.80 (19.81)
3 ($C_{40}H_{30}N_6NiCl_2$)	166-170	2.95	66.33 (66.31)	4.14 (4.11)	11.60 (11.61)
4 ($C_{40}H_{28}N_8O_4NiCl_2$)	188-190	2.83	58.99 (58.96)	3.44 (3.46)	13.76 (13.77)
5 ($C_{16}H_{17}N_6CoCl_2$)	156-158	4.25	45.40 (45.38)	4.02 (4.09)	19.86 (19.85)
6 ($C_{20}H_{20}N_8O_4CoCl_2$)	167	4.52	42.41 (42.43)	3.53 (3.51)	19.79 (19.76)
7 ($C_{40}H_{30}N_6CoCl_2$)	174-178	4.35	66.31 (66.35)	4.14 (4.12)	11.60 (11.61)
8 ($C_{40}H_{28}N_8O_4CoCl_2$)	198	4.55	58.98 (58.97)	3.44 (3.42)	13.76 (13.75)

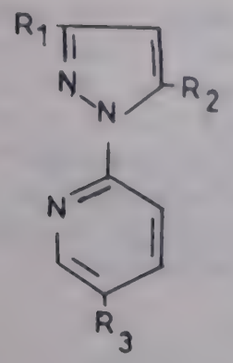

I = $R_1 = R_2 = R_3 = H$
II = $R_1 = R_2 = CH_3, R_3 = NO_2$
III = $R_1 = R_2 = C_6H_5, R_3 = H$
IV = $R_1 = R_2 C_6H_5, R_3 = NO_2$

The metal complexes synthesized are crystalline in nature. They are insoluble in water and common organic solvents but are appreciably soluble in dimethylformamide (DMF).

The analytical data of the complexes (Table 1) indicate that the complexes have 1:2 (metal:ligand) stoichiometry.

The complexes have been found to be electrically non-conducting (7.25 ohm^{-1} cm^2 mol^{-1} in DMF) suggesting that the ligands and the anions are covalently bonded with the central metal atom. The magnetic moments (Table 1) for CoL_2Cl_2 fall in the range 4.2-4.5 B.M. expected to contain odd number of electron (d^7-system) and the $\mu_{eff.}$ values for Ni(II) complexes are well within the range expected for spin-free octahedral geometry[6].

The electronic spectra of all the metal complexes exhibited bands due to *d-d* transitions (Table 2). A strong band around 3000 cm^{-1} in all the metal complexes, was labelled as a charge transfer band, probably associated with the transition of an electron from a non-bonding metal *d*-orbital to an antibonding ligand π^*-orbital. The nickel(II) complexes exhibited three typical bands in the region 26300-30000, 15200-18500 and 9000-11000 cm^{-1} corresponding to the transitions $^3A_{2g} \rightarrow T_{1g}(P)$, $^3A_{2g} \rightarrow {}^3T_{1g}(F)$ and $^3A_{2g} \rightarrow {}^3T_{2g}(F)$. Similarly, the cobalt(II) complexes exhibited absorption bands around 30000-33000, 17100-19000 and 8350-11000 cm^{-1}; the latter two bands have been assigned to the transitions $^4T_{1g}(F) \rightarrow {}^4T_{2g}(P)$ and $^4T_{1g}(F) \rightarrow {}^4T_{1g}(P)$ respectively[6]. The first band is already assigned to metal → ligand charge-transfer because of its high intensity.

A comparative scrutiny of the infrared spectral data of the complexes with those of the uncomplexed ligands gave clues regarding the donor sites of the ligand molecules. A strong and broad band due to ν(C=N) of pyrazole ring, which appeared

Table 2—Infrared and Electronic Spectral Data of the Complexes

Complex No.*	IR bands (cm^{-1})	λ_{max} (cm^{-1})
1	2910, 1570, 1205, 1270, 1910, 275 (M−N)	9530, 15200, 26500
2	3128, 1560, (NO_2), 1350, (NO_2), 1290, 290 (M−N)	9525, 17500, 29100
3	3080, 3040, 1575, 1280 920, 280 (M−N)	9530, 16550, 27200
4	3130, 3060, 1570, 1490, (NO_2), 1340 (NO_2), 915, 285 (M−N)	10200, 18500, 30000
5	3010, 2840, 1580, 1420, 1275, 270 (M−N)	10210, 17100, 29900
6	3090, 1585, 1570, (NO_2), 1345, 910, 280 (M−N)	10220, 18550, 31500
7	3070, 2805, 1575, 1285, 915, 285 (M−N)	10200,17700, 30150
8	3090, 1570, 1480, (NO_2), 1350, (NO_2), 920, 280 (M−N)	10900, 19000, 32900

*Numbering same as in Table 1

Table 3—Antimicrobial Activity Data of the Complexes

Complex No.	Conc. (μg/ml)	Microbial species		
		a	b	c
1	1000	—	—	—
	500	+	+	+
	250	+	+	+
2	1000	—	—	—
	500	+	+	+
	250	+	+	+
3	1000	—	—	—
	500	—	+	+
	250	+	+	+
4	1000	—	—	—
	500	+	—	+
	250	+	+	+
5	1000	—	—	—
	500	—	+	—
	250	+	+	+
6	1000	—	—	—
	500	+	—	+
	250	+	+	+
7	1000	—	—	—
	500	—	+	—
	250	+	+	+
8	1000	—	—	—
	500	+	—	+
	250	+	+	+

Microbial effect (−inhibition, +growth)
a = *Staphylococcus aureus*
b = *Escherechia coli*
c = *Pseudomonas aeruginosa*
*Numbering same as in Table 1

at 1520 cm^{-1} in the ligands, shifted to higher frequency side (~ 1570-1585 cm^{-1}) in the spectra of complexes. Furthermore, the appearance of new bands in the regions 300 and 270 cm^{-1} is attributed to $\nu(M-N)$ mode[7], thus confirming that complex formation takes place by coordination of the C = N group to the metal ion.

Antimicrobial activity

Antimicrobial action of the compounds under investigation was studied on three bacteria species, *Staphylococcus aureus* (a), *Escherechia coli* (b) and *Pseudomonas aeruginosa* (c). Paper disc diffusion method was adopted to measure the inhibition (−) and growth (+) of the microorganisms. The compounds were tested at concentrations 250,500 and 1000 μg/ml. DMF was used as the solvent, its final concentration being 0.01 ml/10 ml in the culture medium (Table 3).

The results show (Table 3) that all the metal complexes have significant antimicrobial activity at concentration 250 μg/ml, but their toxicity decreases markedly on dilution (at 500 μg/ml and 1000 μg/ml).

The metal complexes are more potent against (a), (b) and (c) than the parent compounds. This may be due to the fact that the chelation reduces considerably the polarity of the metal ions in the complexes (due mainly to the partial shairing of its positive charge with the donor group and possible π-electron delocalisation over the whole chelate ring system through *pπ-pπ* or *dπ-dπ* interactions of the orbitals of the ligand and metal ions). This in turn increases the hydrophobic character of the metal chelate favouring its permeation through lipoid layer of microorganism.

References

1 Gupta R R, Yadav B N, Tiwari O P & Srivastava A K, *Inorg chim Acta*, **32** (1979) 295.

2 (a) Saha N & Kar S K, *J inorg nucl Chem*, **39** (1977) 1236.
(b) Saha N & Kar S K, *J inorg nucl Chem*, **41** (1979) 1233.

3 (a) Chohan Z H & Moazzam M, *J pure & applied Sc*, **5** 2 (1986) 33.
(b) Chohan Z H & Sheikh Q I, *J Sc Research*, (Accepted).
(c) Cleare M J, *Coord Chem Rev*, **12** (1974) 349.

4 Khan M A & Pinto A A A, *Mh Chem*, III (1980) 883.

5 Vogel A I, *A text book of quantitative inorganic analysis*, 3rd Ed (Longmans, London) 1961, 531.

6 (a) Allan J R, Brown D H, Nuttal R H & Sharp D W A, *J inorg nucl Chem*, **27** (1965) 1305.
(b) Lever A B P, *Inorg Chem*, **4** (1965) 763.
(c) Figgis B N & Lewis J, *Prog inorg Chem*, **6** (1964) 87.
(d) Balhausen C J, *Introduction to ligand fields* (McGraw Hill, New York) 1962, 256.

7 (a) Vos J G & Groeneveld W L, *Inorg chim Acta*, **24** (1977) 123 and references therein.
(b) Dorrity I A & Orrel K G, *J inorg nucl Chem*, **36** (1974) 230.

Indian Journal of Chemistry
Vol. 27A, December 1988, pp. 1105-1108

Synthesis & Characterization of Thorium(IV) & Dioxouranium(VI) Complexes of 4-{(N-Benzoyl)amino}antipyrine†

R K AGARWAL* & H K RAWAT
Department of Chemistry, Lajpat Rai (Post-Graduate) College, Sahibabad 201 005
and
A K SRIVASTAVA
Department of Chemistry, Meerut College, Meerut 250 001

Received 19 *August* 1987; *revised* 9 *February* 1988; *accepted* 25 *March* 1988

Complexes of 4-{(N-benzoyl)amino}antipyridine (BAApy) with thorium(IV) and dioxouranium(VI), having the general formulae $ThX_4 \cdot n$BAApy (X = Cl, Br, NO_3 or NCS; n = 2; X = I or ClO_4; n = 3) and $UO_2X_2 \cdot n$BAApy (X = Cl, Br, NO_3 or NCS; n = 1; X = I, or ClO_4; n = 2), have been synthesized and characterized by analytical molecular weight, conductance, magnetic moment, IR and TG data. The IR spectra of the complexes suggest that the ligands acts as O,O-chelating agent. The probable coordination number of Th(IV) is 6,8 or 12 and that of U(VI) is 6 or 8 in the present complexes.

Complexes of thorium(IV) and dioxouranium(VI) with pyrazolone ligands have been investigated extensively[1-3]. Their stoichiometries were found to be dependent chiefly on the bulkiness of the ligands. The linear dioxouranium(VI) ion is known to form a wide variety of compounds with different ligands where uranium(VI) is usually 6-,7- or 8-coordinated[4,5]. The high positive charge and an effective ionic size of 0.99 Å enable Th(IV) to form many compounds with coordination numbers greater than six[6,7]. In the present investigation, we wish to report the synthesis and characterization of thorium(IV) and dioxouranium(VI) complexes of 4-{(N-benzoyl)amino}antipyrine (BAApy).

Hydrated thorium(IV) nitrate and dioxouranium(VI) nitrate were BDH reagents. Thorium(IV) halides and perchlorates were prepared by established methods[8,9]. Dioxouranium(VI) salts were prepared as reported previously[10]. The ligand 4-{(N-benzoyl)amino}antipyrine (BAApy) was prepared by N-benzoylation (Schotton and Baumann reaction) of 4-aminoantipyrine. All the solvents used were of AR grade.

† Presented at the 57th annual session of the National Academy of Sciences (India) held on 8-10 October 1987 at Bharathidasan University, Tiruchirapalli.

Synthesis of the complexes

$Th(ClO_4)_4 \cdot 3$BAApy—Hydrated thorium(IV) perchlorate was dissolved in ice-cold water and an excess of 10% non-aqueous solution of BAApy was added dropwise with constant stirring. On continued stirring, a crystalline compound separated out. It was filtered, washed thoroughly with ice cold water to remove excess of the ligand and dried *in vacuo* over P_4O_{10}.

$Th(NO_3)_4 \cdot 2$BAApy—To a solution of thorium(IV) nitrate in ethyl acetate, an excess of the ligand in the same solvent was added. A solid compound precipitated immediately which was filtered, washed with ethyl acetate and then with solvent ether and dried *in vacuo* over fused $CaCl_2$.

$ThX_4 \cdot n$BAApy (n = 2; X = Cl, Br or NCS; n = 3; X = I)—All these complexes were prepared by mixing methanolic solutions of metal salt and ligand in the required molar proportions. The reaction mixture was refluxed for ~2 hr on a water bath and excess solvent removed by disillation. The residual mass on treatment with diethyl ether yielded crystalline solid which was filtered, washed several times with small amounts of methanol and finally with solvent ether and dried *in vacuo* over fused $CaCl_2$. In the case of $ThCl_4$ complex 2-3 drops of HCl were added to prevent solvolysis.

$UO_2X_2 \cdot$BAApy (X = Cl, Br, I or NCS)—The complexes were prepared by mixing the dioxouranium(VI) salt (1 mmol in 20 ml ethanol) and the ligand (1.2 mmol in 25 ml boiling ethanol). On cooling the reaction mixture, desired complexes crystallized out. They were filtered and dried as reported earlier.

$UO_2(NO_3)_2 \cdot$BAApy—This complex was prepared by treating $UO_2(NO_3)_2$ (1 mmol) with BAApy (1.2 mmol) in acetone (45 ml) and heating under reflux (~½ h). On cooling, the complex crystallized from the solution. It was filtered, washed with acetone and dried as above.

$UO_2(ClO_4)_2 \cdot 2$BAApy—To an ethanolic solution containing 1 mmol of the metal salt (1 mmol), the ligand (2.25 mol) in 25 ml of absolute ethanol was added at room temperature. On vigorous stirring, the desired complex precipitated. It was filtered, washed with absolute ethanol and dried *in vacuo* over P_4O_{10}.

All the physical measurements and analyses were performed as reported earlier[10,11].

The analytical data (Table 1) indicate that the

Table 1—Analytical Data of Thorium(IV) & Dioxouranium(VI) Complexes of 4-{(N-benzoyl)amino}antipyrine

Complex	Found (Calc.) %					Λ *M* (ohm^{-1} cm^2 mol^{-1})	Mol. wt Found (Calc.)
	Metal	N	C	H	Anion		
$ThCl_4 \cdot 2BAApy$	23.30 (23.48)	8.37 (8.50)	43.42 (43.72)	3.33 (3.44)	14.09 (14.37)	4.2	973 (988)
$ThBr_4 \cdot 2BAApy$	19.53 (19.87)	7.06 (7.20)	36.72 (37.04)	2.82 (2.91)	27.01 (27.44)	4.3	1152 (1166)
$ThI_4 \cdot 3BAApy$	13.78 (13.96)	7.47 (7.58)	38.62 (39.01)	2.97 (3.07)	29.82 (30.58)	55.3	561 (1661)
$Th(ClO_{44} \cdot 3BAApy$	14.76 (14.95)	8.01 (8.12)	41.39 (41.77)	3.13 (3.28)	24.92 (25.66)	96.4	316 (1551)
$Th(NO_3)_4 \cdot 2BAApy$	21.02 (21.20)	12.63 (12.79)	39.09 (39.48)	3.02 (3.10)	—	4.0	1083 (1094)
$Th(NCS)_4 \cdot 2BAApy$	25.58 (25.52)	12.80 (12.98)	44.28 (44.52)	3.04 (3.15)	21.06 (21.52)	4.3	1063 (1078)
UO_2Cl_2BAApy	36.41 (36.72)	6.36 (16.48)	33.12 (33.33)	2.56 (2.62)	10.66 (10.95)	3.7	632 (648)
$UO_2Br_2 \cdot BAApy$	32.02 (32.29)	5.52 (5.69)	29.13 (29.30)	2.21 (2.30)	21.32 (21.70)	4.2	326 (737)
$UO_2I_2 \cdot 2BAApy$	20.70 (20.91)	7.19 (7.38)	37.70 (37.96)	2.83 (2.98)	22.05 (22.31)	50.1	383
$UO_2(ClO_4) \cdot 2BAApy$	21.78 (21.97)	7.59 (7.75)	39.54 (39.88)	3.02 (3.13)	18.20 (18.37)	53.9	367 (10.83)
$UO_2(NO_3)_2 \cdot 2BAApy$	33.72 (33.95)	9.82 (9.98)	30.69 (30.81)	2.30 (2.42)	—	3.6	691 (701)
$UO_2(NCS)_2 \cdot BAApy$	34.21 (34.34)	9.90 (10.10)	34.39 (34.63)	2.32 (2.45)	16.52 (16.73)	4.9	679 (693)

complexes have the general compositions $ThX_4.nBAApy$ (n = 2, X = Cl, Br, NO_3 or NCS; n = 3, X = I or ClO_4) and $UO_2X_2 \cdot nBAApy$ (n = 1, X = Cl, Br NO_3 or NCS; n = 2, X = I or ClO_4). All the complexes are fairly soluble in acetone, nitrobenzene, DMSO and DMF. The molar conductivities of thorium(IV) complexes in nitrobenzene suggest that the chloro, bromo, nitrato and thiocyanato complexes are nonelectrolytes, while the perchlorate and the iodide complexes are 1:4 and 1:2 electrolytes, respectively. Thus, all perchlorate groups are ionic in the former complex, whereas only two of the four iodide groups may be ionic in nature. All the dioxouranium(VI) complexes, $UO_2X_2 \cdot BAApy$ (X = Cl, Br, NO_3 or NCS), are essentially nonelectrolytes in nitrobenzene. The conductance values for the iodo and perchlorato complexes in nitrobenzene suggest that they are 1:2 electrolytes and thus both the anions are present outside the coordination sphere.

Molecular weight data of the complexes in freezing nitrobenzene (Table 1) show that the complexes are monomeric. In the case of $ThI_4 \cdot 3BAApy$, $UO_2(ClO_4)_2 \cdot 2BAApy$ and $Th(ClO_4)_4 \cdot 3BAApy$, the ratios of found and calculated molecular weights are 0.33, 0.33 and 0.20 respectively. These data further support that 3 species are formed in the case of the former two complexes and 5 species are formed in the latter complex.

The dioxouranium(VI) and Th(IV) complexes were found to be diamagnetic as expected[10,11].

In the free ligand IR spectrum, the ν(C = O) modes occur at 1660 and 1635 cm^{-1} (refs 1, 2, 12). The IR spectra of the complexes show a considerable shift of these absorptions to lower stretching frequencies, indicating coordination through the carbonyl oxygen. The N − H stretching occurs at 3205 and 3100 cm^{-1} in the free ligand and remains unaffected on complexation. This precludes the possibility of coordination through imino nitrogen atom. Of the amide bands, the CO stretching (amide-I) and out-of-plane bending (amide-VI) modes can be used to distinguish between O- and N-coordination of the amide group[13,14]. The decrease in frequency of band I and the increase in frequency of band VI on complex formation indicate that the amide group is O-bonded in all the complexes. A band in the 410-360 cm^{-1} region has been tentatively assigned to the ν(M − O) vibration[1-3].

In all the dioxouranium(VI) complexes, the ν_1 and ν_3 modes of O = U = O are assigned in the ranges of 840-825 and 930-920 cm^{-1} respect-

Table 2—Uranyl Frequencies (cm^{-1}), Force Constants and U – O Bond Distances of Dioxouranium(VI) Complexes

Complex	ν_1 (cm^{-1})	ν_3 (cm^{-1})	U – O force constant (mdyne/Å)	Calc. U – O distance (Å)
$UO_2Cl_2 \cdot BAApy$	840	930	6.9188	1.7369
$UO_2Br_2 \cdot BAApy$	830	920	6.7632	1.7414
$UO_2I_2 \cdot 2BAApy$	825	920	6.7242	1.7420
$UO_2(NO_3)_2 \cdot BAApy$	835	925	6.8408	1.7390
$UO_2(ClO_4)_2 \cdot 2BAApy$	837	927	6.8719	1.7381
$UO_2(NCS)_2 \cdot BAApy$	835	925	6.8526	1.7384

ively[1,3,15,16] (Table 2). Wilson's G-F matrix method[17] was used to determine the stretching and interaction force consants from which the U-O bond distances were calculated following Badger's formula[18]. It is apparent from the calculated data that the U-O bond length decreases with the increase in the value of symmetric stretching frequency (ν_1)[19]. A plot of ($\nu_1 + \nu_3$) vs force constants gave a straight line. The U-O bond distances in dioxouranium salts generally range from 1.60 to 1.92 Å depending on the nature of the equatorial ligands[20]. The calculated values of the U-O bond distances in the present complexes are close to 1.73-1.74 Å (Table 2).

In the perchlorato complexes of Th(IV) and dioxouranium(VI) the ν_3 and ν_4 bands of perchlorate ions are observed as strong absorptions at ~ 1090 and 625 cm^{-1} respectively[21,22]. The absence of the ν_3 band of ionic nitrate (D_{3h}) around 1360 cm^{-1} and the occurrence of two strong bands at ~1510 and 1305 cm^{-1} in the spectra of $Th(NO_3)_4 \cdot 2BAApy$ and $UO_2(NO_3)_2 \cdot BAApy$ suggest the coordination of nitrate in these complexes[23]. The bidentate nature of nitrato groups in $Th(NO_3)_4 \cdot 2BAApy$ has been established by comparing its spectral bands with those of $Th(NO_3)_4 \cdot 5H_2O$, where the bidentate character of the nitrato groups has been established on the basis of the X-ray analysis[7,24]. In $Th(NO_3)_4 \cdot 2BAApy$ the NO_3^- vibrations occur at 1510 (ν_1), 1305 (ν_4), 1040 (ν_2), 820 (ν_6), 760 (ν_3) and 700 (ν_5) while in $Th(NO_3)_4 \cdot 5H_2O$ the corresponding bands occur at 1520, 1290, 1030, 808, 745 and 715 cm^{-1} respectively. Similarly, in $UO_2(NO_3)_2 \cdot BAApy$, the bands at 1510 (ν_1), 1305 (ν_4), 1032 (ν_2), 810 (ν_6), 750 (ν_3) and 725 (ν_5) cm^{-1} suggest the bidentate nature of NO_3^- groups[10,25,26] in this complex, because they occur in almost the same ranges as in $UO_2(NO_3)_2 \cdot 2H_2O$. In both the thiocynato complexes, the appearance of IR bands at ~2080 ($\nu C \equiv N$), 820 ($\nu C = S$) and 430 cm^{-1} (δNCS) suggests the presence of N-bonded isothiocyanate[27,28].

Thermal studies

The thermograms of Th(IV) complexes show the absence of water molecules. The halo and nitrato complexes decompose endothermally while the perchlorato complex decomposes exothermally with a slight explosion and evolution of smoke[29]. The exo peak at ~480°C is due to the oxidation of carbon formed during the decomposition of the complexes. The exo peak in the range 630-670°C is due to metal oxidation. The TG curves of chloro, bromo, nitrato and thiocyanato complexes indicate that in the first step, only one mole of ligand is lost indicating a loose bonding. The remaining ligand is lost at ~400°C. At ~590°C, oxohalide and oxothiocyanate formation takes place. At ~650°C, the final product is ThO_2. The TG curve of $[Th(BAApy)_3](ClO_4)_4$ shows that the complex starts to decompose at ~220°C and continues to do so upto 580°C, after which ThO_2 remains. No stable intermediate perchlorate-BAApy complex has been isolated.

The TG and DT curves of these complexes clearly indicate the absence of water molecules. Except the perchlorate, which decomposes exothermally, all other complexes decompose endothermally. The pyrolysis curves of these complexes are similar in major details. The break in the TG curves in the temperature range 210-290°C, indicates that at this stage only 0.5 mol of ligand is lost (22-25%) in the case of halo and nitrato complexes and one mole of ligand is lost (29.5%) in the case of perchlorato complex. In the 320-395°C temperature range, there is additional mass loss due to loss of all the ligand molecules. The oxide U_3O_8 is formed at ~635°C via the formation of UO_3, following which there is no appreciable change in weight[30].

The preferred coordination number of thorium(IV) is 6 or 8, but higher coordination numbers have also been observed[31]. In $[Th(BAApy)_2X_4]$ (X = Cl, Br or NCS) and $[Th(BAApy)_3I_2]I_2$ the coordination number of Th(IV) is eight. The conductance, molecular weight and IR data show that in the perchlorate complex, all the four perchlorato groups are present outside the coordination sphere and hence Th(IV) is six-coordinated in this complex. In $Th(BAApy)_2(NO_3)_4$, the coordination number of Th(IV) is 12.

In $[UO_2(BAApy)X_2]$ (X = Cl, Br or NCS), the coordination number of uranium is 6. Since in $UO_2(BAApy)_2X_2$ (X = I or ClO_4) both the anion-ligands are ionic in nature, in these complexes uranium is hexa-coordinated. The IR data of $UO_2(BAApy)(NO_3)_2$ suggest bidentate nature of the

nitrate groups in this complex. Thus, it may be considered to have a 8-coordinate uranium atom.

The authors are thankful to Dr. G.D. Sharma, Principal, Lajpat Rai (Post-Graduate) College, Sahibabad for taking keen interest in the work. One of them (RKA) is also thankful to the UGC, New Delhi for financial support of this work.

References

1 Savant V V, Ramamurthy P & Patel C C, *J less-common Metals*, **22** (1970) 479.
2 Agarwal R K, Srivastava A K & Srivastava T N, *Proc Nat Acad Sci (India)*, **51A** (1981) 79.
3 Agarwal R K & Rastogi S C, *Thermochim Acta*, **95** (1985) 279.
4 Zachariasen W H, *Acta Crystallogr*, **7** (1954) 795.
5 Wells A F, *Structural inorganic chemistry*, 3rd Edn (Oxford University Press, London) 1968.
6 Lippard S J, *Progress in inorganic chemistry*, Vol. 8, edited by F A Cotton (Wiley, New York) 1967, 109.
7 Taylor J C, Mueller M H & Hitterman R L, *Acta Crystallogr*, **20** (1966) 842.
8 Ramamurthy P & Patel C C, *J inorg nucl Chem*, **25** (1963) 310.
9 Savant V V & Patel C C, *J less-common Metals*, **24** (1971) 459.
10 Srivastava A K, Sharma S & Agarwal R K, *Inorg chim Acta*, **61** (1982) 235.
11 Agarwal R K, Srivastava A K & Srivastava T N, *Transition Met Chem*, **5** (1980) 95.
12 Baily R A & Peterson T R, *Can J Chem*, **47** (1969) 1681.
13 Katritzky A R, *J chem Soc*, (1958) 2202.
14 Bould J & Brisdon B J, *Inorg chim Acta*, **19** (1976) 159.
15 Vigato P A, Casellato U & Vidali M, *Gazz chim ital*, **107** (1977) 61.
16 Rastogi V K, Pandey A N, Gupta S L & Saxena R C, *Indian J pure appl Phys*, **18** (1980) 379.
17 Wilson L B, *J chem Phys*, **7** (1939) 1047; **9** (1941) 76.
18 Badger R M, *J chem Phys*, **2** (1934) 128; **3** (1935) 710.
19 Garga C L, Gupta S D & Narasimhan K V, *Indian J pure appl Phys*, **8** (1970) 108.
20 Zachariasen W H, *Acta Crystallogr*, **7** (1954) 783.
21 Hathaway B J, Holah D G & Hudson M, *J chem Soc*, (1963) 4856.
22 Madan S K & Donohue A M, *J inorg nucl Chem*, **28** (1966) 1303.
23 Addison C C & Logan N, *Adv inorg Chem Radiochem*, **6** (1964) 95.
24 Ferraro J R & Walker A, *J chem Phys*, **45** (1966) 550.
25 Topping G, *Spectrochim Acta*, **21** (1965) 1743.
26 Agarwal R K, Chopra J R & Rastogi S C, *J Indian chem Soc*, **62** (1985) 154.
27 Burmeister J L, *Coord Chem Rev*, **1** (1966) 205; **3** (1968) 225.
28 Al-Kazaz Z M S, Bagnall K W & Brown D, *J inorg nucl Chem*, **35** (1973) 1501.
29 Srivastava A K, Srivastava M & Agarwal R K, *Ind Engg Chem Products Res & Dev*, **21** (1982) 135.
30 Wendlandt W W, *J inorg nucl Chem*, **5** (1957) 118; **9** (1959) 136.
31 Smith B C & Wassef M A, *J chem Soc (A)*, (1968) 1817.

Indian Journal of Chemistry
Vol. 27A, December 1988, pp. 1109-1110

Thorium Nitrate Complexes of Some Schiff Bases Derived from Substituted Benzaldehydes & Amino Compounds

BABU KUNCHERIA & P INDRASENAN*

Department of Chemistry, University of Kerala, Trivandrum 695 034

Received 7 *September* 1987; *revised and accepted* 29 *February* 1988

A series of thorium nitrate complexes with some schiff bases derived from substituted benzaldehydes and amino compounds has been synthesised and characterised. The schiff bases employed are N-(3-methoxy-4-hydroxybenzylidene)isonicotinylhydrazone (MHBIH), N-(3-methoxy-4-hydroxybenzylidene)benzhydrazone (MHBBH), N-(3-methoxy-4-hydroxybenzylidene)salicyloylhydrazone (MHBSH), N-(3-methoxy-4-hydroxybenzylidene)anthranilic acid (MHBAA), 4-N-(3-methoxy-4-hydroxybenzylidene)aminoantipyrine (MHBAAP), 1,2-N,N-(3-methoxy-4-hydroxybenzylidene)phenylenediamine (MHBPDA), N-(3,4-dimethoxybenzylidene)isonicotinylhydrazone (DMBIH), N-(3,4-dimethoxybenzylidene)benzhydrazone (DMBBH), N-(3,4-dimethoxybenzylidene)salicyloylhydrazone (DMBSH), N-(3,4-dimethoxybenzylidene)anthranilic acid (DMBAA),4-N-(3,4-dimethoxybenzylidene)aminoantipyrine (DMBAAP) and 1,2-N,N-3,4-dimethoxybenzylidene)phenylenediamine (DMBPDA). Elemental analysis and molecular weight data of the complexes indicate that they have composition $ThL_2(NO_3)_4$ (L = MHBIH, MHBBH, MHBSH, MHBAA, MHBAAP, DMBIH, DMBBH, DMBSH, DMBAA and DMBAAP) and $ThL(NO_3)_4$ (L = MHBPDA and DMBPDA). IR spectral and conductance data show that all the ligands act as neutral bidentate ones and nitrate groups are coordinated to the metal ion in a monodentate fashion.

As a part of our programme on the synthesis and characterisation of solid actinide complexes[1,2], we report here some thorium(IV) nitrate complexes with schiff bases derived from substituted benzaldehydes and amino compounds.

Throium(IV) nitrate was a BDH reagent (99.9% pure) and was used as such. The schiff bases were prepared by a known method[3] and their purities were checked by TLC and IR spectral analyses.

The complexes were prepared as described. For the preparation of the complexes of MHBIH, MHBBH, MHBSH, MHBAA, MHBAAP, DMBIH, DMBBH, DMBSH, DMBAA and DMBAAP, solutions of thorium nitrate (2 mmol) and the ligand (4 mmol) in hot dry acetone were mixed and refluxed on a water bath for 3-4 h. The reaction mixture was concentrated and the precipitated complexes of DMBIH, DMBSH, DMBAA and DMBAAP were filtered and washed with acetone whereas the complexes of MHBIH, MHBBH, MHBSH, MHBAA, MHBAAP and DMBBH were separated by the addition of benzene to the viscous mass obtained on concentration. These were filtered, washed several times with hot benzene to remove excess ligand, redissolved in minimum amount of hot dry acetone and precipitated by the addition of dry diethylether. For the preparation of the complexes of MHBPDA and DMBPDA, thorium nitrate (2 mmol) and the ligand (MHBPDA or DMBPDA, 2 mmol) in hot dry acetonitrile were mixed and refluxed on a water bath for 3 h. The complexes so precipitated were filtered and washed several times with hot acetonitrile. All the complexes were dried *in vacuo* over phosphorus(V) oxide. These complexes were analysed for the thorium content by the oxalate-oxide method[4]; C, H, N data were obtained from the Central Drug Research Institute, Lucknow. IR spectra of the ligands and the complexes in the 400-4000 cm^{-1} region were recorded on a Perkin-Elmer 397 double beam IR spectrophotometer using the KBr disc technique. Molar conductivities of the complexes in acetonitrile, methanol and nitrobenzene ($\sim 10^{-3}$ *M* solutions) were measured at room temperature ($28 \pm 2°C$) using an ELICO conductivity bridge type CM82 with a dip-type cell (type CC-03) having platinum electrodes (cell constant, 1.30 cm^{-1}). Magnetic susceptibilities were also measured at room temperature using the Gouy method with $Hg[Co(CNS)_4]$ as the calibrant. Molecular weights of the complexes ($\sim 10^{-3}$ *M* solutions) were determined by the cryoscopic method in nitrobenzene[5].

Analytical data of the complexes (Table 1) indicate that they may be formulated as $ThL_2(NO_3)_4$ (L = MHBIH, MHBBH, MHBSH, MHBAA, MHBAAP, DMBIH, DMBBH, DMBSH, DMBAA and DMBAAP) and $ThL(NO_3)_4$ (L = MHBPDA and DMBPDA). All the complexes are intensely coloured non-hygroscopic solids which are soluble in acetone, acetonitrile, ethanol, methanol and nitrobenzene and insoluble in benzene, carbon tetrachloride, petroleum ether and diethylether. Molar conductance values indicate that all the complexes exhibit non-electrolytic behaviour in nitrobenzene[6] ($\acute{\Lambda}_M$ = 1.3-9.5 ohm^{-1} cm^2 mol^{-1}) suggesting that the nitrate groups are coordinated to the metal ion. However, almost all the complexes show higher conductance values in acetonitrile (35.2-63.4 ohm^{-1} cm^2 mol^{-1}) and methanol (45.6-108.3 ohm^{-1} cm^2 mol^{-1}). These higher values are approximately equal to those of 1:1 electrolytes and are probably due to partial displacement of the anionic nitrates with the polar acetonitrile or methanol molecules[7]. All the complexes show almost zero magnetic moments as expected for the Th^{4+} ion.

Table 1—Analytical and Molecular Weight Data of Thorium(IV) Nitrate Complexes of Some Schiff Bases

Complex	Found (Calc.)				
	Metal %	C %	H %	N %	Mol wt
$[Th(MHBIH)_2(NO_3)_4]$	22.5 (22.7)	30.9 (31.1)	2.5 (2.4)	12.9 (13.0)	1052 (1022)
$[Th(MHBBH)_2(NO_3)_4]$	22.6 (22.8)	35.4 (35.3)	2.8 (2.7)	10.9 (11.0)	1060 (1020)
$[Th(MHBSH)_2(NO_3)_4]$	22.0 (22.1)	34.3 (34.2)	2.9 (2.7)	10.8 (10.7)	1008 (1052)
$[Th(MHBAA)_2(NO_3)_4]$	22.5 (22.7)	35.0 (35.2)	2.3 (2.5)	8.0 (8.2)	1050 (1022)
$[Th(MHBAAP)_2(NO_3)_4]$	20.0 (20.1)	39.1 (39.5)	3.5 (3.3)	12.1 (12.1)	1123 (1154)
$[Th(MHBPDA)(NO_3)_4]$	27.0 (27.1)	30.5 (30.8)	2.2 (2.3)	9.7 (9.8)	837 (856)
$[Th(DMBIH)_2(NO_3)_4]$	22.0 (22.1)	34.5 (34.2)	3.2 (2.9)	13.1 (13.3)	1018 (1050)
$[Th(DMBBH)_2(NO_3)_4]$	21.9 (22.1)	36.5 (36.6)	3.0 (3.1)	10.3 (10.7)	1010 (1048)
$Th(DMBSH)_2(NO_3)_4]$	21.3 (21.5)	35.7 (35.6)	2.9 (3.0)	10.2 (10.4)	1040 (1080)
$Th(DMBAA)_2(NO_3)_4]$	22.1 (22.1)	36.3 (36.6)	2.7 (2.9)	7.7 (8.0)	1032 (1050)
$[Th(DMBAAP)_2(NO_3)_4]$	19.5 (19.6)	40.6 (40.6)	3.9 (3.6)	11.6 (11.8)	1210 (1182)
$[Th(DMBPDA)(NO_3)_4]$	26.1 (26.3)	32.3 (32.6)	2.6 (2.7)	9.2 (9.5)	856 (884)

All the twelve ligands show a strong or medium IR band in the region 1580-1610 cm^{-1}, which is assigned to νC = N. This band is shifted to lower frequency region by 30-40 cm^{-1} in the spectra of all the complexes indicating that the nitrogen of the azomethine group is coordinated to the metal ion.

The IR spectra of MHBIH, MHBBH, MHBSH, DMBIH, DMBBH and DMBSH show a sharp band in the region 1630-1650 cm^{-1} which is attributed to the side chain νC = O mode. This band is shifted by ~ 30 cm^{-1} to the lower frequency side in the spectra of the complexes indicating the coordination of side chain carbonyl group. The strong band at 1680 cm^{-1} observed in the spectra of MHBAA and DMBAA is assigned to the stretching vibration of the side chain carbonyl group. This band is shifted to lower frequency side by ~ 55 cm^{-1} in both the complexes indicating the coordinative participation of the side chain carbonyl group. The spectra of MHBAAP and DMBAAP exhibit a sharp band around 1640 cm^{-1} assignable to ring νC = O mode. This band is shifted to 1610 cm^{-1} indicating that the ring carbonyl group is coordinated to the metal ion. The ligands MHBIH, MHBSH, MHBBH, MHBAA, MHBAAP, MHBPDA and DMBSH show a broad medium intensity band in the region 3430-3450 cm^{-1} and a rather weak one in the region 1320-1330 cm^{-1}, which may be assigned to νO − H (phenolic) and νC − O, respectively. These bands occur in the same region without any shift showing that the phenolic oxygen is not involved in coordination[8,9].

In the spectra of all the complexes three additional bands, which are not present in the spectra of the ligands, are observed at 1390, 1280 and 1020 cm^{-1}. These are assigned to ν_4, ν_1 and ν_2 vibrations, respectively of the nitrate group. The bands at 1390 cm^{-1} (ν_4) and 1280 cm^{-1} (ν_1) are the split bands of ν_3 mode of the free nitrate group and the difference ν_4-ν_1 is ~ 110 cm^{-1} indicating that the nitrate groups are coordinated to the metal ion monodentately[10]. The conductance values of the complexes confirm this evidence of nitrate coordination.

On the basis of the above observations the complexes are assigned the stoichiometries $[ThL_2(NO_3)_4]$ (where L = MHBIH, MHBBH, MHBSH, MHBAA, MHBAAP, DMBIH, DMBBH, DMBSH, DMBAA and DMBAAP) and $[ThL(NO_3)_4]$ (where L = MHBPDA and DMBPDA). All the ligands are bonded to the Th^{4+} ion in a neutral bidentate fashion and the nitrate ions in a monodentate fashion resulting in a coordination number of 8 in the first set of complexes and 6 in the second set of complexes.

The authors sincerely thank Prof. C.G.R. Nair for his helpful suggestions and the UGC, New Delhi for awarding a Teacher-fellowship to one them (B K).

References

1 Sobhana Devi G & Indrasenan P, *Inorg chim Acta*, **133** (1987) 157.
2 Babu Kuncheria & Indrasenan P, *Polyhedron*, **7** (1988) 143.
3 Shukla P R, Jaiswal A M & Narain G, *J Indian chem Soc*, **60** (1983) 1014.
4 Vogel A I, *A text-book of quantitative inorganic analysis* (Longmans, London), 1961, 541.
5 Palmer W G, *Experimental physical chemistry* (The University Press, Cambridge), 1954, 119.
6 Geary W J, *Coord Chem Rev*, **7** (1971) 81.
7 Sathyanarayana D N & Patel C C, *Indian J Chem*, **5** (1967) 367.
8 Kovacic J E, *Spectrochim Acta*, Part A **23** (1967) 183.
9 Doretti L, Sitran S, Madalosso P, Bandoli G & Paolucci G, *J inorg nucl Chem*, **42** (1980) 1060.
10 Curtis N F & Curtis Y M, *Inorg Chem*, **4** (1965) 804.

Indian Journal of Chemistry
Vol. 27A, December 1988, pp. 1111-1113

Evaluation of Formation Constants of Pyridine Adducts of (Resacetophenone oximato)nickel(II)

ARVIND T RANE* & DEEPAWATI R NEPALI
Tata Institute of Fundamental Research, Bombay 400 005

Received 22 *December* 1987; *revised* 7 *March* 1988; *accepted* 24 *March* 1988

Changes in the absorbance of nickel chelate of resacetophenone oxime are observed, on the addition of heterocyclic N-bases to a solution of the nickel chelate in cyclohexanone. This behaviour is attributed to the adduct formation of nickel chelate with pyridine or substituted pyridines. All the N-bases form monoadducts with the nickel chelate, except 1,10-phenanthroline which forms a diadduct. The stabilities of the nickel adduct increase in the following order of the bases: 3,5-lutidine < 2,4,6-collidine < 3-picoline < 4-picoline < pyridine < 2,2′-bipyridyl < 2,9-neocuproin < 1,10-phenanthroline.

Resacetophenone oxime (2,4-dihydroxyacetophenone oxime; abbreviated as RAPOX) has been used as an analytical reagent in spectrophotometry for several metal ions[1].

Recently, cobalt-RAPOXimate complex was isolated in solid state and a spectrophotometric study of the pyridine and substituted pyridine adducts of the said complex was undertaken in monophase system of cyclohexanone and formation constants of the pyridine adducts were evaluated[2]. The present investigation is an extension of our earlier work[2].

2-Picoline, 3-picoline, 4-picoline, 2,4-lutidine, 3,5-lutidine (all Fluka AG), pyridine and 2,4,6-collidine (both BDH, AR) were dried over KOH and purified by distillation. *o*-Phenanthroline (Fluka AG), 2,2′-bipyridyl (Eastman) and neocuproin (2,9-dimethyl-1,10-phenanthroline, BDH, AR) were used as such. Nickel ammonium sulphate and methanol (BDH, AR) were used for the preparation of nickel chelate complex.

The reagent RAPOX ($C_8H_9O_3N$) was synthesized in the laboratory and recrystallised from ethanol. Nickel-RAPOXimate was prepared as reported earlier[3].

Procedure

Stock solution of nickel RAPOXimate was prepared by dissolving requisite quantity of the nickel complex in freshly distilled cyclohexanone. Specific volumes of cyclohexanone solution of the nickel complex were pipetted into standard volumetric flasks containing solutions of varying amounts of the adducting base in cyclohexanone and the volume was adjusted to the mark with cyclohexanone.

The absorption spectra were recorded on a Cary 17D spectrophotometer in the range 500-650 nm employing 10 mm cuvettes.

The spectrum of Ni-RAPOXimate in cyclohexanone exhibits one distinct peak at 595 nm ($\varepsilon_{max} = 132$ g mol^{-1} cm^{-1}). No shift in the wavelength of maximum absorbance was observed on the addition of base but the absorbance decreased gradually and the peak subsequently disappeared when the adduct formation was complete, i.e. $[B] \geqslant [NiR_2]$. Below 530 nm, all the curves merge and go beyond the scale. The absorbance at 595 nm was taken for the calculation of adduct formation constant.

The formation of the nickel adduct with base B can be represented by Eq. (1)

$$[NiR_2] + nB \rightleftharpoons [NiR_2.nB] \qquad \ldots (1)$$

The adduct formation constants were evaluated using Eq. (2) which was originally derived by Math and Freiser for the pyridine adducts of nickel dithiozonate and 8-mercaptoquinolinate[4].

$$\log K_{AD} = npB + \log \frac{A_0 - A}{A} \qquad \ldots (2)$$

In Eq. (2) A_0 and A are the absorbances in the absence and presence of the pyridine base (B), the concentration of which is denoted by its negative logarithm, *p*B.

Plots of log $(A_0 - A)/A$ versus [B] for various bases are shown in Fig. 1. Intercepts of these plots for various adduct forming bases, on y-axis give directly the values of adduct formation constants. The values of adduct formation constants at different temperatures are given in Table 1. From Fig. 1, it could be seen that the slopes of all the plots excepting that of 1,10-phenanthroline are one indicating that only one molecule is involved in the formation of the adduct, $NiR_2.B$. In case of 1,10-phenanthroline, however, the slope of the plot happens to be two, giving rise to the formation of a diadduct, $NiR_2.2B$. Surprisingly, 4-picoline and 3,5-lutidine, though contain reactive methyl groups and no other groups at 2 and 6-positions capable of offering steric hindrance fail to

Table 1—Adduct Formation Constants of Nickel RAPOXimate with Pyridine Bases and Thermodynamic Parameters of Adduct Formation at 26°C

Base	pK (ref. 7)	log K_{AD} in cyclohexanone at			$-E_a$ (kJ mol^{-1})	$-\Delta H^{\dagger}$ (kJ mol^{-1})	$-\Delta S^{\dagger}$ (JK^{-1} mol^{-1})
		26°	35°	44°C			
Pyridine	5.2	0.93	0.85	0.72	20.84	23.33	297
4-Picoline	6.08	0.72	0.55	0.27	66.4	68.9	369
3-Picoline	5.68	0.57	—	—	—	—	—
3,5-Lutidine	6.14	0.33	0.24	0.15	16.4	18.88	302
2,2′-Bipyridyl	4.37	2.53	1.97	1.5	87.36	89.85	497
1,10-Phenanthroline	4.95	6.23	6.14	6.18	16.9	19.4	564
2,9-Neocuproin	5.85	2.82	2.83	—	—	—	—
2,4,6-Collidine	7.48	0.43	—	—	—	—	—

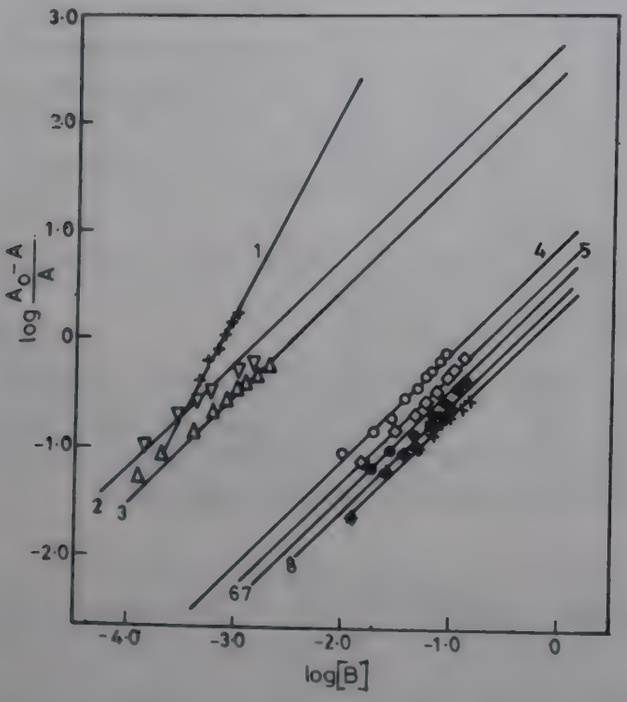

Fig. 1—Plots showing adduct formation between [Ni(RAPOX)$_2$] and various heterocyclic nitrogen bases in cyclohexanone [(1) 1,10-phenanthroline; (2) 2,9-neocuproin; (3) 2,2′-bipyridyl; (4) pyridine; (5) 4-picoline; (6) 3-picoline; (7) 2,4,6-collidine; (8) 3,5-lutidine]

form diadducts. Thus, amongst all the bases used, 1,10-phenanthroline forms a stable adduct, as seen from the log K_{AD} value (Table 1) and favours hexacoordinate structure for the nickel adduct which is the most stable configuration. In the remaining cases, the adducts contain only one mol of base, accounting for five coordination sites around the nickel atom. The presence of any water molecule occupying the sixth position is ruled out as the experiments were carried out in the monophase system of anhydrous cyclohexanone and using oven-dried nickel complex. It is not uncommon to have a pentacoordinate structure around nickel ion. Pentacoordination in nickel has been observed in 1:1 adducts of the N-bases with nickel chelates of other S-containing ligands[4,5] and oxines[6]. Only ligands such as 1,10-phenanthroline behave like bidentate ligands as indicated by the substantial increase in log K_{AD}. Similar monoadducts were observed in the case of cobalt(II) RAPOXimate where all the pyridine derivatives, except the parent pyridine, gave rise to monoadducts. Pyridine, however, showed diadduct formation[2]. No shift as well as change in the absorbance in the spectrum of Ni-RAPOXimate was observed on the addition of 2,4-lutidine, 2,6-lutidine and 2-picoline. These bases were unable to produce any adduct with nickel RAPOXimate. The adduct formation constants with various pyridine bases decreased in the following order of the bases: 1,10-phenanthroline > 2,9-neocuproin > 2,2′-bipyridyl > pyridine > 4-picoline > 3-picoline > 2,4,6-collidine > 3,5-lutidine. Surprisingly 2,4,6-collidine formed a stronger adduct than 3,5-lutidine. This may be due to the fact that 2,4,6-collidine is more basic than 3,5-lutidine because of the presence of one additional methyl group. The methyl group at position-4 is stronger and more reactive. Its reactivity and basicity neutralise the steric hindrance caused by methyl groups at 2 and 6 positions, giving rise to a stronger adduct.

Absorption spectra of Ni-RAPOXimate with most of the pyridine bases were also recorded at 35° and 44°C besides at ambient temperature (26°) and the adduct formation constants were calculated as usual. These values are given in Table 1. The values were found to decrease with increase in temperature. In the case of 2,9-neocuproin, however, the values at different temperatures were almost identical. The energy of activation, E_a, was calculated from the slope of the Arrhenius plot of log K_{AD} versus 1/T, by the formula ln $K_{AD} = -E_a/RT$. Preexponential factor A was

obtained from the vertical intercept of this plot. The activation enthalpy $\Delta H^{\dagger}$ and the activation entropy $\Delta S^{\dagger}$ were obtained from Eqs (3) and (4)

$$\Delta H^{\dagger} = E_a - RT \quad \ldots (3)$$

$$\Delta S^{\dagger} = R[\ln(Ah/kT) - 1] \quad \ldots (4)$$

In Eq. (4) h is the Plank constant; k, the Boltzmann constant; and R, the gas constant. These thermodynamic adduct formation constants of nickel RAPOXimate at 26°C, are also given in Table 1.

References

1 Rane A T, *J Scient ind Res*, **43** (1984) 88.
2 Rane A T & Nepali D R, *Trans Met Chem* **12** (1987) 330.
3 Bhatki K S, Rane A T & Kabadi M B, *Bull chem Soc Japan*, **36** (1963) 1689.
4 Math K S & Freiser H, *Analyt Chem*, **41** (1969) 1682.
5 Sgamelloti A, Furlani C & Magrini F, *J inorg nucl Chem*, **30** (1968) 2655.
6 Bhatki K S, Rane A T & Freiser H, *Inorg chim Acta*, **26** (1978) 183.
7 Clarke K & Well R, *J Am chem Soc*, (1960) 1885.

Indian Journal of Chemistry
Vol. 27A, December 1988, pp. 1114-1115

Spectrophotometric Determination of Co(II), Ni(II) & Cu(II) Using Sodium 1-Amidinoazo-2-hydroxynaphthalene-4-sulphonate

V PRADHAN & R P SINGH*
Department of Chemistry, University of Delhi, Delhi 110 007

Received 15 *May* 1987; *revised and accepted* 28 *January* 1988

Sodium 1-amidinoazo-2-hydroxynaphthalene-4-sulphonate forms 1:2 [in the case of Co(II) and Ni(II)] and 1:1 [in the case of Cu(II)] complexes which property has been utilized for the spectrophotometric determination of these metal ions in the concentration ranges of 4.6-40.6 (Co), 4.6-27.6 (Ni) and 6.2-31.0 (Cu) μg/10 ml.

Sodium 1-amidinoazo-2-hydroxynaphthalene-4-sulphonate (AAHN-4S) was synthesised by refluxing aminoguanidine and 1,2-naphthaquinone-4-sulphonic acid (Na salt) in 1:1 ratio in ethanol for 2 hr. The yellow orange crystalline product which separated out upon cooling overnight was recrystallised from ethanol to obtain a TLC pure product; m.p. >350°C (did not melt) yield (~70%) (Found: C, 41.5; H, 2.8; N, 17.7; Reqd: C, 41.8; H, 2.8; N, 17.7%); IR(KBr): 3480 (νOH), 3350 (νNH), 1630 (bending NH) and 1560 (νN=N−); AAHN-4S is neither soluble in ethanol nor in water. However, on addition of 2-3 drops of aq. ammonia it dissolves because the ammonium salt so formed is soluble in water or ethanol.

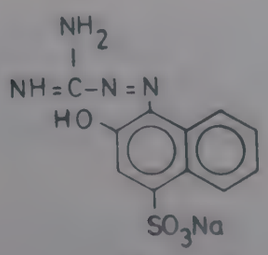

AAHN-4S

A Unicam SP 600 spectrophotometer with optically matched cells of 1 cm light path was used for absorbance measurements. A Beckman Expandomatic SS-2 *p*H meter, with glass and calomel electrodes, was used for *p*H measurements.

Solution (2.5×10^{-4} *M*) of AAHN-4S was prepared in 50% ethanol containing 2-3 drops of aq. ammonia. Cobalt sulphate heptahydrate, nickel ammonium sulphate and copper sulphate pentahydrate (all AR BDH) were dissolved in doubly distilled water and standardised using standard methods.

When 50% ethanolic solution of AAHN-4S was added to aqueous solution of respective metal ion solution and *p*H was adjusted with sodium acetate-acetic acid buffer or dil. sodium hydroxide, coloured complexes were formed, which exhibited maximum absorbances at 590, 560 and 560 nm respectively. The absorbances remained constant in the *p*H ranges 4.0-10.0, 8.5-10.0 and 5.0-7.5 for Co, Ni and Cu respectively in the recommended procedure. Estimation of Co, Ni and Cu was carried out at *p*H 7.0, 9.5 and 6.0, respectively using ten-fold molar excess of AAHN-4S for full colour development.

The systems obeyed Beer's law upto 47.5, 32.3 and 37.2 μg/10 ml for Co, Ni and Cu respectively. The optimum estimation ranges, as evaluated from Ringbom plots, come out to be 4.6-40.6 (Co), 4.6-27.6 (Ni) and 6.3 to 31.0 (Cu) μg/10 ml. The sensitivities of colour reactions according to Sandell's definition are 0.0054 μg Co/cm^2, 0.00534 μg Ni/cm^2 and 0.00792 μg Cu/cm^2. The corresponding molar absorptivities are 10700, 11750 and 7600.

Job's method of continuous variation established 1:2 stoichiometry (metal-ligand) for Co(II) and Ni(II) complexes and 1:1 for Cu(II) complex.

Recommended procedure

To a suitable aliquot (5 ml) containing 4.6 to 40.6 μg Co(II) or 4.6-27.6 μg Ni(II) or 6.3 to 31.0 μg of Cu(II) was added the reagent solution in ten-fold molar excess and the *p*H adjusted at 7.0, 9.5 and 6.0 for Co(II), Ni(II) and Cu(II) respectively by adding sodium acetate-acetic acid buffer or dil. sodium hydroxide and the volume was made up to 10 ml. The amount of cobalt, nickel of copper was then read from the calibration curves drawn under similar conditions.

Effect of diverse ions

For 23.2 μg/10 ml of cobalt, the following ions did not interfere (when present in concentration in μg/10 ml given in parentheses). Masking agents, wherever used, have been mentioned against each: F^-, Cl^-, Br^-, I^-, acetate and sulphate (30000 each); SO_3^{-2}, NO_3^-, NO_2^- (20000 each); thiosulphate, citrate (10000 each); thiourea (5000); Ca^{+2}, Ba^{+2}, Sr^{+2}, Mg^{+2} (10000 each); Mn(II), Pb(II) (1000 each); Cd^{+2} (1000) (I^-), Hg^{+2} (500), (I^-); Cu^{+2} (500) ($S_2O_3^{-2}$), Fe^{+3} (500) (F^-).

Table 1—Simultaneous Determination of Cobalt and Nickel in Synthetic Mixtures

Co(II)		Ni(II)	
Present μg	Found* μg	Present μg	Found* μg
5.8	5.8	11.5	11.4
11.6	11.5	5.8	6.0
11.6	11.5	11.5	11.4
23.2	23.0	8.7	7.7

*Average of four determinations.

For 23.0 μg/10 ml of nickel(II) the tolerance limits in the μg/10 ml are: F^-, Cl^-, Br^-, I^-, SO_4^{-2}, NO_3^- and acetate (3000 each); oxalate, citrate, tartrate (10000 each); SO_3^{-2}, $S_2O_3^{-2}$ (7500); NO_2^- (5000); thiourea (2500); Ca(II), Ba(II), Sr(II) (10000 each); Mn(II), Mg(II) (1000 each); Cu(II) (500) ($S_2O_3^{-2}$).

For 24.8 μg/10 ml of copper(II) the tolerance limits in μg/10 ml are: F^-, Cl^-, Br^-, SO_4^{-2}, NO_3^- (30000); oxalate, tartrate, citrate, nitrate (10000); sulphite (500); Ca(II), Ba(II), Sr(II) (10000 each); Mn(II), Mg(II) (2500 each); Pb(II), (500) (SO_4^{-2}); Fe(III) (500) (F^-); Zn(II) (500) (tartrate).

Nickel in hydrogenated vegetable oils has been determined by this procedure after subjecting the oil sample to wet oxidation[1].

Cobalt(II) and nickel(II) in synthetic solutions could be determined simultaneously as follows.

The spectra of cobalt(II) and nickel(II) complexes indicate a difference of 30 nm in the values of λ_{max}. In view of this the equation derived by Sandell[2], for simultaneous determination of two components in solution, was employed. The results of simultaneous determination of cobalt and nickel in synthetic mixtures (volume 10 ml) are given in Table 1.

The recommended procedure could be extended to the determination of Cu(II) in alloys (brass and gun metal) with an accuracy better than ± 1.5%.

References

1 Reitz L L, Smith W H & Plumlee M P, *Analyt Chem*, **32** (1960) 1728.

2 Sandell E B & Onishi H, *Photometric determination of traces of metals* (John Wiley, New York), 1978.

Indian Journal of Chemistry
Vol. 27A, December 1988, p. 1116

BOOK REVIEWS

Chemical Crystallography with Pulsed Neutrons and Synchrotron X-rays, edited by M A Carrondo & G A Jeffrey (D. Reidel Publishing Co., P.O. Box 989, 3300 AZ Dordrecht), 1988, pp. XI + 616, Price $ 119.00

The development of synchrotron X-rays and pulsed neutrons and of fast detection systems in recent years has greatly widened the scope of research in chemical crystallography; structural studies which require fast recording of diffraction data such as those on solid state chemical reaction kinetics have now become possible because of these advances. Publication of this book is, therefore, most timely for research workers in crystallography. The lectures delivered at the NATO Advanced Study Institute, Alvot, Algarve, Portugal during 17-27 March, 1987 on chemical crystallography with pulsed neutrons and synchrotron X-rays are published in this book in the same sequence in which these were delivered in the meeting; the main points of the discussion following each lecture are also recorded. Sixteen posters presented at the meeting are also included at the end of the book.

In the first chapter, Jeffrey traces the development of crystallography from its early days up to the present time when crystal structure analysis has become a robotic procedure. In the next three chapters, a brief introduction to neutron elastic and inelastic scattering, the method of production of pulsed neutrons and their various applications, and inelastic (one phonon) scattering in a crystal using pulsed neutrons are given. Chapter 5 includes a discussion on various applications of neutron scattering in chemistry such as structural studies of hydrogen containing compounds, electron density studies using (X-N) deformation maps, magnetization density studies using polarized neutrons as well as studies of liquids and amorphous solids and adsorbates. In Chapters 6-9, single crystal pulsed neutron diffraction, pulsed neutron powder diffraction and pulsed neutron diffraction in special sample environments are described; the description of the instruments used in these cases is also given. The next three chapters give application of synchrotron X-rays in protein crystallography and in electron density studies; a brief discussion is also given of the application of neutron radiation in the determination of proton positions in proteins. There is a long chapter (Chapter 13) on the structural applications of X-ray absorption spectroscopy in coordination chemistry using synchrotron radiation sources. Chapter 14 discusses the application of Mössbauer method in crystallography. In the next chapter, the Rietveld profile analysis of powder diffraction data is given.

Chapter 16 on *Real time neutron powder diffraction* discusses how the use of high flux neutron source together with large curved one-dimensional position sensitive detectors allows a complete powder pattern to be recorded simultaneously on a time scale of a few minutes or less, so that transient phenomenon such as chemical reactions in the solid state could be studied. Of particular interest is the study of the thermal transformation of icosahedral quasicrystals of Al-Mn system into orthorhombic Al_6Mn at a temperature of about 630K.

New theoretical developments for investigating macromolecular structures by the use of anomalous dispersion and isomorphous replacement techniques are outlined in Chapter 17 by J Karle; reprints of four publications which give details of the theory are also attached. In Chapter 18, I L Karle illustrates, by examples, some approaches that have been successful in overcoming difficulties encountered in direct phase determining methods.

The last four chapters give the applications of synchrotron radiation in the study of polymers, biological macromolecules and of very small crystals. Examples of real time experiments on polymers are given to show morphological changes during crystallization and melting. Of particular interest are also investigations of conformational changes in proteins during biological reactions by means of structure analysis of intermediate states.

All the chapters are followed by detailed references. The chapters are generally well written although, as often happens in a multi-author book, the presentation in different chapters is rather uneven, and there is also some probably unavoidable repetition. The book should be most useful to readers having a good background of crystallography and in particular, to those who are likely to make use of pulsed neutrons or synchrotron X-rays in their research programmes on chemical crystallography.

L M Pant
National Chemical Laboratory
Pune 411 008

THE WEALTH OF INDIA

An Encyclopaedia of Indian Raw Materials and Industrial Products, published in two series :
(i) Raw Materials, and **(ii) Industrial Products.**

RAW MATERIALS

The articles deal with Animal Products, Dyes & Tans, Essential Oils, Fats & Oils, Fibres & Pulps, Foods & Fodders, Drugs, Minerals, Spices & Flavourings, and Timbers and other Forest products. Names in Indian languages, and trade names are provided.

For important crops, their origin, distribution, evolution of cultivated types and methods of cultivation, harvesting and storage are mentioned in detail. Data regarding area and yield and import and export are provided. Regarding minerals, their occurrence and distribution in the country and modes of exploitation and utilization are given. The articles are well illustrated. Adequate literature references are provided.

Eleven volumes of the series covering letters A–Z have been published.

Vol. I : A (Revised) Rs. 300.00; Vol. I (A-B) Rs. 120.00; Vol. II (C) Rs. 143.00; Vol. III (D-E) with index to Vols. I-III Rs. 158.00; Vol. IV (F-G) Rs. 150.00; Vol. IV Suppl. Fish & Fisheries Rs. 84.00; Vol. V (H-K) Rs. 171.00; Vol. VI (L-M) Rs. 135.00; Vol. VI : Suppl. on Livestock including poultry Rs. 153.00; Vol. VII (N-Pe) Rs. 150.00; Vol. VIII (Ph-Re) Rs. 129.00; Vol. IX (Rh-Sc) Rs. 200.00; Vol. X (Sp-W) Rs. 338.00; Vol. XI (X-Z) with Cumulative Index to Vols. I-XI Rs. 223.00.

INDUSTRIAL PRODUCTS

Includes articles giving a comprehensive account of various large, medium and small scale industries. Some of the major industries included are : Acids, Carriages, Diesel Engines, Fertilizers, Insecticides & Pesticides, Iron & Steel, Paints & Varnishes, Petroleum Refining, Pharmaceuticals, Plastics, Ship & Boatbuilding, Rubber, Silk, etc.

The articles include an account of the raw materials and their availability, manufacturing processes, and uses of products, and industrial potentialities. Specifications of raw materials as well as finished products and statistical data regarding production, demand, exports, imports, prices, etc. are provided. The articles are suitably illustrated. References to the sources of information are provided.

Nine volumes of the series covering letters A–Z have been published.

Part I (A-B) Rs. 87.00; Part II (C) Rs. 111.00; Part III (D-E) with Index to Parts I-III Rs. 150.00; Part IV (F-H) Rs. 189.00; Part V (I-L) Rs. 135.00; Part VI (M-Pi) Rs. 42.00; Part VII (Pl-Sh) Rs. 90.00; Part VIII (Sl-Tl) Rs. 99.00; Part IX (To-Z) with Index to Parts I-IX Rs. 120.00.

HINDI EDITION : BHARAT KI SAMPADA–PRAKRITIK PADARTH

Vols. I to VII and two supplements of Wealth of India—Raw Materials series in Hindi already published.

Published Volumes :

Vol. I (अ-औ) Rs. 57.00; Vol. II (क) Rs. 54.00; Vol. III (ख-न) Rs. 54.00; Vol. IV (प) Rs. 125.00; Vol. V (फ-मेरे) Rs. 90.00; Vol. VI (मेल-स्) Rs. 120.00; Vol. VII (रे-वाटा) Rs. 203.00; Vol. VIII (वाय-सीसे) Rs. 300.00.

Supplements :

Fish & Fisheries (Matsya & Matsyaki) Rs. 74.00;
Livestock (Pashudhan aur Kukkut Palan) Rs. 51.00

Vols. IX to XI under publication.

Please contact :

SENIOR SALES AND DISTRIBUTION OFFICER

PUBLICATIONS & INFORMATION DIRECTORATE, CSIR
Hillside Road, New Delhi 110 012

RN 7090/63

CSIR PUBLICATIONS

WEALTH OF INDIA

An encyclopaedia of the economic products and Industrial resources of India issued in two series

RAW MATERIALS SERIES – Contains articles on plant, animal and mineral resources.

	Rs.	$	£
Vol. I(A) (Revised)	300.00	94.00	74.00
Vol. I (A-B)	120.00	60.00	26.00
Vol. II (C)	143.00	66.00	34.00
Vol. III (D-E)	158.00	64.00	40.00
Vol. IV (F-G)	98.00	54.00	24.00
Supplement (Fish & Fisheries)	84.00	32.00	21.00
Vol. V (H-K)	171.00	68.00	42.00
Vol. VI (L-M)	135.00	68.00	30.00
Supplement (Livestock including Poultry)	153.00	68.00	39.00
Vol. VII (N-Pe)	150.00	60.00	38.00
Vol. VIII (Ph-Re)	129.00	64.00	28.00
Vol. IX (Rh-Se)	156.00	70.00	38.00
Vol. X (Sp-W)	338.00	150.00	85.00
Vol. XI (X-Z)	223.00	77.00	44.00

INDUSTRIAL PRODUCTS SERIES – Deals with major, Small-Scale and Cottage Industries

Part I (A-B)	87.00	40.00	22.00
Part II (C)	111.00	48.00	28.00
Part III (D-E)	150.00	67.00	39.00
Part IV (F-H)	189.00	84.00	48.00
Part V (I-L)	135.00	46.00	34.00
Part VI (M-Pi)	42.00	16.00	5.60
Part VII (Pl-Sh)	90.00	36.00	12.00
Part VIII (Si-Ti)	99.00	54.00	20.00
Part IX (To-Z)	120.00	68.00	24.00

BHARAT KI SAMPADA (Hindi Edition of Wealth of India, Raw Materials):

Vol. I (अ-औ)	57.00	32.00	13.00
Vol. II (क)	54.00	30.00	12.00
Vol. III (ख-ज)	54.00	30.00	12.00
Vol. IV (ट)	125.00	68.00	32.00
Vol. V (ठ-मेरे)	90.00	44.00	20.00
Vol. VI (मेल-रू)	120.00	54.00	26.00
Vol. VII (रे-सटा)	203.00	80.00	50.00
Vol. VIII (सात-सीसे)	300.00	80.00	50.00
Livestock (Kukkut Palan)	51.00	30.00	12.00
Fish & Fisheries (Matsya aur Matsyaki)	74.00	42.00	10.00
A Dictionary of Generic & Specific Names of Plants & Animals Useful to Man	45.00	22.00	10.00

Please Contact :

SENIOR SALES & DISTRIBUTION OFFICER
PUBLICATIONS & INFORMATION
DIRECTORATE, CSIR
HILLSIDE ROAD, NEW DELHI - 110012

OTHER PUBLICATIONS

	Rs.	$	£
The Useful Plants of India	192.00	64.00	48.00
A Dictionary of the Flowering Plants in India by H. Santapau & A.N. Henry	63.00	28.00	16.00
Glossary of Indian Medicinal plants by R.N. Chopra, S.L. Nayar & I.C. Chopra	93.00	32.00	20.00
Supplement to Glossary of Indian Medicinal Plants by R.N. Chopra, I.C. Chopra & B.S. Verma	51.00	18.00	12.00
The Flora of Delhi by J.K. Maheshwari	42.00	16.00	5.50
Illustrations to the Flora of Delhi by J.K. Maheshwari	105.00	44.00	26.00
Herbaceous Flora of Dehra Dun by C.R. Babu	216.00	120.00	44.00
Gnetum by P. Maheshwari & Vimla Vasil	30.00	12.00	4.00
Marsilea by K.M. Gupta	62.00	27.00	16.00
Aquatic Angiosperms	30.00	12.00	4.00
Indian Fossil Pteridophytes by K.R. Surange	99.00	44.00	25.00
Cedrus by P. Maheshwari & Chhaya Biswas	63.00	28.00	16.00
Proteaceae by C. Venkata Rao	108.00	48.00	27.00
Pinus by P. Maheshwari & R.N. Konar	45.00	22.00	16.00
Loranthaceae by B.M. Johri & S.P. Bhatnagar	83.00	37.00	21.00
Abies & Picea by K.A. Chowdhury	21.00	12.00	4.20
Indian Thysanoptera by T.N. Ananthakrishnan	39.00	16.00	5.20
The Millipede Thyropygus by G. Krishnan	18.00	7.00	2.40
Indian Sardines by R.V. Nair	33.00	14.00	4.40
Drug Addiction with special Reference to India by R.N. Chopra & I.C. Chopra	19.00	7.00	2.40
Diosgenin & other Steroid Drug Precursors by L.V. Asolkar & Y.R. Chandha	54.00	26.00	12.00
Cholera Bacteriophages by Dr. Sachimohan Mukerjee	45.00	20.00	12.00
Cottonseed Chemistry & Technology by K.S. Murti & K.T. Achaya	116.00	64.00	26.00
Corrosion Map of India	27.00		3.60
Rural Development and Technology: A Status Report-cum-Biblio-graphy by PR Bose and V.N. Vashist	150.00	76.00	34.00
Termite Problems in India	14.00	6.00	1.80
Research & Development Management	38.00	20.00	
Proceedings of the Seminar on Primary Communica-tions in Science & Technology in India by R.N. Sharma & S. Seetharama	78.00	35.00	68.00

Packing and Postage Extra

Printed & Published by Shri S.S. Saksena, Editor, Publications & Information Directorate (PID) Hillside Road, New Delhi 110012, at PID Photocomposition-cum-Printing Unit

Regd No. D(C)-1018